

ISSN 0973-8916

Current Trends in Biotechnology and Pharmacy

Volume- 16

Supplementary Issue 2

2022



www.abap.co.in

Current Trends in Biotechnology and Pharmacy

ISSN 0973-8916 (Print), 2230-7303 (Online)

Editors

Prof.K.R.S. Sambasiva Rao, India
krssrao@abap.co.in

Prof.Karnam S. Murthy, USA
skarnam@vcu.edu

Editorial Board

Prof. Anil Kumar, India
Prof. P.Appa Rao, India
Prof. Bhaskara R.Jasti, USA
Prof. Chellu S. Chetty, USA
Dr. S.J.S. Flora, India
Prof. H.M. Heise, Germany
Prof. Jian-Jiang Zhong, China
Prof. Kanyaratt Supaibulwatana, Thailand
Prof. Jamila K. Adam, South Africa
Prof. P.Kondaiah, India
Prof. Madhavan P.N. Nair, USA
Prof. Mohammed Alzoghaibi, Saudi Arabia
Prof. Milan Franek, Czech Republic
Prof. Nelson Duran, Brazil
Prof. Mulchand S. Patel, USA
Dr. R.K. Patel, India
Prof. G.Raja Rami Reddy, India
Dr. Ramanjulu Sunkar, USA
Prof. B.J. Rao, India
Prof. Roman R. Ganta, USA
Prof. Sham S. Kakar, USA
Dr. N.Sreenivasulu, Germany
Prof.Sung Soo Kim, Korea
Prof. N. Udupa, India

Dr.P. Ananda Kumar, India
Prof. Aswani Kumar, India
Prof. Carola Severi, Italy
Prof. K.P.R. Chowdary, India
Dr. Govinder S. Flora, USA
Prof. Huangxian Ju, China
Dr. K.S.Jagannatha Rao, Panama
Prof.Juergen Backhaus, Germany
Prof. P.B.Kavi Kishor, India
Prof. M.Krishnan, India
Prof. M.Lakshmi Narasu, India
Prof.Mahendra Rai, India
Prof.T.V.Narayana, India
Dr. Prasada Rao S.Kodavanti, USA
Dr. C.N.Ramchand, India
Prof. P.Reddanna, India
Dr. Samuel J.K. Abraham, Japan
Dr. Shaji T. George, USA
Prof. Sehamuddin Galadari, UAE
Prof. B.Srinivasulu, India
Prof. B. Suresh, India
Prof. Swami Mruthinti, USA
Prof. Urmila Kodavanti, USA

Assistant Editors

Dr.Giridhar Mudduluru, Germany

Dr. Sridhar Kilaru, UK

Prof. Mohamed Ahmed El-Nabarawi, Egypt

Prof. Chitta Suresh Kumar, India

www.abap.co.in

ISSN 0973-8916

Current Trends in Biotechnology and Pharmacy

(An International Scientific Journal)

Volume 16

Supplementary Issue 2

2022



www.abap.co.in

Indexed in Chemical Abstracts, EMBASE, ProQuest, Academic SearchTM, DOAJ, CAB Abstracts, Index Copernicus, Ulrich's Periodicals Directory, Open J-Gate Pharmoinfonet.in Indianjournals.com and Indian Science Abstracts.

Association of Biotechnology and Pharmacy (Regn. No. 28 OF 2007)

The Association of Biotechnology and Pharmacy (ABAP) was established for promoting the science of Biotechnology and Pharmacy. The objective of the Association is to advance and disseminate the knowledge and information in the areas of Biotechnology and Pharmacy by organising annual scientific meetings, seminars and symposia.

Members

The persons involved in research, teaching and work can become members of Association by paying membership fees to Association.

The members of the Association are allowed to write the title MABAP (Member of the Association of Biotechnology and Pharmacy) with their names.

Fellows

Every year, the Association will award Fellowships to the limited number of members of the Association with a distinguished academic and scientific career to be as Fellows of the Association during annual convention. The fellows can write the title FABAP (Fellow of the Association of Biotechnology and Pharmacy) with their names.

Membership details

(Membership and Journal)		India	SAARC	Others
Individuals	– 1 year	Rs. 600	Rs. 1000	\$100
	LifeMember	Rs. 4000	Rs. 6000	\$500
Institutions (Journal only)	– 1 year	Rs. 1500	Rs. 2000	\$200
	Life member	Rs.10000	Rs.12000	\$1200

Individuals can pay in two instalments, however the membership certificate will be issued on payment of full amount. All the members and Fellows will receive a copy of the journal free.

Association of Biotechnology and Pharmacy

(Regn. No. 28 OF 2007)

#5-69-64; 6/19, Brodipet

Guntur – 522 002, Andhra Pradesh, India

Current Trends in Biotechnology and Pharmacy

ISSN 0973-8916

Volume 16 (Supplementary Issue 2)	CONTENTS	2022
Research Papers		
Comparative <i>in vivo</i> evaluation of simvastatin after oral and transdermal administration in rabbits <i>B. Manjula*</i> , <i>V. Rama Mohan Gupta</i> and <i>K. B. Chandra Sekhar</i>		1 - 8
Phytochemical investigation and heavy metal analysis of a miracle plant <i>Eryngium foetidum</i> Linn. <i>Shaik Chand Basha*</i> and <i>M Alagusundaram</i>		9 - 14
Preparation, characterization, <i>in vitro</i> evaluation, cytotoxic and antitumor activity of rubitecan inclusive liposomes with 2-hydroxy propyl- β -cyclodextrins as potential antitumor drug delivery system <i>Farsiya Fatima</i> and <i>Dr. M. Komala*</i>		15 - 24
Microwave irradiated green synthesis of novel isoxazole derivatives as anti-epileptic agent <i>Krishna Chandra Panda*</i> , <i>Bera Venkata Varaha Ravi Kumar</i> and <i>Biswa Mohan Sahoo</i>		25 - 30
RP-HPLC Method Development and Validation for Simultaneous Determination of Decitabine and Cedazuridine in Pure and Tablet Dosage Form <i>Alimunnisa</i> and <i>Lakshmana Rao A*</i>		31 - 39
Development and evaluation of capecitabine loaded human serum albumin nanoparticles for breast cancer <i>J. Josephine Leno Jenita*</i> , <i>A. R. Mahesh</i> , <i>B. P. Sudarshan</i> , <i>Seema S Rathore</i> and <i>Shanaz Banu</i>		40 - 49
Development and Validation of Stability Indicating RP-UPLC Method for Quantitative Estimation of Safinamide Mesylate in Bulk and its Tablet Dosage Form <i>Madhu Medabalimi*</i> , <i>K. Saravanakumar</i> and <i>S.V. Satyanarayana</i>		50 - 59
RP-HPLC Method for Determination of Favipiravir (RdRp of RNA Viruses) in Pharmaceutical Dosage Form <i>P. Ravisankar*</i> , <i>B. Divya</i> , <i>A. Bhavani Sailu</i> , <i>K. Neelima</i> , <i>A. Viswanath</i> and <i>P. Srinivasa Babu</i>		60 - 69
Spectroscopic Analysis of DNA Binding Mode of Novel Schiff Base Vanadium Complex <i>Poonam R. Inamdard</i> and <i>A. Sheela*</i>		70 - 74

Anti-Tubercular Activity of Neem Flower Extract <i>K. Purna Nagasree*</i> , <i>B. Hima Bindu</i> , <i>I. Priyanka</i> , <i>T. Divya</i> and <i>S. Mansha Afroz</i>	75 - 77
Comparative Effects of <i>Ocimum tenuiflorum</i> and <i>Ocimum basilicum</i> on Isoniazid Microsphere Formulation Characteristics Prepared by Different Methods <i>Rupali A. Patil</i> , <i>Prashant L. Pingale*</i> and <i>Sunil V. Amrutkar</i>	78 - 86
Development and Validation of a Sensitive and Rapid Bioanalytical RP-HPLC Method for the Quantification of Nebivolol Hydrochloride in Rat Plasma <i>S.N.H. Pratap*</i> and <i>Prof. J. Vijaya Ratna</i>	87 - 95
Comparative <i>In Vivo</i> Evaluation of Optimized Formulation of Teneligliptin and Metformin Bilayered Tablet with Pure Drugs <i>Rajani V*</i> , <i>Rajendra Prasad Y</i> and <i>Lakshmana Rao A</i>	96 - 102
Formulation and Evaluation of Cilnidipine Solid Dispersions and Oral Controlled Release Formulations <i>Ramakrishna Vydana*</i> and <i>Chandra Sekhar Kothapalli Bonnoth</i>	103 - 110
<i>In Silico</i> Design and Solvent Free Synthesis of Some Novel Dihydropyrimidinthione Derivatives and Study of its Antimicrobial Activity <i>G. Revathi *</i> and <i>Dr. K. Girija</i>	111 - 130
Ultrasonication Extraction Techniques for a New Approach for Development of Pharmacognostical and Phytochemical Screening of <i>Syzygium aromaticum</i> <i>Reena Gupta *</i> , <i>Ittishree</i> and <i>Jitendra Gupta</i>	131 - 138
<i>Syzygium cumini</i> Protects Diabetic Wistar Rats Against Rosiglitazone-Induced Cardiotoxicity and Hepatotoxicity <i>Prashant L. Pingale</i> , <i>Rupali A. Patil*</i> , <i>Aishwarya S. Gadkari</i> and <i>Sunil. V. Amrutkar</i>	139 – 154
Comparative anti-anaemic activity of methanolic extracts of <i>Momordica charantia</i> and <i>Luffa acutangula</i> <i>Doppalapudi Sandeep*</i> , <i>Suryadevara Vidyadhara</i> and <i>Pottella Srinivasulu</i>	155 - 161
Synthesis, Spectral Characterization and <i>In vitro</i> Anti Cancer Activity of Pyrimidine – Imidazole coupled Heterocyclic compounds against Human Lung Cancer Cell Line <i>S. Shakila Banu*</i> , <i>G. Krishnamoorthy</i> , <i>R. Senthamarai</i> and <i>A. M. Ismail</i>	162 - 170
Preparation and characterization of oral fast dissolving film of hydralazine HCL <i>M. Sudhir *</i> , <i>V. Sruthi</i> , <i>T.Venkata Siva Reddy</i> , <i>Ch. Naveena</i> , <i>B. Pamula Reddy</i> and <i>Sk. A. Rahaman</i>	171 - 178
Design and development of itraconazole loaded nanosponges for topical drug delivery <i>Swalin Parija *</i> and <i>V.Sai kishore</i>	179 - 186

Comparative *in vivo* evaluation of simvastatin after oral and transdermal administration in rabbits

B. Manjula*, V. Rama Mohan Gupta and K. B. Chandra Sekhar

¹Research Scholar, JNTU Ananthapuram, Ananthapuram

²Department of Pharmaceutics, G. Pulla Reddy College of Pharmacy, Hyderabad

³Vice Chancellor, Krishna University, Machilipatnam, Andhra Pradesh

*Corresponding author: betholimanjula@gmail.com

Abstract

Membrane-moderated transdermal systems of Simvastatin liposomes were prepared by incorporating the drug reservoir within a shallow compartment moulded from a drug-impermeable backing membrane and 2% w/v cellulose acetate rate-controlling membrane. The pharmacodynamic and pharmacokinetic performance of Simvastatin following transdermal administration was compared with that of oral administration. This study was carried out in a randomized cross-over design in male New Zealand albino rabbits. The estimation of Simvastatin in plasma was carried out by LC-MS/MS method. The parameters such as maximum plasma concentration (C_{max}), time for peak plasma concentration (t_{max}), mean residence time (MRT) and area under curve (AUC_{0 - ∞}) were significantly (P < 0.001) differed following transdermal administration compared to oral administration. The relative bioavailability of Simvastatin was increased about nine fold after transdermal administration as compared to oral delivery. This may be due to the avoidance of first pass effect of Simvastatin. The concentration of Simvastatin in plasma was found to be stabilized and maintained in a narrow range over the study period up to 24 hrs for transdermal formulation where as the concentration was decreased rapidly up on oral administration. It was concluded that the relative rate of extensive first pass metabolism was significantly reduced in transdermal administration, resulted in increased relative bioavailability and reduced frequency of administration.

Keywords: Simvastatin, Liposomes, Transdermal Systems, LC-MS/MS, *In vivo* Studies.

Introduction

The transdermal route of drug delivery has gained great interest of pharmaceutical research, as it circumvents number of problems associated with oral route of drug administration. The barrier nature of skin inhibits the penetration of most drugs. The use of lipid vesicles as delivery system for skin treatment has gained attention in recent years(1). Liposomes are microscopic or submicroscopic particles and are concentric bilayered vesicles in which an aqueous volume is entirely enclosed by a membranous lipid bilayer mainly composed of natural or synthetic phospholipids. Liposomes are microscopic vesicles that contain amphipathic phospholipids arranged in one or more concentric bilayers enclosing an equal number of aqueous compartments. The thermodynamically stable, lamellar structures form spontaneously when a lipid is brought into contact with an aqueous phase(2).

The aim of the present study was to develop and evaluate the potential use of liposome vesicles in the transdermal drug delivery for delivery of Simvastatin. Simvastatin is an effective drug in the treatment of hyperlipidemic patients, simvastatin is a methylated derivative of lovastatin that acts by competitively inhibiting 3-hydroxy-3-methylglutaryl-coenzyme A (HMG-CoA) reductase, the enzyme that catalyzes the rate limiting step in cholesterol biosynthesis. Administration of conventional tablets of simvastatin has been reported to exhibit

fluctuations in plasma drug levels, results either in manifestation of side effects or reduction in drug concentration at the receptor sites also is a cholesterol-lowering agent and is structurally similar to the HMG, a substituent of the endogenous substrate of HMG-CoA reductase. Simvastatin lowers hepatic cholesterol synthesis by competitively inhibiting HMG-CoA reductase, the enzyme that catalyzes the rate-limiting step in the cholesterol biosynthesis pathway via the mevalonic acid pathway(3). Due to short biological half life (5.3 hours) and low bioavailability (5%) due to extensive first pass metabolism makes it suitable candidate for transdermal drug delivery system. An *in vivo* evaluation study was conducted to ascertain pharmacokinetic parameters in rabbits after oral and transdermal administration of simvastatin in rabbits.

Materials and Methods

The *in vivo* study of the optimized formulations were performed as per the guidelines approved by the Committee for the Purpose of Control and Supervision of Experiments on Animals (CPCSEA), Ministry of social Justice and Empowerment, Government of India. Prior approval by Institutional animals ethics committee was obtained for conduction of experiments (Ref: IAEC/IX/10/ACOP/ CPCSEA, Dated 21-12-19).

Preparation of Liposomes by Thin Film Hydration Technique: Liposomes were prepared by rotary evaporation-sonication method. ⁴The lipid mixture (500mg) consist of phospholipid (Soya Lecithin), edge activator (Tween 80) and drug (10 mg/ml) in different ratios was dissolved in an organic solvent mixture consist of chloroform and methanol (2:1, v/v) then placed in a clean, dry round bottom flask. The organic solvent was carefully evaporated by rotary evaporation (Buchi rotavapor R-3000, Switzerland) under reduced pressure above the lipid transition temperature(at 60°C for 1 hr) to form a lipid film on the wall of the flask. The final traces of the solvents were removed by subjecting the flask to vacuum over night. The dried thin lipid

film deposited on the wall of the flask was hydrated with a phosphate buffer solution (pH 6.4) by rotation for 1hr at room temperature at 60 rpm. The resulting vesicles were swollen for 2 hrs at room temperature to get large multilamellar vesicles. To prepare small Liposome vesicles, the resulting vesicles were sonicated at 100 kHz, 80 Amp for 30 minutes at pulse on 30sec and pulse off 50 sec using a probe sonicator (OrchidScientifics, Nasik).The obtained suspension was passed through a series of 0.45 μ and 0.22 μ polycarbonate filters and then stored at 4°C(4).

Preparation of Rate Controlling Membrane: Solvent evaporation technique was employed in the present work for the preparation of Cellulose acetate films. The polymer solutions were prepared by dissolving the polymer (2% w/w Cellulose acetate) in 50 ml of Ethyl acetate Methanol (8:2). Dibutyl phthalate at a concentration of 40% w/w of the polymer was used as a plasticizer. 20 ml of the polymer solution was poured in a Petri plate (9.4 cm diameter) placed on a horizontal flat surface. The rate of evaporation was controlled by inverting a funnel over the Petriplate. After 24 hours the dried films were taken out and stored in a desiccators(5).

Preparation of Liposomes Loaded Gels: Accurately weighed quantity of 500 mg of Hydroxy propyl methyl cellulose was dispersed in 5 ml of distilled water and was allowed for swelling over night. The swollen carbopol was stirred for 60 minutes at 800 rpm. The previously prepared required Simvastatin equivalent Liposomes, methylparaben and propylparaben were incorporated into the polymer dispersion with stirring at 500 rpm by a magnetic stirrer for 1 hour. The pH of above mixture was adjusted to 7.4 with tri ethanolamine (0.5%). The gel was transferred in to a measuring cylinder and the volume was made up to 10ml with distilled water(6).

Design of Membrane Moderated Transdermal Therapeutic System: A circular silicon rubber ring with an internal diameter of 2.5 cm and a thickness of 3mm was fixed on to a backing membrane (an imperforated

adhesive strip was supplied by Johnson and Johnson Limited ,Mumbai). This serves as a compartment for drug reservoir. Gel equivalent to 40 mg of Simvastatin was taken into the compartment as a drug reservoir. Cellulose acetate membrane of known thickness was fixed on the ring with glue to form a membrane moderated therapeutic systems. A double sided adhesive strip was fixed on the rim of the ring above Cellulose acetate membrane(7).

In Vivo Evaluation

Subject Selection: Twelve New Zealand healthy rabbits with a mean age of 10±2 weeks and with a mean body weight of 3±0.2 kg were used in this study. Each group consisted of six rabbits (n=6) each and were subjected for overnight fasting, it was taken care that there was no stress on the animals. Rabbits were randomly divided into two groups for different sampling time and each group was housed in one cage. Food and water were available ad libitum at all times during the experiment. The study was conducted in a crossover design with 2 weeks washout periods in between the two experiments. The animal dose of Simvastatin was calculated relevant to human dose by using the following formula(8).

Human dose of Simvastatin = 40 mg.
 Animal dose = $\frac{\text{Human Dose} \times \text{Animal Weight}}{\text{Human Weight}}$ =
 $40 \times 3 / 70 = 1.71 \text{ mg /kg}$

Blood Sampling: About 1 ml of blood samples were collected from the tracheal lobular vein of the rabbit using and the blood was stored in screw top heparinized plastic tubes, the sampling time for blood was done at 0 min (predose), 1, 2, 4, 6, 8, 10, 12, 14, 16, 18, 20 and 24 hr. The plasma was immediately separated by aspiration after centrifugation at 4000 rpm for 5 minutes and frozen at -20°C until analysed by LC-MS/MS method(9).

Determination of Pharmacokinetic Parameters: Various pharmacokinetic parameters such as peak plasma

concentration (C_{max}), time at which peak occurred (T_{max}), area under the curve (AUC), elimination rate constant (K_{el}), biological half-life ($t_{1/2}$) and mean residence time (MRT) were calculated using the noncompartmental pharmacokinetics data analysis software PK Solutions 2.0™ (Summit Research Services, Montrose, CO, USA) (10).

Statistical Analysis of the Pharmacokinetic Parameters:

The pharmacokinetic parameters of the tested formulations were statistically analyzed using paired sample's t-test for normal distributed results of C_{max} , K_a , K_e , MRT and $AUC_{0-\infty}$ values. All tests were performed at 0.001 level of significance(10).

Estimation of Simvastatin in Rabbit Plasma:

LC-MS/MS Method: A summary of the chromatographic and mass spectrometric conditions is as follows:

UPLC: WATERS

Mass spectrometer: API 2000

Ion source: Heated nebulizer

Polarity: Negative

Detection ions

Simvastatin: 240.2 * amu (parent), 196.0* amu (product), d3-Simvastatin: 244.2* amu (parent), 200.2 amu (product)

Column: Phenomenax,synergi 4 μ Polar- RP80 A, 4.6x75 mm

Column oven temperature: 35°C

Peltier temperature: 10°C

Mobile phase: Ammonium formate: Acetonitrile (30:70)

Flow rate: 1 ml/min.

Volume of injection: 10 μL

Retention time: Simvastatin - 0.5 to 1.20 minutes: ISTD - 0.5 to 1.20 minutes

Run time: 2.00 minutes

Preparation of Working Standard Solutions:

1. Preparation of Simvastatin Standard Stock Solution: Simvastatin working standard equivalent to 5 mg

Simvastatin was accurately weighed and transferred into a 5 ml volumetric flask and dissolved in methanol. The solution was made up to the volume with methanol. The concentration of resulting solution was calculated by considering the purity of Simvastatin. The solutions were labeled and stored in a cold store at 2-8°C.

2. Preparation of Internal Standard Stock Solution: 0.005 g of d3-Simvastatin was weighed accurately and transferred in to a 5 ml volumetric flask and dissolved in methanol. The solution was made up to the volume with methanol. The concentration of resulting solution was calculated by considering the purity of Simvastatin-d4. The solutions were labeled

and stored in a cold store at 2-8°C. Stock solution was diluted with 60% Acetonitrile in water solution to get a concentration of 75.00 µg/ml.

Calibration Curve Standards:

1. Preparation of Stock Dilutions of Standard Simvastatin Solution: Stock solution of Simvastatin was diluted with 60% Acetonitrile in water solution to get a concentrations ranging from 1 to 140 µg/ml (Figure 1).

2. Spiking of Plasma for Calibration Curve Standards: Concentrations of Simvastatin ranging from 50 to 7000 ng/ml were prepared with plasma and labeled them as CC1 to CC8 in (Table 1). The calibration

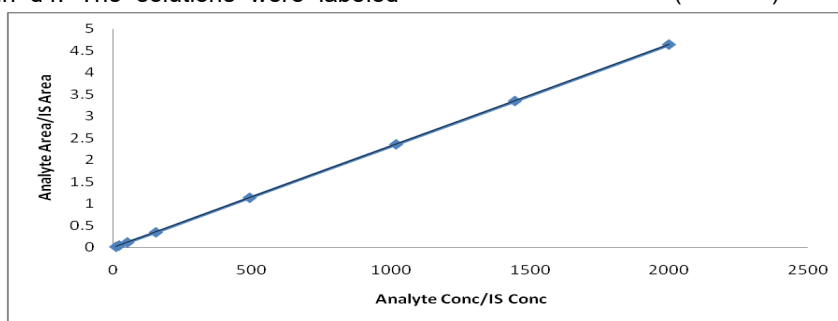


Fig 1. Calibration Curve for Estimation of Simvastatin in Plasma

Table 1: Analyte Concentrations of Stock Dilutions of Standard Simvastatin Solution with Plasma

S No	Sample Name	Analyte Concentration (ng/ml)	Analyte peak area	IS Peak Area	Area Ratio	Calculated Concentration (ng/ml)	Accuracy (%)
1	Plasma Blank	0	0	0	0	N/A	N/A
2	Blank+ISTD	0	254	513643	0	N/A	N/A
3	CC1	50.05	3879	528938	0.01	50.407	100.71
4	CC2	100.15	6997	506198	0.01	97.939	97.79
5	CC3	250.300	17284	484351	0.04	258.119	103.12
6	CC4	500.650	34646	504084	0.07	500.215	99.91
7	CC5	1001.250	77371	577631	0.13	978.007	97.68
8	CC6	2002.500	134349	520675	0.26	1887.085	94.24
9	CC7	5006.250	345626	529110	0.65	4782.401	95.53
10	CC8	7008.750	578109	544120	1.06	7780.670	111.01

curve standards were prepared freshly for each validation run.

Extraction Procedure:

Step 1: Blank, calibration curve standards and the subject samples were withdrawn from the deep freezer and allowed them to thaw. The thawed samples were vortexed to ensure complete mixing of contents. To 0.25 ml of plasma sample in a vial, 25 μ l of d3-Simvastatin standard (75 μ g/ml) was added. To plasma blank, 25 μ l of 60% Acetonitrile in water solution was added and vortexed the samples to ensure complete mixing of contents.

Step 2: Add 2.5 ml of tertiary butyl methyl ether, place on a shaker for 15 minutes and centrifuge for 10 minutes at 4000 rpm at 20°C. Transfer supernatant (organic layer) into the another vial. Evaporate this layer under a stream of nitrogen at 45°C. The residue was reconstituted with

0.5 ml of mobile phase and vortexed. The samples were transferred in to auto-injector vials and loaded the vials in to auto sampler. 10 μ l of sample was injected in to LC-MS/MS system.

Data Processing: The chromatograms were obtained by using the computer-based Analyst 1.4.2 version software supplied by the Applied Biosystems, Canada. The concentrations of the unknown samples were calculated from the equation using regression analysis of spiked plasma calibration standard with $1/x^2$ as weighting factor. $y = mx + c$ Where, y = Ratio of Simvastatin peak area and ISTD peak area (analyte area / ISTD area); x = Concentration of Simvastatin; m = Slope of the calibration curve; c = y-axis intercept value. Linear regression analysis equation of stock dilutions of standard Simvastatin solution with plasma is, $y = 0.000136x + 0.000454$.

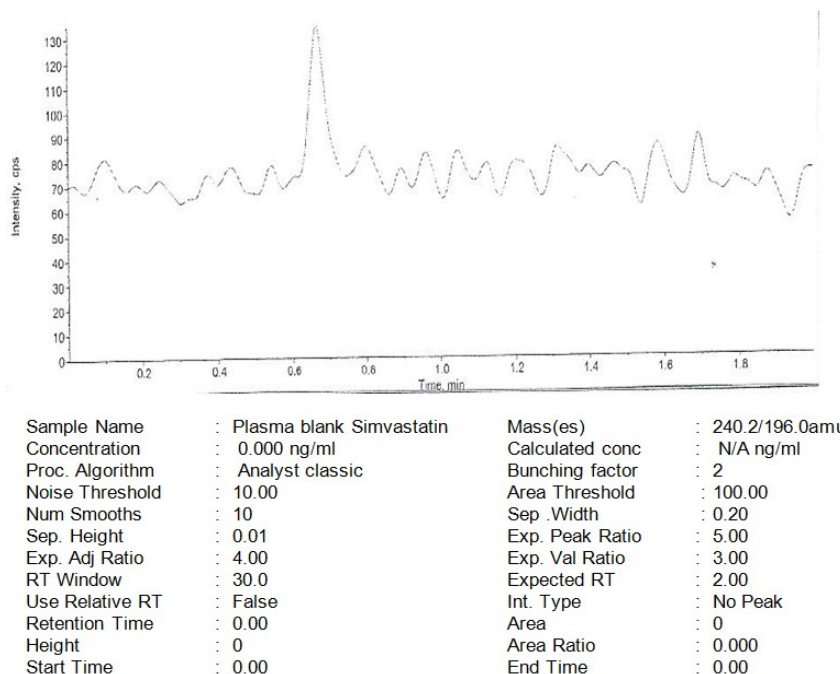


Fig. 2. Chromatograms of Blank Plasma

Comparative *In Vivo* Evaluation of Simvastatin

Results and Discussion

The *in vivo* experiments were conducted as per the protocol and procedure described earlier. The ability of core in cup tablet as a drug delivery system to release drugs in a predetermined time release manner was investigated in rabbits after oral administrations was investigated. Bioanalytical methods employed for the quantitative determination of drugs and their metabolites in biological matrix (plasma, urine, saliva, serum etc) play a significant role in evaluation and interpretation of pharmacokinetic data. For the successful conduct of pharmacokinetic study, the development of selective and sensitive bioanalytical methods plays an important role for the quantitative evaluation of drugs and their metabolites (analytes). The LC-MS/MS methods were highly sensitive and suitable for the detection of drug in plasma even in low concentrations. Various pharmacokinetic parameters such as peak plasma concentration (C_{max}), time at which peak occurred (T_{max}), area under the curve (AUC), elimination rate constant

(K_{el}), biological half-life ($t_{1/2}$) and mean residence time (MRT) were calculated using the noncompartmental pharmacokinetics data analysis software PK Solutions 2.0™ (Summit Research Services, Montrose, CO, USA).

The pharmacokinetic parameters of the tested formulations were statistically analyzed using paired sample's t-test for normal distributed results of C_{max} , K_a , K_{el} , MRT and $AUC_{0-\infty}$ values. All tests were performed at 0.001 level of significance.

Calibration curves were constructed from blank sample (plasma sample processed without IS), blank+IS samples and eight point calibration standards for Simvastatin in plasma. Plasma concentrations of Simvastatin at different times were calculated. Pharmacokinetic parameters such as absorption rate constant, elimination rate constant, half life, AUC, and MRT were calculated from the plot of time versus plasma concentration and subjected to statistical analysis and the results were shown in (Table 2).

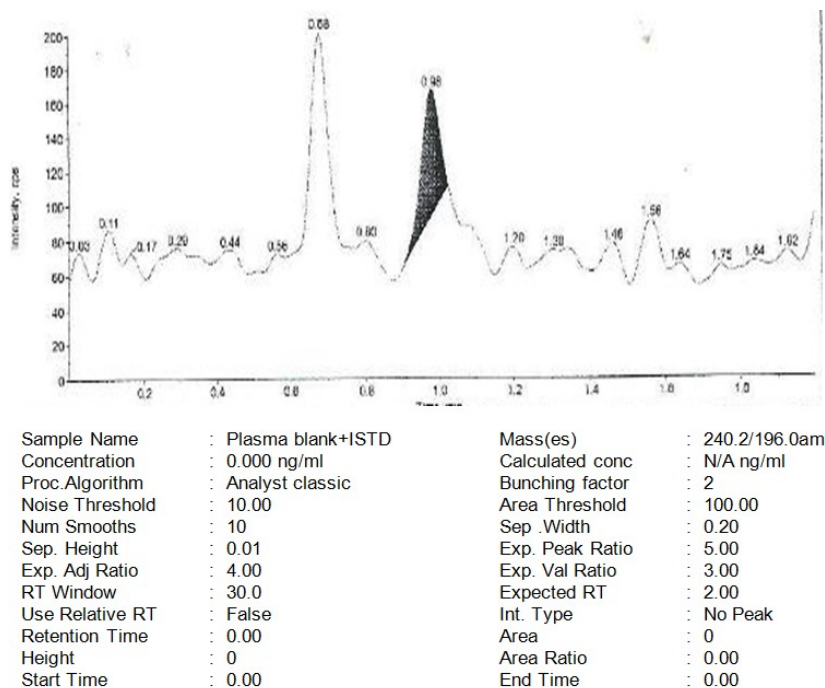


Fig. 3. Chromatogram of Stock Solution of Standard Simvastatin Solution with Plasma
 Comparative *In Vivo* Evaluation of Simvastatin

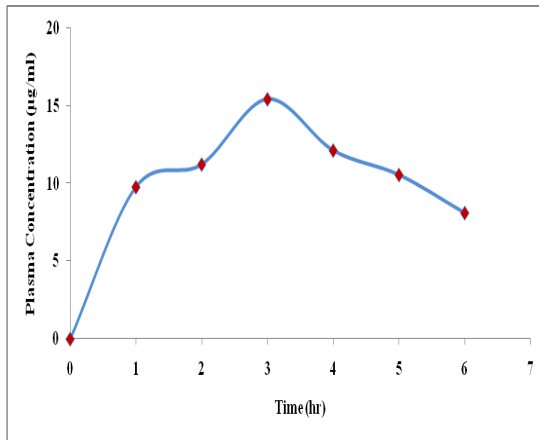


Fig. 4. Plasma Concentration-Time Curve of Simvastatin Following Oral Administration of Oral Suspension

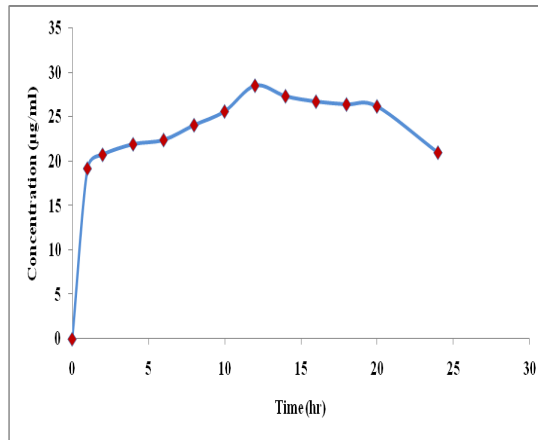


Fig. 5. Plasma Concentration-Time Curve of Simvastatin Following Topical Administration of Optimized Transdermal Formulation

Table 2: Statistical Treatment of Pharmacokinetic Parameters (Mean \pm S.D.) of Following Oral Administration of Oral Suspension and Optimized Transdermal Formulation of Simvastatin

Pharmacokinetic Parameter	Oral Suspension	Optimized Transdermal Formulation	Calculated Value of 't'
C_{max} (ng/ml)	23.4 ± 0.31	28.6 ± 0.41	16.70***
T_{max} (h)	3 ± 0.13	12 ± 0.08	21.36***
MRT (h)	5.1 ± 0.05	24.3 ± 0.15	25.50***
$t_{1/2}$ (h)	2.62 ± 0.03	12.52 ± 0.013	7.75***
K_{el} (h^{-1})	0.26 ± 0.04	0.055 ± 0.007	3.87***
K_a (h^{-1})	1.14 ± 0.01	0.33 ± 0.02	12.67***
$AUC_{0-\infty}$ (ng h/ml)	105.9 ± 1.56	958.0 ± 3.07	156.60***

Null hypothesis (H_0): There is no significant difference between the pharmacokinetic parameters of oral administration of oral suspension and optimized transdermal formulations of Simvastatin.

Table value of 't' with 10 DF at the 0.001 level is 4.587.

Result: H_0 is not accepted as the calculated 't' value more than the table Value of 't' with 10 DF at 0.001 levels of significance. It was therefore concluded that there was significant difference between the pharmacokinetic parameters of oral administration of oral suspension and optimized transdermal formulations of Simvastatin.

Values are presented in Mean \pm SD

Plasma Concentration of Simvastatin following oral and transdermal administration in rabbits at different times were calculated. The results from the oral administration of Simvastatin indicated the maximum plasma concentration (C_{max}) 23.4 ± 0.31 ng/ml at 3 hrs (t_{max}) while transdermal administration exhibited the maximum plasma concentration (C_{max}) of 28.6 ± 0.41 ng/ml at 12 hrs (t_{max}). The oral administration of Simvastatin resulted in a low and quite variable AUC of 105.9 ± 1.56 ng.hr/ml, where as the transdermal resulted in AUC of 958.0 ± 3.07 ng.hr/ml. The mean residence time of transdermal administration (24.3 ± 0.15 hrs) was found to be more than oral administration (5.1 ± 0.05 hrs). The results indicated that the parameters significantly differed following transdermal administration, compared to oral administration. The concentration of selected drugs in plasma was found to be stabilized and maintained in a narrow range over the study period up to 24 hrs for transdermal formulation where as the concentration was decreased rapidly up on oral administration. The maximum plasma concentration (C_{max}) was attained at 3 hrs after oral administration and it was observed after 12 h upon application of transdermal formulation of same dose.

The *in vivo* pharmacokinetic studies revealed that the transdermal formulations of Simvastatin exhibited controlled release and absorption kinetics over longer periods of time which in turn maintained the desired plasma concentrations over longer periods of time.

References

1. Sivannarayana P, Prameela Rani A, Saikishore V. Liposomes: Ultra Deformable Vesicular Carrier Systems in Transdermal Drug Delivery System. Research J. Pharma.Dosage Forms and Tech 2012; 4(5): 243-255.
2. Walve JR, Bakliwal SR, Rane BR, Pawar SP. Liposomes: A syrrigated carrier for transdermal drug delivery system. Int J App Bio Pharm Tech. 2011; 2(1):204-13.
3. Singh S K, Verma P R P , Razdan B., Development and characterization of a simvastatinloaded self-microemulsifying drug delivery system, Pharm. Dev. Tech. 2010; 15 (2): 469–483.
4. Amin SG, Shah DA and Dave RH: Formulation and evaluation of liposomes of fenofibrate prepared by thin film hydration technique. Int J Pharm Sci & Res 2018; 9 (9): 3621-37.
5. Sai Kishore V, Murthy T. E. G. K. Formulation and Evaluation of Transdermal Gels of Diltiazem Hydrochloride. Indian J. Pharma. Educ. Res 2008; 42 (3): 272-276.
6. Kusum Devi V, Saisivam S, Maria G R, Deepti PU. Design and evaluation of matrix diffusion controlled transdermal patches of verapamil hydrochloride. Drug Dev. Ind. Pharm, 2003; 29 (5): 495-503.
7. Sai Kishore, V., Gopala krishnamurthy, T. E., Mayuren, C. (2011). Comparative In Vivo Evaluation of Diltiazem hydrochloride following Oral and Transdermal administration in Rabbits, Research J.Pharm. and Tech, 4 (1): 150-154.
8. Sai Kishore, V., Gopala krishnamurthy, T. E., Mayuren, C. (2011). Comparative In Vivo Evaluation of Propranolol hydrochloride following Oral and Transdermal administration in Rabbits, Asian J. Research Chem, 4 (3): 461-465.
9. Nageswararao P, Ramesh M, Jaswanth KI, Indira KN, Seshagirirao JVLN. Simultaneous determination of simvastatin, lovastatin and niacin in human plasma by LC-MS/MS and its application to a human pharmacokinetic study. Biomed Chromatogr. 2012; 26:476–484.
10. Pradeep P, Vandana P, Anant P. Formulation of a self-emulsifying system for oral delivery of simvastatin: in vitro and in vivo evaluation:Acta pharm. 2007;57: 111–122.

Phytochemical investigation and heavy metal analysis of a miracle plant *Eryngium foetidum* Linn.

Shaik Chand Basha* and M Alagusundaram

¹ Jawaharlal Nehru Technological University Anantapur, Anantapuramu

² Department of Pharmaceutics, Ratnam Institute of Pharmacy, Nellore

*Corresponding Author: E-Mail Id: schandbasha20@gmail.com

Abstract

Herbs are rich source of secondary metabolites that have been found to have medicinal properties. The present study was conducted to evaluate the phytochemical and heavy metal analysis whole plant of *Eryngium foetidum* Linn. The obtained results revealed that Petroleum ether and Chloroform extract contains less phytochemical constituents when compared with, Ethyl acetate and Ethanolic extracts in maximum quantity. The Heavy metals analysis for powder were determined by atomic absorption spectroscopy method (AAS). The results showed doesn't contains high toxic levels of heavy metals; (Arsenic-0.022 mg/L; below the detectable level, Chromium 0.005 mg/L; and Lead 0.006 mg/L below the detectable level).

Keywords: Phytochemical Constituents, Atomic Absorption Spectroscopy Method, *Eryngium foetidum* Linn.

Introduction

Medicinal herbs have played a crucial role in maintaining human health and improving the quality of human life for thousands of years. They often contain highly active pharmacological principles including minerals and trace metals(1). According to World Health Organization (WHO) estimates, nearly 70–80% of the world population still primarily relies on nonconventional medications, mostly derived from herbs(2,3). India is known for its rich tradition of herbal medicine, and Indians are quite familiar with the medicinal and flavoring properties of several herbs. Herbs are traditionally used for the treatment and prevention of chronic ailments. The toxicity of herbal plants may be related to contaminants

such as pesticides, microbes, heavy metals, chemical toxins, and adulterants(4,5). In general, the geography, the geochemical soil characteristics, contaminants in the soil, water, and air, and other growth, transport, and storage conditions can significantly affect the properties and the quality of the herbal plants and their constituents(6,7).

Materials and Methods

Plant Materials: The whole plant of *Eryngium foetidum* Linn. was collected from the Marthandam, Kanya kumari Dist., Tamilnadu in the month of December. Healthy and mature plants were selected for the study. The taxonomic identification of plant was authenticated by Dr. C. Madhava Chetty, Professor, Dept. of Botany, SV University, Tirupati, Chittoor Dist., A.P, India and deposited to the department as a sample herbarium. The plants were thoroughly washed with tap water followed by second distilled water to remove the dirt and specks of dust.

Drying: The cleaned plants were cut into small pieces and were left for shade drying for 15 days. Afterwards, they were dried in hot air oven at 40°C for 2 h to remove the equilibrium moisture before the extraction process.

Extraction: Extraction was performed by Soxhelt extraction technique(11). Whole plants of *Eryngium foetidum* Linn. were pulverized by using a mechanical grinder, which was later sieved through mesh size 80 to get the powder of uniform size. Around 10 g of the powder was packed in a thimble of whatmann's filter paper. The apparatus was then assembled and the extractions were carried out using 250 ml each of as Petroleum ether, Chloroform, Ethyl acetate

and Ethanol as solvent. The temperature was maintained at 35-40°C. The extraction was continued for 10 h for Ethanol, 5 h for Petroleum ether, Chloroform, Ethyl acetate following the color of the solvent collected in the thimble chamber. Ten milliliters each of concentrated extract was kept for phytochemical screening and remaining extracts were dried. The dried extract was used for isolation of phytoconstituents and Pharmacological activities. Preliminary Characters and percentage yield of Petroleum ether, Chloroform, Ethyl acetate and Ethanol extracts of *Erygium foetidum* L. is presented in Table 1 & Fig. 1

Phytochemical Screening:

Phytochemical screenings were carried out for Petroleum ether, Chloroform, Ethyl acetate and Ethanol extracts as per the standard methods(6,7,8,9) and following tests were performed:

Test for Alkaloids

a. Mayer's Test: To 2 ml of each extract, few ml of 2N HCl along with few drops of Mayer's reagent was added. Gelatinous white precipitation confirms the presence of alkaloids.

b. Wagner Test: To 2 ml of extract few drops of Wagner reagent was added, a reddish brown precipitation observed confirms the presence of alkaloids.

Test for Saponin

Froth Flotation Test: 2 ml of sample was added in a test tube with few ml of water, a froth observed and persisted on constant shaking confirms the presence of saponin.

Test for Tannins and Phenolic Compound: To a 2 ml of extract few drop of 5% FeCl₃ solution was added, blue black precipitation confirms the presence of tannins and phenolic compound.

Table 1: Preliminary Characters and % Yield of Various Extracts of *Erygium Foetidum* Linn.

S No	Solvent	Color of Extract	Percentage Yield
1.	Petroleum ether	Dark Green	33.3%
2.	Chloroform	Light Green	8.41%
3.	Ethyl acetate	Light Green	8.31%
4.	Ethanol	Brown	20.0%



Fig. 1. Preliminary Characters of Various Extracts of *Erygium Foetidum* Linn.

Phytochemical Investigation and Heavy Metal Analysis

Test for Flavonoids: To 2 ml of extract, 1 ml of lead acetate solution was added. An intense yellow color was appeared which confirms the presence of flavonoids.

Test of Cardiac Glycoside: To 2 ml of plant extract, 2 ml of glacial acetic acid containing 1 drop of ferric chloride solution and 1 ml of concentrated H_2SO_4 was added. Appearance of a brown ring indicates the presence of cardiac glycoside.

Test for Reducing Sugars: Fehling test: 1ml each of Fehling's A and Fehling's B solutions was mixed and boiled for 1 min and equal volume of test solution was added. The whole solution is heated in a boiling water bath for 5–10 min. Formation of brick red ppt. confirmed the presence of carbohydrate.

Test for Glycoside (Killer Killiani Test): To 2 ml of extract, 1 ml of glacial acetic acid, few drop of $FeCl_3$, and few drops of concentrated H_2SO_4 were added. Green/blue precipitation indicates the presence of glycoside.

Test for Emodins: To 2 ml of extract, 2 ml of NH_4OH and 3 ml of benzene were added. Red coloration indicates the presence of emodins.

Test for Phlobatannins: To 2 ml of extract, 2 ml of 1% HCl was added and heated. Red precipitate indicates the presence of phlobatannins.

Test for Terpenoids: To 2 ml of extract, 2 ml of chloroform and 2 ml of concentrated H_2SO_4 was added. A reddish brown coloration indicates the presence of terpenoids.

Test for Protein: To 2 ml of extract, few drops of concentrated H_2SO_4 was added on it. White precipitate indicates the presence of protein.

Test for Steroid (Salkowski Test): To 2 ml of extract, 2 ml of $CHCl_3$ and 2 ml of conc. H_2SO_4 were added on it. A reddish brown ring at the junction indicates the presence of steroid.

Heavy Metal Analysis

The quantification of heavy metals in the plant powder was done by flame AAS

technique equipped in ICE 3000 series atomic absorption spectrometer. For this, 1.0 g of dried plant powder was taken in a 250ml conical flask, and 5 ml of conc. HNO_3 (GFS Chemicals Inc., Columbus, 69%) was added slowly. The mixture was heated on the hot plate till the brown fumes disappeared yielding the white fumes. Water was added to make the solution, and it was then filtered in a 50 ml volumetric flask. Finally, the volume was adjusted to 50 ml by adding triple distilled water up to the mark(16,17). This filtrate was then introduced in flame AAS for the detection of metals.

Results and Discussion

The phytochemical screening revealed the presence of phenols were present in all extracts. Flavanoids, were present in all three petroleum ether, Ethyl acetate and ethanol extracts(10). Terpenoids were present in Chloroform, Ethyl acetate and ethanol extracts and but were absent in petroleum ether extract. Anthraquinones, emodins and glycoside were present only in Ethyl acetate extract and tannins were present only in ethanol extract and absent in all three extracts. The concentration of alkaloid by Mayer's test was medium in the ethanol extract. Similarly, in Wagner's test, it was high in ethanol and low in petroleum ether extract. The reducing sugar was at high concentration in petroleum ether and low in ethanol. Proteins were absent only in petroleum ether extract and remaining have extracts with low concentration. The report of phytochemical screening is presented in (Table 2).

Environment, pollution, atmosphere, soil, harvesting and handling are some of

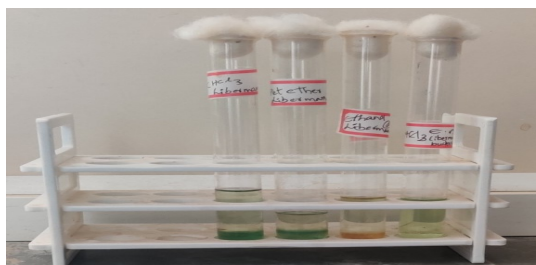


Figure. 2 Test for Steroids Various Extracts of *Erygium Foetidum* Linn.

Table 2: Phytochemical Compositions of Various Extracts of *Erygium Foetidum Linn.*

Chemical Test	<i>Erygium foetidum</i> Extract			
	Pet. Ether	Chloroform	Ethyl Acetate	Ethanol
Test for alkaloid				
1. Mayer's test	–	–	+	++
2. Wagner test	–	–	+	++
Test for saponin	–	–	–	+++
Test for phenol	+	+	++	++
Test for flavonoids	+	–	++	+++
Test for glycoside	–	–	++	+++
Test for reducing sugar	+	+	+	–
Test for steroid	+	–	+	++
Test for tannins	–	–	–	+
Test for protein	–	–	–	–
Test for terpenoids	–	+	+	+++
Test for emodins	–	–	–	–
Test for anthraquinone	–	–	+	–

Table 3: Heavy Metal Analysis of Dried Powder of Plant *Erygium Foetidum Linn.*

S. No.	Heavy Metal	Wavelength	Concentration	Normal Level
1.	Arsenic [As]	188.979	0.022 mg/L [BDL]	0.053mg/L
2.	Chromium [Cr]	267.716	0.005 mg/L	0.007 mg/L
3.	Lead [Pb]	220.353	0.006 mg/L	0.042 mg/L

the factors, which play a major role in contamination of medicinal plants by metals and also by microbial growth. Therefore it is necessary to measure and establish the levels of metallic elements in the herbal plants as these elements when consumed at higher levels become toxic(10-12). The dried powder of plant *Erygium foetidum L.* analyzed for the presence of important heavy metals such as Arsenic, Chromium and Lead in this study. The results showed doesn't contains high toxic levels of heavy metals; (Arsenic-

0.022 mg/L; below the detectable level, Chromium 0.005 mg/L; and Lead 0.006 mg/L below the detectable level) (Table 3). The heavy metal content did not exceed the limit given according to the WHO guidelines 2005(12-15).

Conclusion

The outcome of the present studies revealed that various phytochemicals including alkaloids, steroids, terpenoids, glycosides, anthraquinones, etc., are present while tannins

and emodins were found absent in this plant. Heavy metals like As, Cr, Pb are below the detectable level according to the WHO guidelines, which provide biological significance of the studied plant. The studies therefore suggest that the folklore use though is very resourceful; the authenticity yet needs serious research. The closely resembling species may sometimes create ambiguity that even leads to fatal disorders. With more resources and time, further investigation and isolation of phytochemical constituents of plant *Erygium foetidum* L. can be revealed.

Conflict of Interests

The authors declare that there is no conflict of interests regarding the publication of this paper.

Acknowledgement

The authors would like to thank the Annamacharya College of Pharmacy, Rajampet, Kadapa Dist, Andhra Pradesh, India for providing the facilities of this study.

References

1. Azwanida N. (2015). A review on the extraction methods use in medicinal plants, principle, strength and limitation, Medicinal Aromatic Plants. 4:3–8.
2. Fabricant D. S. and Farnsworth N. R. (2001). The value of plants used in traditional medicine for drug discovery, Environmental Health Perspectives. 109: 69–75.
3. Sahoo N., Manchikanti P. and Dey S. (2010). Herbal drugs standards and regulation, Fitoterapia. 81:462–47.
4. World Health Organization (WHO), Traditional Medicine Strategy 2002–2005. (2002). World Health Organization, Geneva, Switzerland.
5. Saad B., Azaizeh H., Abu Hijleh G., and Said O. (2006). Safety of traditional Arab herbal medicine, Evidence-Based Complementary and Alternative Medicine. 3: 433–439.
6. Gavamukulya Y., Abou-Elella F., Wamunyokoli F., AEI-Shemy H. (2014). Phytochemical screening, anti-oxidant activity and in vitro anticancer potential of ethanolic and water leaves extracts of *Annona muricata* (Graviola). Asian Pac J Trop Med 7:S355–S363.
7. Aiyegoro O A., Okoh AI. (2010). Preliminary phytochemical screening and In vitro antioxidant activities of the aqueous extract of *Helichrysum longifolium* DC. BMC Complement Altern Med.
8. Geetha TS., Geetha N. (2014). Phytochemical screening, quantitative analysis of primary and secondary metabolites of *Cymbopogon citrates* (DC) stapf. Leaves from Kodaikanal hills, Tamilnadu. Int J PharmTech Res. 6:521–529.
9. Kaur GJ., Arora DS. (2009). Antibacterial and phytochemical screening of *Anethum graveolens*, *Foeniculum vulgare* and *Trachyspermum ammi*. BMC Complement Altern Med.
10. Rania D., Safa A. K., Husna R., and Munawwar A. K. (2015). Determination of Heavy Metals Concentration in Traditional Herbs Commonly Consumed in the United Arab Emirates, Journal of Environmental and Public Health, 1-6.
11. Ashish P., Pawan K. O., Biswash G. and Narendra K. C. (2019). Phytochemical screening, metal concentration determination, antioxidant activity, and antibacterial evaluation of *Drymaria diandra* plant, Beni-Suef University Journal of Basic and Applied Sciences. 8:16.
12. World Health Organization, WHO Guidelines for Assessing Quality of Herbal Medicines with Reference to Contaminants and Residues. (2006). World Health Organization, Geneva, Switzerland.
13. World Health Organization (WHO), Quality Control Methods for Medicinal Plant Materials. (2005). World Health Organization, Geneva, Switzerland.
14. Thakuri B. C., Chanotiya C. S., Padalia R. C, Mathela C. S. (2006). Leaf essential oil of

Eryngium foetidum L. from far Western Nepal. J Essent Oil Bear Plants. 9:251–256.

15. Cardozo E., Rubio M., Rojas LB., Usubiliaga A. (2004). Composition of the essential oil from the leaves of *Eryngium foetidum* L. from the Venezuelan Andes. J Essent Oil Res.16:33–40.

16. Thi N D T., Anh T H., Thach L.(2008). The essential oil composition of *Eryngium foetidum* L. in South Vietnam extracted by hydrodistillation under conventional heating and microwave irradiation. J Essent Oil Bear Plants. 11:154-161.

17. Martin K P. (2004). Efficacy of different growth regulators at different stages of somatic embryogenesis in *Eryngium foetidum* L.- a rare medicinal plant. *In Vitro Cell Dev Biol Plant*, 40:459–63.

18. Gayatri M C., Madhu M., Kavyashree R., Dhananjaya SP. (2006). A protocol for in vitro regeneration of *Eryngium foetidum* L. *Indian J Biotech*, 5:249–51.

19. Li Z., Xu L., Gao X.(2007). *In vitro* culture and plant regeneration of *Eryngium foetidum* L. *Plant Phys Commun*, 43:496.

Preparation, characterization, *in vitro* evaluation, cytotoxic and antitumor activity of rubitecan inclusive liposomes with 2-hydroxy propyl- β -cyclodextrins as potential antitumor drug delivery system

Farsiya Fatima and Dr. M. Komala*

¹Department of Pharmaceutics, School of Pharmaceutical Sciences, Vels Institute of Science, Technology and Advanced Studies (VISTAS), Chennai.

²Department of Pharmaceutics, School of Pharmaceutical Sciences, Vels Institute of Science, Technology and Advanced Studies (VISTAS), Chennai

*Corresponding author: farsiya@gmail.com

Abstract

It is an oral topoisomerase inhibitor, having oral absorption of about 25-30% leading to low bioavailability of the drug due to low permeability and poor water solubility. The aim of the present study is to improve the solubility and dissolution rate and in turn the sufficient activity against pancreatic cancer of the drug, by formulating its inclusion complex with beta (β)-cyclodextrin, using different methods. The phase solubility analysis indicates the formation of 1:1 molar inclusion complex of the drug with beta cyclodextrin. Phase solubility analysis of Rubetecan-HP β CD mixture provided $k_{1:1}$ value of 1188 M^{-1} . The prepared complexes were characterized using differential scanning calorimetry, scanning electron microscopy, and x-ray diffractometry. The results suggest that using "drug-in-CD-inclusion complex in liposome" approach is a feasible strategy to formulate. These prepared liposomes by double-loading technique seem to be a suitable targeted drug delivery system because they have a fast onset action with prolonged drug release process and the significantly enhanced drug-loading capacity.

Keywords: 2-Hydroxy Propyl- β –Cyclodextrins, Inclusion complexes, Liposomes

Introduction

Nanocarriers are able to change the physicochemical properties of the

incorporated molecules, affect the pharmacokinetic profiles of embedded drugs, as well as allow the incorporated molecules to overcome biological barriers. For these reasons nanovehicles are used to enhance the effectiveness of the drug, decrease severe side effects, and protect the drug from chemical degradation that may compromise their efficiency, or lead to the formation of secondary products, which are sometimes toxic. Liposomes are microscopic spherical lipid vesicles in which an aqueous volume is entirely enclosed by a membrane(1). They can encapsulate hydrophilic molecules in the aqueous core, lipophilic ones in the membrane and amphiphilic substances at the aqueous–lipid interface. Liposomes are usually made of natural, biodegradable, non-toxic and non-immunogenic lipid molecules. These aggregates are useful in biological, biomedical, and biotechnological applications as drug delivery systems due to their extraordinary capacity to encapsulate hydrophilic drugs in the aqueous core and to trap lipophilic compounds within the membrane. In doing so, this carrier system protects the entrapped molecules from degradation and thinning down in the systemic circulation. Because of their properties, liposomes when formed, their physicochemical properties like size, lamellarity, membrane rigidity, etc. are able to influence and enhance the performance of products by increasing ingredient solubility, improving ingredient bioavailability, enhance intracellular

uptake, alter pharmacokinetics and biodistribution and *in vitro* and *in vivo* stability(2). Liposomes are also known to prevent local irritation, increase drug potency and reduce toxicity. However, the amount of drug that can be encapsulated within the liposomes impedes its employment as a carrier system. Both the properties of the liposome as well as that of the entrapped drug can manipulate the encapsulation efficiency. Liposomes offer an excellent opportunity to selective drug targeting which is expected to optimize the pharmacokinetic parameters and the pharmacological effects, prevent local irritation, and reduce the drug toxicity(2). Drugs may be incompatible with vesicle formation, and the accommodation of water-insoluble drugs in the lipid bilayers of the liposomes can be detrimental to the bilayer formation and stability and require the use of suitable organic solvents. Increasing the lipid load in order to incorporate sufficient drug for adequate therapeutic efficacy may not be acceptable, particularly with chronic use. Simultaneous entrapment of the drug into the lipid bilayers as well as into the aqueous phase of the liposome by virtue of the water-soluble cyclodextrin (CD) inclusion complexes is a prospective approach for surmounting such shortcomings and combining the relative advantages of the two types of carriers into a single system by formulating drug-in cyclodextrin-in liposome (CLDDS) systems(11).

Nevertheless, the incorporation of highly hydrophobic molecules into liposomes can destabilize the lipid membrane, leading to a rapid release of the drug from the bilayer. In an attempt to overcome this problem, in 1994, McCormack and Gregoriadis engineered, for the first time, the possibility of forming a combined system of cyclodextrins (CDs) and liposomes called drug-in-cyclodextrin-in-liposomes (DCLs). These systems are able to combine the capability of CDs to form CD/drug inclusion complexes with the use of liposomes as shuttle systems. Recently, different DCLs have been designed to overcome drawbacks such as the low

solubility and low stability of many type of active compounds comprising aromatics, essential oils, and hydrophobic drugs. The possibility of using such a combined strategy aimed to concurrently exploit the CD-solubilizing power toward the drug and the tailored release mechanisms offered by liposomes.

Rubitecan [Orathecin™] is a topoisomerase I inhibitor extracted from the bark and leaves of the *Camptotheca acuminata* tree, which is native to China. It is a pyrano-indolizino-quinoline that is camptothecin in which the hydrogen at position 9 has been replaced by a nitro group. It is a C-nitro compound, a semisynthetic derivative, a tertiary alcohol and a delta-lactone. It is a prodrug for 9-aminocamptothecin. Investigated for use/treatment in pancreatic cancer, leukemia (unspecified), melanoma, ovarian cancer. Rubitecan is an effective drug against pancreatic cancer(4).

We decided to formulate inclusion complexes of 2-Hydroxy Propyl-β-Cyclodextrins containing Rubetecan in liposome as the anticancer agent. However, the inherent bioavailability of the molecule is very low. This molecule has an aberrant solubility pattern and attempts to improve its bioavailability are plenty in the literature. A nanoparticulate delivery system for Rubetecan has been designed; 2-Hydroxy Propyl-β-Cyclodextrins has been used as a complexing agent. Liposomes of Rubetecan have been formulated as a stable carrier for delivering Rubetecan to the hepatocytes is desired, warranting its delivery as CLDDS. All liposomal formulations were characterized for encapsulation efficiency, particle size, drug loading and morphology. *In vitro* release profiles were determined and an *in vitro* cytotoxicity and antitumor activity was performed to ascertain the effectiveness of the formulation developed(12).

Material

HP-β-CD (molecular weight, 1.460 Da) and dimethyl sulfoxide-d6 (DMSO- d6) were obtained from Sigma-Aldrich. The average degree of substitution in the purchased HPβCD was 0.8 hydroxypropyl groups per glucose unit.

All other chemicals used were of standard reagent grade.

Preparation of Rubitecan Inclusion

Complexes: Preparation of Rubitecan Inclusion is prepared by neutralization-agitation method: 1.500 g 2-Hydroxy Propyl- β -Cyclodextrins was weighed and placed into 50 mL beaker. 30 mL distilled water was added into the beaker to make a solution. Accurately weighed (0.3849 g) RUBITECAN (RUBITECAN to 2-Hydroxy Propyl- β -Cyclodextrins' molar ratio 1:1) was then added into the 2-Hydroxy Propyl- β -Cyclodextrins solution. 1 mol/L NaOH solution was then added dropwise to adjust the pH to alkaline. RUBITECAN, all in the open ring form, was dissolved in 2-Hydroxy Propyl- β -Cyclodextrins solution, followed by magnetic stirring for 2 h at room temperature. 1 mol/Litre hydrochloric acid solution was then dropped into the above solution to adjust the pH to neutral and kept overnight. The solution was then filtered and the filtrate was concentrated under reduced pressure at 40°C vacuum drying. The RUBITECAN 2-Hydroxy Propyl- β -Cyclodextrins inclusion complex was then obtained and verified(4).

Liposome Preparation: Small uni-lamellar liposomes containing Rubitecan and Rubitecan: 2-Hydroxy Propyl- β -Cyclodextrins inclusion complexes were obtained by the method of formation-and- hydration-sonication of lipid film, as described by Lira et al. Briefly, to obtain Rubitecan liposomes, Rubitecan pure substance (10 mg) mixed with combined blend of lipids containing soya phosphatidyl choline, cholesterol and stearyl-amine) and was solubilized in the organic phase with the in a biphasic mixture solvent system composed of chloroform: methyl alcohol (3:1 v/v) under magnetic stirring. Next, a thin film was formed and hydrated with 10 mL of Tris buffer solution (pH 7.4) containing trehalose (10% m/v). The resulting multi-lamellar liposomes were then subjected to ultrasonication to obtain micro-uni-lamellar liposomes. Finally, the liposomes were freeze-dried and the lyophilized liposomes

maintained at 25°C \pm 1°C in a desiccator equipped with vacuum control. Alternatively, in order to obtain Rubitecan inclusion complex form of liposomes, the Rubitecan: 2-Hydroxy Propyl- β -Cyclodextrins inclusion complexes were added to the Tris-buffer solution (aqueous phase) forming liposomes at a drug concentration of 1000 micrograms/mL(5).

Characterization of Inclusion Complexes in Liposomes:

Phase Solubility Test: It is commonly utilized to measure the binding constant calculated from the equations of Higuchi and Connors. Briefly, an excess of RUBITECAN (2 mg) was added in 2 mL of distilled water containing various amounts of HP β CD (0-200 mM). The dispersions were mixed by orbital stirring (Model TS2000A VDRL, Bio mixer, Brazil) at 150 rpm for 72 h at 25°C \pm 2°C. Then, the samples were filtered through the hydrophilic cellulose acetate membrane (0.22 μ m, Kasvi, Brazil). The RUBITECAN concentrations were determined spectrophotometrically at λ = 286 nm (model SP-2000 UV, Spectrum, USA). For Rubitecan, the apparent stability constant (Ks) was calculated from the linear relationship between the molar concentration of Rubitecan in the solution medium as a function of the HP- β -CD molecular concentration according to the following equation:

Slope- is the corresponding slope of the phase solubility diagram

$$K_s = \frac{\text{Slope}}{S_0(1-\text{slope})}$$

S₀ (the intercept) denotes the solubility of Rubitecan in the absence of 2-Hydroxy Propyl- β -Cyclodextrins(13).

Morphological Studies: The morphology was evaluated and photo scanned by using scanning electron microscopy (SEM) (MEV-FEG Auriga 40, Zeiss, Germany) with an accelerating voltage of 5 kV. The test samples were previously covered with a layer of

palladium by sputter coating. SEM reveals the inclusion cyclodextrins complexes to analyse whether the inclusion linkage had been completely obtained by comparing and contrasting the pictorial variations among the 2-HP- β -CD and final inclusion complex(6).

Particle Size Measurements: The average diameter of the liposomal particles and their polydispersity index (PI) of liposomes, at pre-and-post lyophilization/rehydration stage, were measured by photon-correlation-spectroscopic method (PCS) using a laser particle size analyzer Delsa-TM Nano-S at 25°C with a 90-degree fixed angle (Beckman Coulter, UK). Liposome samples (n = 3) were diluted suitably in highly purified water for particle counting.

Zeta Potential Measurements: The surface charge of the vesicles (zeta potential) was measured by determining their electrophoretic mobility using a Zetatrac Legacy (Nanotracs®, USA). The measurements (n = 3) were carried out at 25°C with sample dispersions at 0.3% (w/v) in a NaCl (1 mM) aqueous electrolyte.

Encapsulation Efficiency: It was estimated by UV-Visible spectrophotometry. The Rubitecan was determined by taking an aliquot of liposomal suspension (50 microliters). The aliquot was solubilized in methyl alcohol and is further subjected to sonication for 5 min to increase the solubility of aliquot in methanol. The analyte was then estimated by spectrophotometry at the absorption maxima of 276 nm (λ_{max}), using the Rubitecan standard calibration curve with in working dilutions ranging from 2 to 20 micrograms/mL in methanol. To quantify the Rubitecan content that was not inclusively complexed into 2-HP- β -Cyclodextrins liposomes, the microfiltration/dialysis/ultracentrifugation, a widely used technique, was used. Initially, an aliquot of liposomal dispersion (400 microliters) was centrifuged at 10,000 rpm for 20 minutes at 4°C. Next, the filtrate, whose free analyte in liposomes was quantified by UV-Vis spectrophotometry (276 nm). Dilution factors

were applied to measure the correlation. Entrapment efficiency was calculated by the following equation: $EE\% = (\text{total-DCTN free Rubitecan})/\text{total Rubitecan} \times 100\%$ (7).

In Vitro Release Kinetics: The kinetic profiles of Rubitecan liposomes and Rubitecan: 2-Hydroxy Propyl- β -Cyclodextrins inclusion complexes encapsulated into liposomes in pH 7.4 Tris buffer solution for 1.5 days.

In Vitro Cytotoxicity and Antitumor Activity: The cytotoxicity and antitumor activity were studied by 3-(4,5-Dimethylthiazol-2-yl)-2,5-diphenyltetrazolium bromide (MTT) assay with various cancer cell lines (HCT116, KB), and L929 cells (regular homosapeins cell line). The cells were inoculated into 96-well plates and incubated for 24 hours at 37°C ambiances under controlled relative-humidity atmosphere in Dulbecco's Modified Eagle Medium-(DMEM) or Roswell Park Memorial Institute Medium-(RPMI 1640) with 10% (v/v) foetal bovine serum (FBS) and 1% (v/v) streptomycin sulphate. After 24-hours of inoculation cell agglomerates received drug, drug loaded in liposomes, inclusive complexes of drug and incubated for 48 h. After incubation, 30 μ L of MTT solution (1000 ppm) was added to each well, mixed and incubated for 4 hours at 37°C. The media was withdrawn and then 100 microliters of DMSO was added to each well to and mix gently to solubilize the Formazan crystals developed by the viable and live cells. Further, the absorbance was measured at 550 nm (optical density) and 660 nm (for background subtraction). %-Cell viability was calculated according to the following equation: Optical Density- (OD) value = (OD 560 nm-670 nm)(8).

$$\text{Cell Viability (\%)} = \frac{\text{OD}_{\text{Sample}} - \text{OD}_{\text{Blank}}}{\text{OD}_{\text{Control}} - \text{OD}_{\text{Blank}}}$$

Cellular-Uptake Study by Confocal-Laser-Scanning-Microscopy: The cellular uptake of optimized and prepared inclusion complex is established by using the method confocal laser scanning microscopy in HCT-119 and KB cell linings. The HCT-119 and KB cells were inoculated on Octa-well plate with RPMI 1640 medium and incubated for

24 hours. After incubation, the cells are treated with Rubitecan-2-HP-CD-inclusion complex and blend thoroughly for uniform distribution and then are incubated for 4 hours. The medium was collected and rinsed with Phosphate Buffer Solution for 2 times. Then the cell linings were stabilized by fixation with 4% paraformaldehyde for 10 min at 37°C. The micro-cellular machinery and other components including the nucleus of the cells were smeared and colour with Acti-stain-TM-488-phalloidin and DAPI for 15 min, and the slides were slightly treated with glycerol as dehydrating agent kept a side for 5 minutes. Further the slides are mounted and examined by CLSM(9).

Stability Assessment of Liposomes: These testing procedures include the physicochemical evaluations such as physical appearance, particle size measurement and distribution, poly-dispersity index and pH-variations were studied. The objective of accelerated stability study is to verify the liposomal preparations on short-term degradation by subjecting to stressed conditions. In this context, liposomal suspensions were undergoing the high-speed centrifugation at 10000 rpm for 1 hr at 4°C and to mechanical stress at 180 strokes/minute at 37°C during 48 hrs (Polytest@20 Bio-block Scientific). Long-term bench-top stability evaluation of liposomes

was also recommended to perform immediately after the preparation of liposomes and subsequently at predetermined time intervals at 7, 15, and 30 days(10).

Results and Discussion

Phase Solubility Test: The concentration of RUBITECAN solubilized form in deionized water is raised in linear fashion with the addition of 2-Hydroxy Propyl- β -Cyclodextrins. The S_0 value (solubility of RUBITECAN in the absence of 2 HP- β -CD) was 0.000274 mM and the slope value of the linear plot was 0.00028, the slope value and S_0 value are important to obtain the stability constant (K_s) value. The determination coefficient was 0.9982, suggesting a equimolar ratio of 1:1 stoichiometry of the complex formation, and indicating an A_L -type phase solubility diagram according to Higuchi and Connors. In our study, the stability constant for the complexation was 1188 M^{-1} , the higher K_s value, the higher the chance of occurring an inclusion-complex between the active drug molecule and cyclodextrin and, henceforth, acquires the maximum drug solubility and successful complexation in the cyclodextrin cavity. The solubility profile of RUBITECAN in aqueous solutions containing 2-Hydroxy Propyl- β -Cyclodextrins (Figure 1).

Morphological Studies: The SEM images depicted that free Rubitecan is present as

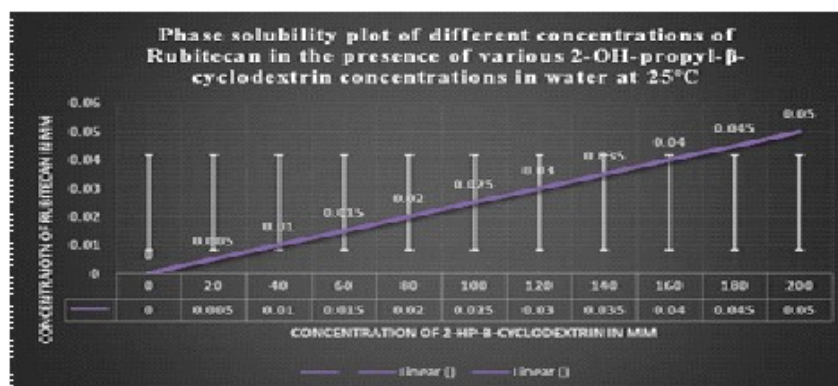


Fig 1. Phase Solubility Plot of Different Concentrations of Rubitecan in the Presence of Various 2-Hydroxy-Propyl β -Cyclodextrin Concentrations in Water at 25°C

asymmetrical crystals with non-uniform shape and appearance. (Figure 2A) and 2-HP-β-CD are visible as spherical shaped particles with rough, uneven texture with high degree of crevices and pores on surface of the particles. (Fig. 2B). On the other hand, in the pictures of the Rubitecan: 2-Hydroxy Propyl-β-Cyclodextrins inclusion complexes (Figure 2C) the intrinsic morphological characters of both molecules are modified and a uniform amorphous flat structure with highly variable in particle size distribution was observed. These variations in particle morphological features were attributed to the formation of linkage between the drug and cyclodextrins during inclusion complexation process, which suggests the formation of the inclusion complex.

Particle Size Measurements: The average particle sizes of plain liposomes and inclusive complexed cyclodextrin liposomes were measured to be 82.45 ± 6.6 nm and 87.33 ± 3.00 nm, respectively. There were no remarkable variations ($p < 0.05$) in the equivalent mean diameters of particle sizes of

plain and inclusive complex liposomes of Rubitecan. Also, the respective poly-dispersity index values of plain and inclusive complex liposomes of Rubitecan were found to be 0.35 and 0.39. The liposomes are ultimately had a uniformly distributed and populated particles.

In Vitro Release Kinetics: A quick release effect (25%) to native liposomes and cyclodextrins liposomes occurred in the first four hours. This might be attributed to the quick release of Rubitecan adsorbed on the surface of liposomes. Henceforth, a slow and persistent release of the Rubitecan has observed in both formulations within a period of 6 hours (4–10 h). After 8 h, there was a drug release of almost 80% to both plain and cyclodextrin liposomes. The highest concentration of drug released to Rubitecan (95%) and to Rubitecan:2-Hydroxy Propyl-β-Cyclodextrins inclusion complexes (98%) was obtained at 24 h. As shown in Figures (a) and (b), there was substantial agreement about the finding indicates that a simple diffusion mechanism is involved in the mass transport of liposomal systems Figs 3-10.

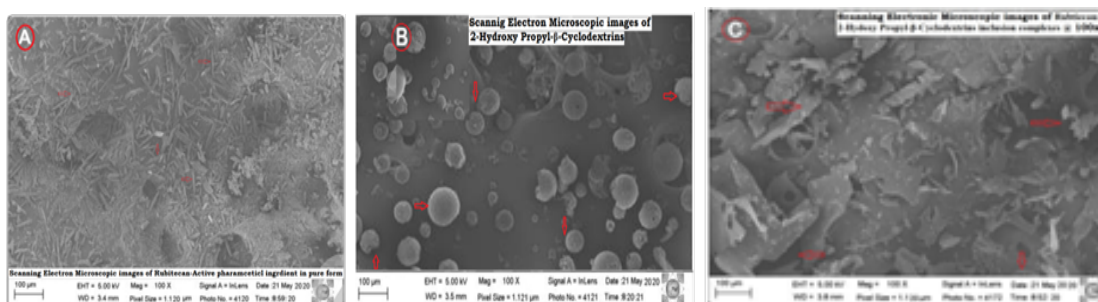


Fig 2. (A) Scanning Electron microscopy, (B) SEM Image, (C) SEM Image (SEM) of Rubitecan-API in pure form

Table 1: Illustrates Particle Size, Zeta Potential and Encapsulation Efficiency

Liposomes	Particle Size in nm	Poly Dispersity Index	Zeta Potential in mV	Encapsulation Efficiency
Rubitecan Liposomes (Native)	73.65±5.24	0.31±2.78	36.45±2.74	94.72±2.64
Rubitecan: 2-HP-CD-Inclusive Complex Liposomes	88.58±2.84	0.39±6.85	38.76±3.65	92.18±3.42

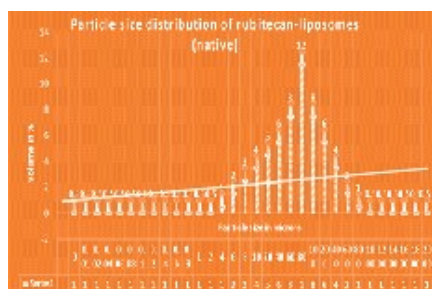


Fig 3. Particle Size Distribution of Rubitecan Liposomes

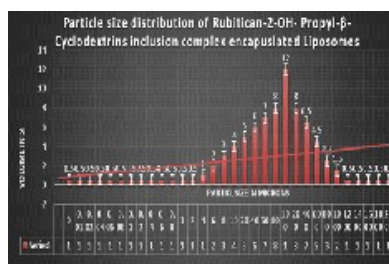


Fig 4. Particle Size Distribution of Rubitecan-2-Hydroxy Propyl-Beta-Cyclodextrins Inclusion Complexes Encapsulated Liposomes

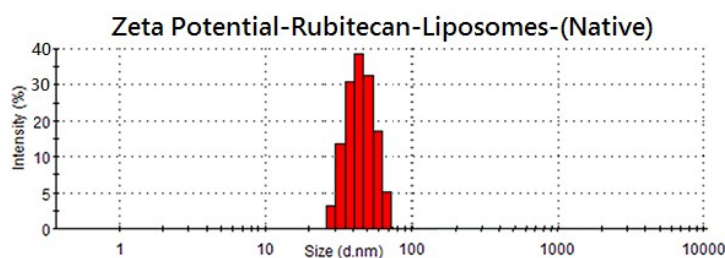


Fig 5. Zeta Potential Study of Rubitecan Liposomes

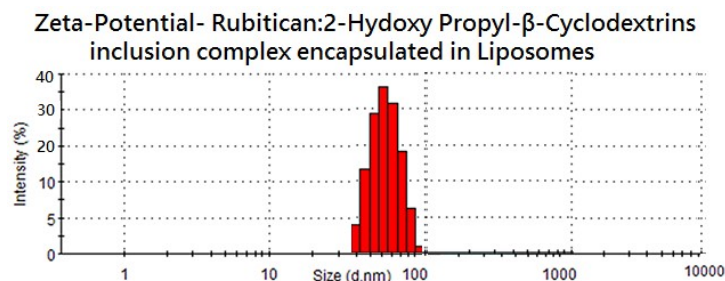


Fig 6. Zeta Potential Study of Rubitecan-2 Hydroxy Propyl-Beta-Cyclodextrins Inclusion Complexes Encapsulated Liposomes

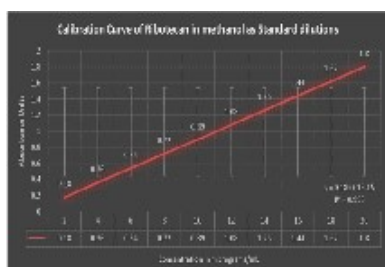


Fig 7. Calibration Curve of Rubitecan In methanol as standard dilutions

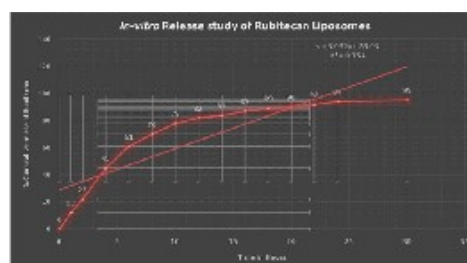


Fig 8. *In Vitro* Release Study of Rubitecan Liposomes

Antitumor Drug Delivery System

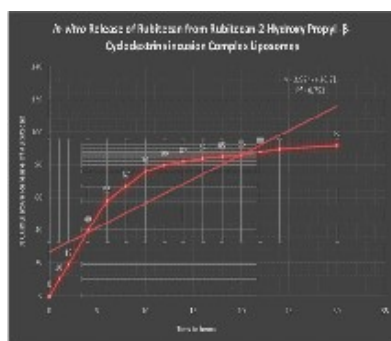


Fig 9. *In Vitro* Release Study of Rubitecan-2-Hydroxy propyl-Beta-Cyclodextrins Inclusion complexes

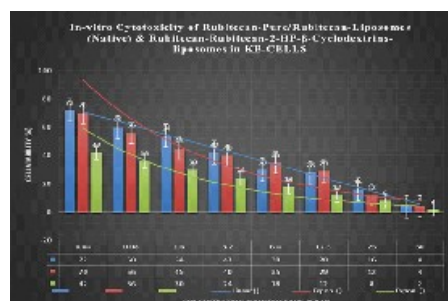


Fig 10. *In Vitro* Cytotoxicity Study of Rubitecan (Pure)/Rubitecan 2-Hydroxy propyl -Beta Cyclodextrins Inclusion Complexes in KB Cells

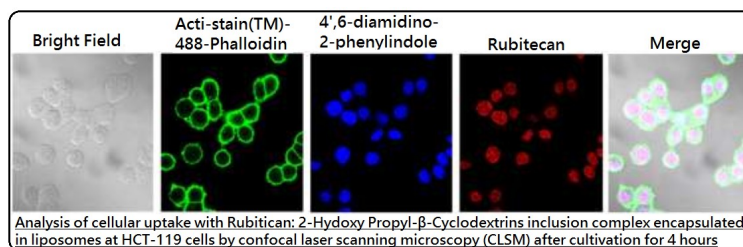


Fig 11. Analysis of cellular uptake with Rubitecan-Hydroxy propyl -Beta-cyclodextrins Inclusion Complexes at KB cells by Confocal laser Scanning Microscopy (CLSM) after Cultivation for 4 Hours

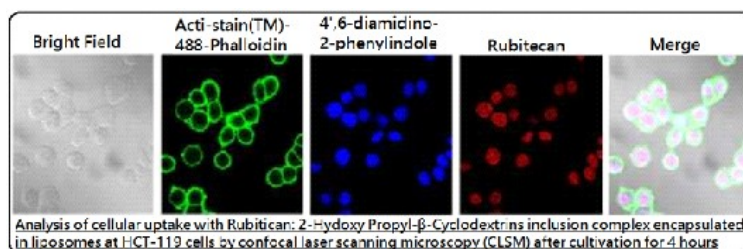
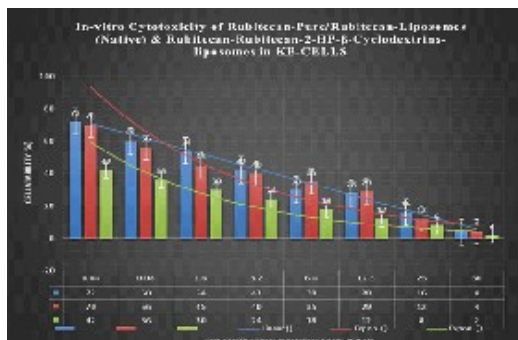


Fig 12. Analysis of Cellular Uptake with Rubitecan-2-Hydroxy Propyl-Beta-Cyclodextrins Inclusion Complexes at HCT-119 Cells by CLSM after Cultivation for 4 Hours

***In vitro* Cytotoxicity and Antitumor Activity:** The cytotoxicity and antitumor activity of free Rubitecan, Rubitecan-loaded-liposomes, and Rubitecan: 2-Hydroxy Propyl-β-Cyclodextrins inclusion complex encapsulated in liposomes were evaluated by MTT assay [3-(4, 5-dimethyl thiazol-2-yl)-2, 5-diphenyl tetrazolium bromide] HCT119 and KB cell

(cancer cell) (Figure). Viable cells at the time of test agent addition (T0) and following 72 hours of drug exposure were determined. In addition, anticancer activity shown (Fig. (B), (C)) that anticancer activity of Rubitecan-inclusion complex was improved than free Rubitecan and Rubitecan-loaded-liposomes in HCT 116 and KB cell Figure 11-13.



12. Marwa Mohamed, Eman Alaaeldin, Amal Hussein, Hatem A. Sarhan, Liposomes and PEGylated liposomes as drug delivery systems, *J. Adv. Biomed. & Pharm. Sci.* 3 (2020) 80- 88.
13. Mohammed Maher Mehanna, Nouran Abd El-Kader, Magda Wadih Samaha, Liposomes as potential carriers for ketorolac ophthalmic delivery: formulation and stability issues, *Braz. J. Pharm. Sci.* 2017; 53(2):e16127.
14. Yan Chen, Qingqing Wu, Zhenghai Zhang, Ling Yuan, Xuan Liu and Lei Zhou, Preparation of Curcumin-Loaded Liposomes and Evaluation of their Skin Permeation and Pharmacodynamics, *Molecules* 2012, 17, 5972-5987.
15. Abdulrahman K Al Asmari, Zabih Ullah, Mohammad Tariq, Amal Fatani, Preparation, characterization, and in vivo evaluation of intranasally administered liposomal formulation of donepezil, *Drug Design, Development and Therapy* 2016:10, 205–215.

Microwave irradiated green synthesis of novel isoxazole derivatives as anti-epileptic agent

Krishna Chandra Panda*, Bera Venkata Varaha Ravi Kumar and Biswa Mohan Sahoo

¹Roland Institute of Pharmaceutical Sciences, Berhampur-760010 affiliated to Biju Patnaik University of Technology (BPUT), Rourkela, Odisha.

*Corresponding author: krishnachandrapanda@gmail.com

Abstract

Green synthetic tools involve the design, synthesis and use of chemical substances by eliminating the generation of chemical hazards. This technique is advantageous in terms of atom economy, use of safer chemicals, energy efficient and decomposition of the waste materials to non-toxic substances which are eco-friendly. So, microwave irradiated heating method is applied for the generation of novel isoxazole derivatives. The structure of isoxazoles moiety contains three carbon atoms, one oxygen atom and one nitrogen atom in the five membered ring. Isoxazole scaffold exhibits diverse pharmacological activities such as anti-viral, anti-tubercular, anti-diabetic, anticancer, anthelmintic, antimicrobial, antifungal, antioxidant, anti-epileptic, antipsychotic etc. A series of novel isoxazole derivatives are synthesized under microwave irradiation. By the help of microwave, the rate of the reaction is enhanced which leads to high selectivity with better product yield as compared to the conventional heating methods. The titled compounds are evaluated for their antiepileptic activity by using maximal electroshock (MES) method. The screening results revealed that some of the compounds exhibited promising antiepileptic activity as compared to the standard drug.

Keywords: Microwave, Green, Synthesis, Epilepsy, Chemistry, Isoxazole, Evaluation

Introduction

Green synthetic protocol involves the utilization of set of principles that eliminates

the production of any hazardous substances during the design, manufacture and utilization of chemical substances(1). This method plays a major role to control the pollution of environment by using safer organic solvents, catalysts, suitable reaction conditions there by augments the atom economy and energy efficiency of the synthetic procedure(2). So, the microwave irradiated synthesis of organic compounds is considered a green protocol as it offers numerous benefits over conventional heating techniques(3). The synthesis of organic compounds under microwave irradiation mainly depends on the ability of the reaction medium to absorb microwave energy efficiently and also depends on the selection of organic solvents to complete the chemical synthesis(4,5). Hence, microwave induced synthesis is more advantageous in terms of uniform heating, homogeneity, increased rate of chemical reactions, improvement of product yield and cleaner reaction conditions(6).

Based on this concept, the isoxazole derivatives are synthesized *via* chalcones under microwave irradiated heating method to reduce the by-products formation so that the yield of the final product can be improved in lesser reaction time(7). Isoxazole moiety possess three carbon atoms, one oxygen atom and one nitrogen atom in five-membered ring system(8). Isoxazoles derivatives exhibits diverse biological activities such as antifungal, anti-viral, antimicrobial, anti-tubercular, anti-diabetic, anticancer, antioxidant, anti-epileptic, antipsychotic etc.(9-15).

Isoxazole scaffold forms the basis for different drug molecules such as leflunomide,

valdecoxib, zonisamide. Similarly, isoxazole derivatives such as sulfamethoxazole, sulfisoxazole and oxacillin are used clinically to treat a wide variety of bacterial infections. (Figure 2) (16-18).

Similarly, chalcone possess α,β -unsaturated carbonyl system that makes these molecules more pharmacologically active (Figure 3) (19-21).

Experimental Section

All the chemicals and reagents used to conduct experiments were of synthetic grade with high purity. The scientific microwave oven was used for the synthesis of isoxazole derivatives. The synthesis of the titled compounds was performed at power level-2 which corresponds to 210W [22-24]. The melting points of the synthesized compounds were determined in open capillary tubes and were observed to be uncorrected. TLC was monitored to check the completion of reaction condition. For TLC study, the solvents such chloroform and ethyl acetate (60: 40) was selected as mobile phase. The

sample spots were visualized under ultraviolet lamp. IR spectra of selected compounds was recorded with the help of FT-IR spectrometer (SHIMADZU) by using KBr. Similarly, the $^1\text{H-NMR}$ spectra was recorded on $^1\text{H-NMR}$ spectrometer (Brucker 400 MHz) by using DMSO as solvent and TMS as an internal standard. The synthetic route for the title compounds 4a-e was presented (Scheme1).

General Synthesis of Isoxazole Derivatives

Isoxazole derivatives were obtained from chalcone. First of all, chalcone (3a-e) were synthesized by Claisen-Schmidt condensation of 2-hydroxy acetophenone (0.01 mol) and substituted benzaldehydes (0.01 mol) in the presence of sodium hydroxide solution. TLC was monitored to confirm the completion of reaction. Further, the mixture of various chalcones (3a-e) (0.01 mol), hydroxylamine hydrochloride (0.01 mol) in ethanolic sodium hydroxide solution was refluxed under microwave irradiation at 210 W for 10-15 min. TLC was checked to determine the completion of reaction. After completion of the reaction, it was kept on ice bath to obtain solid product of isoxazole derivatives (4a-e).

Antiepileptic Activity

The newly synthesized isoxazole derivatives were evaluated for their

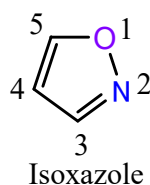


Figure 1. Structure and Nomenclature of Isoxazole Moiety

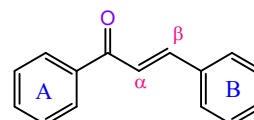


Figure 3. Structure and Nomenclature of Chalcone

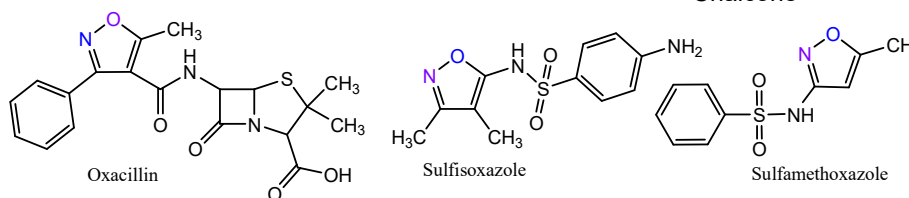
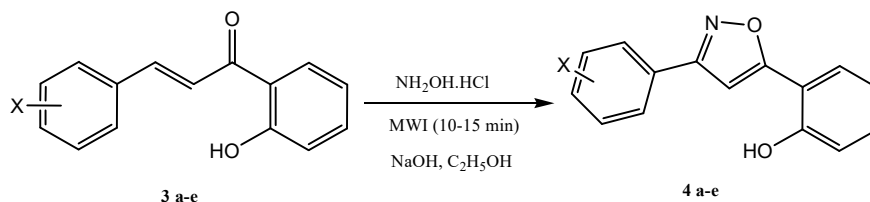


Figure 2. Medicinal Agents containing Isoxazole Pharmacophore

Green Synthesis



Scheme 1. Synthesis of isoxazole derivatives

Table 1. Antiepileptic Activity of Title Compounds 4(a-e)

Group	Treatment Group	Dose (mg/kg)	HLTE phase duration (sec)	Percentage Protection	Recovery/ Death
Group-I	Control	-	67	-	Death
Group-II	Standard	25	14	79	Recovered
Group-III	4a	300	26	61	Recovered
	4b	300	22	67	Recovered
	4c	300	24	64	Recovered
	4d	300	20	70	Recovered
	4e	300	21	68	Recovered

antiepileptic activity as per the protocols designed by the National Institute of Neurological Disorders and Stroke, NIH (USA). All the animal experiments performed were approved by Institutional Animal Ethics Committee (IAEC), India with protocol no. 926/PO/Re/S/06/ CPCSEA. The antiepileptic activity was performed by using the maximal electroshock (MES) method(25-27). For this study, the rats were selected randomly and each group contains six animals. Group-I was considered as control while Group-II was selected as standard. The remaining groups of animals were administered with all the test compounds with dose of 300 mg/kg. The standard drug (Phenytoin) was injected intraperitoneally 30 min before and the test compounds were administered orally 1h prior to induce the convulsion. Electro convulsive shock (150 mA for 0.2 sec) was given through the corneal electrode to induce convulsions to each group of rats. There are different phases of convulsion which include flexion, extension,

clonus and stupor. Prior to delivery, the current output was measured by a multimeter. After the occurrence of electric stimulation, the duration of different phases was determined and the HLTE (Hind limb tonic extension) phase was compared with the control group. A decrease in the duration of hind limb extension was considered as protective action (Table 1, Figure 4). In case of anti-epileptic activity, the percentage protection was calculated as follows.

$$\% \text{ Protection} = \frac{(\text{MEPD}_{nc} - \text{MEPD})}{\text{MEPD}_{nc}} \times 100$$

Where MEPD_{nc} is the mean extensor phase duration of normal control in sec., MEPD is the mean extensor phase duration of sample or standard in sec.

Results and Discussion

A new series of isoxazole derivatives (4a-e) was obtained *via* chalcones by

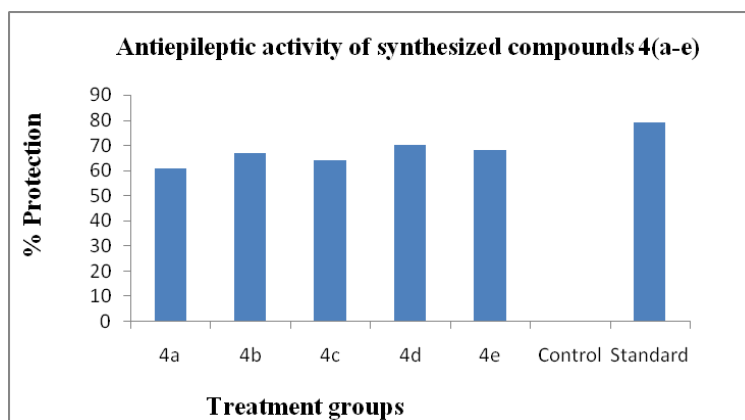


Fig 4. Percentage protection of title compounds

Table 2. Optimization Study of Reaction Time and Product Yield

Comp. Code	X	R _f	M.P (°C)	Conventional Synthesis		Microwave Synthesis	
				Reaction (min)	Yield	Reaction (min)	Yield
4a	H	0.54	148-150	60	64%	10	74%
4b	2-Cl	0.62	150-153	120	56%	12	68%
4c	4-Cl	0.63	155-157	90	63%	13	87%
4d	4-F	0.55	154-159	90	58%	12	65%
4e	4-OH	0.61	162-165	120	60%	10	75%

cyclization of chalcones (3a-e) in the presence of hydroxyl amine hydrochloride and ethanolic sodium hydroxide solution. By the help of microwave irradiation, the product yield was improved 65%-87% in short reaction time. The characteristic spectra of α,β unsaturated carbonyl (ketone) group of chalcone was observed near 1640-1650 cm^{-1} . Similarly, the absorption at λ_{max} for various groups are 3220-3300 cm^{-1} (-OH), 2924-3116 cm^{-1} (Ar-CH), 3029.39 cm^{-1} (aliphatic-C-H), 1630 cm^{-1} (C=N), 1735-1750 cm^{-1} (C=O, Ester), 1242-1258 cm^{-1} (-C-O-N Str), 1000-1360 cm^{-1} (-C-F), 600-800 cm^{-1} (-C-Cl) respectively. In the ^1H NMR spectrum, the aromatic protons were observed as multiplet at δ 6.86-8.56 and

singlet at δ 6.46 for -OH. The mass spectra of the chalcone and isoxazole derivative exhibited molecular ion peak corresponding to their molecular formula(29-30). The titled compounds were screened for their antiepileptic activity with concentration of 300 mg/ml and the results were compared with standard drug Phenytoin.

Conclusion

Isoxazole derivatives were synthesized by using both the conventional method and microwave irradiation technique to check the product yield. By the help microwave irradiation technique, the product yield was improved from 54% to 87% in a short period of time with

cleaner reaction conditions. Maximal electroshock method was used for evaluating the antiepileptic activity of the titled compounds. The screening results revealed the most of the compounds exhibited promising antiepileptic activity as compared to the standard drug. Further, it is required to focus on optimization study of biological activity in relation to the structural features of isoxazole derivatives to potentiate the development of the therapeutically active compounds.

Acknowledgement

The authors would like to thank Roland Institute of Pharmaceutical Sciences, Berhampur affiliated to Biju Patnaik University of Technology (BPUT), Rourkela, Odisha, India for providing the necessary facilities to carry out this research work.

References

1. Gupta, P., Mahajan, A. (2015). Green chemistry approaches as sustainable alternatives to conventional strategies in the pharmaceutical industry. *RSC Adv.*, 5, 26686-26705.
2. Clarke, C.J., Tu, W.-C.; Levers, O.; Brohl, A.; Hallett, J.P. (2018). Green and sustainable solvents in chemical processes. *Chem. Rev.*, 118, 747-800.
3. Sahoo, B.M. (2016). Microwave Assisted Drug Synthesis (MADS): A Green Technology in Medicinal Chemistry, *J. App. Pharm.* 8 (1), 1-2.
4. Mavandadi, F.; Lidstrom, P. Microwave assisted chemistry in drug discovery. (2004). *Curr Top Med Chem.*, 4, 773-792.
5. Sahoo, B.M.; Panda, J.; Banik, B.K. (2018). Thermal and non-thermal effects of microwaves in synthesis, *J. Ind. Chem. Soc.*, 95, 1311-1319.
6. Polshettiwar, V.; Nadagouda, M.N.; Varma, R.S. (2009). Microwave assisted chemistry: A rapid and sustainable route to synthesis of organics and nanomaterials. *Aust J. Chem.*, 62, 16-26.
7. Kapubalu, S.K.; Reddy, K.T.; Vamsikantha, A. (2011). Synthesis and characterization of some novel isoxazoles via chalcone intermediates. *Der Pharma Chemica*, 3(5), 113-122.
8. Ajay Kumar, K.; Jayarooma, P. (2013). Isoxazoles: Molecules with potential medicinal properties. *IJPCBS*, 3(2), 294-304.
9. Chikkula, K.V.; Raja, S. (2017). Isoxazole-A potent Pharmacophore. *Int. J. Pharm. Pharm. Sci.*, 9(7), 13-24.
10. Sahoo, B.M.; Sahoo, B.; Panda, J.; Kumar, A. (2017). Microwave-Induced Synthesis of Substituted Isoxazoles as Potential Antimicrobial Agents, *Curr. Microwave Chem.*, 4(2), 1-6.
11. Parikh, A.R.; Merja, B.C.; Joshi, A.M.; Parikh, K.A. (2004). Synthesis and biological evaluation of isoxazoline derivatives. *Ind. J. Chem.*, 43B, 955-9.
12. Lincy, J.; Mathew, G. (2016). Evaluation of *in vivo* and *in-vitro* anti-inflammatory activity of novel isoxazole series. *Eur. Int. J. Sci. Tech.*, 5, 35-42.
13. Sevim, R.; Sila, K.; Bedia, K.K.; Suna, O.T.; Julide, A. (2011). Synthesis and evaluation of cytotoxic activities of some substituted isoxazolone derivatives. *Marmara Pharm. J.*, 15, 94-9.
14. Renuka, S.; Kota, R.K. (2011). Medicinal and Biological Significance of Isoxazole A Highly Important Scaffold for Drug Discovery. *Asian J. of Res. in Chem.*, 4(7), 1038-1042.
15. Balaji, N.V.; HariBabu, B.; Rao, V.U.; Subbaraju, G.V.; Nagasree, K.P.; Kumar, M.M.K. (2019). Synthesis, screening and docking analysis of hispolonpyrazoles and isoxazoles as potential antitubercular agents. *Curr. Top. Med. Chem.* 19, 662-682.
16. Pradeep K.Y.; Ruthu, M.; Chetty, C.M.; Prasanthi, G.; Reddy, V.J. (2011).

- Pharmacological activities of isoxazole derivatives. *J. of Global Trends in Pharmac. Sci.*, 2(1), 55- 62.
17. Shaik, A.; Kishor, P.; Kancharlapalli, V. (2020). Synthesis of Novel and Potential Antimicrobial, Antioxidant and Anticancer Chalcones and Dihydropyrazoles Bearing Isoxazole Scaffold. *Proceedings*, 41(1), 1-12.
18. Hamama, W.S.; Ibrahim, M.E.; Zoorob, H.H. (2017). Synthesis and biological evaluation of some novel isoxazole derivatives. *J. Heterocyc. Chem.*, 54, 341-3.
19. Mahapatra, D.K.; Bharti, S.K.; Asati, V. (2017). Chalcone Derivatives: Anti-inflammatory Potential and Molecular Targets Perspectives. *Curr. Top. Med. Chem.* 17, 3146–3169.
20. Singh, S.; Sharma, P.K.; Verma, N.K.; Dudhe, R. (2011). A Review on aversatile molecule: Chalcone. *Asian J. Pharm. Biol. Res.*, 1(3), 412-418.
21. Sahu, N.K.; Balbhadra, S.S.; Choudhary, J.; Kohli, D.V. (2012). Exploring pharmacological significance of Chalcone scaffold: A Review. *Cur. Med. Chem.*, 19(2), 209.
22. Kapubalu, S.K.; Reddy, K.T.; Vamsikantha, A. (2011). Synthesis and characterization of some novel isoxazoles via chalcone intermediates. *Der Pharma Chemica*, 3(5), 113-122.
23. Lidstrom, P.; Tierney, J.; Wathey, B.; Westman, J. (2009). Microwave assisted organic synthesis-A Review. *Tetrahedron*, 57, 9225-9283.
24. Santagada, V.; Frecentese, F.; Perissutti, E.; Fiorino, F.; Severino, B.; Caliendo, G. (2009). Microwave assisted synthesis: A new technology in drug discovery. *Mini Rev Med Chem.*, 9, 340-358.
25. Vogel, H.G. (2006). Drug Discovery and Evaluation: Pharmacological Assays. 2nded. New York: Springer 25-28.
26. Rubio, C.; Rubio-Osornio, M.; Retana-Márquez, S.; VerónicaCustodio, M.L.; Paz, C. (2010). In vivo experimental models of epilepsy. *Cent. Nerv. Syst. Agents Med. Chem.*, 10, 298-309.
27. Porter, R.J. (1983). Antiepileptic drug development program. *Prog. Clin. Biol. Res.*, 127, 53–66.
28. Dunham, M.S.; Miya, T.A. (1957). A note on a simple apparatus for detecting neurological deficit in rats and mice. *J. Am. Pharmac. Assoc. Sci Edit.*, 46(3), 208-209.
29. Khobare, R.; Pawar, R.P.; Warad, K.D.; Tayade, A.; Mane, C.B. (2020). An Efficient Synthesis of Substituted Isoxazole derivatives using ultra Sound Sonication Method. *Eur. J. of Mol. & Clin. Med.*, 7(7), 319-325.
30. Hushare, V.J.; Rajput, P.R. (2012). Synthesis, characterization and antimicrobial activity of some novel isoxazoles. *Rasayan J. Chem.*, 5(1), 121-126.
31. Goel, A.; Madan, A.K. (1997). Structure-activity study of antiepileptic N-aryl-isoxazolecarboxamides/N-isoxazolylbenzamide analogs using Wiener's topological index. *Struct Chem.*, 8, 155-159.
32. Barmade, M.A.; Murumkar, P.R.; Sharma, M.K.; Yadav, M.R. (2018). Medicinal Chemistry Perspective of Fused Isoxazole derivatives. *Curr. Topics in Med. Chemx* 16, 2863.
33. Zimmermann, L.A.; de Moraes M.H.; da Rosa R.; de Melo E.B.; Paula, F.R.; Schenkel, E.P.; Steindel, M.; Bernardes, L.S.C. (2018). Synthesis and SAR of new isoxazole-triazolebis-heterocyclic compounds as analogues of natural lignans with antiparasitic activity. *Bioorg Med Chem.*, 26(17), 4850-4862.

RP-HPLC Method Development and Validation for Simultaneous Determination of Decitabine and Cedazuridine in Pure and Tablet Dosage Form

Alimunnisa and Lakshmana Rao A*

Department of Pharmaceutical Analysis, V. V. Institute of Pharmaceutical Sciences, Gudlavalleru, Andhra Pradesh, India.

*Corresponding author: dralrao@gmail.com

Abstract

A simple, rapid, accurate and precise isocratic reversed phase high performance liquid chromatographic method has been developed and validated for simultaneous estimation of Decitabine and Cedazuridine in tablet dosage form. The chromatographic separation was carried out on Zorbax C18 column (150 mm x 4.6 mm I.D., 5 μ m particle size) with a mixture of 0.01N potassium dihydrogen phosphate buffer and acetonitrile in the ratio of 65:35% v/v as a mobile phase at a flow rate of 1.0 mL/min. UV detection was performed at 245 nm. The retention times were 2.263 minutes and 3.001 minutes for Decitabine and Cedazuridine respectively. Calibration plots were linear ($r^2=0.999$ for both Decitabine and Cedazuridine respectively) over the concentration range of 8.75-52.5 μ g/mL for Decitabine and 25-150 μ g/mL for Cedazuridine. The method was validated for linearity, precision, accuracy, ruggedness and robustness. The proposed method was successfully used for simultaneous estimation of Decitabine and Cedazuridine in tablet dosage form. Validation studies revealed that the proposed method is specific, rapid, reliable and reproducible. The high % recovery and low % RSD confirms the suitability of the proposed method for routine quality control analysis of Decitabine and Cedazuridine in bulk and tablet dosage form.

Keywords: Decitabine, Cedazuridine, Validation, HPLC.

Introduction

Decitabine is indicated for the treatment of patients with myelodysplastic syndromes (MDS) including refractory anaemia, refractory anaemia with ringed sideroblasts, refractory anaemia with excess blasts, refractory anaemia with excess blasts in transformation and chronic myelomonocyticleukaemia (1). Chemically it is, 4-amino-1-[(2R,4S,5R)-4-hydroxy-5-(hydroxymethyl)oxolan-2-yl]-1,2-dihydro-1,3,5-triazin-2-one (2) (Fig. 1). It acts as nucleoside metabolic inhibitor, Decitabine is recognized as a substrate by DNA methyl transferase enzymes (DNMTs). This mode of action depletes DNMTs and results in global DNA hypomethylation (3).

Cedazuridine is acytidine deaminase inhibitor co-administered with the hypomethylating agent. Decitabine is indicated for the treatment of variable forms of myelodysplastic syndrome (MDS) (4). Chemically it is, (4R)-1-[(2R,4R,5R)-3,3-difluoro-4-hydroxy-5-(hydroxymethyl)oxolan-2-yl]-4-hydroxy-1,3-diazinan-2-one (Fig.2). It acts as DNA methyltransferase (DNMT) inhibitor

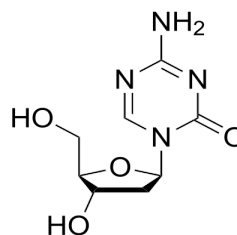


Fig 1. Chemical structure of decitabine

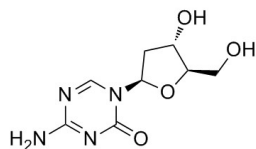


Fig 2. Chemical structure of cedazuridine

which is co-administered with hypomethylating agents like Decitabine. Cedazuridine inhibits major mechanism by which Decitabine is degraded in the gut and liver, and the combination therefore permits the efficient delivery of Decitabine orally (5).

Literature survey reveals that there is only one HPLC method was reported for simultaneous estimation of Decitabine and Cedazuridine in pharmaceutical formulations (6). Therefore, an attempt has been made to develop a novel, rapid, accurate and precise RP-HPLC method for simultaneous estimation of Decitabine and Cedazuridine in tablet dosage form and validated in accordance with ICH guidelines (7).

Materials and Methods

Instrumentation: To develop a high-performance liquid chromatographic method for simultaneous estimation of Decitabine and Cedazuridine using Waters 2695 HPLC system on Zorbax C18 (150 mm x 4.6 mm I.D., 5 μ m particle size) column was used. The instrument is equipped with UV-Visible detector. Data was analysed by using Empower 2 software. A Eutech pHmeter was used for pH measurements.

Chemicals and solvents: The marketed formulation of Decitabine and Cedazuridine tablets (Decitabine of 35mg and Cedazuridine of 100mg) were procured from local market. HPLC grade water and acetonitrile were purchased from Rankem Ltd., India. Methanol and potassium dihydrogen phosphate of AR grade was obtained from Rankem Ltd., India.

Determination of working wavelength (λ_{max}): In simultaneous estimation of two drugs isobestic wavelength was used. Isobestic point is the wavelength where the molar absorptivity is the same for two substances that are inter convertible. So this wavelength was used in simultaneous estimation to estimate two drugs accurately. The wavelength of maximum absorption of the solution of the drugs in mixture of 0.01N KH_2PO_4 buffer and acetonitrile (65:35% v/v) were scanned using PDA detector within the wavelength region of 200-400 nm against 0.01N KH_2PO_4 buffer and acetonitrile (65:35% v/v) as blank. The absorption curve shows isobestic point at 265 nm. Thus 265 nm was selected as detector wavelength for the HPLC chromatographic method.

Chromatographic conditions: 0.01N Potassium dihydrogen phosphate buffer and acetonitrile in the ratio of 65:35% v/v was found to be the most suitable mobile phase for ideal chromatographic separation for simultaneous estimation of Decitabine and Cedazuridine. The solvent mixture was filtered through 0.45 μ m membrane filter and sonicated before use. It was pumped through the column at a flow rate of 1.0 mL/min. Injection volume was 10 μ L and the column was maintained at a temperature of 25°C. The column was equilibrated by pumping the mobile phase through the column for at least 30 minutes prior to the injection of the drug solution. The detection of the drug was monitored at 245 nm. The run time was set as 5 minutes.

Preparation of standard stock solution: Accurately weighed 17.5 mg of Decitabine, 50 mg of Cedazuridine and transferred to 50 mL volumetric flask separately. 3/4th of diluents was added to both of these flasks and sonicated for 10 minutes. Flasks were made up with diluents and labelled as standard stock solution 1 and 2. (350 μ g/mL of Decitabine and 1000 μ g/mL of Cedazuridine).

Sample solution preparation: 5 tablets were weighed and the average weight of each tablet was calculated, then the weight

equivalent to 1 tablet was transferred into a 100 mL volumetric flask, 50 mL of diluents was added and sonicated for 25 min, further the volume was made up with diluent and filtered by HPLC filters (350 µg/mL of Decitabine and 1000 µg/mL of Cedazuridine). 1 mL of filtered sample stock solution was transferred to 10 mL volumetric flask and made up with diluent. (35 µg/mL of Decitabine and 100 µg/mL of Cedazuridine).

General Preparations:

0.01N KH_2PO_4 buffer: Accurately weighed 1.36 gm of potassium dihydrogen ortho phosphate in a 1000 mL of volumetric flask add about 900 mL of milli-Q water added and degas to sonicate and finally make up the volume with water then pH adjusted to 5.4 with dil. ortho phosphoric acid solution.

0.1%OPA buffer: 1 mL of ortho phosphoric acid was diluted to 1000 mL with HPLC grade water.

Preparation of mobile phase: Mobile phase was prepared by mixing 0.01N KH_2PO_4 buffer and acetonitrile taken in the ratio 65:35% v/v. It was filtered through 0.45 µ membrane filter to remove the impurities which may interfere in the final chromatogram.

Preparation of diluent: Based up on the solubility of the drugs, diluent was selected, acetonitrile and watertaken in the ratio of 50:50% v/v.

Assay: Inject 10 µL of the standard, sample into the chromatographic system and measure the areas for Decitabine and Cedazuridine peaks and calculate the % Assay.

Method Validation

System suitability: System suitability is checked by using standard chemical substance to ensure that the analytical system is working properly. In this peak area and % of drug of six determinations is measured and %RSD should be calculated.

Specificity: Specificity of an analytical method is ability to measure specifically the analyte of interest without interference from blank and known impurities. For this purpose blank chromatogram, standard chromatogram and sample chromatogram were recorded. The chromatogram of blank shows no response at the retention times of drugs which confirms the response of drugs was specific.

Linearity: The linearity of the method was obtained by preparation of the calibration standards of six different concentrations in 6 replicates. The calibration curve plots for Decitabine and Cedazuridine were obtained by plotting the peaks areas on y-axis and concentrations on x-axis over the concentration ranges of 8.75-52.5 µg/mL for Decitabine and 25-150 µg/mL for Cedazuridine. The correlation coefficient should be greater than 0.99.

Range: The range of an analytical method is the interval between the upper and lower levels of analyte (including these levels) that have been demonstrated with precision, accuracy and linearity.

Accuracy: The accuracy of the method was assessed by recovery experiments by adding a known quantity of pure standard drug into the sample solution and recovering the same in terms of its peak areas. The sample was spiked with standard at levels of 50%, 100% and 150% of test concentrations. The resultant spiked sample was assayed in triplicate.

Precision: Precision is the degree of repeatability of an analytical method under normal operation conditions. Precision is of 3types,

1. System precision
2. Method precision
3. Intermediate precision (a. intra-day precision, b. Inter-day precision)

System precision is checked by using standard chemical substance to ensure that the analytical system is working properly. In

this peak area and % of drug of six determinations is measured and %RSD should be calculated. In method precision, a homogenous sample of single batch should be analyzed 6 times. This indicates whether a method is giving constant results for a single batch. In this analyze the sample six times and calculate the %RSD. The precision of the instrument was checked by repeatedly injecting (n=6) solutions of 35 µg/mL of Decitabine and 100 µg/mL of Cedazuridine.

Robustness: As part of the Robustness, deliberate change in the flowrate, mobile phase composition, temperature variation was made to evaluate the impact on the method.

A. The variation of flow rate: Standard solution 35 µg/mL of Decitabine and 100 µg/mL of Cedazuridine was prepared and analyzed using the varied flow rates 0.9 mL/min & 1.1 mL/min flow rate instead of 1.0 mL/min, remaining conditions are kept constant. On evaluation of the above results, it can be concluded that the variation in flow rate affected the method significantly. Hence it indicates that the method is robust even by change in the flow rate $\pm 20\%$.

B. The variation of organic phase ratio: Standard solution of 35 µg/mL of Decitabine and 100 µg/mL of Cedazuridine was prepared and analyzed using the varied in mobile phase ratio.

C. The variation of temperature: Temperature minus (25°C) and temperature plus (35°C) were maintained and samples were injected in duplicate manner system.

LOD Sample preparation: 0.25 mL each from two standard stock solutions was pipetted out and transferred to two separate 10 mL volumetric flasks and made up with diluents. From the above solutions 0.1 mL each of Decitabine and Cedazuridine solutions respectively were transferred to 10 mL volumetric flasks and made up with the same diluents.

LOQ Sample preparation: 0.25 mL each from two standard stock solutions was pipetted out and transferred to two separate 10 mL volumetric flask and made up with diluent. From the above solutions 0.3 mL each of Decitabine and Cedazuridine, solutions respectively were transferred to 10 mL volumetric flasks and made up with the same diluent.

Forced Degradation Studies

Decitabine and Cedazuridine standard samples were subjected to degradation under different stress conditions like acidic, alkali, oxidative, thermal, photo stability and neutral conditions. For acidic & alkali degradation samples were refluxed with 2N HCl & 2N NaOH at 60°C for 30 min. For oxidative degradation 20% v/v, H₂O₂ was used and the same was refluxed at 60°C for 30 min. For thermal degradation, sample was placed in oven at 105°C for 1 hr; and for photo stability degradation, drug was exposed to UV light by keeping the sample in UV chamber for 7 days or 00 watt hours/m² in photo stability chamber; for neutral degradation, the drugs were refluxed in water for 1 hours at a temperature of 60°C. All the samples were diluted to obtain a final concentration of 35 µg/mL of Decitabine & 100 µg/mL of Cedazuridine. Ten micro liters of the samples were injected into the system and the chromatograms were recorded to assess the stability of the sample.

Results and Discussion

The HPLC procedure was optimized with a view to develop an accurate, precise and reproducible method for simultaneous estimation of Decitabine and Cedazuridine in tablet dosage form using Zorbax C18 column (150 mm x 4.6 mm; 5 µm) in isocratic mode with mobile phase composition of 0.01N potassium dihydrogen phosphate buffer and acetonitrile in the ratio 65:35% v/v. The use of 0.01N phosphate buffer and acetonitrile in the ratio of 65:35% v/v

resulted in peak with maximum separation, good shape and resolution. Flow rates between 0.9 to 1.1 mL/min were studied. A flow rate of 1.0 mL/min gave an optimum signal-to-noise ratio with reasonable separation time, the retention times for Decitabine and Cedazuridine were found to be 2.263 minutes and 3.001 minutes respectively. Total run time was 5 minutes. The drug components were measured with UV detector at 245 nm. The results of optimized chromatographic conditions were shown in Table 1.

Linearity was obtained in the range of 8.75-52.5 µg/mL for Decitabine and 25-150 µg/mL for Cedazuridine. The correlation coefficient (r^2) was found to be 0.999 for both Decitabine and Cedazuridine respectively. The regression equation of the linearity plot of concentration of Decitabine over its peak area was found to be $y=37806x+10196$, where x is the concentration of Decitabine (µg/mL) and y is the corresponding peak area. The regression equation of the linearity plot of concentration of Cedazuridine over its peak area was found to be $y=31736x+21050$, where x is the concentration of Cedazuridine (µg/mL) and y is the corresponding peak area. The results show that an excellent correlation exists between peak area and concentration of

drugs within the concentration range indicated. The linearity results were shown in Table 2.

The % RSD for intra-day precision and inter-day precision for Decitabine were found to be 0.6% and 1.0% respectively (limit % RSD<2.0%). The % RSD for intra-day precision and inter-day precision for Cedazuridine were found to be 0.7% and 1.0% respectively (limit % RSD<2.0%) and hence the method is precise. The precision data of Decitabine and Cedazuridine were furnished in Table 3 & Table 4.

The % recovery of the drugs Decitabine and Cedazuridine were found to be 99.71 to 100.17% and 99.91 to 100.50% respectively and the high percentage of recovery of Decitabine and Cedazuridine indicates that the proposed method is highly accurate. The results of accuracy studies of Decitabine and Cedazuridine were shown in Table 5 & Table 6.

The retention times for the drugs Decitabine and Cedazuridine was 2.263 minutes and 3.001 minutes respectively. The number of theoretical plates calculated for Decitabine and Cedazuridine was 6633 and 11974 respectively. The tailing factor for Decitabine and Cedazuridine was 1.52 and 1.305 respectively, which indicates efficient

Table 1. Optimized chromatographic conditions

S. No.	Parameters	Conditions
1	Instrument used	Waters HPLC 2695 System
2	software	Empower 2.0 version
3	Injection volume	10 µL
4	Mobile Phase	0.01N KH ₂ PO ₄ Acetonitrile (65:35% V/V)
5	Column	Zorbax C 18 (150 mm x 4.6 mm, 5 µm)
6	Detection Wavelength	245 nm
7	Flowrate	1 mL/min
8	Runtime	5 min
9	Temperature	Ambient (25°C)
10	Diluent	Water and Acetonitrile (50:50% V/V)

performance of the column. The limit of detection (LOD) and limit of quantification (LOQ) for Decitabine were found to be 0.58 µg/mL and 1.92 µg/mL; 0.99 µg/mL and 3.01

µg/mL for Cedazuridine respectively, which indicate the sensitivity of the method. The summary of system suitability parameters and validation parameters were shown in Table 7.

Table 2. Results of linearity for decitabine and cedazuridine

S. No.	Decitabine		Cedazuridine	
	Conc. (µg/mL)	Peak area	Conc. (µg/mL)	Peak area
1	0	0	0	0
2	8.75	338918	25	809643
3	17.5	668059	50	1614417
4	26.25	1010116	75	2409485
5	35	1362686	100	3225114
6	43.75	1669573	125	4026519
7	52.5	1968823	150	4723591
Regression Equation	$y = 37806x + 10196$		$y = 31736x + 21050$	
Slope	37806		31736	
Intercept	10196		21050	
R2	0.999		0.999	

Table 3. Intra-day precision for decitabine and cedazuridine

S. No.	Area for Decitabine	Area for Cedazuridine
1	1338456	3118026
2	1354590	3155597
3	1352438	3180969
4	1333754	3169152
5	1336688	3163536
6	1342507	3178497
Average	1343072	3160963
S.D	8597.6	23038.0
%RSD	0.6	0.7

The robustness studies indicated that no considerable effect on the determination of the drugs. Therefore, the test method is robust for the quantification of the drugs. In all deliberately varied conditions, the %RSD for replicate injections of Decitabine and

Cedazuridine were found to be within the acceptable limits.

Validated method was applied for the simultaneous estimation of Decitabine and Cedazuridine in commercial tablet dosage

forms. The % Assay of Decitabine and Cedazuridine were found to be 101.60% and 100.54% respectively. The results for the drugs assay showed good agreement with label claims. No interfering peaks were found

in the chromatogram of the tablet formulation within the run time indicating that excipients used in tablet formulation did not interfere with the simultaneous estimation of the drugs Decitabine and Cedazuridine by the proposed

Table 4. Inter-day precision for decitabine and cedazuridine

Day	Aea for Decitabine	Area for Cedazuridine
1	1310462	3123728
2	1314676	3094017
3	1305798	3154633
4	1338991	3082297
5	1314841	3128306
6	1332908	3076085
Average	1319613	3109844
SD	13221.2	30622.4
%RSD	1.0	1.0

Table 5. Accuracy results of decitabine

% Concentration (at specification level)	Amount Added (µg)	Amount Found (µg)	% Recovery	Mean Recovery
50%	17.5	17.52	100.14	100.01%
100%	35	34.89	99.71	
150%	52.5	52.59	100.17	

Table 6. Accuracy results of cedazuridine

% Concentration (at specification level)	Amount Added (µg)	Amount Found (µg)	% Recovery	Mean Recovery
50%	50	49.95	99.91	100.29%
100%	100.0	100.38	100.38	
150%	150.0	150.87	100.50	

Table 7. System suitability parameters for decitabine and cedazuridine

S. No.	Parameter	Decitabine	Cedazuridine
1	Retention time (min)	2.252	2.979
2	Plate count	6633	11974
3	Tailing factor	1.52	1.305
4	Resolution	----	6.317
5	%RSD	0.9	0.5

Table 8. Assay of decitabine and cedazuridine

S. No.	Assay of Decitabine			Assay of Cedazuridine		
	Standard Area	Sample Area	% Assay	Standard Area	Sample Area	% Assay
1	1331358	1338456	101.25	3160242	3118026	99.17
2	1331197	1354590	102.47	3144319	3155597	100.36
3	1330607	1352438	102.30	3151862	3180969	101.17
4	1307769	1333754	100.89	3140695	3169152	100.80
5	1312164	1336688	101.11	3129029	3163536	100.62
6	1310781	1342507	101.55	3119742	3178497	101.09
Avg	1320646	1343072	101.60	3140982	3160963	100.54
SD	11492.4	8597.6	0.6504	14795.6	23038.0	0.7327
%RSD	0.9	0.6	0.6	0.5	0.7	0.7

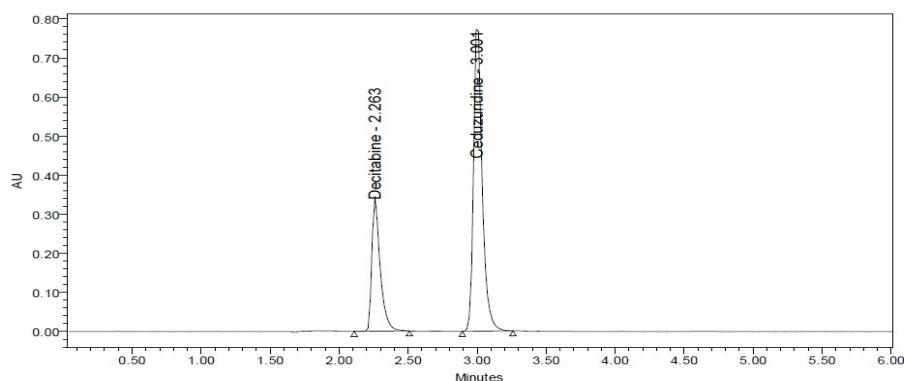


Fig 3. Optimized chromatogram of decitabine and cedazuridine

HPLC method. The assay results are shown in Table 8.

The chromatograms were checked for appearance of any extra peaks under optimized conditions, showing no interference from common tablet excipients and impurities. Also the peak areas were compared with standard and were found to be within limits. As shown in chromatogram, two analytes are eluted by forming symmetrical peaks. The typical chromatogram of Decitabine and Cedazuridine standard were shown in Fig. 3.

Conclusion

The developed RP-HPLC method for the estimation of selected drugs is simple, rapid, accurate, precise, robust and economical. The mobile phase and solvents are simple to prepare and economical, reliable, sensitive and less time consuming. The sample recoveries were in good agreement with their respective label claims and they suggested non-interference of formulation recipients in the estimation and can be used in laboratories for the routine analysis of selected drugs. The present work concluded that stability

indicating assay method by RP-HPLC was simple, accurate, precise, and specific and has no interference with the placebo and degradation products. Hence these can be used for routine analysis of Decitabine and Cedazuridine.

Conflict of interest

The authors declare that no conflict of interest.

References

1. Jabbar E and Issa JP. Evolution of Decitabine. *American Cancer Society Journal*. 2008; 112(11): 2341-2351.
2. IUPAC. Compendium of Chemical Terminology, 2nd edn. (The Gold Book). PAC69. Glossary of terms used in computational drug design (IUPAC Recommendations). 1997; 1137.
3. Metin K and Richard LM. Pharmacokinetic and Pharmacodynamic Analysis of Decitabine in the Design of its Dose-schedule for Cancer Therapy. *Clinical Epigenetics Journal*. 2013; 5(1): 1-16.
4. Sohita D. Decitabine/Cedazuridine: First Approval. *Springer Link*. 2021; 8(1): 1373-1378.
5. Patel AP and Cahill K. Cedazuridine/Decitabine: From Pre-Clinical to Clinical Development in Myeloid Malignancies. *Journal of Blood Advances*. 2021; 5(8): 2264-2271.
6. Ishaq BM and Reddy LSS. RP-HPLC-PDA Method Development, Validation and Stability Studies of the Novel Antineoplastic Drug Combination-Decitabine and Cedazuridine. *Journal of Pharmaceutical Research International*. 2020; 32(32): 10-16.
7. ICH Harmonized Tripartite Guideline: Text on Validation of Analytical Procedures, Text and Methodology, Q2(R1), International Conference on Harmonization, Geneva 2005; 1-17.

Development and evaluation of capecitabine loaded human serum albumin nanoparticles for breast cancer

J. Josephine Leno Jenita*, A. R. Mahesh, B. P. Sudarshan, Seema S Rathore and Shanaz Banu

¹Department of Pharmaceutics, College of Pharmaceutical Sciences, Dayananda Sagar University, Bangalore- 560078, Karnataka

²Faculty of Pharmacy, MS Ramaiah University of Applied Sciences, Bengaluru-560070, Karnataka

³Department of Pharmacognosy, College of Pharmaceutical Sciences, Dayananda Sagar University, Bangalore- 560078, Karnataka

*Corresponding Author: jenita79@gmail.com

Abstract

Capecitabine is an orally-administered chemotherapeutic agent used in the treatment of metastatic breast and colorectal cancers. Albumin nanoparticles indicated high drug loading capacity in a composite with biodegradability and biocompatibility. The aim of the present study is to develop capecitabine loaded albumin nanoparticles and their evaluation. Capecitabine loaded albumin nanoparticles were prepared by desolvation method. The prepared nanoparticles were characterised for mean particle size, zeta potential, and drug loading capacity. The process yields and drug loading ranged between 66%w/w to 84.6%w/w and 5.06%w/w to 15.36%w/w respectively. The mean particle size of nanoparticle size of various batches F1 to F4 were found to be 151.18nm, 134.9nm, 178.8nm, and 151.3nm respectively. The zeta potential of the batch F2 was found to be -21.1mV. The drug release was ranged from 32.75% to 51.2% for 24h depending on drug polymer ratio. The *in vitro* release studies showed a biphasic release pattern with an initial burst effect followed by sustained release. Release kinetic model revealed that the mechanism of drug release from human serum albumin nanoparticles followed Fickian model.

Keywords: Capecitabine, Human Serum Albumin, desolvation method.

Introduction

Capecitabine is a potentially effective anticancer drug which can be administered orally. It is a prodrug of fluorouracil (1). The fluorinated analogue of uracil was first synthesized in 1957. Fluorouracil is used as a chemotherapeutic agent against various types of solid tumours those of the head and neck, prostate, breast, liver, pancreas, and genitourinary and gastrointestinal tracts (2). Capecitabine itself is not an active drug. It is converted to activated 5-fluorouracil through a series of enzymatic steps. Selective conversion of its final metabolite 50-deoxy-5-fluorouridine to 5-Fluorouracil takes place within the human cancer cells and in healthy liver tissue also. The adverse effects associated with capecitabine include cardiotoxicity, bone-marrow depression, nausea and vomiting, stomatitis, diarrhoea, dermatitis, etc... Both the inclusion of the drug into replicating RNA and depletion of thymidine causes cytotoxicity (3). In order to reduce its toxicity and to enhance its bioavailability Capecitabine can be formulated to various formulations like extended-release tablets, controlled release tablets, microspheres, nanoparticles etc. (4) Capecitabine can be formulated as a controlled release dosage form which may provide greater *in vitro* and *in vivo* antitumor activity, and thus reduces its toxic side effects. The controlled release can be achieved using various biocompatible polymers (5).

The adverse effects associated with capecitabine include cardiotoxicity, bone-marrow depression, nausea and vomiting, stomatitis, diarrhoea, dermatitis, etc. Both the inclusion of the drug into replicating RNA and depletion of thymidine causes cytotoxicity (6). In order to reduce its toxicity and to enhance its bioavailability Capecitabine can be formulated to various formulations like extended-release tablets, controlled release tablets, microspheres, nanoparticles etc. (7) Capecitabine can be formulated as a controlled release dosage form which may provide greater *in vitro* and *in vivo* antitumor activity, and thus reduces its toxic side effects. The controlled release can be achieved using various biocompatible polymers (8).

Capecitabine oral administration simplifies care and hence it is increasingly used for off-label indication including monotherapy in the advanced or metastatic cancers, combination therapy in conjunction with other drugs in the advanced or metastatic cancers, and with radiation therapy for the neoadjuvant treatment of rectal cancer (9). Capecitabine offers the patients more freedom from hospital visits as it can be taken by own and have less inconvenience.(10) Its toxicity profile is manageable, but it requires a strong recognition and prompt intervention by the clinicians (11).

Nanoparticles are defined as particulate dispersions or solid particles with a size in the range of 10-1000nm (12). The drug dissolved, entrapped, encapsulated or attached to nanoparticle matrix. Nanoparticles have been shown to increase bioavailability, decrease side effects of highly toxic drugs, and prolong drug release (13). The drug accumulation in cells is particle size dependent with an increasing effect for smaller particle size and highest efficiency for the nanoparticles of around 100 nm. Appropriate surface modification of NPs enhances their localisation and specific accumulation in cancer cells (14).

Materials and Methods

Materials

Capecitabine was a kind gift from Shilpa Medicare Ltd. Raichur (India); Human

serum albumin and Glutaraldehyde were purchased from SD Fine Chemical Ltd, Mumbai, India; Ethanol was supplied by Shri Maruti enterprises Pvt. Ltd. Mumbai; and all other chemicals were used of analytical grade.

Method

Preparation of Capecitabine Loaded Albumin Nanoparticles

The desolvation method was used for the preparation of capecitabine loaded human serum albumin nanoparticles (15). 10mM NaCl solution was taken and accurately weighed quantity of human serum albumin and the drug capecitabine was dissolved in this solution. Using 1M NaOH solution pH was adjusted to 7 to 8. Ethanol was added at a rate of 1ml/min dropwise to the drug polymer solution under magnetic stirring at the speed of 500 rpm until the turbidity appears. After 30 min 25 μ l of 4% v/v of glutaraldehyde was added as a cross linking agent to this turbid solution and stirred continuously for 8h at room temperature. The nanosuspensions were purified by centrifugation at 10,000 rpm for 10min. The settled down nanoparticle mass was subjected to freeze drying. The dried nanoparticles were then stored in vials at 4°C.

Characterisation of Capecitabine Loaded Albumin Nanoparticles

Drug - Polymer Compatibility Study

Any possible interaction between drug capecitabine and polymer human serum albumin were determined by drug polymer compatibility studies. Required amount of sample was taken in a mortar and gently triturated. The physical mixture of drug capecitabine and polymer human serum albumin is taken as sample. A little quantity of this sample mixture was taken and placed in a sample holder and scanned at 4000 cm^{-1} to 400 cm^{-1} in Bruker alpha 2 analyzer. This study was carried out for drug, polymer and physical mixture of drug and polymer and also for nanoparticles. The spectra obtained were

compared and interpreted for functional group peaks.

The physical state of capecitabine in the nanoparticles was analysed by differential scanning calorimeter (DSC). The thermogram of the drug and nanoparticles gives information regarding the physical properties and melting point of the drug.

Determination of % Process Yield

To determine % process yield of capecitabine loaded albumin nanoparticles the final dried nanoparticles were weighed and the yield was calculated with respect to initial weight of capecitabine and human serum albumin used for preparation of nanoparticles (16).

$$\text{Process Yield (\%)} = \frac{\text{Practical Yield}}{\text{Theoretical Yield}} \times 100$$

Determination of % Drug Loading

The % drug loading was determined by completely extracting the capecitabine from known weight of capecitabine loaded albumin nanoparticles in pH 7.4 phosphate buffer. Weighed quantity of nanoparticles were taken from each batch and the drug was completely extracted using pH 7.4 phosphate buffer. The drug concentration was determined by using a UV spectrophotometer (Shimadzu 160A, Japan) at a wavelength of 295nm against blank and % drug loading was calculated using the formula.

$$\% \text{ Drug Loading} = \frac{\text{Actual drug content}}{\text{Weight of NPs taken}} \times 100$$

Determination of Particle Size Distribution and Zeta Potential

The nanoparticles size and polydispersity were determined by Malvern zetasizer (17). It is the routine method to determine the mean hydrodynamic diameter and the particle size distribution of

nanoparticles. The dynamic light scattering measurement were done at 25°C with an angle detection of 90° and 173°. The zeta potential of nanoparticles was measured from the mobility of the electrons of nanoparticles using laser doppler electrophoresis via Malvern zetasizer. The measurement was carried out at 25°C in a carbon electrode cell.

Determination of Surface Morphology

The Transmission electron microscope (TEM) is a type of electron microscope that gives images of the sample surface by scanning it with a high-energy beam of electrons in a raster scan pattern. Transmission electron microscopy was performed to characterize the surface morphology of the formed nanoparticles at 20 kV. Prior to examination, samples were gold-coated to render them electrically conductive and then examined under the microscope.

Determination of In Vitro Drug Release Studies

The *in vitro* release studies of capecitabine loaded albumin nanoparticles were performed using dialysis membrane method (18). The prepared nanoparticles equivalent to 5mg of drug were placed in a dialysis membrane and 5ml of pH 7.4 phosphate buffer. The membrane was knotted at both ends and immersed in 50mL of pH 7.4 phosphate buffer, ensuring that it was thoroughly immersed in the dissolution fluid. It was stirred at 100rpm at 37 °C temperature and the receptor compartment was closed to prevent dissolution media from evaporating. At predetermined time intervals 5ml of the dissolution medium was withdrawn by replacing fresh dissolution medium. The amount of capecitabine released was determined by measuring the absorbance at 295 nm using UV- Visible spectrophotometer.

Determination of Release Kinetics

Release kinetics studies was carried out to understand the mechanism behind the

release and to figure out the best fit plot with the kinetic model (19). The data obtained from the *in vitro* release studies were fitted to various kinetic model such as Zero order, First order, Higuchi model and Korsmeyer-Peppas model.

Results and Discussion

The drug capecitabine was subjected to various preformulation studies namely solubility, melting point and drug-polymer compatibility. The solubility of capecitabine in 10 mg/10 ml of solvent was carried out and it reveals that it is soluble in water, phosphate buffer pH7.4 and sparingly soluble in ethanol. The melting point of capecitabine was found to be 113°C and it was within the range, which supports the drug to formulate into nanoparticles.

Drug - Polymer Compatibility Study

Drug-polymer interaction was studied using FT-IR analysis and it showed that there

were no changes in the IR spectra of pure drug capecitabine in presence of albumin. Figure 1 which showed that the polymer did not alter the performance characteristics of drug, thus revealing compatibility of the selected drug with the polymer.

Preparation of Nanoparticles

The preparation of capecitabine loaded HSA nanoparticles was performed by desolvation method using ethanol as a desolvating agent. Four different batches were prepared by varying the concentration of the polymer HSA and keeping the drug concentration constant Table 1.

The % process yield for capecitabine loaded HSA nanoparticles was in the range 66%w/w to 84.6%w/w depending on the drug polymer ratio. Due to the presence of many binding sites in their molecules, protein nanoparticles have a high drug loading capacity. Covalent bonding, electrostatic

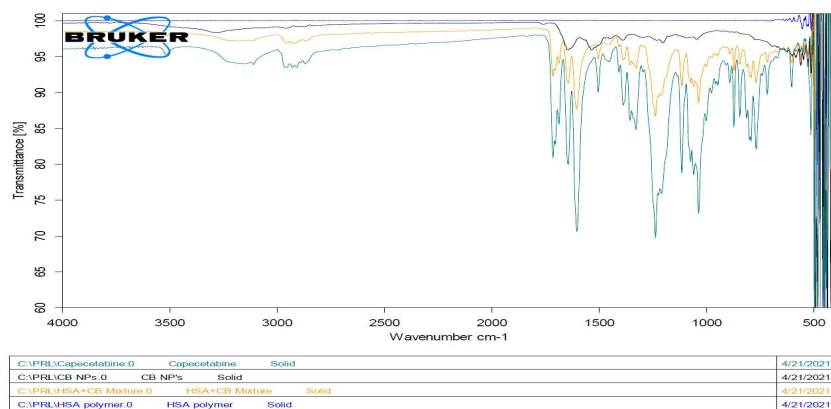


Fig 1. FT-IR Spectrum of drug, polymer, Drug-polymer mixture and nanoparticles

Table 1. Formula for Preparation Capecitabine Loaded Albumin Nanoparticles

S No	Ingredients	F1	F2	F3	F4
1	Capecitabine	10 mg	10 mg	10 mg	10 mg
2	Human Serum Albumin	10 mg	20 mg	30 mg	40 mg
3	10 mM Sodium Chloride solution	5 ml	5 ml	5 ml	5 ml
4	1% Glutaraldehyde	25 ul	25 ul	25 ul	25 ul

Nanoparticles for Breast Cancer

attraction, and hydrophobic interactions are all plausible drug loading methods. All carriers should have a high drug loading capacity in order to reduce the quantity of solid materials required per millilitre of injection (20). Albumin nanoparticles have showed a strong affinity for a wide range of pharmaceuticals (21). The drug loading into the albumin nanoparticles can be achieved in two ways; pre-loading and post-loading. We have employed the later technique, in which the medication is entrapped before the glutaraldehyde solution is used to crosslink the molecules. The prepared HSA nanoparticles showed a drug loading capacity in the range of 5.06%w/w to 15.36%w/w. The table 2 represents the

process yield and the percentage drug loading of different formulation of nanoparticles.

Particle Size and Surface Charge

The particle size was determined by dynamic light scattering, using Malvern system. The mean particle size of HSA nanoparticles containing capecitabine was found to be 151.18nm, 134.9nm, 178.8nm, and 151.3nm respectively (Fig. 2). The ability of nanoparticles to alter the biodistribution and pharmacokinetics of drugs, have important in vivo therapeutic applications. In this respect, the size and surface characteristics of nanoparticles are of prime importance.

Table 2. Data of Process Yield and Percentage Drug Loading of F1 to F4

Batch Code	Process Yield (w/w)	Drug Loading (%w/w)
F1	73.1±0.786	5.06±1.234
F2	80.2±0.924	15.36±0.456
F3	84.6±0.916	7.97±1.098
F4	66±0.745	5.82±0.976

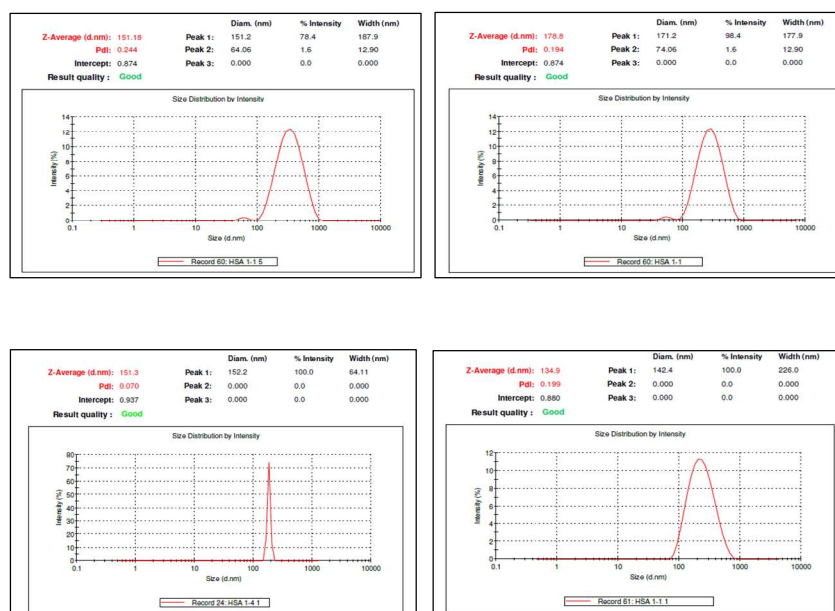


Fig 2. Particle size distribution of capecitabine loaded human serum albumin nanoparticles (F1- F4)

Nanoparticles of fewer diameters with hydrophilic surface have longer circulation in blood. Such systems prolong the duration of drug activity and also increase the targeting efficiencies to specific sites. Smaller the size of the particle better is the chance for permeation. In addition to the albumin concentration, pH also affects the coagulation of albumin molecules (22). It was also reported that pH also plays a vital role in formation of particle. In this study, the pH of solution mixture containing drug-polymer was adjusted to 8 to enhance the electrostatic repulsion which in turn minimizes the chances of coagulation among albumin molecules which otherwise may lead to the formation of larger particles. Small particles, due to their Brownian motion, can get adequate energy through to keep them agitated preventing the precipitation of nanosuspension and hence enhances the stability. Polydispersity index talks about the homogeneity of the particles. Closer the value of polydispersity to zero better is the homogeneity of the nanoparticles. The zeta potential of the nanoparticles was measured in 0.1 mM NaCl using Malvern Zetasizer. Surface charge plays a vital role in the stability of nanoparticle suspension. Larger the value of zeta potential more is the number of charged particles and in turn more is the repulsion between the particles, leading to the enhancement in the

stability of nanoparticles. Ideally the nanoparticles with the zeta potential values above 30 mV and below -30 mV are considered to have better stability. Zeta potential of HSA nanoparticles it was found to be -21.1 mV (Fig. 3).

Surface Morphology

The surface morphology of capecitabine loaded albumin nanoparticles was studied by Transmission electron microscopy and the study revealed that the nanoparticles were spherical and uniform in size (Fig.4).

In Vitro Drug Release Studies

One of the main criteria to examine the performance of a nanosystem before it is utilized on a biological system is to assess its *in vitro* drug release profile using a suitable release media at physiological pH. This study helps in understanding the release patterns of the drug and thus give us an idea of what modification might be required to achieve the objective of the research. The *in vitro* release of drug capecitabine from the various nanoparticle formulations was carried out by using dialysis method in 7.4 pH phosphate buffer for 24 h. The slow sustained release is highly desirable as it minimizes the drug release from the nanoparticles before they

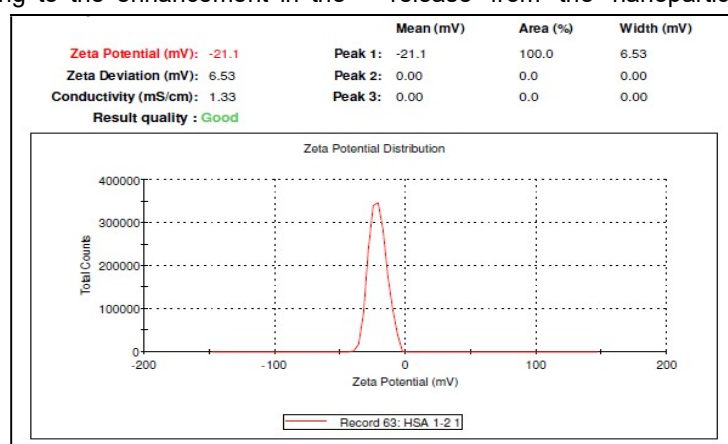


Fig 3. Zeta potential of capecitabine loaded human serum albumin nanoparticles (F2)

reach the target organ/tissue. The results shown in Fig. 5 indicated that the formulations showed a sustained release of drug over a period of 24 h. The cumulative percentage release of capecitabine from prepared HSA nanoparticles varied from 46.2%, 51.2 %, 47.55 %, 32.75 %. These results demonstrated the sustained release of drug from various formulations

Release Kinetics

The *in vitro* release data obtained from formulations were fitted to various kinetic models to reveal the drug release mechanism from nanoparticles (Table 3 & Fig. 6). Diffusion controlled drug release was observed with higher r^2 value in Higuchi model for all the formulations. The diffusion exponent (n) value is used to characterize different release mechanism in

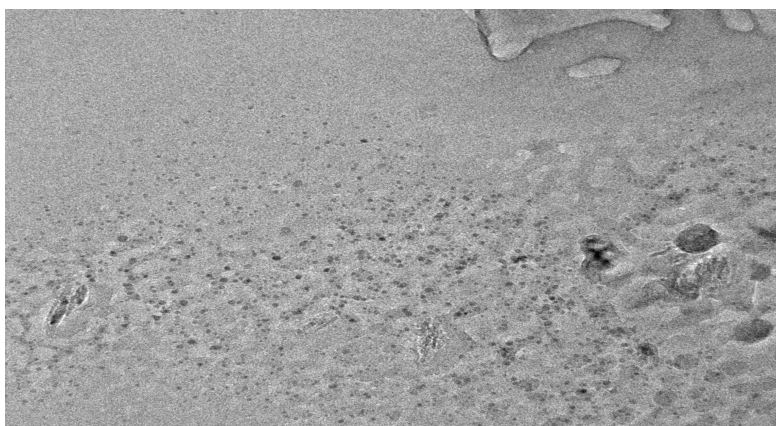


Fig 4. Transmission electron microscopic image of capecitabine loaded human serum albumin nanoparticles (F2)

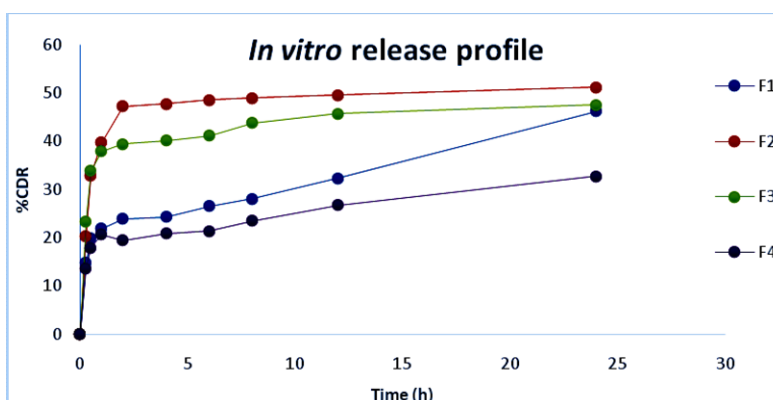


Fig 5. *In vitro* drug release profile of capecitabine loaded human serum albumin nanoparticles

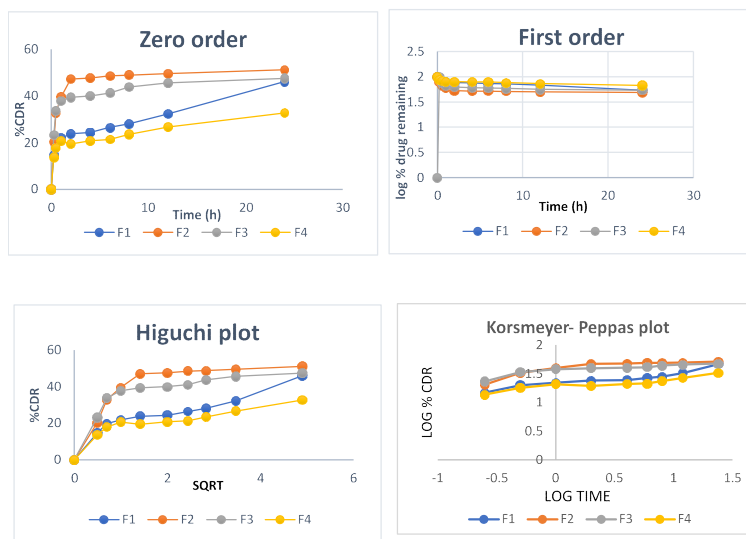


Fig 6. Release kinetics of capecitabine loaded human serum albumin nanoparticles

Table 3. Data of release kinetics of capecitabine loaded human serum albumin nanoparticles

S No	Formulation Code	Release kinetics							
		Zero order		First order		Higuchi		Korsmeyer-peppas	
		r ²	n	r ²	n	r ²	n	r ²	n
1	F 1	0.4449	2.703	0.4808	-0.0141	0.7021	8.8662	0.8782	0.1589
2	F 2	0.5099	5.7315	0.5745	-0.0368	0.7704	18.395	0.8288	0.2518
3	F 3	0.3759	4.0654	0.4203	-0.0241	0.6398	13.849	0.7407	0.1518
4	F 4	0.3371	1.9783	0.3551	-0.0099	0.593	6.8509	0.727	0.1171

Korsmeyer-Peppas model. The n value was found to be in the range of 0.1171 and 0.2518 for all the formulations indicating that drug release was controlled by anomalous diffusion, i.e. the mechanism of drug release is controlled simultaneously by diffusion and erosion of the matrix type formulations.

Conclusion

Anticancer drug - capecitabine loaded HSA nanoparticles were developed by

desolvation method. This method was able to produce desired size and uniformly shaped nanoparticles. All the formulations showed good process yield and % drug loading. Particle size analysis showed that the formed particles were in nano size and the mean zeta potential studies demonstrated that the nanoparticles possess a negative surface charge which indicates high degrees of stability due to inter particle repulsions. The *in vitro* drug release profile of all formulation was able to sustain the release of drug for 24h. The

release kinetics data showed that capecitabine release from nanoparticles was diffusion controlled and the n value of Korsmeyer- Peppas model indicates the release mechanism followed Fickian model. Based on this observation, it can be concluded that the formulated nanoparticle drug delivery system containing drug capecitabine is safe and able to sustain the release of drug for 24h. Overall it can be concluded that the prepared nanoparticles can be an efficient platform for the treatment of breast cancer by animal studies furtherly.

Conflict of Interests

The authors that there is no conflict of interests regarding the publication of this paper.

References

1. Ceylan Hepokura Ishak Afşin Kariper, Sema Mısır, Ebrunur Ay, Servet Tunoglu et al., Silver nanoparticle/capecitabine for breast cancer cell treatment. *Toxicol In Vitro*. 2019; 61:104600.
2. Wagstaff AJ, Ibbotson T, Goa KL. Capecitabine A Review of its Pharmacology and Therapeutic Efficacy in the Management of Advanced Breast Cancer. Adis International Limited. *Drugs*. 2003; 63 (2): 217-236
3. Muthadi Radhika Reddy, Hrushitha Reddy M. Preparation and Development of Capecitabine Microspheres for Colorectal Cancer. *J. Pharm. Sci. & Res*. 2017; 9(1): 37-43.
4. Narendar Dudhipala, Goverdhan Puchchakayala. Capecitabine lipid nanoparticles for anti-colon cancer activity in 1,2-dimethylhydrazine-induced colon cancer: preparation, cytotoxic, pharmacokinetic, and pathological evaluation, *Drug Development and Industrial Pharmacy*. 2018; 44 :10,1572-1582.
5. Suzuki M, Hori K, Abe I, Saito S, Sato H. A new approach to cancer chemotherapy: selective enhancement of tumor blood flow with angiotensin II. *The Journal of the National Cancer Institute*. 1981; 67(3):663-9.
6. J K McGavin, KL Goa. Capecitabine A Review of its Use in the Treatment of Advanced or Metastatic Colorectal Cancer. Adis International Limited. *Drugs*. 2001; 61 (15): 2309-2326.
7. Storp Bv, Engel A, Boeker A, Ploeger M, Langer K. Albumin nanoparticles with predictable size by desolvation procedure. *J Microencapsul*. 2012; 29(2):138-46.
8. Ghadiria M, Farahania EV, Atyabib F, Kobarfardc F, Hosseinkhani H. *In-Vitro* Assessment of Magnetic Dextran-Spermine Nanoparticles for Capecitabine Delivery to Cancerous Cells. *Iranian Journal of Pharmaceutical Research*. 2017; 16 (4): 1320-1334.
9. Kimura K, Yamasaki K, Nakamura H, Haratake M, Taguchi K, Otagiri M. Preparation and in Vitro Analysis of Human Serum Albumin Nanoparticles Loaded with Anthracycline Derivatives. *Chem Pharm Bull*. 2018; 66(4):382-390.
10. Zhao S, Wang W, Huang Y, Yuhang Fu and Yi Cheng. Paclitaxel loaded human serum albumin nanoparticles stabilized with intermolecular disulfide bonds, *Medicinal Chemistry Communication*. 2014;5(11):1658-1663.
11. Sebak S, Maryam S, Meenakshi M, Arun M, Satya Prakash K. Human serum albumin nanoparticles as an efficient noscapine drug delivery system for potential use in breast cancer: preparation and in vitro analysis. *Int J Nanomedicine*. 2010; 5(1):525-32.
12. Jenita JL, Chocalingam V, Wilson B. Albumin nanoparticles coated with polysorbate 80 as a novel drug carrier for the delivery of antiretroviral drug—Efavirenz. *International journal of pharmaceutical investigation*. 2014; 4(3):142-148.
13. Lu B, Xiong SB, Yang H, Yin XD, Chao RB. Solid lipid nanoparticles of mitoxantrone for local injection against breast cancer and its lymph node metastases. *Eur J Pharm Sci*. 2006;28(1-2):86-95.

14. Shenoy DB, Amiji MM. Poly(ethylene oxide)-modified poly(epsilon-caprolactone) nanoparticles for targeted delivery of tamoxifen in breast cancer. *Int J Pharm.* 2005; 11;293(1-2):261-70.
15. Lopes T, Cuevas JL, Jardon G, Gomez E, Ramirez P, Navaro O. Preparation and characterization of antiepileptic drugs encapsulated in sol gel titania nanoparticles as controlled release system. *Med. Chem.* 2015; S2: 003.
16. Rohiwal SS, Pawar SH. Synthesis and characterization of bovine serum albumin nanoparticles as a drug delivery vehicle. *Int. J. Pharm. Bio. Sci.* 2014; 5(4): 51-57.
17. Kumar PV and Jain NK. Suppression of agglomeration of ciprofloxacin loaded human serum albumin nanoparticles. *AAPS. Pharm. Sci. Tech.* 2007; 8(1): E1-E6.
18. S.R. Mudshinge, A.B. Deore, S. Patil, C.M. Bhalgat. Nanoparticles. *Emerging carriers for drug delivery, Saudi Pharm J.* 2011; 19: 129–141.
19. M.C. Roco, C.A. Mirkin, M.C. Hersam. Nanotechnology research directions for societal needs in 2020: summary of international study. *J. Nanoparticle Res.* 2011; 13: 897–919.
20. J. Jeevanandam, A. Barhoum, Y.S. Chan, A. Dufresne, M.K. Danquah. Review on nanoparticles and nanostructured materials: history, sources, toxicity and regulations. *Beilstein J. Nanotechnol.* 2018; 9 1050–1074.
21. Wilson, T.V. Ambika, R.D.K. Patel, J.L. Jenita, S.R.B. Priyadarshini. Nanoparticles based on albumin: preparation, characterization and the use for 5-fluorouracil delivery. *Int. J. Biol. Macromol.* 2012; 51: 84–88.
22. Rohiwal SS, Pawar SH. Synthesis and characterization of bovine serum albumin nanoparticles as a drug delivery vehicle. *Int. J. Pharm. Bio. Sci.* 2014; 5(4): 51-57.

Development and Validation of Stability Indicating RP-UPLC Method for Quantitative Estimation of Safinamide Mesylate in Bulk and its Tablet Dosage Form

Madhu Medabalimi*, K. Saravanakumar and S.V. Satyanarayana

¹JNTUA, Ananthapuramu-515002, Andhra Pradesh, India

²Department of Pharmaceutics, Sree Vidyanikethan College of Pharmacy, A. Rangampet, Tirupathi-517102, Andhra Pradesh, India

³Department of Chemical Engineering, JNTUA, Ananthapuramu-515002, Andhra Pradesh, India

*Corresponding author: creativemadhum@gmail.com

Abstract

Currently, there was an increasing interest on the development of a simple, rapid and sensitive method for safinamide mesylate due to its well- documented anti parkinsonism activity. This study aims to develop and validate a UPLC method for determination of the Safinamide mesylate in bulk and its tablet dosage forms. The chromatographic separation was achieved by using an ACQUITY BEH C18 column (50 mm × 2.1 mm, 1.7 μm; Waters), with an isocratic elution of 0.02 M diammonium hydrogen phosphate buffer pH 9.0 and Acetonitrile (80:20 v/v), at a flow rate of 0.25 ml/min with the help of UV detection at 272nm. The results of the analysis were validated statistically as per the International Conference on Harmonization (ICH) guidelines. Linearity studies were carried out in the range of 10 - 60 μg/ml and the linear response (r^2) was found to be 0.9999 with limits of detection and quantification being 0.081 and 0.271μg, respectively. The precision was performed by analysis of standard and sample solutions of SAF at working concentration level for six times. The % RSD values of the system and method precisions were found to be 0.527 and 0.324 respectively. Then, the precision of the method was confirmed by intra-day and inter-day analysis. The % RSD value of the intra-day and inter-day precisions were found to be 0.324, 0.531 respectively. Recovery studies were performed for determining accuracy of the method and the percentage

recovery was found to be 99.48-100.85%. The Robustness were performed at different flow rates and different temperatures, and the % RSD value were found to be 0.5965, 0.6276 respectively. Thus, a highly sensitive, simple and the stability indicating method were developed for the estimation of SAF in bulk and tablet dosage forms.

Keywords: Safinamide Mesylate, ICH Guidelines, ACQUITY BEH C18 Column, Ultra Performance Liquid Chromatography, Diammonium Hydrogen Phosphate Buffer

Introduction

Safinamide Mesylate (SAF) is a novel sodium and calcium channel blocker, capable with selective and reversible inhibition of monoaminoxidase type B (MAO-B) (1-7), chemically, it is (S)-(+)-2-[4-(3-fluoro benzyloxy benzyl amino) propanamide] methane sulfonate. (Figure: 1) which acts as Neuro protective with antiparkinsonian and anticonvulsion activity for the treatment of Parkinson's disease (8-11). Along with these activities, a well documented literature reports that there are few analytical methods like HPLC [12-14], HPTLC [15], LC-MS/MS (16, 17) are available for quantitative estimation and therapeutic effectiveness of SAF in bulk as well as formulation.

The development and validation of analytical methods for the accurate detection and quantification of active compounds in

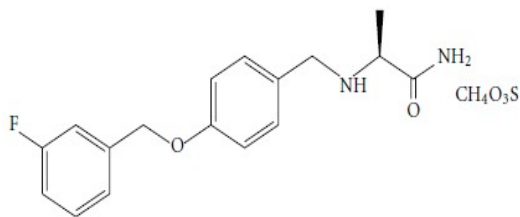


Figure: 1. Safinamide Mesylate

pharmaceutical samples with absence of interference of degradation products are a key consideration in the pharmaceutical field. Assay of SAF was mainly focused on its quantification by UPLC, mainly due to reward in terms of sensitivity and accuracy. The use of UPLC technology has been proposed to get out of the drawbacks like reducing the time of analysis and accordingly decreasing the environmental impact by reducing solvent consumption.

Herein we described the UPLC method development and validation of SAF in bulk and its tablet dosage forms for quantification and it was optimized and validated as per the ICH guidelines (18-20).

Material and Methods

Chemicals and Reagents: The SAF reference standard with a purity greater than 98% was gratis from Radiant Pharma, Mumbai, India. SAF tablets were purchased from commercial stores within their shelf life period. The reagents and solvents used (Acetonitrile, diammonium hydrogen phosphate) were of AR grade obtained from Merck Chemicals, Mumbai, India.

Instrumentation and UPLC Conditions: The estimation of SAF was performed using Waters' Acquity UPLC system (Waters, Milford, MA, USA) equipped with a quaternary gradient pump, auto sampler, column oven, and photodiode array detector and empower 2 software was used for analysis. An ultrasonic device, a sensitive balance, Sartorius analytic balance and a pH meter, glass electrode, were used for the

preparation of solutions. Thermo Scientific Heraeus microbiological incubator, Digital Dry Baths, Labnet International and Spectroline E-Series UV lamp were used for stability studies.

0.02 M diammonium hydrogen phosphate and acetonitrile in a ratio of 80:20 v/v was selected as the mobile phase and the pH was adjusted by adding liquid ammonia (pH=9). The detector wavelength was set at 272nm. The flow rate is maintained at 0.25 ml/min, at an ambient column temperature with 5 μ L injection volume.

Preparation of Mobile Phase: Freshly prepared solutions of 200 ml acetonitrile and 800 ml of 0.05 M ammonium acetate are transferred into a 1000ml standard flask and mixed well. Adjust the pH to 9 by adding a liquid ammonia solution with constant stirring and then filtered through 0.45 mm membrane filters.

Preparation of Stock Solution: The stock solution of SAF was prepared by taking 100mg of standard and transferred into a 100 ml standard flask having mobile phase and stirred continuously about 15 to 30 min. Finally made the final volume with the same solution to get the desired concentration (1mg/mL).

Preparation of Standard Solutions: 4 ml of stock solution of SAF was transferred with a calibrated pipette into a 100 ml flask. The final volume was made with the diluent to get 40 μ g/mL.

Preparation of Sample Solution: 20 tablets of SAF were weighed, powdered and transferred 673.45mg of powder which is equivalent to 100 mg of SAF into a 100ml standard flask with the mobile phase. Mix thoroughly using a stirrer for half an hour and made the final volume and filtered through a 0.45 mm filter. Further dilutions were made with the same diluent to get the optimum concentration of 40 μ g/mL.

UPLC Method Validation: UPLC developed method was validated by performing specificity/ selectivity, linearity, precision, accuracy, stability and robustness according to ICH guidelines for the estimation of SAF in bulk and tablet dosage form.

Linearity: Different dilutions were prepared in the concentration range of 10-60 µg/ml of the stock solution (1mg/mL) of SAF. A standard curve was plotted by taking the peak area on 'y' axis and concentrations on 'x' axis. Regression analysis was used to evaluate the linearity of the method by the least square method.

Precision: The precision was performed by estimating standard, sample solutions of SAF (40µg/ml) at working concentration level for 6 times. Further the precision of the method was confirmed by the analysis of the formulation for three times in a day and one time in the three successive days.

Accuracy: Accuracy was established by recovery studies, carried out by spiking a known amount of SAF at three levels (20, 40 and 60µg/ml) to the tablet excipients. The sample solutions were analyzed in triplicate at each level and percentage recovery was calculated. The accuracy was evaluated based on the correlation between experimental value and theoretical value.

Robustness: The Robustness of the method was performed by altering the parameters like flow rate, column temperature. The method was analyzed at different flow rates and at different column temperatures using working standard and sample solutions of SAF.

Specificity: The specificity was verified by comparing chromatograms of the standard solution, matrices spiked with SAF and a solution containing only matrices (blank samples). In order to confirm the presence or absence of interferences from matrices, the peak corresponding to SAF was analyzed and identified in each spiked matrix by UV spectra between 250 and 370nm, peak purity and retention time (from UPLC).

Forced Degradation: Forced degradation studies were also performed to know the stability of SAF. Acid hydrolysis and alkaline hydrolysis were investigated by adding hydrochloric acid (0.1 M HCl) and sodium hydroxide (0.1 M NaOH) to the

standard solution of SAF, in order to prevent temperature and photolytic degradation, these solutions were kept at 25°C and protected from light. After different periods of exposure, solutions were neutralized and analyzed. To evaluate peroxide degradation, to the standard solution hydrogen peroxide (3% H₂O₂) was added. UV degradation was performed by placing the standard solution in a UV chamber (250-370nm) with controlled temperature (25°C). To assess the thermal degradation, standard solutions were exposed to 70°C.

Results and Discussion

Method Development: Detection and quantification of SAF have been analyzed by using different methodologies including chromatography and spectroscopy. Most of chromatographic methods are time consuming. In this study, UPLC method was selected based on its ability to endorse ultra pressure analysis and less time consuming with high precision, therefore increasing analysis efficiency.

Optimization of UPLC Method: Initially, different ratios of mobile phase, different column were tried for better separation of SAF. After performing various trials, finally mobile phase with the ratio of 80:20 %v/v of 0.02 M diammonium hydrogen phosphate buffer (pH 9.0) and acetonitrile and Waters Acquity BEH C18, 50 × 2.1 mm, 1.7µm column were selected for analysis as they produced a sharp and symmetrical peak with a retention value of 0.285 at 272nm. The flow rate was maintained all over analysis at 0.25 ml/min at ambient column temperature with the injection volume was 5 µL (Figure: 2).

Optimized Chromatographic Conditions: UPLC method development and validation of SAF was carryout by using Waters Acquity BEH C18, 50 × 2.1 mm, 1.7µm column, 0.02 M diammonium hydrogen phosphate buffer pH 9 and acetonitrile as mobile phase in the ratio of 80:20 v/v. Detection was done using a photo diode array detector at 272 nm. The flow rate was

optimized to 0.25 ml/min at ambient temperature.

Application of Proposed Method to Tablet Formulation: To determine the concentration of SAF in tablets (Label claim: 100 mg per tablet), the contents of 20 tablets were weighed, finely powdered and their mean weight was determined. The powder equivalent to 100 mg of SAF was weighed and extracted with 100 ml of mobile phase; it was sonicated for 20 min. The resulting solution was filtered using 0.41 μ m filter.

Method Validation: The proposed method was validated as per the ICH

guidelines in terms of its linearity, accuracy, specificity, Intraday and interday precision, robustness, ruggedness, LOD and limit LOQ.

Linearity (Calibration Curve): For linearity study, aliquots of 10, 20, 30, 40, 50, and 60 μ g/ml of SAF from standard stock solution were injected into the waters acquity system (Figure: 3). The calibration curve was plotted using concentration against peak area and analyzed through least squares regression. The assay was found to be linear in the range from 10 -60 μ g/mL. The calibration curve was linear with an average correlation coefficient of r^2 0.999. Hence the selected

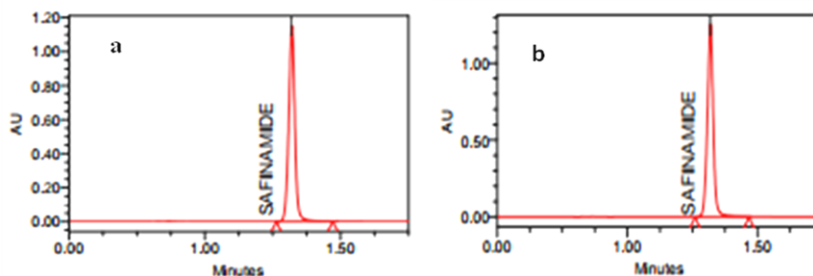


Figure: 2. Chromatograms of SAF Standard (a) and Sample (b)

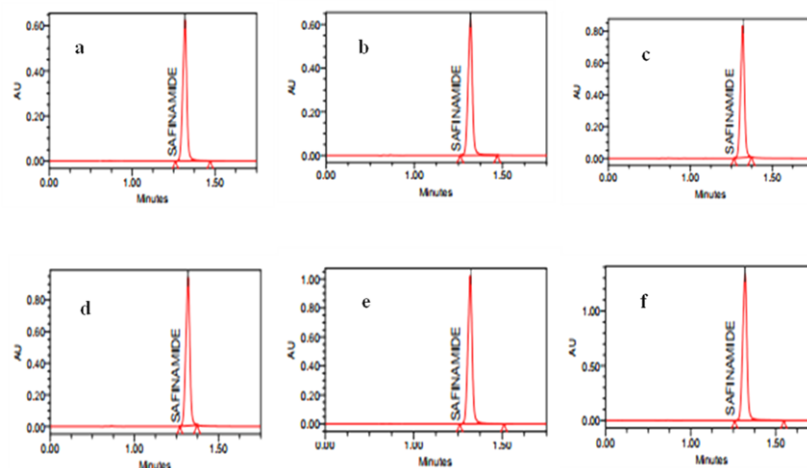


Figure: 3. Linearity Chromatograms of SAF; 10 μ g/ml (a), 20 μ g/ml (b), 30 μ g/ml (c), 40 μ g/ml (d), 50 μ g/ml (e) and 60 μ g/ml (f)

RP-UPLC Method

concentrations were found to be linear (Figure: 4). Results are shown in Table: 1.

Accuracy: The accuracy of the method was performed by recovery studies. A known quantity of Safinamide mesylate raw material solutions was added at different levels (50,100 and 150%). The peak areas of the solutions were measured and the percentage recovery was calculated. The percentage recovery was found to be in the range of 99.85–100.11% (Figure: 5). Results of recovery data were shown in (Table 2).

Specificity: The specificity of the method was ascertained by analyzing blank, placebo, standard solution and tablet formulation. There were no interferences

between excipients and Safinamide mesylate. Hence the method was specific (Figure: 6).

Precision: The precision was performed by analyzing standard and sample solutions of Safinamide mesylate at working concentration level for 6 times. The % RSD value of system precision and method precision were found to be 0.527 and 0.324 respectively. The amount present in tablet formulation was in good concord with the label claim. The results showed that the precision of the methods was confirmed.

Further the precision of the method was confirmed by intra-day and inter-day analysis. The analysis of the formulation was carried out for three times in the same day and one time in the three consecutive days. The results were shown in (Table: 3).

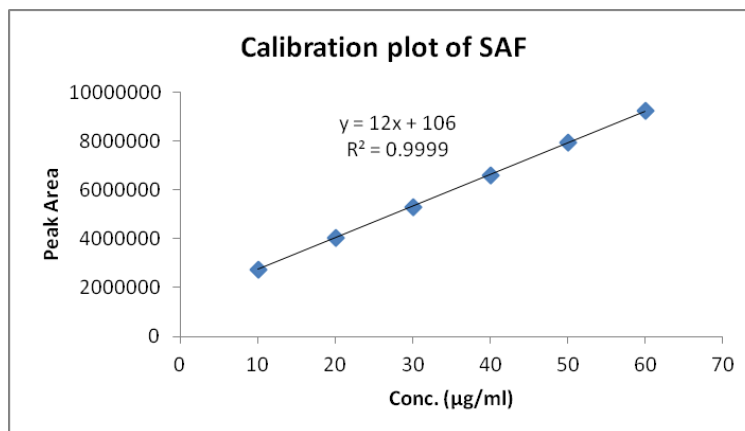


Figure: 4. Calibration Plot of SAF

Table 1: Linearity Data of SAF

S No	Linearity Level	Concentration (µg/ml)	Area
1	25	10	2756378
2	50	20	4042136
3	75	30	5296681
4	100	40	6594914
5	125	50	7923328
6	150	60	9236630
Correlation Coefficient			0.9999

RP-UPLC Method

Robustness: The Robustness were performed at different flow rates (0.2ml/min, 0.25ml/min and 0.3ml/min.) and at different column temperatures (20°C, 25°C, and 30°C) by using working standard and sample solutions of Safinamide mesylate. . The % RSD value of flow rate variation and column temperature variation were found to be

0.5965 and 0.6558 respectively (Figure: 7). Results are shown in Table: 4.

Limit of Detection (LOD) and Limit of Quantification (LOQ): In order to determine detection and quantification limit, concentrations in the lower part of the linear range of the calibration curve were used. SAF solutions of 10,

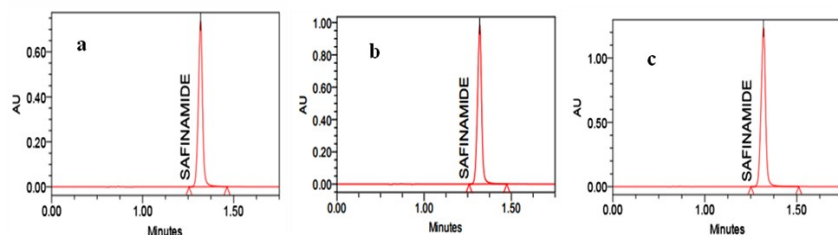


Figure: 5. Accuracy Chromatograms of SAF; 50% (a), 100% (b) and 150% (c)

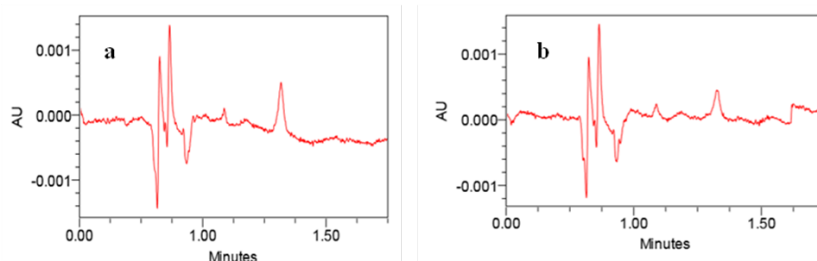


Fig 6. Chromatograms of Blank (a), Placebo (b)

Table: 2. Accuracy Data of SAF

Sample No	Spiked Level	Sample Weight (mg)	Sample Area	µg/ml Added	µg/ml Found	% Recovery	% Mean Recovery
1	50%	33.673	3631749	20.07	20.12	99.75	99.91
2		33.673	3611606	20.07	20.01	100.29	
3		33.673	3630428	20.07	20.13	99.70	
1	100%	67.345	6761150	40.13	40.15	99.95	100.11
2		67.345	6781061	40.15	40.14	100.02	
3		67.345	6805563	40.23	40.22	100.02	
1	150%	101.018	7304679	60.20	59.96	100.40	99.85
2		101.018	77375024	60.20	60.26	100.09	
3		101.018	7663028	60.20	59.64	99.06	

RP-UPLC Method

Table 3. Method Precision, System Precision, Inter Day Precision Data of SAF

S No	Method Precision		System Precision		Inter Day Precision Data	
	Peak Area	% Assay	Peak Area	% Assay	Peak Area	% Assay
1	7222699	100.07	7219579	100.01	7278394	100.84
2	7242606	100.34	7289022	101.00	7283002	100.90
3	7218974	100.01	7289022	101.00	7293728	101.05
4	7276367	100.81	7216189	100.00	7209387	99.88
5	7265881	100.66	7216189	100.00	7218593	100.01
6	7232006	100.20	7214002	99.90	7218940	100.01
Average		100.35		100.31		100.45
SD		0.325		0.529		0.533
%RSD		0.324		0.527		0.531

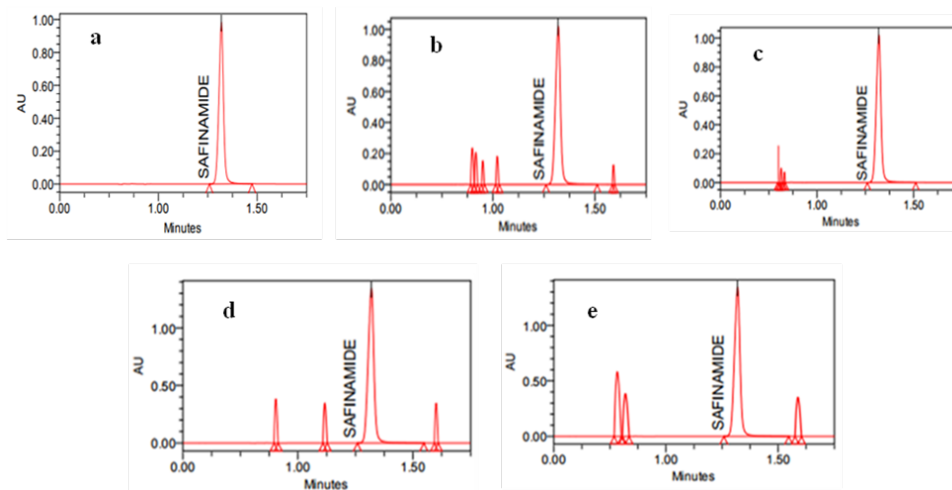


Figure: 7. Chromatograms of Untreated SAF (a), Acid-Degraded (b), Alkali-Degraded (c), Peroxide-Degraded (d), UV Light-Degraded (e)

20, 30, 40, 50, and 60 $\mu\text{g}/\mu\text{L}$ were prepared and applied in triplicate. The LOQ and LOD were calculated using equation $\text{LOD} = 3.3 \times \text{N}/\text{B}$ and $\text{LOQ} = 10 \times \text{N}/\text{B}$, where N is the standard deviation of the peak areas of the drugs ($n = 3$), taken as a measure of noise, and B is the slope of the corresponding calibration curve. Results are shown in Table: 5.

Degradation Studies

Stress Degradation Studies: The specificity of the method can be demonstrated through forced degradation studies performed under acidic, basic, oxidative, and ultraviolet light conditions. A specific method should be able to separate and equivocally identify the test compound from the various degradation products

(Fig. 7). All experiments were conducted in triplicate (n=3). Results were shown in Table: 6.

Acid Hydrolysis: SAF (40 µg/ml) was prepared in HCl (1 M). Aliquots were kept at 25 °C for 24 h (Thermo Scientific Heraeus microbiological incubator, USA) and 80°C

(AccuBlock™ Digital Dry Baths, Labnet international, USA) for 12 h.

Base Hydrolysis: SAF (40 µg/mL) was prepared in NaOH (1 M). Aliquots were kept at 25 °C for 24 h (Thermo Scientific Heraeus microbiological incubator, USA) and 80 °C (AccuBlock™ Digital Dry Baths, Labnet international, USA) for 12 h.

Table 4. Robustness Data of SAF

S No	Parameter	Change	Peak Area	% Assay
1	Flow Rate (ml/min)	0.2	7157652	99.16
2		0.25	7243089	100.35
3		0.3	7208459	99.87
4	Temp (°C)	20	7242750	100.24
5		25	7250341	100.45
6		30	7325339	101.49

Oxidative Degradation: SAF (40µg/mL) was prepared using 30% (v/v) hydrogen peroxide (H₂O₂). Aliquots were incubated at 25 °C for 24 h and 80 °C for 12 h.

UV Degradation: SAF (40µg/mL) was prepared in the mobile phase and aliquots were kept in clear plastic vials to avoid unwanted UV absorption which may occur with glass vials. Samples were then exposed to UV light (365nm, Spectroline E-Series UV lamp, Spectronics Corp, USA) for a duration of 7 h.

Table 5. Analytical Performance Summary Data of SAF

S No	Validation Parameter	Results	Acceptance Criteria
1	Accuracy (%Recovery) (n=9)	Mean Recovery 101 %	% Recovery - 98% to 102%
2	Precision (n=6)	Mean assay -100.35 % % RSD – 0.324	Mean assay – 98% -102% % RSD should be < 2
3	Linearity	y = 12x + 106 R ² = 0.9999	R ² = 0.995
4	Degradation Studies (Acid, Base, Light, Peroxide)	Mean Assay – 90.775% % RSD – 1.619	The assay should be between 85-115% % RSD should be < 2
5	Limit of Detection	0.1454 µg/ml	--
6	Limit of Quantification	0.4408 µg/ml	--

Table 6. Degradation Studies in Different Stress Conditions

Nature of the Sample	Sample Area	% Assay	Difference of Assay
Acid	4242136	89.25	10.75
Base	4273248	90.64	9.36
Peroxide	5696681	92.78	7.22
UV	5526886	90.43	9.57

RP-UPLC Method

Discussion

SAF is a novel drug with multiple actions to treat Parkinson's disease which is a neurodegenerative disease. A stability indicating UPLC method was developed and validated for the quantitative determination of a Safinamide in tablet dosage form. The optimum concentration of SAF was found to be 40µg/ml. The chromatographic separation was achieved by using an ACQUITY BEH C18 column (50 mm × 2.1 mm, 1.7 µm; Waters, USA), with an isocratic elution of 0.02 M diammonium hydrogen phosphate buffer pH 9.0 and Acetonitrile (80:20, v/v), at a flow rate of 0.25 ml/min with UV detection at 272nm. The results of the analysis were validated statistically as per the ICH guidelines. Linearity studies were carried out and the linear response ($r^2 = 0.9999$) was observed in the range of 10 - 60µg/mL with limit of detection (LOD) and quantification (LOQ) being 0.081 and 0.271 µg, respectively.

Precision was performed by injecting six replicate solutions of Safinamide standards and samples having the concentration of 40µg/ml. The % RSD value of system precision and method precision were found to be 0.527 and 0.324 respectively. The accuracy of the method was performed by recovery studies. The percentage recovery was found to be in the range of 99.48–100.85%. The Robustness were performed at different flow rates and different temperatures, and the % RSD value were found to be 0.5965, 0.6276 respectively. Hence the proposed method was successfully applied to a routine analysis of Safinamide mesylate in bulk and in tablet dosage form. Analytical performance summary data of Safinamide mesylate are shown in Table 6.

Conclusion

In the present study, a simple, rapid, sensitive and accurate UPLC method was successfully developed and validated for the quantitative determination of Safinamide in bulk and tablet dosage form. The results

demonstrated a highly sensitive and selective method, without any interferences from the matrices and degradation products, able to quantify Safinamide mesylate with precision, accuracy and robustness. Hence it was concluded that the developed analytical method was successfully used for the routine quality control analysis of the Safinamide in marketing tablet dosage form.

Conflict of Interest

The authors declare no conflict of interest.

References

1. Deeks ED., Safinamide: first global approval *Drugs*. 75 (2015) 705-11.
2. US Food and drug administration. "FDA approves a drug to treat Parkinson's disease" FDA news release 2017.
3. Marzo A., Dal Bo L., Monti N. C. (2004). Pharmacokinetics and pharmacodynamics of safinamide, a neuroprotectant with antiparkinsonian and anticonvulsant activity, *Pharmacological Research*. 50 (1): 77–85.
4. Caccia C, Maj R, Calabresi M (2006). Safinamide: from molecular targets to a new anti-Parkinson drug, *Neurology*. 67: S18-23.
5. Caccia C, Salvati P, Rossetti S, Anand R (2007). Safinamide: beyond MAO-B inhibition. *Parkinsonism Relat Disord*. 13: (Suppl 2) S99.
6. Onofrj M., Bonanni L., Thomas A. (2008). An expert opinion on safinamide in Parkinson's disease, *Expert Opinion on Investigational Drugs*. 17(7): 1115–1125.
7. Schapira AH, Stocchi F, Borgohain R (2013). Long-term efficacy and safety of safinamide as add-on therapy in early Parkinson's disease, *Eur J Neurol*. 20: 71-80.
8. Schapira AH, Fox S, Hauser RA 2013. Safinamide add on to Ldopa: a randomized, placebo-controlled, 24-week global trial in patients with Parkinson's Disease (PD) and

Motor fluctuations (SETTLE), 65th AAN Annual Meeting, American Academy of Neurology.

9. Gregoire L, Jourdain VA, Townsend M (2013). Safinamide reduces dyskinesias and prolongs L-DOPA antiparkinsonian effect in parkinsonian monkeys. *Parkinsonism Relat Disord.* 19 (5): 508-14.

10. Borgohain R, Szasz J, Stanzione P (2014). Randomized trial of safinamide add-on to levodopa in Parkinson's disease with motor fluctuations, *Mov Disord*, 29: 229-237.

11. Kandadai RM, Jabeen SA, Kanikannan MA, Borgohain R (2014). Safinamide for the treatment of Parkinson's disease, *Expert Rev Clin Pharmacol*, 7(6): 747-59.

12. Dal Bo L., Mazzucchelli P., Fibbioli M., and Marzo A. (2006). Bioassay of safinamide in biological fluids of humans and various animal species, *Drug Research.*, 12: 814–819.

13. Zhang K., Xue N., Shi X., Liu W., Meng J., and Du Y. (2011). A validated chiral liquid chromatographic method for the enantiomeric separation of safinamide mesilate, a new anti-Parkinson drug, *Journal of Pharmaceutical and Biomedical Analysis*, 55(1): 220–224.

14. Mali Bhushan J., Vivekkumar K., Redasani K., Amod S. Patil, Atul Shirkhedkar A. (2013). Development and validation of RP-HPLC method for determination of safinamide mesylate in bulk and in tablet dosage form, *Analytical Chemistry An Indian Journal*, 13(4): 127-130.

15. Vivekkumar K., Redasani K., Mali Bhushan J., and Sanjay J. Surana (2012). Development and Validation of HPTLC Method for Estimation of Safinamide Mesylate in Bulk and in Tablet Dosage Form, *International Scholarly Research Network Analytical Chemistry*, 1-4.

16. Gotze L., Hegele A., Metzelder S.K. (2012). Development and clinical application of a LC-MS/MS method for simultaneous determination of various tyrosine kinase inhibitors in human plasma, *Clin. Chim. Acta.*, 413: 143–149.

17. Zou Liang, Sun Lili, Zhang Hui, Hui Wenkai, Zou Qiaogen, Zhu Zheyang (2017). Identification, Characterization, and Quantification of Impurities of Safinamide Mesilate: Process-Related Impurities and Degradation Products. *Journal of AOAC International*, 100 (4): 1029-1037.

18. FDA, ICH-Q2 (R1): Validation of Analytical Procedures: Text and Methodology, vol. 60, US Food and Drug Administration, DC, USA, 1995.

19. FDA, ICH-Q1A (R2): Stability Testing of New Drug Substances and Products, vol.68, US Food and Drug Administration, DC, USA, 2nd edition, 2003.

20. FDA, ICH-Q1B (R2): Photo-Stability Testing of New Drug Substances and Products, vol.62, US Food and Drug Administration, DC, USA 1997.

RP-HPLC Method for Determination of Favipiravir (RdRp of RNA Viruses) in Pharmaceutical Dosage Form

P. Ravisankar*, B. Divya, A. Bhavani Sailu, K. Neelima, A. Viswanath and P. Srinivasa Babu

Department of Pharmaceutical Analysis, Vignan Pharmacy College, Vadlamudi, Guntur-522 213, Andhra Pradesh

*Corresponding Author: E-Mail Id: banuman35@gmail.com

Abstract

A simple, sensitive, precise, accurate, rapid, and reproducible HPLC method was developed and validated for the determination of Favipiravir (RdRp of RNA viruses) in pharmaceutical dosage form. Good quality chromatographic separation of Favipiravir (FAV) was conceded out by using Nucleosil C₁₈ column (4.6 mm i.d., X 250 mm., 5 µm particle size) (based on 99.999 % ultra-high purity silica) using mobile phase consisting acetonitrile: methanol: HPLC Grade water (50:40:10 % v/v) at flow rate of 1 ml/minute. The λ_{max} of the Favipiravir was found to be 365 nm. The retention time of Favipiravir was found to be 2.794 min and the calibration curve was linear function of drug in the conc. range of 10-50 µg/mL ($r^2 = 0.9998$). The LOD and LOQ were found to be 1.042995 µg/mL and 3.160591 µg/mL respectively. The recovery (accuracy) studies were performed and the percentage recovery was found to be 99.34 - 99.42 %. Percentage assay of Favipiravir tablets were found to be 99.85 %. Infact the % RSD values for all validation key parameters were less than 2 %. Thus, the developed method found to be fruitfully practicable for the determination of Favipiravir in quality control analysis in pharmaceutical formulations.

Keywords: RP - HPLC, Favipiravir, Validation, ICH guidelines.

Introduction

The chemical name for FAV is 6-fluoro-3-hydroxypyrazine-2-carboxamide. It

has molecular formula C₅H₄FN₃O₂ and a molecular weight of 157.104 g/mol. FAV is an antiviral used to manage influenza, and that has the potential to target other viral infections (1). Literature Survey, it is revealed that the drug has been estimated by UV Spectroscopy (2) UPLC MS/MS (3), LC-MS/MS (4,5), HPLC (6-8) But only a few UV Spectroscopic methods and Liquid Chromatography analyses have been reported for the determination in pharmaceutical dosage forms. In general view, HPLC has been proven to be useful in diagnostic purposes and the pharmaceutical industry. The aim and Objective of the present work was to develop and validate a rapid, precise, and sensitive for FAV in pharmaceutical dosage form. The chemical structure of FAV is shown in (Figure 1).

Materials and Methods

Chemicals and Reagents

Sample of FAV was gifted from Hetero Labs Ltd., Hyderabad, India. HPLC grade Methanol, HPLC grade Acetonitrile, HPLC grade Water, AR grade Triethylamine, AR grade Sodium Hydroxide and AR grade ortho phosphoric acid were purchased from Merck specialties Pvt. Ltd., Mumbai, India and AR grade potassium dihydrogen phosphate purchased from Glaxo SmithKline Pharmaceuticals Ltd., Mumbai. Other excipients were prepared in our laboratory.

Instrumentation

For the detection of sample using UV, ELICO SL-210 spectrophotometer, having 1

cm matched quartz cells, was used for all spectral and absorbance measurements, and solutions were prepared in methanol, acetonitrile and HPLC grade water (50:40:10). For HPLC, the chromatographic system used consists Agilent technologies-1260 series with G1311C Quat pump VL, Thermo scientific C₁₈ column, 1260 series with G1511D DAD VL. having diode array detector was used for higher data quality for more confidence. The data that was acquired, was processed by utilizing EZ chrome elite software.

Method Development and Optimization of Chromatographic Conditions

For HPLC development, a variety of mobile phases containing HPLC grade water,



Fig 1. Chemical Structure of FAVIPRAVIR

acetonitrile, methanol in different ratios with or without buffers, and also various flow rates were performed. A good symmetrical peak was found when the mobile phase containing of a mixture of acetonitrile: methanol: HPLC grade water (50:40:10% v/v).

Selection of Detection Wavelength

The UV spectrum of diluted solutions of various concentrations of FAV in methanol was recorded by using UV spectrophotometer. The wavelength of maximum absorbance was scanned over a range of 200 - 400 nm and the UV overlay absorption spectrum is represented in (Figure 1a). The maximum absorbance was found at 365 nm.

Preparation of the Mobile Phase

Mobile phase consisting a mixture of acetonitrile: methanol: HPLC grade water (50:40:10 % v/v) was prepared and filtered through Whatman's filter paper and degassed by sonication.

Preparation of Standard Stock Solution

Exactly weighted 100 mg of FAV was transferred into 100 ml of volumetric flask, dissolved and diluted up to the mark with mobile phase to get stock solution containing

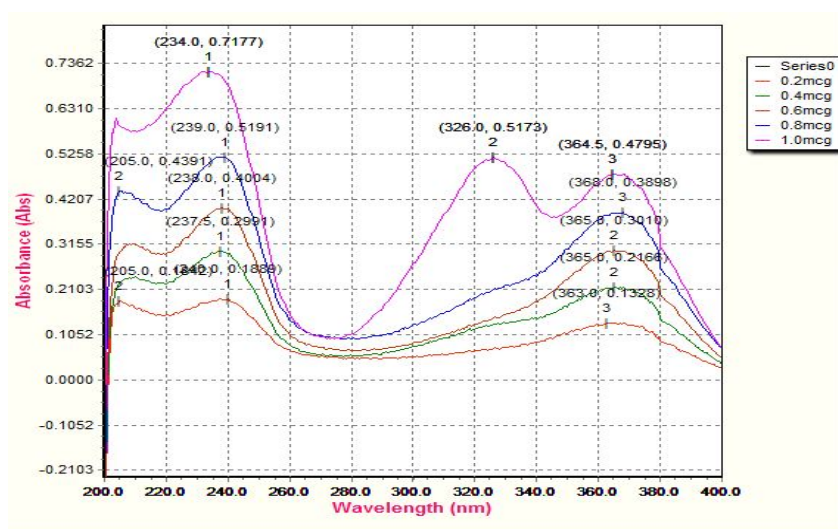


Fig 1a. Overlay Spectrum of FAV for UV Method

RP-HPLC Method for Determination

1.0 mg/mL of FAV. Aliquots from stock solution were diluted with mobile phase to attain the calibration standard solutions over the range of 10, 20, 30, 40, 50 µg/mL FAV for high pressure liquid chromatographic method (n=5). As a matter of fact, the calibration curve was constructed by plotting the peak area on Y- axis and concentrations on X-axis.

Preparation of Sample Solution

For the assay twenty tablets containing FAV were precisely weighed and was shifted into a cleaned and dry mortar and ground to a fine powder and mixed homogenously. An exactly weighed amount of powder equivalent to 100 mg of FAV was taken and transferred into a 100 ml volumetric flask. The drug was extracted with mobile phase. The mixture was sonicated for 10 minutes and volume was filled up to mark and filtered through whatman filter paper and degassed by sonication. From this stock

solution 4.0 ml was transferred to 100 ml volumetric flask and diluted with the mobile phase to obtain an intermediate solution of 40 µg/mL of FAV. Indeed, this solution was filtered through whatman filter paper, degassed by sonication and 20 µL was injected in chromatographic system. Infact sample solution was injected in to the developed high performance liquid chromatographic system and area of the peak was measured and percent assay was determined.

Method Development Optimization

The optimized HPLC conditions of several mobile phases with different compositions have been tested to develop an optimized chromatographic conditions like tailing factor, peak shape, and the number of theoretical plates as shown in (Table 1). For the selection of the mobile phase, primarily acetonitrile: methanol: HPLC grade water has been tested for different compositions. Eventually, the gradient mode and mobile

Table1. Optimized Chromatographic Conditions for FAV

Parameter	Chromatographic conditions
Instrument	Agilent SPD 20A prominence UV- Vis detector LC-20AT prominence liquid chromatograph, 1260 Quat Pump VL,1260 Diode Array Detector
Column	Nucleosil C18 column (4.6 mm i.d., X 250 mm., 5 µm particle size) (based on 99.999% ultra high purity silica)
Detector	1260 Diode Array Detector.
Mobile phase	ACN: MeOH: HPLC Grade Water (50: 40:10 v/v)
Flow rate	1 mL/minute
Detection wave length	UV at 365 nm
Run time	12 minutes
Temperature	Ambient temperature (25°C)
Volume of injection loop	20 µL
Retention time (R _t)	2.794
Theoretical plates [th.pl] (Efficiency)	6051
Theoretical plates per meter [t.p/m]	12102
Tailing factor (asymmetry)	1.20

RP-HPLC Method for Determination

phase containing a mixture acetonitrile: methanol: HPLC grade water (50:40:10% v/v) at a flow rate of 1 ml/ minute was found to be satisfactory and proper system suitability parameters obtained as shown in Table 2.

Method Validation (9,10,11,12,13)

Validation is the process of establishing documented evidence, which provides a high degree of assurance, that a specific activity will consistently produce desired results or products, meeting its pre-determined specifications and quality characteristics. The method was validated as per ICH guidelines (14).

System Suitability

System suitability parameters can be defined as tests to ensure that the method can generate results of acceptable accuracy and precision. The requirements for system suitability are usually developed after method development and validation has been completed. The system suitability parameters like theoretical plates, retention time, tailing factor, were studied and found satisfactory.

Specificity

Specificity of the method was evaluated by assessing whether excipients and other additives that are usually present in pharmaceutical formulations of FAV do not interfered with the peaks of the analyte under optimum conditions as shown in Table 3.

Linearity

The linearity of the method was determined at five concentration levels ranging from 10-50 µg/ml for FAV. Evaluation of the drug was performed with a PDA detector at 365.0 nm peak area was recorded for all the peaks. The correlation coefficient value of FAV was found to be 0.9998 as shown in Table 4.

Accuracy (Recovery Studies)

The accuracy of the method was evaluated by standard addition method. Recovery tests were carried out by analyzing drug with different compositions. Known amounts of standard drugs were added to pre analyzed sample at three different levels 10%, 30%, 50 % and the mixed standard solutions were analyzed in triplicate at every level as per suggested

Table 2. System suitability parameters

System suitability parameters	FAV
Tailing factor (T)*	1.20
Number of theoretical plates	6051
Theoretical Plates per meter (N)*	1,21,020
Retention time*	2.794 minutes
Peak area*	702331
SD for peak area	4.324349662
% RSD for peak area	0.000615712
*Average of six determinations, SD = Standard deviation, RSD = relative standard deviation.	

Table 3. Results of Specificity Study for FAV

Name of the Solution	Retention Time (t _R) Minutes
Mobile phase (blank)	No interference at RT of analyte peak
Placebo	No interference at RT of analyte peak
FAV 50 µg/mL (sample)	2.793 minutes

method. The accepted limits are 98 % - 105 % and all observed data are within the required range which indicates good recovery values and hence the accuracy of the method developed.

Precision

Method precision was determined by performing assay of sample under the tests of repeatability (Intraday precision) and intermediate precision (Interday precision) performed during three consecutive days by three different analysts, at different working concentrations. The percent relative standard deviation (% RSD) was calculated which is within the acceptable criteria of not more than 2.0.

Robustness

The robustness of an analytical procedure is the measure of its capacity to remain unaffected by small but deliberate variations in method parameters and provides an indication of its reliability during normal usage. For the determination of a method's robustness, parameters such as variation in detector wavelength are varied within a realistic range and the quantitative influence of the variables is determined. If the influence of the parameter is within a previously specified tolerance, the parameter is said to be within the method's robustness range. The absorbance was

Table 4. Linearity Data of FAV by HPLC

S. No	Concentration (µg/m)	Retention Time (RT) Minutes	Peak Area, mV.s.
1	0	-	0
2	10	2.793	147397
3	20	2.793	281672
4	30	2.794	429690
5	40	2.793	69493
6	50	2.793	702331

Table 4a. The Summary Output of ANOVA Study of FAV

SUMMARY OUTPUT								
Regression Statistics								
Multiple R	0.99985							
R Square	0.9997							
Adjusted R Squ	0.99959							
Standard Error	4448.22							
Observations	5							
ANOVA								
	df	SS	MS	F	Significance F			
Regression	1	1.95E+11	1.95E+11	9873.01	2.25E-06			
Residual	3	5.9E+07	2E+07					
Total	4	1.95E+11						
	Coefficien	Standard	t Stat	P-value	Lower 95%	Upper 95%	Lower 95.	Upper 95.0%
Intercept	6809.9	4665.33	1.45968	0.24049	-8037.254	21657.05	-8037.3	21657.1
X Variable 1	13976.9	140.665	99.363	2.25E-06	13529.231	14424.55	13529.2	14424.5

RP-HPLC Method for Determination

measured and assay was calculated as shown in Table 5.

Linearity and Range

A graph of peak area versus concentration ($\mu\text{g/mL}$) were plotted for FAV at concentration range between 10-50 $\mu\text{g/ml}$. The linear regression equation and correlation coefficient (r^2) were $y = 14074x + 3242.8$ and 0.9998 respectively.

LOD and LOQ

LOD

Limit of Detection is the lowest concentration in a sample that can be detected, but not necessarily quantified under the stated experimental conditions.

LOQ

The limit of quantitation is the lowest concentration of analyte in a sample that can be determined with acceptable precision and accuracy.

Analysis FAV in Tablet Formulation

FAV standard solution and FAV sample solution were prepared. The samples were analyzed using the developed chromatographic method and the % content of the FAV in the tablets was estimated. The % content of the FAV was calculated using the following formula.

$$\text{AT/AS} \times \text{WS/25} \times 9/100 \times 250/5 \times 100/5 \times \text{P}/100 \times 100/\text{LC}$$

Where, AT = Peak area response of FAV in the chromatogram obtained from the test solution.
 AS = Average peak area response of FAV in the chromatograms obtained from replicate injections of standard solution.
 WS = Weight of FAV standard taken in mg in standard solution.
 P = % Purity of FAV standard.
 LC = Label claim of FAV in mg per tablet.

Results and Discussion

The objective of the proposed work was to develop some new, sensitive and

Table 5. Robustness Results of FAV

S No	Parameter	optimized	Used	Retention time (t_R), min	Plate count [§]	Peak asymmetry [#]	Remark
1.	Change in flow rate (± 0.2 mL/minute)	1.0 mL/min	0.8 mL/min	2.896	9,054	1.20	*Robust
			1.0 mL/min	2.794	8,998	1.21	*Robust
			1.2 mL/min	2.673	8,834	1.3	*Robust
2.	Detection wavelength (± 1 nm)	365 nm	364 nm	2.794	8,790	1.1	Robust
			365 nm	2.794	8,998	1.6	Robust
			366 nm	2.794	8,890	1.2	Robust
3.	Mobile phase composition (Acetonitrile :Methanol:HPLC Grade water)	50:40:10 v/v	45:45:10 v/v	2.684	8,634	1.8	*Robust
			50:40:10 v/v	2.794	8,998	1.4	*Robust
			40:40:20 v/v	2.854	8,713	1.22	*Robust
Acceptance criteria (Limits): [#] Peak Asymmetr (AS) < 1.5, [§] Plate count (PC) > 2000, * Significant change in Retention time							

selective analytical method for the determination of FAV and to validate the developed method according to the ICH guidelines and applying the same for its estimation in marketed formulation. FAV is a purine analogue and is incorporated in place of guanine, adenine and inhibits viral replication. Literature survey reveals that very few analytical methods have been reported for the determination of FAV in bulk and pharmaceutical dosage form. Hence, on the basis of literature survey it was thought to develop a rapid, precise, accurate, simple, specific and reliable RP-HPLC methods for routine analysis of FAV in bulk and pharmaceutical dosage forms. In HPLC method, the conditions were optimized to obtain an adequate separation of eluted compounds. Initially, various mobile phase compositions were tried to separate title ingredients. The objective of this study was to develop a rapid and sensitive RP-HPLC method for the analysis of FAV in bulk drug and pharmaceutical dosage form by using the most commonly employed C_{18} column with UV-detection. Initially, various mobile phase compositions were tried (numerous trials were performed) to elute the drug. From all the trials finally awesome reproducibility results, good peak shape, minimal peak

tailing and short runtime were identified when mobile consisting of Acetonitrile: Methanol: HPLC Grade water in the proportion of (50:40:10 v/v) and 1 mL/minute flow rate was selected. The retention time for FAV was found to be 2.794 min. The calibration was linear in the concentration range of 10 – 50 $\mu\text{g/mL}$ for FAV. Calibration graph of FAV is shown in Fig 2, and standard chromatograms of FAV are shown in Fig 3 – 3d. Specificity of the chromatographic method was tested by injecting sample concentration prepared from marketed formulation. The response was compared with that obtained from the standard drug. The chromatogram confirms the presence of FAV at 2.794 minutes without any interference. Precision study was determined to find out intra-day and inter-day variation in the test methods of FAV for 3 times on the same day. The % RSD of the intra-day and inter day precision obtained was <2 which indicates that the proposed method is precise. Method validation following ICH guidelines indicated that the developed method had high sensitivity with LOD of 1.0429 $\mu\text{g/mL}$ and LOQ of 3.1605 $\mu\text{g/mL}$. The robustness of an analytical method was determined by analysis of aliquots from homogenous lots by differing physical parameters such as change in flow

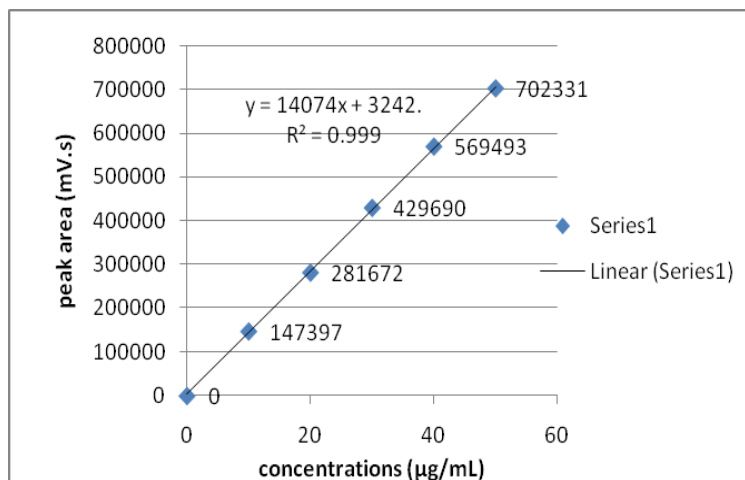


Fig 2. Calibration Graph of FAV by RP- HPLC

RP-HPLC Method for Determination

rate to 1.0 ± 0.2 mL and changing detection wavelength $365 \text{ nm} \pm 1 \text{ nm}$ and mobile phase composition change to $50:40:10 \text{ v/v} \pm 5 \text{ v/v}$. The obtained values were given in Table 6.

These values indicated that the method was quite robust. The proposed method was validated in accordance with ICH parameters and was applied for analysis of the same in

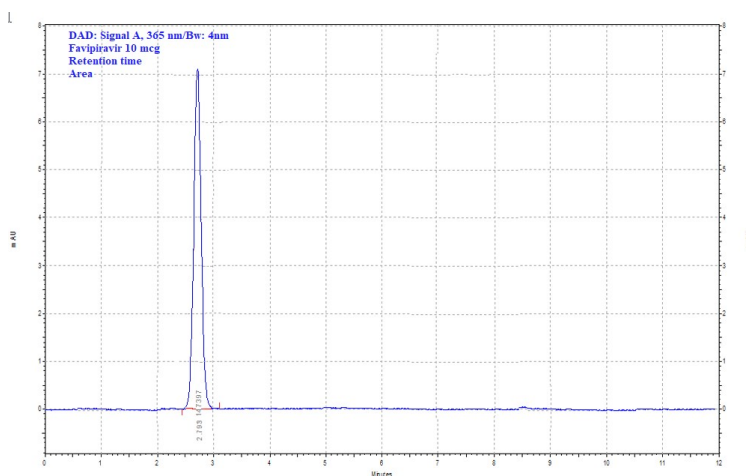


Fig 3. Standard Chromatogram of FAV (10 µg/mL)

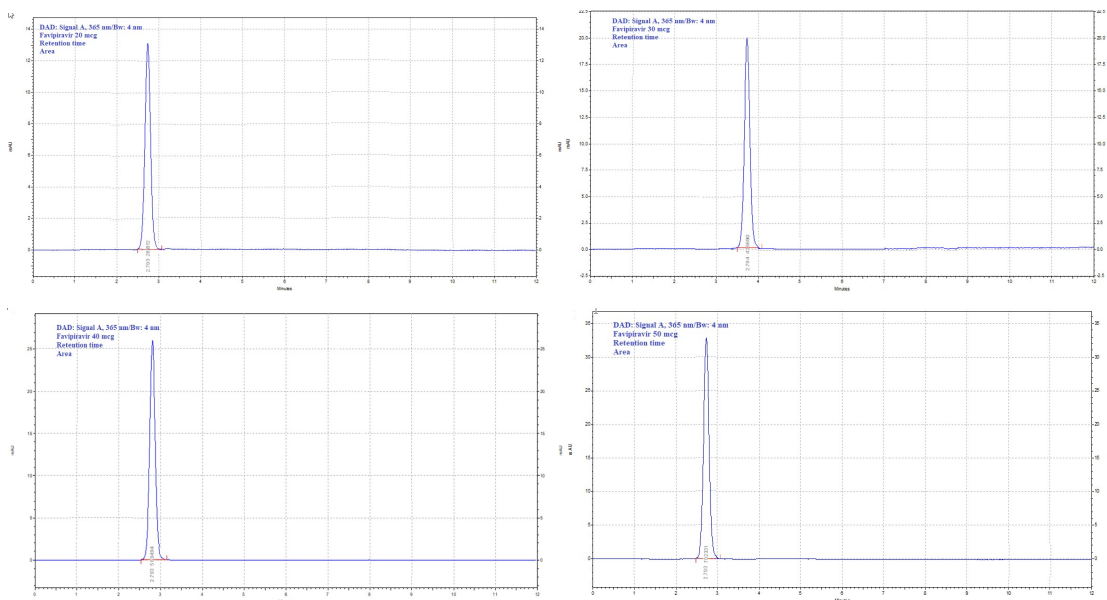


Fig 3. Standard Chromatogram of FAV (A) (20 µg/mL), (B) (30 µg/mL), (C) (40 µg/mL), (50 µg/mL)

RP-HPLC Method for Determination

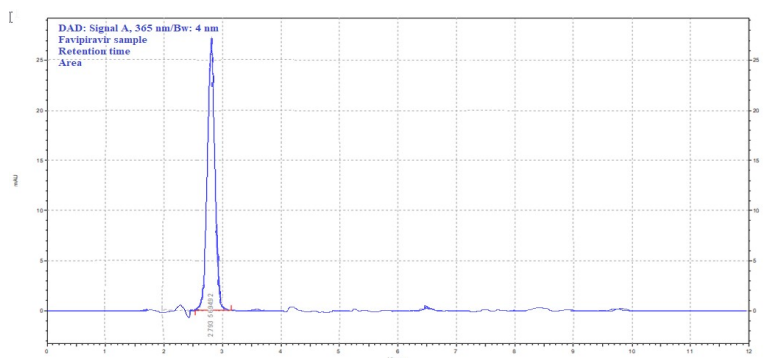


Fig 4. Sample Chromatogram of FAV

marketed formulations. The content of each component in the formulation was estimated by comparing the peak area of the test sample with that of the peak area of the standard which were found to be 99.85 % w/w for FAV sample chromatogram representing marketed formulation was shown in Fig 4. The development of an analytical method for the determination of drugs by Reverse Phase HPLC has received considerable attention in recent years because of their importance in quality control of drugs and drug products. Hence, the developed RP-HPLC methods can be adopted for the routine analysis of FAV in bulk and pharmaceutical dosage forms in quality control laboratories.

Conclusion

The present study demonstrated validated Reverse Phase High Performance Liquid Chromatography method for the determination of FAV available as tablet dosage form. The method was completely validated and showed satisfactory results. The method was free from interference of the other active ingredients and additives used in the formulation. The RP-HPLC method for the determination of FAV has various advantages like low solvent consumption, less retention time, excellent peak symmetry, highly sensitive, precise, accurate and robust. In fact, results of the study indicates that the developed methods were found to be accurate, precise, linear,

sensitive, simple, economical, reproducible have short run time which makes the method rapid. Hence it can be concluded that this method may be employed for the routine quality control analysis of FAV in active pharmaceutical dosage forms.

References

1. Ravi Sankar, P., Viswanath, A. (2020). Potential Anti-Covid-19 drug options. *Int.J. Pharm.Sci. Rev.Res*, 62(1): 199-204.
2. Jeevana Jyothi, B., Venkata Kavya, R. (2021). Ultraviolet spectrophotometric method development for estimation of new antiviral repurposing drug Favipiravir. *Asian journal of pharmaceutical repurposing drug Favipiravir*, Vol-14:67-69.
3. Mamdouh, R., Rezk Emad, B., Basalious, Kamal, A., Badr. (2021). A novel, rapid and simple UPLC-MS/MS method for quantification of favipiravir in human plasma: Application to a bioequivalence study. *Biomedical Chromatography*, 35(2): 1-9. <https://doi.org/10.1002/bmc.5098>.
4. Duygu Eryavuz Onmaz, Sedat Abusoglu, Mustafa Onmaz, Fatma Humeyra Yerlikaya, Ali Unlu. (2021). Development and validation of a sensitive, fast and simple LC-MS / MS method for the quantitation of favipiravir in human serum. *J Chromatogr B Analyt Technol Biomed Life Sci*, 1176:122768.

5. Morsy, M.I., Nouman, E.G., Abdallah, Y.M., Zainelabdeen, M.A., Darwish, M.M., Hassan, A.Y., Gouda, A.S., Rezk, M.R., Abdel-Megied, A.M., Marzouk, H.M. (2021). A novel LC-MS/MS method for determination of the potential antiviral candidate favipiravir for the emergency treatment of SARS-CoV-2 virus in human plasma: Application to a bioequivalence study in Egyptian human volunteers. *J Pharm Biomed Anal*, 199: 114057.
6. Hailat, M., Al-Ani, I., Hamad, M., Zakareia, Z., Abu, Dayyih, W. (2021). Development and Validation of a Method for Quantification of Favipiravir as COVID-19 Management in Spiked Human Plasma. *Molecules*, 26, 3789. <https://doi.org/10.3390/molecules26133789>.
7. Nadendla, R., Patchala, A. (2021). A Validated High Performance Liquid Chromatographic Method for the Quantification of Favipiravir by PDA Detector. *Int. J. Pharma Bio Sci*, 11(2), 181–188.
8. Ibrahim bulduk. (2021). HPLC-UV method for quantification of Favipiravir in pharmaceutical formulations. *Acta Chromatographica*, 1233-2356:33 (3):209-215.
9. Ravisankar, P., Naga Navya, Ch., Pravallika, D., Navya Sri, D. (2015). A review on step-by-step analytical method validation. *IOSR Journal of Pharmacy*, 5, 7-19.
10. Ravisankar, P., Gowthami, S., Devala Rao, G. (2014). A review on analytical method development. *Indian journal of research in pharmacy and Biotechnology*, 2, 1183-1195.
11. Ravi Sankar, P., Sai Geethika, A., Rachana, G., Srinivasa Babu, P., Bhargavi, J. (2019). Bioanalytical Method Validation. A Comprehensive Review. *Int. J. Pharm. Sci. Rev. Res.*, 56(1), 50-58.
12. Ravisankar, Panchumarthy., Anusha, S., Supriya, K., Ajith Kumar, U. (2019). Fundamental chromatographic parameters. *Int. J. Pharm. Sci. Rev. Res*, 55(2), 46-50.
13. Ravisankar, P., Abhinav, Pentyala., Baladatta Sai, Ch., Hemasri, P., Srinivasa Babu, P. (2021). Validation characteristics and statistics in analytical method development. *High technology letters*, 21(7),76-88.
14. ICH Q2 (R1), (2005). Validation of analytical procedures, Text, and methodology. *International Conference on Harmonization, Geneva*, 1-17.

Spectroscopic Analysis of DNA Binding Mode of Novel Schiff Base Vanadium Complex

Poonam R. Inamdar and A. Sheela*

¹Department of Pharmaceutical Chemistry, School of Pharmacy, Vishwakarma University, Pune, 411048, Maharashtra

²Department of Chemistry, School of Advanced Sciences, Vellore Institute of Technology, Vellore, 632014, Tamilnadu

*Corresponding Author: E-Mail Id: asheela@vit.ac.in

Abstract

Vanadium metal complexes based on wide range of the ligands have been explored at a greater extent for their various biological potential, in the recent times. Schiff bases are one of such fascinating ligands with donor sites varying according to the ketone or aldehyde group used. Based on these, a novel PS1V1, bis-vanadium complex was synthesized using schiff base backbone. It was characterized by using UV, FTIR, EPR and Mass spectral studies. The DNA binding ability of the characterized complex, PS1V1, was explored using UV and Fluorescence spectroscopic techniques. Furthermore, DNA binding mode of PS1V1 was also ascertained using competitive fluorescent displacement assay performed in the presence of minor groove binding agent, Hoechst.

Keywords: Vanadium complexes, Piperonal, Schiff base, DNA interaction, DNA binding

Introduction

Metal complexes have developed as Metallo drugs due to their multifaceted biological applications. The discovery of cisplatin, has paved a path in metallopharmaceutical field and chemotherapy as a DNA intercalator (1). The severe clinical side effects and thus limited therapeutic efficiency of platinum based drugs have triggered a research in other metal core compounds (2).

In current times, the application of the metal complexes as anti proliferative, apoptotic

and cytotoxic agents (3-6) has been reported in detail. Vanadium is a bio essential element, playing an important role in signal transduction. Currently, vanadium based metal complexes have been explored as chemotherapeutic compounds due to their wide scope of biological applications such as insulin mimetic (7,8), antibacterial (9), antioxidant (10) and anticancer (11,12) activities. Few diketone and hydrazone based vanadium complexes have also exhibited oxidative DNA cleavage and DNA binding efficacies (13,14). A number of piperonal based Schiff bases ruthenium(II) (15) complexes have been reported for cytotoxic activity.

We report, herein, the synthesis and characterization Schiff base based vanadium complex, PS1V1. Furthermore, its DNA binding mode has also been explored elaborately using spectroscopic techniques.

Experimental

Materials

All the chemicals were purchased from commercial sources and used without further purification for the experiments. 4-chlorobenzhydrazide, Piperonal (1,3-benzodioxole-5-carbaldehyde), Vanadyl acetyl acetone were purchased from Sigma Aldrich. All the solvents such as acetonitrile, methanol, ethanol and diethyl ether were purchased in AR grade and used. CT DNA, Tris HCl buffer and Hoechst 33258 were procured from Merck Genei.

Methods

Electronic spectra were recorded on a JASCO UVVIS-NIR-V-670 spectrophotometer.

FTIR spectra were measured using KBr pellets on a Shimadzu IR affinity-1CE model with resolution IV. MS spectra were recorded by GCMS instrument. EPR was recorded on a JEOL Model JES FA200 instrument. The fluorescence spectra were recorded on a Hitachi F-7000 FL Spectrophotometer UV absorbance of commercial calf thymus DNA in a buffer gave an absorption ratio (A260/A280) of about 1.9:1, indicating that the DNA was sufficiently free from protein. The concentration of DNA was determined using molar extinction coefficient of 6600M⁻¹cm⁻¹ at λ_{max} 260nm. All the experiments were carried out in a Tris buffer pH 7.2 in Milli-Q triply deionized water.

Synthesis of Ligand PS1

Methanolic solution of 4-chlorobenzhydrazide (1mmol) was added to the methanolic solution of piperonal (1mmol) and mixture was refluxed for an hour in the presence of acetic acid. The resultant pale yellow color hydrazone product was filtered and washed with petroleum ether. It was characterized using UV, FTIR, NMR and mass spectral studies.

Synthesis of Complex PS1V1

10 ml of hot methanolic solution of vanadyl acetyl acetone (1mmol) was added dropwise to the 10 ml of hot methanolic solution of ligand PS1 (3mmol). The reaction mixture was refluxed for 2h. PS1V1 = Yield: 58%. Green solid. Anal. Cald. For C₃₀H₂₆Cl₂N₄O₇V: C: 53.75, H: 3.01, N: 8.36. Found: C: 53.73, H: 3.00, N: 8.34. UV-Vis (methanol): λ_{max} (MeOH)/nm (ε, dm³mol⁻¹cm⁻¹) 220(79,850), 345(61,500), 680(6550). FT-IR (KBr, ν_{max}/cm⁻¹): 1649 (C=O), 1597 (C=N), 939 (V=O). ESI-MS Calcd for C₃₀H₂₆Cl₂N₄O₇V: 675.19, Found: 675.26.

DNA Binding Experiments

UV Absorption spectral titration experiments were carried out by monitoring the electronic spectrum of 20μM of the complex in the presence of varying CT-DNA concentrations (0 -120μM). The fluorescence study was carried out at the constant complex

concentration of 100 μM with varying concentrations of DNA from 0 to 120μM dissolved in Tris HCl buffer.

Results and Discussion

The complex Fig.1 were synthesized and characterized by spectral, elemental and analytical techniques and found to be air stable.

Ultraviolet spectroscopy

The UV-visible spectra of complex PS1V1 is shown in Fig. 2 The vanadium complex, PS1V1, has shown the intraligand π-π* transition at 220 nm and strong metal ligand charge transfer at 345 nm and the complex has shown d-d transitions at 680 nm.

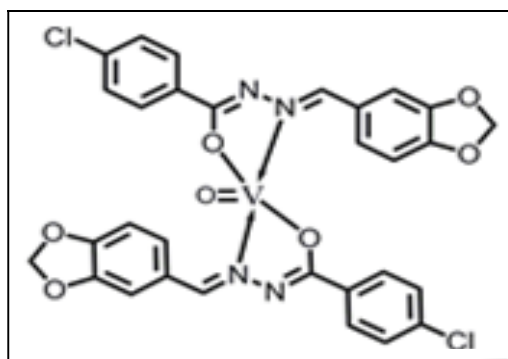


Fig 1. Structure of the Complex PS1V1

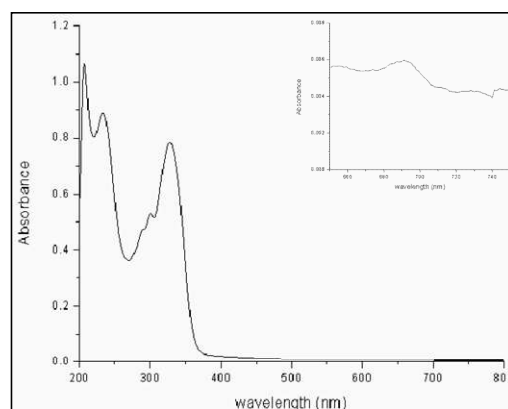


Fig 2. UV-Visible Spectrum of the Complex PS1V1

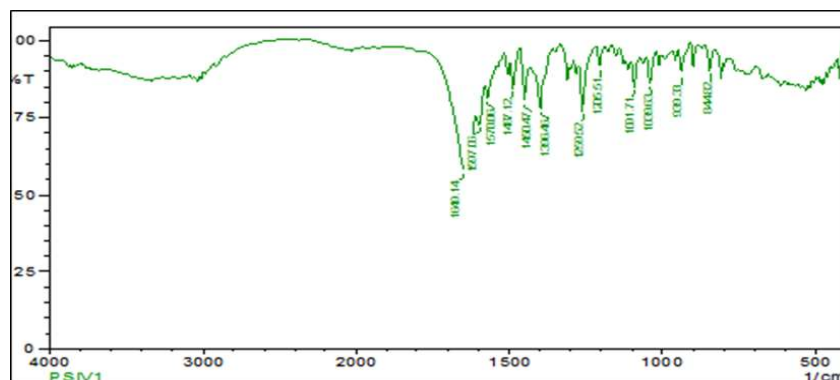


Fig 3. FTIR Spectrum of the Complex PS1V1

IR Spectral Analysis

The FTIR spectrum of complex PS1V1 is shown in Fig. 3. FTIR stretching band of carbonyl carbon was found to be significantly reduced at 1597cm^{-1} compared to the ligand PS1. The typical $\text{V}=\text{O}$ stretching frequency was observed at 939cm^{-1} .

EPR Spectra

The EPR spectra Fig. 4 for the complex in polycrystalline form at RT displayed g value of about 1.925.

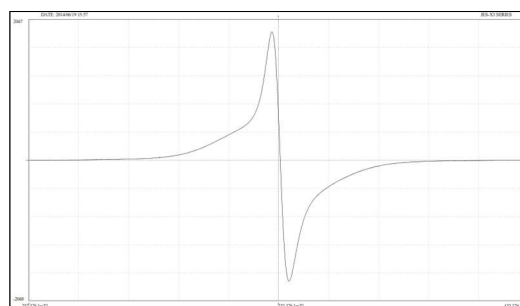


Fig 4. EPR Spectrum of the Complex PS1V1

Mass Spectral Analysis

The Mass spectrum of the complex is shown in Fig. 5. The mass spectrum of the complex was recorded in the methanol and M^+ peak was observed at 675.25 m/z

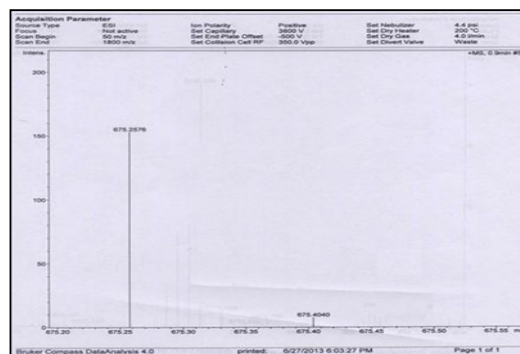


Fig 5. ESI MS Spectrum of the Complex PS1V1 (DNA) / $(\epsilon_a - \epsilon_f) = (\text{DNA}) / (\epsilon_a - \epsilon_f) + 1/ K_b (\epsilon_b - \epsilon_f)$

DNA Binding Studies

UV Absorption Titration

The binding mode of complex PS1V1 was assessed by UV absorption titration with calf thymus (CT) DNA. The UV spectra of $20\mu\text{M}$ solutions of in the absence and with successive increment of CT DNA are shown in Fig.6. The typical hyperchromic effect with negligible shifts in absorption maxima was observed in the bands of the complex (Fig. 6) indicating the groove binding nature. The intrinsic binding constant K_b with the help of the absorbance spectra of the same. K_b was calculated using the formula (16),

where, ϵ_a , ϵ_f and ϵ_b correspond to $A_{\text{obsd}}/(\text{PS1V1})$, the extinction coefficients for free vanadium complex and that of vanadium complex in fully bound form, respectively. Intrinsic binding constant for complex PS1V1 was found to $(2.05 \pm 0.09) \times 10^3\text{M}^{-1}$.

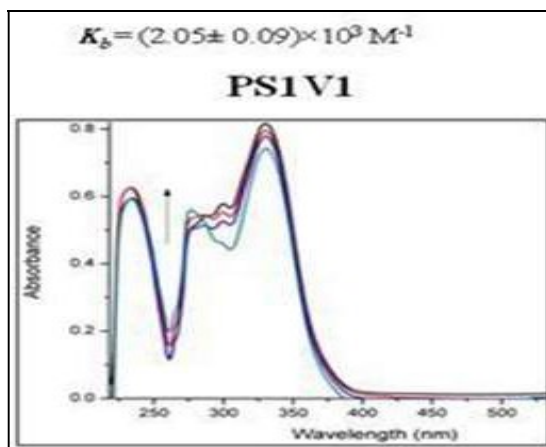


Fig 6. UV Absorption Spectrum of the Complex PS1V1 with CT DNA

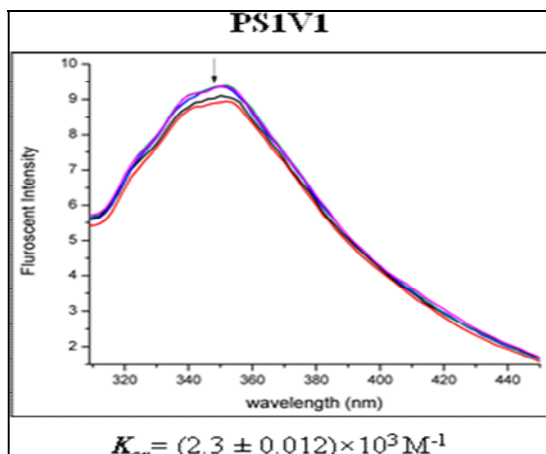


Fig 7. Fluorescence Emission Spectrum of the Complex PS1V1 with CT DNA

Fluorescence Spectral Studies

Emission spectral titrations were carried out to ascertain the binding mode of the complex PS1V1 with CT DNA. Complex PS1V1 was excited at 274nm. The emission maximum of the complex was observed in the presence of DNA. The successive addition of DNA resulted in the quenching of the emission intensities of both the complexes thus suggesting a groove binding mode rather than intercalation (Fig 7)

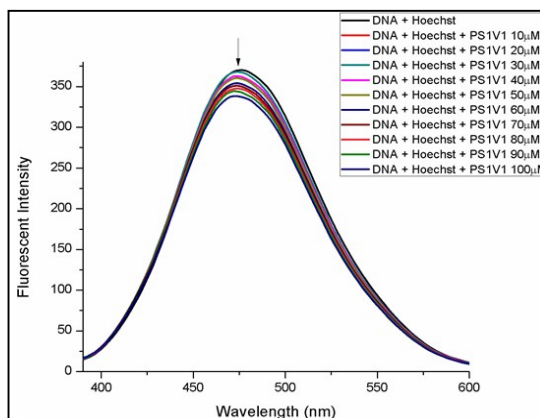


Fig 8. Fluorescence Emission Studies of the Complex PS1V1 in the Presence of Hoechst-DNA

supporting the results of absorption spectral studies. K_{sv} value for PS1V1 was found to be $(2.3 \pm 0.012) \times 10^3 M^{-1}$.

Competitive Fluorescence Displacement Assay

The Hoechst-CT DNA complex containing was excited at 355nm and fluorescence emission spectra were recorded at 480nm by titrating with increasing concentrations of complex. The quenching in the emission intensity of the Hoechst bound DNA was observed (Fig. 8), supporting a groove binding nature. K_{sv} value for PS1V1 was found to be $0.94 \times 10^3 M^{-1}$.

Conclusion

PS1V1, vanadium complex was synthesized based on Schiff base ligand and was characterized using UV, FTIR, EPR and Mass spectral studies. UV absorption titration of the complex PS1V1 with CT DNA suggested the groove binding mode. The fluorescence spectral titration with DNA also supported the groove binding mode of the complex. Later, Hoechst fluorescence displacement assay ascertained the minor groove binding mode of the complex, PS1V1, as the emission intensity of the hoechst-DNA complex was quenched at a greater extent.

Acknowledgement

The authors thank VIT, Vellore and Vishwakarma University for providing the necessary facilities to carry out the research work.

References

1. Rosenberg, B., Lippert, B. (1999). *Cisplatin: Chemistry and Biochemistry of a Leading Anticancer Drug*, Wiley-VCH, Weinheim, Germany, pp. 3-27.
2. Jung, Y., Lippard, S. J. (2007). Direct cellular responses to platinum induced DNA damage. *Chem Rev*, 107 : 1387-1407.
3. Jamshidi, M., Yousefi, R., Nabavizadeh, S. N., Rashidi, M., Haghghi, M. G., Niazi, A., Moosavi-Movahedi, A. (2014). Anticancer activity and DNA-binding properties of novel cationic Pt(II) complexes. *Int. J. of Biological macromolecules*, 66 : 86-96.
4. Khan, N.H., Pandya, Ch. Maity, N., Kumar, M., Patel, R. M., Kureshy, R.I., Abdi, S.H.R., Mishra, S., Das, S., Bajaj, H.C. (2011). Influence of chirality of V(V) Schiff base complexes on DNA, BSA binding and cleavage activity. *Eur. J. Med. Chem.* 46 : 5074-5085.
5. Dharmaraja, J., Subbaraj, P., Esakkidurai, T., Shobana, S. (2014). Coordination behavior and bio-potent aspects of Ni(II) with 2-aminobenzamide and some amino acid mixed ligands – Part II: Synthesis, spectral, morphological, pharmacological and DNA interaction studies. *Spectrochim. Acta A*. 132: 604–614.
6. Arjmand, F., Muddassir, M., Yousuf, I. (2014). Design and synthesis of enantiomeric (R)- and (S)- copper (II) and diorganotin (II)-based antitumour agents: Their in vitro DNA binding profile, cleavage efficiency and cytotoxicity studies. *J. Photochem. Photobio. B*. 136 : 62-71.
7. Sheela, A., Mohana Roopan, S., Vijayaraghavan, R. (2008). New diketone based vanadium complexes as insulin mimetics. *Eur. J. Med. Chem.* 43: 2206-2210.
8. Sheela, A., Vijayaraghavan, R. (2010). A study on the glucose lowering effects of ester-based oxovanadium complexes. *Transition Met. Chem.* 35 : 865-870.
9. Raman, N., Selvan, A. (2011). DNA interaction, Enhanced DNA photocleavage, electrochemistry, thermal investigation and biopotential properties of new mixed-ligand complexes of Cu(II)/VO(IV) based on Schiff bases. *J. Mol. Str.* 985 : 173-183.
10. Sheela, A., Sarada, N.C., Vijayaraghavan, R. (2013). A possible correlation between antioxidant and antidiabetic potentials of oxovanadium(IV) complexes. *Med. Chem. Res.* 22 : 2929-2937.
11. Balaji, B., Somyajit, K., Banik, B., Nagaraju, G., Chakravarty, A. R. (2013). Photoactivated DNA cleavage and anticancer activity of oxovanadium(IV) complexes of curcumin. *Inorg. Chim. Acta.* 400 : 142-150.
12. Jabeen, M., Ali, S., Shahzadi, S., Sharma, S. K., Qanungo, K. (2014). Synthesis, characterization, theoretical study and biological activities of oxovanadium(IV) complexes with 2-thiophene carboxylic acid hydrazide. *J. Photochem. Photobio. B* 136 : 34-45.
13. Inamdar., P.R., Sheela. A. (2015). Exploration of DNA binding mode, chemical nuclease, cytotoxic and apoptotic potentials of diketone based oxovanadium(IV) complexes. *Int. J Bio Macro.* 76 : 268-278
14. Inamdar., P.R., Sheela. A. (2017). DNA binding behaviour of mixed ligand vanadium(V) complex based on novel tridentate hydrazone and benzhydroxamic acid ligand systems. *Applied Organometallic Chem.* 31: 3573.
15. Beckford, F.A., J. Thessing, M. Shaloski Jr., P. C. Mbarushimana, J. Didion, J. Woods, A. Gonzalez-Sarrías, N. P. Seeram and A. Brock. (2011). Synthesis and characterization of mixed-ligand diimine-piperonal thiosemicarbazone complexesruthenium(II): Biophysical investigations and biological evaluation as anticancer and antibacterial agents. *J. Mol. Struct.*, 992 : 39-47.
16. Neidle., S. (2001). DNA minor groove recognition by small molecules. *Nat. Prod. Rep.* 18 : 291-309.

Anti-Tubercular Activity of Neem Flower Extract

K. Purna Nagasree*, B. Hima Bindu, I. Priyanka, T. Divya and
S. Mansha Afroz

¹Department of Pharmaceutical chemistry and analysis, Raghu College of Pharmacy,
Visakhapatnam –531162, Andhra Pradesh, India

²Department of Pharmaceutical chemistry, Vignan Institute of Pharmaceutical Technology,
Visakhapatnam – 530049, Andhra Pradesh, India

*Corresponding author: E-mail id: kpurna2104@gmail.com

Abstract

Neem – *Azadirachta indica*, has been used in ayurvedic medicine for more than 4000 years due to its medicinal properties. Neem has many biological activities like anti-inflammatory, anti-fungal, anti-bacterial, anti-oxidant and anti-viral etc. In our research, we collected neem flowers and shade dried them. The flowers were extracted using ethanol solvent. Initially weighed quantities of shade dried flowers (100g) were soaked in ethanol (500mL) for 48hrs. Then the soaked mixture was filtered and flowers are kept aside. The ethanol is separated from the extract using rotavapour at a temperature of 120°C. The thick extract was collected at the end and stored separately. Flowers were soaked again with ethanol for 24 hrs and the process was continued. All the collected extracts were combined and chemical analysis was done to find out the presence of chemical constituents like triterpenoids, phenols, flavonoid etc. Anti-tubercular activity was performed using MABA method for the ethanolic extract of neem flowers with a standard rifampicin. The MIC of the standard was found to be 12.5 µg/mL, whereas the MIC of neem flower ethanolic extract was found to be 25 µg/ml.

Keywords Neem flower, Ethanolic extract, Anti-tubercular activity, MABA, MIC, Rifampicin

Introduction

Neem or Margosa is a botanical cousin of mahogany. It belongs to the family

Meliaceae. The latinized name of Neem – *Azadirachta indica* - is derived from the Persian. It has great potential in the fields of pest management, environment protection and medicine. Neem tree is about 12-18 metres in height with a circumference up to 1.8-2.4 metres (1). Neem is a flowering plant which will produce flower on 3-5 years of age in which the flowers are 4-7mm in length and 6-10mm in width. The neem tree can be found growing in countries located in the equatorial belt. Two species of *Azadirachta* have been reported, *Azadirachta indica* A. Juss – native to Indian subcontinent and *Azadirachta excelsa* Kack. – confined to Philippines and Indonesia (2). The most important active constituent is Azadirachtin and the others are Nimbolin, Nimbin, Nimbidin (3), Quercetin and β-sitosterol (4).

Materials and Methods

Neem flowers were taken and shade dried. The solvent used was ethanol AR.

Extraction Procedure of Neem Flower

500 ml round bottomed flask was taken, to this added 50gm of shade dried neem flowers and soaked in 250ml ethanol for 48hrs. The above mixture was refluxed for 10 mins. Cooled and filtered the mixture and collected the filtrate. Poured this filtrate into pear shaped flask and fixed this to rota evaporator in Fig. 1. Rotavapour apparatus (Roteva) was set with temperature below the boiling point of ethanol (78.37°C). Set the specific rotation to 70 rpm, after stabilization



Fig 1. Shade dried Neem flowers soaked in ethanolic extract in round bottomed flask



Fig 2. Rotavapour (Roteva)

and switch on the vacuum (Equitron vacuum pump- 40 mbar). Separated ethanol solvent was collected and poured into flowers for re-extraction in Fig. 2.

Measure the extract and ethanol volume, extract was kept aside. The obtained ethanol was poured into the pre soaked neem

flowers. It was soaked again for 24 hrs, again the extract and solvent are separated. The above process was repeated with 5 batches of neem flowers with each batch weighing 50 gm. All the collected extracts were combined and kept at room temperature.

Results and Discussion

Test For Chemical Constituents

Test for Flavonoids(5)

1ml of ethanolic extract of plant material was taken in a test tube and added few drops of dilute NaOH. An intense yellow colour was observed in the test tube and it becomes colourless on addition of few drops of dilute acid. This shows the presence of Flavonoids.

Test for Triterpenoids(6)

5 ml ethanolic extract was dissolved in 2 ml chloroform and 1ml acetic anhydride was added. Concentrated sulphuric acid was added to the above solution. Formation of reddish-violet colour appeared. This shows the presence of Triterpenoids.

Test for Phenols(7,8)

Take 3 ml of ethanolic extract of neem flowers in a test tube, add freshly prepared ferric chloride solution in it drop wise, Blue colour appeared. This indicates the presence of Phenols.

Anti Tubercular Activity

Maba Method

A blue colour in the well was interpreted as no bacterial growth and pink colour was scored as growth(9). The MIC was defined as lowest drug concentration which prevented the colour change from blue to pink(10). From the extract of neem flower we got comparable results with the standard drug rifampicin. Rifampicin has showed the anti tubercular activity i.e 25 µg/ml in Fig. 3. The anti- mycobacterial activity of the ethanolic extract of neem flowers could be due to its



Fig 3. MABA METHOD- Standard Drug : Rifampicin 12.5 µg/ml

chemical constituents like flavonoids, triterpenoids or phenols. The preliminary evaluation gave a positive result with these chemical constituents.

Conclusion

The neem extract MIC was 25 µg/ml compared to that of standard first line drug i.e Rifampicin 12.5 µg/ml. The chemical constituents identified were triterpenoids, flavanoids, phenols.

Acknowledgements

The authors are thankful to Mr. K. Raghu, Dr. Jagadeesh Panda and Dr. L. Rataiah for providing the necessary facilities.

References

1. Ogbuewu IP, Odoemenam VU, Okoli IC.(2011).The Growing importance of in agriculture, industry, medicine and environment. *Res J Med Plant*, 5: 230-245.
2. Glri RP, Ajit, Sucheta.(2019). Neem the wonder herb. *Int j trend res dev*,3: 2456-6470.
3. Nassem F, Aparna M. (2019). An update on therapeutic potential if neem and its active constituents. *Era's j med res*, 6: 369-410.

4. Ahmad E, NidalJ. (2017). A review of chemical constituents and traditional usage of neem plant. *Palest med pharm j*, 2: 75-81.

5. Shrirangasami SR, Murugaragavam, Rakesh SS. (2020). Chemistry behind in neem (*A.indica*) as medicinal value to living form. *Jpharmacognphytochem*,9: 467-469.

6. Syed TA, Siddiqui S, Bina, Muhammed NK. (2003). Chemical constituents of the flowers of *Azadirachta.indica*. *HelvChimActa*, 86: 2787-2796.

7. Mohammad AH, Qasim AR. (2013). Study of total phenol, flavonoids contents and phytochemical screening of various leaves crude extracts. *Asian Pac J Trop Biomed*, 3: 705-710.

8. Constantine SD. (2007). Extraction, separation, and detection methods for phenolic acids and flavonoids. *J SepSci*, 30:3268-3295.

9. Mebly MA, Laura A. (2012). The use of the MABA to assess the susceptibility of *mycobacterium* to anti-leprosy and other drugs. *J InfectChemother*, 18: 652-661.

10. Mario J, Luis L. (2013). The MABA approach: A new option to improve bronchodilator therapy. *Eur Respir J*, 42: 885-887.

Comparative Effects of *Ocimum tenuiflorum* and *Ocimum basilicum* on Isoniazid Microsphere Formulation Characteristics Prepared by Different Methods

Rupali A. Patil, Prashant L. Pingale* and Sunil V. Amrutkar

Sir Dr. M. S. Gosavi College of Pharmaceutical Education and Research,
Nashik-422005

*Corresponding Author: E-mail Id: prashant.pingale@gmail.com

Abstract

Due to difficulties such as bacterial resistance, unpleasant effects, and low patient compliance with anti-tubercular drugs, tuberculosis treatment remains a challenge. Microspheres are a sort of multiparticulate drug delivery system that is used to distribute a drug for a longer period of time, boost bioavailability or stability, and target specific locations. Isoniazid is an important first-line anti-tubercular drug used in tuberculosis treatment in a fixed-dose combination. We attempted a unique way to address the above-mentioned obstacles of tuberculosis therapy by merging both these methodologies of microspheres and bioenhancers in the current work. Bioenhancers are 'bioavailability enhancers,' which have no therapeutic effect but enhance the action of drug molecules when administered in combination. The comparative effect of *Ocimum tenuiflorum* and *Ocimum basilicum* as a bioenhancer was studied and compared to a formulation without bioenhancers. Two processes are used to make microspheres: Complex Coacervation and Modified Emulsion Method. *In-vitro* release, drug entrapment efficiency, % bioadhesion, and permeability of the microspheres were all assessed using the intestinal sac method. *In-vitro* drug release from formulations containing *Ocimum tenuiflorum* and *Ocimum basilicum* as bioenhancers was reported to be around 56-84% in 12 hours. The microspheres were discovered to be smaller than 120 microns in

diameter. The DEE was shown to be between 39-78%. The bioadhesion of the microsphere was determined to be 38-82% (increased in formulations where bioenhancers incorporated). The major findings of the USP paddle apparatus *in-vitro* release study concern the extraordinarily large increase in drug release due to the presence of bioenhancers.

Keywords: Microspheres, Double emulsion method, Complex coacervation method, Isoniazid, *Ocimum tenuiflorum*, *Ocimum basilicum*

Introduction

Tuberculosis is a leading source of illness and mortality around the world. Every year, over 2 million people are killed by the disease. Treatment regimens now offered are lengthy, putting excessive demands on destitute people. As a result, the tide of medication resistance is rising. The flexibility to adapt drug release rates to the needs of a specific application, as well as the capacity to dispense at a constant or pulsatile rate, are two potential advantages of the drug delivery system. It safeguards medications, particularly proteins, from being rapidly destroyed by the body. By substituting occasional (once a month or fewer) injections for regular (e.g., daily) injections, microspheres with controlled release systems might increase patient comfort and compliance (1).

As a result, using bioenhancers in combination therapy to improve release performance and, eventually, maximise their effectiveness while using microspheres as a drug

delivery vehicle would be an appropriate formulation method for optimising anti-tubercular drugs' pharmacokinetic properties [2].

Bioenhancers are substances that, when taken with an active medicine, increase the drug's pharmacological activity while having no therapeutic benefit. The use of herbal ingredients to improve drug bioavailability has resulted in a major paradigm shift in therapeutics. Bioenhancers increase permeability and alter drug bioavailability for therapeutic efficacy, which may lead to a reduction in dose while maintaining therapeutic availability. Anti-TB drug therapy has a number of difficulties, including loss of efficacy due to bacterial resistance, unpleasant effects, and low patient compliance. C.K. Atal looked at a list of Ayurvedic compositions used to treat a variety of diseases in ancient India. He noticed that the majority of Ayurvedic formulations contained Trikatu or one of its ingredients, Piper longum (*P. longum*), which is used to cure a variety of diseases (210 formulations out of 370 tested). In the cited study effort, we aimed to address the aforementioned issues by merging the principles of microsphere drug delivery (enhanced bioavailability) with herbal bioenhancers with improved bioavailability [3,4].

Basils (*Ocimum* spp., Lamiaceae) have a variety of essential oils that are high in phenolic compounds, linalool, and other natural products. Basil leaves are dried and used to season stews, sauces, salads, soups, meat, and tea [5,6].

The objectives of cited research work are to:

- formulate isoniazid sustained-release microspheres using a variety of approaches.



Fig 1A. Leaves and Dried Powder of A. *Ocimum Tenuiflorum*; B. *Ocimum Basilicum*

Ocimum Tenuiflorum and *Ocimum Basilicum*

- Study the effect of varying concentrations of herbal bioenhancer (extracts of *Ocimum tenuiflorum* and *Ocimum basilicum*) on *in-vitro* drug release from microspheres, and assess the impact of different processing parameters on microsphere characteristics.

Materials and Methods

Methods

Two methods were used to prepare microspheres including complex coacervation and a modified emulsion method.

Materials

Isoniazid was received as a gift sample from Lupin Pharmaceuticals Ltd., Aurangabad, Maharashtra, as a model anti-tubercular drug. *Ocimum tenuiflorum* (OT) and *Ocimum basilicum* (OB) were obtained from the herbal medicinal garden and authenticated by Department of Botany, SSVPS's Dr. P. R. Ghogrey College of Science in Dhule, Maharashtra. As a bioenhancer, hydro-alcoholic extracts of *Ocimum tenuiflorum* were used. Sodium alginate and Type B gelatin (bloom strength 220) were procured from Loba Chemie, Mumbai. Sigma Aldrich, Germany, provided the sodium tripolyphosphate and Chitosan. All of the other chemicals and polymers that were employed were of analytical quality.

Experimental Work

Extraction and Isolation of *Ocimum Tenuiflorum* (OT) and *Ocimum Basilicum* used as Bioenhancer:

Different components (leaves, stem, flower, root, seeds, and sometimes the entire

plant) of *Ocimum tenuiflorum* and *Ocimum basilicum* are used in traditional medicine in Fig. 1.

The leaves of *Ocimum tenuiflorum* and *Ocimum basilicum* were harvested between October and December and compared to a reference sample. The 50 % ethanolic extract was made by combining 500 g of dried, crushed, and powdered tulsi leaves with 1000 mL of 50 % ethanol in a round bottom flask and keeping it at room temperature for three days in the shade. After filtering the extract, the operation was performed twice more. The resulting extract filtrate was collected and evaporated on a water bath until dry. The yield of extract was approximately 5.00 % w/w [7].

Phytochemical Evaluation of *Ocimum Tenuiflorum* and *Ocimum Basilicum*: The phytochemical examination of dried leaves of Holy basil was carried out according to Ayurvedic Pharmacopoeia [8] provisions for several criteria (Table 1).

Preparation of Isoniazid Microspheres: Sustained release microspheres can be made using a variety of techniques, including emulsion cross-linking and multiple emulsions [9]. This microsphere was prepared using the double emulsification method and complex coacervation method in this investigation.

Method 1 - Complex Coacervation Method (CCM): In a 1:05 ratio, chitosan and gelatin were mixed in a dilute acetic acid solution (1

% v/v) at 3 % w/v and pH adjusted to 5.0. Isoniazid (150 mg) was dissolved in the polymeric mixture mentioned. At 40°C, the medicine in the polymeric mixture was emulsified with 1 mL Tween 80 (2 % w/v) in 100 mL liquid paraffin (1:1 ratio of light and heavy liquid paraffin). A mechanical stirrer was used to emulsify the mixture for 15 minutes at 1200 rpm (Remi Motors, India).

To induce gelatin coagulation, the resulting w/o emulsion was refrigerated to 4°C. Then, at 4°C, 50 ml Na-TPP (1.5 % w/v) with pH 5 was added drop by drop. Stirring was continued for another 30 minutes to obtain cross-linked microspheres. Centrifugation was used to collect microspheres, which were then washed three times with double distilled water, dried at room temperature under vacuum, and washed three times with acetone to remove water. The microspheres were created and stored in a desiccator for further study. Polymer concentration, polymer: copolymer ratio (Chitosan: Gelatin B), cross-linking period, and rpm were all factors in the formulation optimization [10,11]. Components of an optimal formulation comprising varied concentrations of hydroalcoholic extract of *Ocimum tenuiflorum* and *Ocimum basilicum* as a bioenhancer are shown in Table 2.

Method 2 - Double Emulsification Method (MEM): 150 mg isoniazid dissolved in a 3% sodium alginate aqueous solution (10 ml). The aqueous phase was emulsified in light liquid paraffin (in the ratio 1:10) containing 1% (v/v) Span 80 for 45 minutes using a

Table 1: Phytochemical Evaluation of *Ocimum Tenuiflorum* and *Ocimum Basilicum*

Parameter	Value (%w/w)	
	<i>Ocimum Tenuiflorum</i>	<i>Ocimum Basilicum</i>
Total Ash	8.5	8.9
Acid insoluble ash	1.1	1.5
Water soluble ash	3.9	4.4
Loss on drying	3.9	4.7
Swelling index	10 ml	12 ml
Water absorption capacity	10 ml	12.7 ml

Ocimum Tenuiflorum and *Ocimum Basilicum*

mechanical stirrer (Remi Motors, India). 5 ml of 7.5 % calcium chloride dissolved in a 1:1 mixture of methanol and isopropyl alcohol was slowly added to the emulsion and agitated to ensure successful crosslinking. Microspheres were collected via vacuum filtration, then washed three times in isopropyl alcohol before being dried at ambient temperature. Variables like polymer concentration, drug-polymer ratio, cross-linking agent concentration, and cross-linking time were used to optimise the formulation [10,11]. Finally, different concentrations of hydro-alcoholic extracts of *Ocimum*

tenuiflorum and *Ocimum basilicum* were added to the optimised formulation to investigate their effect on drug bioavailability (Table 3).

Characterization of Microspheres

Compatibility Studies: Fourier Transform Infrared Spectroscopy was used to investigate any chemical interactions between the medication and the polymeric substance during the creation of the microspheres (FTIR). Pure drug INH, placebo microspheres, and INH microspheres (2-5 mg) manufactured with and without bioenhancer were weighed and combined appropriately with potassium

Table 2. Isoniazid Microsphere Formulations with Various Polymers and Hydroalcoholic Extract of Bioenhancer Ratios (Complex Coacervation Method)

Formulation Code	INH (mg)	Gelatin:Chitosan (ratio)	Sodium TPP (%)	Cross Linking Time (min.)	BE1 (mg)	BE2 (mg)
CI1	150	0.5:1	1	30	--	--
CI2	150	0.5:1	1	30	5	--
CI3	150	0.5:1	1	30	10	--
CI4	150	0.5:1	1	30	15	--
CI5	150	0.5:1	1	30	--	5
CI6	150	0.5:1	1	30	--	10
CI7	150	0.5:1	1	30	--	15

Table 3. Isoniazid Microsphere Formulations with Various Polymers and Hydroalcoholic Extract of Bioenhancer Ratios (Double Emulsification Method)

Formulation Code	INH (mg)	Sodium Alginate (%)	CaCl ₂ (%)	Cross Linking Time (min.)	BE1 (mg)	BE2 (mg)
MI1	150	3	7.5	45	--	--
MI2	150	3	7.5	45	5	--
MI3	150	3	7.5	45	10	--
MI4	150	3	7.5	45	15	--
MI5	150	3	7.5	45	--	5
MI6	150	3	7.5	45	--	10
MI7	150	3	7.5	45	--	15

MI- Isoniazid microspheres by modified emulsion method, IHN- Isoniazid,
 BE₁- Bioenhancer 1 i.e., hydroalcoholic extract of *Ocimum tenuiflorum* (OT)
 BE₂- Bioenhancer 2 i.e., hydroalcoholic extract of *Ocimum basilicum* (OB)

Ocimum Tenuiflorum and *Ocimum Basilicum*

bromide to make a homogeneous mixture (0.1 to 0.2 g). A small amount of powder was crushed into a thin semi-transparent pellet by applying pressure to it. The pellet's IR spectrum was recorded with FTIR (Perkin Elmer, USA, Spectrum RX1 Model) with air as the reference, and the findings were compared to check if there was any drug-excipient interaction [12].

Particle Size Analysis: The particle size of both plain medicine microspheres and microspheres with bioenhancer was evaluated using a Motic microscope at 40 X magnification. In each of the measurements, at least 100 particles were evaluated in each of the three fields [10,11].

Percent Drug-Entrapment Efficiency: The drug content of the microspheres was evaluated spectrophotometrically (max = 263 nm; Perkin Elmer, USA Lambda 25 model) to estimate the percentage drug entrapment. Sonication was used to dissolve isoniazid-loaded microspheres (10 mg) in 10 ml of isotonic phosphate buffer pH 6.8 for 20 minutes. After filtering the solutions with 0.22 µm Millipore filters, the amount of isoniazid was determined [13]. According to preliminary UV measurements, the presence of dissolved polymers had no effect on the drug's absorbance at 263 nm. The % drug entrapment was calculated using following formula:

$$\text{Percent drug entrapment} = \frac{\text{Mass of drug present in microparticles}}{\text{Mass of drug used in the formulation}} \times 100$$

Percentage Yield: The yield of microspheres was calculated by comparing the total weight of microspheres produced to the total weight of the polymer, drug, and bioenhancers employed in the formulation [14]. The microsphere % yield was calculated using the following formula:

$$\text{Percentage yield} = \frac{\text{Weight of microspheres obtained}}{\text{Total weight of drug, polymer used in formulation}} \times 100$$

Measurement of Bioadhesion: The in-vitro bioadhesion of microspheres (in triplicate) was determined using the falling liquid film method. Microspheres (50 mg) were spreaded over small intestine of albino rat (area 2cm²) and detained for 20-30 minutes in a humidity temperature-controlled cabinet (Thermolab, India) at 75%RH and 25°C to allow the microspheres to hydrate. After that, the mucosal lumen was thoroughly washed with isotonic phosphate buffer pH 6.8 and dried at 70°C in a hot air oven [15].

The following formula was used to calculate the percentage of bioadhesion:

$$\text{Percentage bioadhesion} = \frac{\text{Weight of adhered microspheres}}{\text{Weight of applied microspheres}} \times 100$$

In-vitro Drug Release: The release characteristics of isoniazid from microspheres were examined in simulated gastric fluid (SGF pH 1.2) and simulated intestinal fluid (SIF pH 6.8). The drug-loaded microspheres (equivalent to 10 mg isoniazid) were put in empty capsule shells and spun at 50 rpm in 500 ml of 37°C dissolving fluid. At regular intervals, the aliquots (2 ml) were extracted and replaced with fresh media [16]. The drug content was measured spectrophotometrically at 263 nm after the samples were diluted and filtered.

Statistical Analysis: The results were statistically analysed using the Student's t-test. The zero order, first order, and Higuchi's matrix models were used to compare the *in vitro* release profile [17].

Result and Discussion

FTIR Study: INH had a significant C=O stretch band (Amide I) around 1650 cm⁻¹ and an Amide II due to N-H bend around 1620 cm⁻¹ in its FT-IR spectrum. The FT-IR spectrum of the drug-loaded microspheres, on the other hand, entirely obscured these peaks. Isoniazid drug release *in-vitro* from formulations containing bioenhancer extract was reported to be 85-90% in 12 hours. In formulations without bioenhancers, the similar percentage was

around 45-50%. Other characteristics were investigated as well, such as % bioadhesion and permeability testing utilising the intestinal sac method.

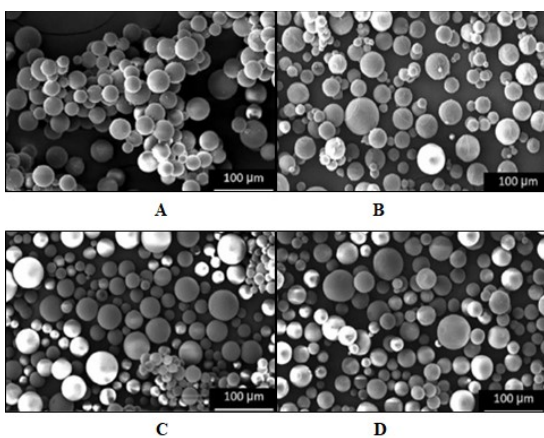


Fig 2. Microspheres by: A, B Complex Coacervation and C, D. Modified Emulsification Method using OT and OB as a Bioenhancer Respectively

Differential Scanning Calorimetry: An empty aluminium pan was utilised as a reference and an isoniazid powder sample (2-8 mg) was weighed into an aluminium pan and assessed as sealed with pinholes. The heat-cool-heat cycle was also utilised to assess the thermodynamic relationship between two forms. At 70°C, the DSC endotherm exhibited a strong melting endotherm. The DSC curve of INH revealed an endothermic event between 50 and 80°C which was connected to the material's dehydration.

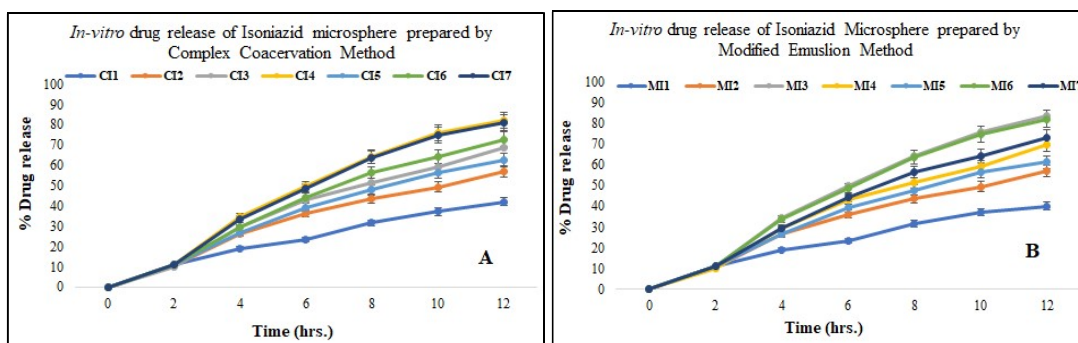
Particle Size: The microspheres were found to have a smoother surface and were distinct and spherical in shape; the morphology of drug-loaded microspheres should not alter as shown in Fig. 2. As indicated in Table 4, the mean particle size of the microspheres generated by the complicated coacervation process was 100-120µm.

Percentage Yield: To estimate the yield of microspheres, the total weight of microspheres collected was compared to the weight of the drug, polymers, and bioenhancer.

Table 4. Isoniazid Microspheres Evaluation Parameters Using Modified Emulsion and Complex Coacervation Method

Formulation Code	Mean Particle Size (µm)	Yield (%) ±SD	Drug Entrapment (%) ±SD	Bioadhesion (%) ±SD	Drug Release (at 12 th hr.) % ±SD
CI1	113-118	35.25±1.01	40.07±0.73	38.17±0.19	42.15±1.11
CI2	112-116	46.25±1.11	60.13±0.47	53.87±1.02	56.81±0.94
CI3	103-108	57.42±1.01	62.21±1.07	66.41±0.98	68.96±1.21
CI4	104-110	69.11±0.79	77.10±0.31	81.91±0.54	82.16±0.81
CI5	111-118	49.17±1.07	51.96±0.72	58.47±0.29	62.64±0.87
CI6	103-108	62.66±0.42	66.18±0.49	66.94±1.07	72.71±0.68
CI7	106-112	69.18±1.01	76.11±0.87	80.41±0.91	81.11±0.53
MI1	116-120	34.25±0.25	39.11±0.37	38.01±0.49	40.17±0.33
MI2	111-114	49.25±1.07	59.87±0.74	53.11±1.22	57.15±1.04
MI3	101-108	71.50±0.19	78.01±0.13	82.50±0.45	83.61±0.18
MI4	108-113	59.24±1.17	64.12±1.11	67.14±0.89	69.71±1.07
MI5	109-114	51.24±0.97	53.69±1.27	59.14±0.92	61.46±0.99
MI6	100-105	71.11±0.39	76.89±1.17	81.14±1.11	82.17±0.33
MI7	106-112	63.16±1.24	67.01±0.94	67.49±1.17	73.17±0.86

Ocimum Tenuiflorum and Ocimum Basilicum



Coacervation and Modified Emulsion Method

Fig 3. *In vitro* Drug Release from Isoniazid Microspheres Prepared by Complex

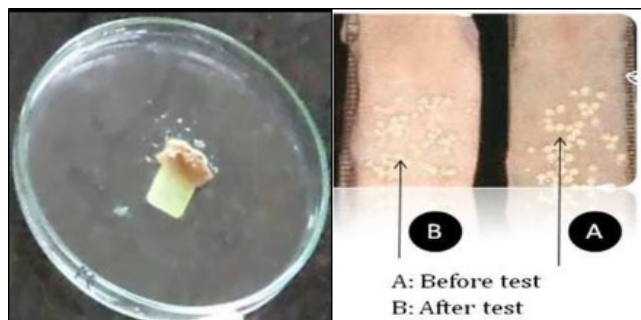


Fig 4. Bioadhesion Study of Isoniazid Microspheres

The percentage yield of the optimised formulations, which spans from 34.50 to 71.50%, is shown in Table 4. Losses accounted for throughout the microsphere hardening, washing, and filtering procedures could account for the loss of medicine in the strategy.

Percent Entrapment Efficiency: The entrapment efficiency was determined to be between 39.50 to 78.14%. The loss of the medication in these approaches could be attributed to the hardening, washing, and filtration processes. As demonstrated in Table 4, during microsphere formulation optimization, polymer concentration, cross-linker concentration, and cross-linking time may have an impact on microsphere entrapment efficiency. The maximum entrapment efficiency values obtained are

higher, or at least comparable, to the highest value reported in prior microsphere formation studies using sodium alginate. The discrepancy is attributable to high water solubility of isoniazid, which results in high drug concentrations in the preparation medium in this approach, as well as the usage of bioenhancer in formulations.

Percent Bioadhesion: The presence and amount of bioenhancer had a substantial impact on the bioadhesion of the microspheres in the optimised formulations. The bioadhesion investigation was carried out using a previously documented method (in triplicate). The percentage bioadhesion ranged from 38.50 to 82.95% in Table 4. Microspheres with bioenhancers have a higher bioadhesive property (Fig. 3) than microspheres without bioenhancers (Fig. 4). The bioadhesive

characteristics of microspheres resulted in long-term retention in the small intestine. It was revealed that microspheres that included a higher concentration of bioenhancer had a 45% increase in bioadhesion. Furthermore, as seen in Table 4, as the amount of bioenhancer increases, the percentage bioadhesion increases. Because of their bioadhesive properties, these particles were able to stay in the small intestine for a long time.

In vitro Drug Release: Figures 4A and 4B show the in-vitro release behaviour of isoniazid microspheres generated by a modified emulsification and complicated coacervation approach using *Ocimum tenuiflorum* and *Ocimum basilicum* as a bioenhancer in simulated gastric fluid (SGF), pH 1.2, and simulated intestinal fluid (SIF), pH 6.8. Approximately 10-15% of the medicine was released over a 2-hour period in the SGF, pH 1.2, and 30-70% over a 12-hour period in the SIF, pH 6.8. Microspheres containing bioenhancer have a very high increase in microsphere release when compared to microspheres without bioenhancer (from 40.50% to 83.79% and 82.50% in case of modified emulsification method and complex coacervation method, respectively). CI1 and MI1 are bioenhancer-free formulations, whereas CI2, CI3, CI4, MI2, MI3, and MI4 are microsphere formulations containing *Ocimum tenuiflorum*, and CI5, CI6, CI7, MI5, MI6, and MI7 are microsphere formulations containing *Ocimum basilicum* as a bioenhancer in 5, 10, and 15 mg concentrations, respectively.

Conclusion

The particle size of microspheres made by both complex coacervation and modified emulsion methods using *Ocimum tenuiflorum* and *Ocimum basilicum* as a bioenhancer was consistent and less than 120 microns in size; however, the particle size may change when bioenhancer extract is added to the formulations. The efficiency of drug encapsulation was determined to be between 39.50 to 78.14% (increased on addition of bioenhancer in the formulations).

When bioenhancers were utilised, the percentage bioadhesion of the microsphere increased by 40% above the baseline value (82.95% from 38.50% from formulation, where no bioenhancer were used. The most important findings from the in-vitro release study were the significant increases in drug release (from 40.50% to 83.79% and 82.50%, respectively) due to the presence of bioenhancers alone and in combination (from 40.50% to 83.79% and 82.50% in case of modified emulsification method and complex coacervation method).

Acknowledgement

We acknowledge GES's Sir Dr. M. S. Gosavi College of Pharmaceutical Education and Research, Nashik for providing research facilities.

Conflict of Interest

Authors declare no conflict of interest.

Funding

None

References

1. Powell, K. M., Vander Ende, D. S., Holland, D. P., Haddad, M. B., Yarn, B., Yamin, A. S., and Ray, S. M. (2017). Outbreak of drug-resistant *Mycobacterium tuberculosis* among homeless people in Atlanta, Georgia, 2008-2015. *Public Health Reports*, 132(2):231-240.
2. Javed, S., Ahsan, W., and Kohli, K. (2016). The concept of bioenhancers in bioavailability enhancement of drugs—a patent review. *Journal of Scientific Letters*, 1:143-65.
3. Chavhan, S. A., Shinde, S. A., and Gupta, H. N. (2018). Current trends on natural bioenhancers: A review. *International Journal of Pharmacognosy and Chinese Medicine*, 2:000123.
4. Kesarwani, K., and Gupta, R. (2013). Bioavailability enhancers of herbal origin: An overview. *Asian Pacific journal of tropical biomedicine*, 3(4):253-266.

5. Al-Maskari, M. Y., Hanif, M. A., Al-Maskri, A. Y., and Al-Adawi, S. (2012). Basil: A natural source of antioxidants and nutraceuticals. In *Natural Products and Their Active Compounds on Disease Prevention* (pp. 463-471). Nova Science Publishers, Inc.
6. Stefanaki, A., and van Andel, T. (2021). Mediterranean aromatic herbs and their culinary use. In *Aromatic Herbs in Food* (pp. 93-121). Academic Press.
7. Hanumanthaiah, P., Panari, H., Chebte, A., Haile, A., and Belachew, G. (2020). Tulsi (*Ocimum sanctum*)—a myriad medicinal plant, secrets behind the innumerable benefits. *Arabian Journal of Medicinal and Aromatic Plants*, 6(1):105-127.
8. Kadam, P. V., Yadav, K. N., Jagdale, S. K., Shivatare, R. S., Bhillwade, S. K., and Patil, M. J. (2012). Evaluation of *Ocimum sanctum* and *Ocimum basilicum* mucilage-as a pharmaceutical excipient. *Journal of Chemical and Pharmaceutical Research*, 4(4):1950-1955.
9. Lengyel, M., Kállai-Szabó, N., Antal, V., Laki, A. J., and Antal, I. (2019). Microparticles, microspheres, and microcapsules for advanced drug delivery. *Scientia Pharmaceutica*, 87(3):20.
10. Pingale, P. L., and Ravindra, R. P. (2013). Effect of Piper nigrum on in-vitro release of Isoniazid from oral microspheres. *International Journal of Pharm and Bio Sciences*, 4(1):1027-1036.
11. Majeed, A., Ranjha, N. M., Hanif, M., Abbas, G., and Khan, M. A. (2017). Development and evaluation of ivabradine HCl-loaded polymeric microspheres prepared with eudragit L100-55 (methacrylic acid-ethyl acrylate copolymer) and ethyl cellulose for controlled drug release. *Acta Pol. Pharm*, 74(2):565-578.
12. Pingale, P. L., and Ravindra, R. P. (2013). Effect of Piper Nigrum on In-Vitro Release of Rifampicin Microspheres. *Asian Journal of Pharmaceutical and clinical research*, 7(5):79-83.
13. El-Say, K. M. (2016). Maximizing the encapsulation efficiency and the bioavailability of controlled-release cetirizine microspheres using Draper–Lin small composite design. *Drug design, development and therapy*, 10:825.
14. Pingale, P. L., and Ravindra, R. P. (2019). Comparative Study of Herbal Extract of Piper Nigrum, Piper Album and Piper Longum on Various Characteristics of Pyrazinamide and Ethambutol Microspheres. *Journal of Drug Delivery and Therapeutics*, 9(4-A):72-78.
15. Zhang, Y., and Liu, H. (2016). Development of bioadhesive microspheres for oral bioavailability enhancement of berberine hydrochloride. *International Journal of Polymer Science*, 2016:4235832.
16. Rastogi, R., Sultana, Y., Aqil, M., Ali, A., Kumar, S., Chuttani, K., and Mishra, A. K. (2007). Alginate microspheres of isoniazid for oral sustained drug delivery. *International journal of pharmaceutics*, 334(1-2):71-77.
17. Pingale, P. L., Boraste, S. S., and Amrutkar, S. V. (2021). Formulation and evaluation of pravastatin fast disintegrating tablets using natural superdisintegrant. *Journal of Medical Pharmaceutical and Allied Science*, 10(3): 2977-2981.

Development and Validation of a Sensitive and Rapid Bioanalytical RP-HPLC Method for the Quantification of Nebivolol Hydrochloride in Rat Plasma

S.N.H. Pratap* and Prof. J. Vijaya Ratna

¹Research Scholar, A. U. College of Pharmaceutical Sciences, Visakhapatnam, Andhra Pradesh.

²Department of Pharmaceutics, A. U. College of Pharmaceutical Sciences, Visakhapatnam, Andhra Pradesh

*Corresponding Author: E-Mail Id: pratappharma2012@gmail.com

Abstract

A simple and specific bioanalytical reverse phase high performance liquid chromatography (HPLC) assay method was established and validated for estimation nebivolol HCl in rat plasma using amlodipine besylate as internal standard. The chromatographic separation was achieved by reversed phase Knauer C18 column and mobile phase composition of acetonitrile, methanol and 0.1N orthophosphoric acid (80:20:10) with ultraviolet detector at the wavelength of 272 nm. The flow rate was maintained at 0.5 mL/min. System suitability parameters of mobile phase composition, flow rate, and wavelength were optimized to provide highly sensitive peaks for the drug samples. The calibration curve was found linear in the range of 400 ng/mL to 1800 ng/mL with a retention time of 5.48 minutes. LOD and LOQ were found at 40.24 ng/mL and 121.94 ng/mL respectively. The developed method was validated in terms of linearity, recovery, precision, robustness, ruggedness, and stability (short term & long-term stabilities and freeze & thaw stability). All the experiments were done as per ICH guidelines and the outcomes were well inside the limits determined.

Keywords: Bioanalytical, Reversed Phase HPLC, Nebivolol HCl, ICH

Introduction

Bioanalytical method is used to determine the concentration of drug and

metabolites present in the biological matrix like serum, plasma, cerebrospinal fluid etc. The developed method can be used to detect the content of drug quantitatively. Validation of an analytical method involve in documentation of laboratory investigations to estimate the performance characteristics of procedures meeting required specifications and proposed applications. Validation of bioanalytical method demonstrate that the method developed is sensitive, accurate, precise and suitable for the intended purpose.

Nebivolol hydrochloride is a cardio selective adrenergic beta-1 blocker used in the treatment of hypertension and chronic heart failure in elderly patients. The drug also has vasodilation property acting through L-arginine/nitric oxide pathway. It is chemically 1-(6-fluoro-3,4-dihydro-2H-chromen-2-yl)-2-((6-fluoro-3,4-dihydro-2H-chromen-2-yl)-2-hydroxyethyl)amino ethanol;hydrochloride. It is generally prescribed for elderly patients with a starting dose of 2.5 mg in tablet dosage form (1). The chemical structure of drug was depicted in (Figure 1). Several methods were developed and reported for the estimation of NBH till date including RP-HPLC (2,3), RP-HPTLC (4) and bioanalytical method development in human plasma were reported (5). In the current study, a sensitive bioanalytical method was developed for the estimation of nebivolol HCl in rat plasma using HPLC equipped with absorbance detector as per the FDA guidance (6). The method involved liquid-liquid extraction of NBH from the plasma using acetonitrile, methanol, and

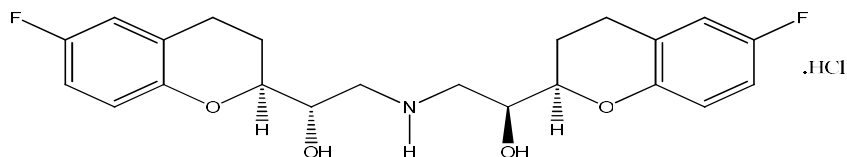


Fig 1. Chemical Structure of Nebivolol Hydrochloride

buffer mixture. The developed method was validated using ICH Q2 (R1) guidelines (7).

Materials and Methods

Materials and Reagents: Waters HPLC system equipped with Knauer C₁₈ (250 X 4.6 mm, 5 μ), column, solvents, and buffers of HPLC grade purchased from Merck Ltd. Nebivolol HCl (NBH) was purchased from Yarrow Chem. Products, Mumbai.

Instruments: Waters HPLC 2695 alliance system with 2487 UV detector, Empower-2 software, Remi vortex shaker.

Plasma Samples: Plasma samples for the method development were collected from animal house facility, Bapatla College of Pharmacy, Bapatla, Guntur with Regd. No. 1032/PO/Re/S/07/CPCSEA. Blood samples were collected from Albino Wistar rats using retro orbital puncture without sacrificing animals. Blood samples were collected in sample tubes with anticoagulant (EDTA), centrifuged at 400 rpm for 20 minutes. The supernatant plasma was collected and stored at -20°C in deep freezer until further use.

Preparation of Standard Solutions: Stock solutions of nebivolol HCl (1 mg/mL) and amlodipine besylate (1 mg/mL) were prepared with methanol-acetonitrile mixture (5:5 v/v) using standard powders. Working standard solution of NBH was prepared by diluting stock solution with above solvent mixture to get 0.4 to 1.8 μ g/mL solution. The same method was used to prepare 1000 ng/mL working standard solution of amlodipine besylate.

Preparation of Plasma Samples: Plasma samples of drug and IS mixture

were prepared using 100 μ L of blank plasma, 100 μ L of NBH standard solution and 100 μ L of IS in an Eppendorf tube. The sample extraction was conducted using liquid-liquid extraction technique (LLE) with 100 μ L of acetonitrile & methanol solution (1:1) to the above drug containing plasma mixture, vortexed for 2 minutes and then centrifuged at 15000 rpm at 4°C for 5 minutes. 100 μ L of supernatant was transferred to the sample tube vial and 20 micro liters solution was then injected into the chromatographic system.

The blank plasma solution was prepared by spiking 0.1 mL of plasma into extraction solution (acetonitrile-methanol mixture), vortexed for 1 minute and further centrifuged at 4°C at 15000 rpm for 10 minutes. The supernatant was collected, filtered, and used as blank solution for analysis.

Method Development: The validation parameters like specificity, linearity, sensitivity, accuracy, precision, and recovery in rat plasma, were determined according to the US-FDA guidance for industry, bio-analytical method development and validation document 2018.

Linearity: The linearity of the proposed method was established from the standard calibration curve constructed at six concentrations (0.4 to 1.8 μ g/mL) of nebivolol HCl with constant concentration of IS (Amlodipine besylate at 1 μ g/mL), on six consecutive days in order to confirm reproducibility of results. Calibration curve was constructed for the drug in the spiked plasma samples by plotting the relative peak area (ratio of peak area of drug to peak area of IS) against their respective concentrations using a linear least squares regression analysis.

Specificity/Selectivity: The specificity/selectivity of the analytical method was investigated by confirming the complete separation and resolution of the required peak area of nebivolol HCl and the IS in plasma samples, spiked with appropriate concentration of these compounds. The tests were accomplished to verify the potential interferences of endogenous plasma components co-eluting with drug and IS.

Accuracy and Precision (8)

Intra-day Accuracy and Precision: The intra-day precision and accuracy of the method were determined by analyzing six spiked samples of nebivolol HCl at three different concentrations LQC, MQC and HQC (0.4, 1.2 and 1.8 µg/mL). The deviation of the mean from the true value serves as the measure of accuracy. The statistical evaluation includes calculation of parameters such as mean, standard deviation, coefficient of variation, and percentage relative error. Accuracy and Precision were determined using % relative error and %RSD respectively.

Inter-day Accuracy and Precision: The inter-day accuracy and precision was determined for six replicates at three different concentrations 0.4, 1.2 and 1.8 µg/mL over three days. The statistical evaluation includes calculation of parameters such as mean, standard deviation, coefficient of variation, accuracy, and percentage relative error. Accuracy was determined using % relative error and precision was determined by calculating %RSD.

Sensitivity: The sensitivity of the method detected using limit of detection (LOD) and limit of quantification (LOQ) concentrations of drug samples. LOD is a parameter used to detect the lowest amount of analyte that can be detected from background noise and cannot be quantitated and LOQ stands for the lowest concentration of analyte that can be detected and quantitated. LOD and LOQ can be measured using signal to noise ratio of 3:1 and 10:1.

They can be determined based on the standard deviation of the response (σ) and the slope of the calibration curve (s) using known concentrations of analyte with those of blank samples. The standard deviation of the response can be determined based on standard deviation of Y-intercepts of regression lines. LOD & LOQ are calculated based on the following formulae (9):

$$\text{Limit of Detection (LOD)} = 3.3 \frac{\sigma}{s}$$

$$\text{Limit of Quantification (LOQ)} = 10 \frac{\sigma}{s}$$

Where,

' σ ' is regression standard deviation of intercept.

' s ' is the slope.

Recovery: Recovery of drug sample can be calculated using analyte response to that of maximum concentration of pure sample. During the bioanalytical development, nebivolol HCl was determined for absolute and relative recoveries of drug and IS from rat plasma using quality control samples. The absolute recovery of drug and IS were calculated using measured values of extracted samples compared with un-extracted pure authentic samples whereas; relative recovery of drug and IS were computed using peak areas (detector response) obtained from the sample injections of the prepared plasma standards compared to the nominal concentration prepared. The standard used was prepared to contain a drug concentration assuming 100% recovery. Recovery of nebivolol HCl was measured at three concentration levels (0.4, 1.2 and 1.8 µg/mL).

Robustness: Robustness of the method developed for the drug was evaluated by changing small but deliberate variations in chromatographic conditions. The parameters studied in this study were flow rate and mobile phase composition.

Stability Study (10)

LOQ, MOQ and HOQ samples of six replicates were retrieved from deep freezer

after three freeze thaw cycles. Samples were frozen at -20°C followed by thawing at the time of experiment. Short term and long-term stabilities of samples were conducted by preserving samples at room temperature for 24 hours and -20°C deep freezer for 45 days respectively. The precision and accuracy of stability samples must be within 15% of nominal concentrations.

Results and Discussion

Selection of Chromatographic Conditions: The chromatographic conditions for the method validation were selected based on the peak resolutions, day-to-day reproducibility of the retention times, peak shapes and back pressure. Selection of mobile phase is the key for reproducible elution of characteristic peaks and different combination of solvents were tested starting with acetonitrile-methanol mixture (80:20, %v/v) where, merging of peaks observed. The mobile phase composition was changed with addition of water to the above composition at acetonitrile-methanol-water (65:35:5, %v/v) that resulted in proximity of two peaks of drug analyte and IS. Finally, the composition was selected with replacing orthophosphoric acid instead of water with a composition of acetonitrile: methanol: 0.1% Orthophosphoric acid (70:20:10) produced sharp reproducible peaks with system suitability conditions at 2.6 and 5.4 minutes for nebivolol HCl and IS respectively.

Linearity: The analytical curves were constructed with standard concentrations ranging 0.4 µg/mL to 1.8 µg/mL of NBH along

with constant concentration of 1.0 µg/mL of IS in rat plasma. All the samples were extracted for the drug and IS contents using the above-mentioned procedure. The baseline was monitored and 20 µL of these solutions were injected into the system. Calibration curves were constructed using ratio of peak areas of drug to IS on Y-axis and concentration of pure drug on X-axis for replicated samples and correlation coefficient was calculated (Table 1). The curve showed enough linearity with 'r' value of 0.998 and regression equation of $Y = 0.8639X (\pm 0.0053) + 0.218 (\pm 0.0059)$ measured using simple regression model as showed in (Figure. 2).

Specificity/Selectivity:

Representative chromatogram of blank plasma was confirmed the presence of very little interference from the endogenous component. Chromatograms of spiked plasma samples of nebivolol HCl at 0.4 µg/mL concentration along with IS at a constant concentration (1.0 µg/mL) confirmed that drug and IS peaks were well resolved and completely separated at retention times of 2.60 and 5.48 minutes respectively.

Accuracy and Precision

Intra-day Accuracy and Precision: Intra-day accuracy of the method for drug ranged from 99.010% to 99.481%, while the intra-day precision ranged from 0.219% to 0.372% at concentrations of 0.4 µg/mL (LQC) 1.2 µg/mL (MQC) and 1.8 µg/mL (HQC).

Inter-day Accuracy and Precision: Inter-day accuracy of the method for drug ranged from 98.361% to 99.083%, while precision of the method for the same ranged

Table 1. Concentration Data for NBH in Wistar Rat Plasma

Concentration (µg/mL)	Peak Area (n=3)		Peak Area Ratio (D/IS)
	Drug	IS	
0	0	0	0
0.4	29547.2±230.49	52649.1±210.42	0.566±0.0044
0.8	48120.4±291.41	52168.7±97.50	0.909±0.0070
1.0	56403.8±70.86	52981.6±127.28	1.064±0.0029
1.2	67217.5±249.53	53012.1±109.27	1.281±0.0041

RP-HPLC Method for the Quantification

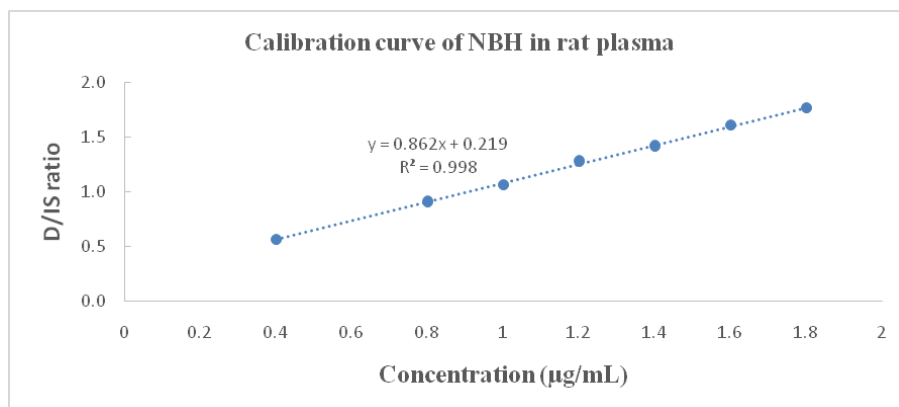


Fig 2. Calibration Curve for the Estimation of Nebivolol HCl in Plasma using HPLC Method

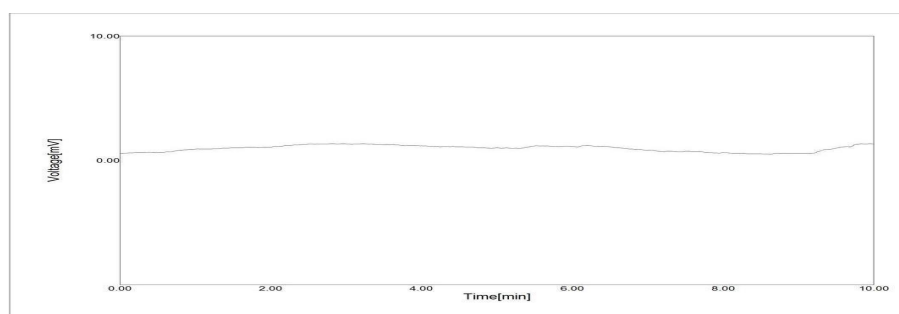


Fig 3. HPLC Chromatogram of Blank Plasma

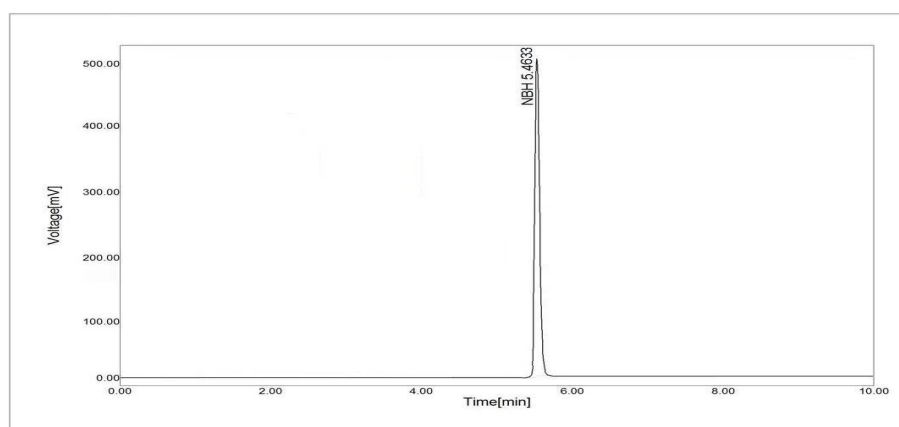


Fig 4. HPLC Chromatogram of Pure Nebivolol HCL
RP-HPLC Method for the Quantification

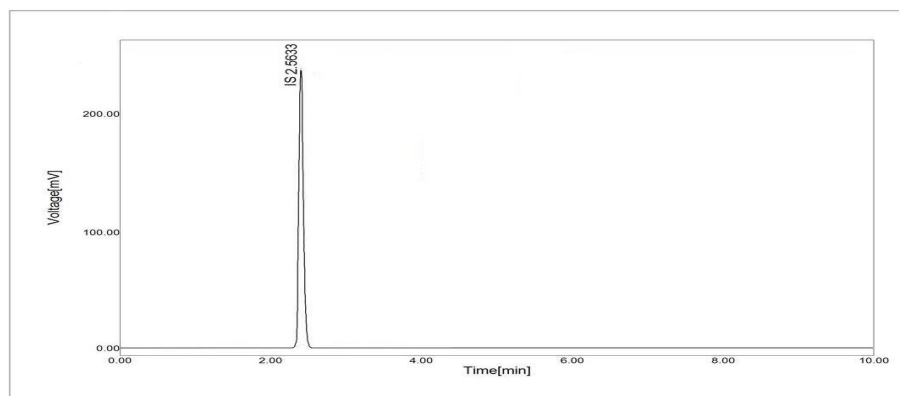


Fig 5. HPLC Chromatogram of Internal Standard (Amlodipine Besylate)

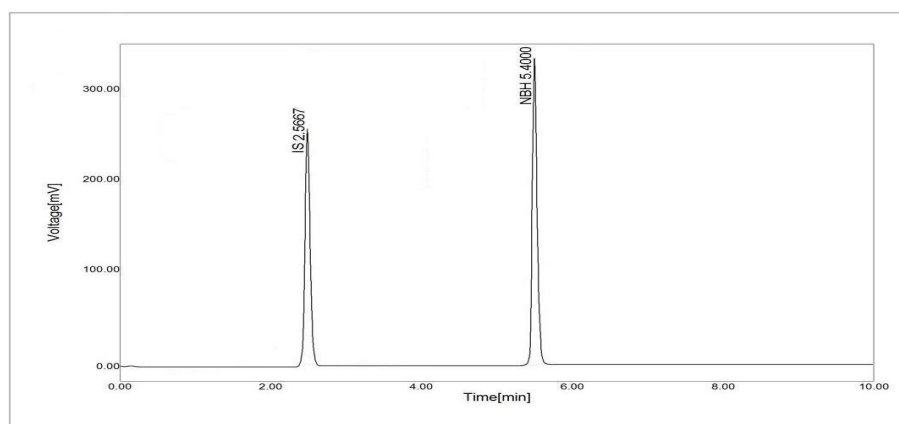


Fig 6. HPLC Chromatogram of Nebivolol Hydrochloride+ Amlodipine Besylate (Drug+IS)

from 0.322% to 0.547% at concentrations 0.4, 1.2 and 1.8 $\mu\text{g/mL}$.

The results were depicted in (Table 2 and 3) for intra and inter day accuracy and precision. The coefficient of variation% for all the levels of nebivolol HCl in the plasma samples were found to be within acceptable limits indicating a reasonable intermediate precision (intra and inter-day) of the proposed method.

Recovery: The absolute and relative recovery was determined for nebivolol HCl

and represented in (Table 4). The values showed to be consistent, precise and reproducible at the three levels 0.4, 1.2 and 1.8 ng/ml. The absolute analytical recovery of internal standard was found to be 95.11%.

By verifying the data for accuracy, precision and linearity it was found that the method developed was justified within the range.

Sensitivity (LOD & LOQ): The LOD and LOQ were defined as the lowest concentration giving a signal-to-noise (S/N)

Table 2. Intra-day Precision, Accuracy, and Relative Error for Nebivolol HCl Measured in Spiked Rat Plasma Samples

Intraday (n=6)			
	0.4 µg/mL	1.2 µg/mL	1.8 µg/mL
Mean	0.397	1.188	1.790
S.D.	0.0013	0.0044	0.0039
Precision as %CV	0.346	0.372	0.219
Accuracy %	99.375	99.010	99.481
Relative error %	0.625	0.990	0.519

Table 3. Inter-day precision, accuracy, and relative error for nebivolol HCl measured in spiked rat plasma samples

Inter day (n=6)			
	0.4 µg/mL	1.2 µg/mL	1.8 µg/mL
Mean	0.396	1.187	1.770
S.D.	0.0019	0.0038	0.0096
Precision as %CV	0.496	0.322	0.547
Accuracy %	99.083	98.972	98.361
Relative error %	0.916	1.028	1.63

ratio of at least 3:1 and 10:1, respectively. In the estimation of lower limit samples of pure drug, sensitivity was established using LOD and LOQ that were considered to be 40.24 ng/mL and 121.94 ng/mL for LOD & LOQ respectively.

Robustness: The developed method for estimation of NBH was tested for robustness using small variations in mobile phase composition (65:25:10), (70:20:10) and (75:15:10) and flow rate (0.9, 1.0, 1.1). The %RSD results of these changes were in the range of 1.5-3.0% which were in accordance with the actual values shown in calibration data. The tailing factor for the drug (nebivolol HCl) was always less than 1.5 and the components were well separated under all the changes carried out (mobile phase composition and flow rate). Considering the factors like modification in the system suitability parameters, specificity of the method and conducting the experiment at

Table 4. Percent Recovery of Nebivolol HCl in Spiked Rat Plasma Samples

Concentration (ng/mL)	Extraction Recovery (%)	Relative Recovery (%)
0.4	93.57	100.90
1.2	96.42	100.86
1.8	92.27	99.49

room temperature it may be indicated that the method was found to be robust. Hence, the newly developed method was considered robust.

Ruggedness: Ruggedness was studied along with precision and accuracy of batches where the effect of the column, and analyst change was observed. The observed value for analyst variation and results obtained for precision and accuracy were within the acceptance criteria (there were no changes in

Table 5. Stability Study of Nebivolol HCl Analytes Stored at Different Conditions

Nominal Concentration (µg/mL)	Fresh Sample Concentration Determined (µg/mL)	Sample Concentration after Storage (µg/mL)	%RSD	% Mean Deviation
Short Term (24h)				
0.4	0.396	0.393	1.47	0.63
1.2	1.202	1.194	0.47	0.77
1.8	1.790	1.729	0.70	3.40
Freeze-thaw Cycles (n=3)				
0.4	0.400	0.397	0.94	0.75
1.2	1.194	1.191	0.44	0.22
1.8	1.791	1.733	0.47	3.21
Long Term (45 days)				
0.4	0.394	0.384	1.63	2.51
1.2	1.198	1.189	0.48	0.75
1.8	1.788	1.702	1.0	4.70

the retention time, recovery, and precision of the drug) according to guidelines.

Stability

The results of stability testing done at various conditions showed within the limits described by standards as depicted in (Table 5). Nebivolol HCl was found to be stable at room temperature for 24 hours and after three freeze thaw cycles. All analytes were stable at room temperature showing consistent results. The long-term storage conditions in freezer for 45 days also showed stability with no large deviations in mean of replicates. Thus, the analytes stored at prescribed conditions showed no degradation and remains stable in plasma samples which was seen with excellent recoveries at different storage conditions.

Conclusion

A validated RP-HPLC method was developed for nebivolol HCl in rat plasma according to the ICH guidelines. The method was optimized with different mobile composition and flow rate for sensitive and

rapid detection of drug in the plasma samples. The method was validated as per the ICH Q2A (R1) guidelines. It consists of a mobile phase composition of acetonitrile, methanol and 0.1N orthophosphoric acid (70:20:10 %v/v) with Knauer C₁₈ column with amlodipine besylate as internal standard. The retention time of NBH was found at 5.48 minutes. The calibration curve for the concentration range of 0.4-1.8 µg/mL was found linear with correlation coefficient of 0.9988. The percentage recoveries for three levels LQC, MQC and HQC were found within the range of 92.27% to 96.42%. All the analytes showed good precision and accuracy with excellent stability at various conditions. Therefore, the developed method was deemed to be accurate, precise, simple, sensitive, and reliable to estimate the drug content in rat plasma. This method can therefore be used in computation of pharmacokinetic parameters of nebivolol HCl in pharmaceutical dosage forms.

References

1. Indian Pharmacopoeia. Volume 3. New Delhi: 2014. Indian Pharmacopoeia commission. Pg. no. 2310.

2. Meyyanathan SN, Rajan S, Muralidharan S, Birajdar AS, Suresh B. A validated RP-HPLC method for simultaneous estimation of nebivolol and hydrochlorothiazide in tablets. *Indian journal of pharmaceutical sciences*. 2008 Sep;70(5):687.
3. Yang LT, Xie HR, Zhang XQ, Wang L, Jiang XH. HPLC-MS/MS determination of nebivolol in human plasma and its application in pharmacokinetic study. *Chinese Journal of Pharmaceutical Analysis*. 2016 Jan 1;36(12):2094-100.
4. Patel LJ, Suhagia BN, Shah PB. RP-HPLC and HPTLC methods for the estimation of nebivolol hydrochloride in tablet dosage form. *Indian journal of pharmaceutical sciences*. 2007;69(4):594.
5. Aruna G, Bharathi K, Prasad K. Development and validation of bioanalytical HPLC method for simultaneous estimation of Cilnidipine and Nebivolol in human plasma. *International Journal of Pharmacy and Pharmaceutical Sciences*. 2017 Oct 2; 9(10):253.
6. US Food and Drug Administration. Bioanalytical method validation. Guidance for Industry. 2018.
7. Guideline ICH. Validation of analytical procedures: text and methodology. Q2 (R1). 2005 Nov;1(20):05.
8. Nandania J, Rajput SJ, Contractor P, Vasava P, Solanki B, Vohra M. Quantitative determination of nebivolol from human plasma using liquid chromatography–tandem mass spectrometry. *Journal of Chromatography B*. 2013 Apr 1;923:110-9.
9. Ravi P, Vats R, Joseph S, Gadekar N. Development, and validation of simple, rapid and sensitive LC-PDA ultraviolet method for quantification of Nebivolol in rat plasma and its application to pharmacokinetic studies. *Acta Chromatographica*. 2015 Jun 1;27(2):281-94.
10. Patel JM, Dhingani AP, Garala KC, Raval MK, Sheth NR. Development and validation of bioanalytical HPLC method for estimation of telmisartan in rat plasma: application to pharmacokinetic studies. *Dhaka University Journal of Pharmaceutical Sciences*. 2012; 11(2): 121-7.

Comparative *In Vivo* Evaluation of Marketed and Optimized Formulations of Teneiglipitin and Metformin Bilayered Tablets

Rajani V^{1*}, Rajendra Prasad Y² and Lakshmana Rao A³

¹Department of Biotechnology, Acharya Nagarjuna University, Nagarjuna Nagar, Andhra Pradesh, India

²College of Pharmaceutical Sciences, Andhra University, Visakhapatnam, Andhra Pradesh, India

³V. V. Institute of Pharmaceutical Sciences, Gudlavalleru, Andhra Pradesh, India

*Corresponding author: E-mail id: rajanivetapalem@gmail.com

Abstract

The combination of Metformin and Teneiglipitin is an attractive approach for the management of type-2 diabetes because the two pharmacological approaches have different and potentially complementary targets. A novel bilayer tablet, consisting of an immediate release layer containing Teneiglipitin (20 mg) and prolonged release layer containing Metformin (500 mg) was developed. *In vivo* studies were carried out in rabbits by using the optimised formulation as a test product and marketed formulation as a reference. Based on the *in vivo* performance, the developed bilayer tablets showed superior bioavailability than the marketed tablets. A simple, sensitive and selective HPLC method was developed for the simultaneous determination for Metformin and Teneiglipitin in rabbit plasma using a novel sample extraction procedure. Method validation was carried out according to ICH guidelines in rabbit plasma in order to evaluate the method for selectivity, linearity of response, accuracy, precision, recovery and stability of analytes during processing and storage. The total area under plasma concentration time curve ($AUC_{0-\infty}$), the maximum plasma concentration (C_{max}), and time to reach the maximum plasma concentration (T_{max}) were selected as parameters for pharmacokinetic evaluation. The C_{max} and T_{max} were obtained directly from the experimental data of plasma concentration versus time. $AUC_{0-\infty}$ was

obtained by adding the AUC_{0-24h} , which was calculated by the trapezoidal rule. The differences in average of data were compared by sample analysis of variance (one way analysis of variance) or independent sample t test. The significance of the difference was determined at 95% confident limit ($P=0.05$).

Keywords: Metformin, Teneiglipitin, Bilayer Tablets, Formulation.

Introduction

Teneiglipitin is a potent and selective inhibitor of dipeptidyl peptidase-IV (DPP-4), orally active, that improves glycemic control in patients with type 2 diabetes (T2DM) primarily by enhancing pancreatic (α and β) islet function. Thus Teneiglipitin has been shown both to improve insulin secretion and to suppress the inappropriate glucagon secretion seen in patients with T2DM. Teneiglipitin reduces HbA_{1c} when given as monotherapy, without weight gain and with minimal hypoglycemia, or in combination with the most commonly prescribed classes of oral hypoglycemic drugs: Metformin, a sulfonylurea, a thiazolidinedione, or insulin. Metformin, with a different mode of action not addressing β -cell dysfunction, has been used for about 50 years and still represents the universal first line therapy of all guidelines (1). However, given the multiple pathophysiological abnormalities in T2DM and the progressive nature of the disease, intensification of therapy with combinations is typically required over time.

Recent guidelines imply that patients will require pharmacologic combinations much earlier to attain and sustain the increasingly stringent glycemic targets, with careful drug selection to avoid unwanted adverse events, especially hypoglycemia (2). The combination of Metformin and Tenelegliptin offers advantages when compared to currently used combinations with additive efficacy and complimentary mechanisms of action, since it does not increase the risk of hypoglycemia and does not promote weight gain. Therefore, by specifically combining these agents in a single tablet, there is considerable potential to achieve better blood glucose control and to improve compliance to therapy (3). A novel bilayer tablet, consisting of an immediate release layer containing Tenelegliptin (20 mg) and prolonged release layer containing Metformin (500 mg) was developed. An *in vivo* evaluation study conducted to ascertain pharmacokinetic parameters in rabbits by using the optimised formulation as a test product and marketed formulation as a reference. Based on the *in vivo* performance, the developed bilayer tablets showed superior bioavailability than the marketed formulation.

Materials and Methods

The *in vivo* study of the optimized formulations was performed as per the guidelines approved by the Committee for the Purpose of Control and Supervision of Experiments on Animals (CPCSEA), Government of India. Prior approval by Institutional animals ethics committee (Ref: P3/IAEC/2016/1/VVIPS/VR) was obtained for conduction of experiments. Marketed Teneinat M (Natco Pharma) and optimized bilayer tablet, consisting of an immediate release layer containing Tenelegliptin (20 mg) and prolonged release layer containing Metformin (500 mg) prepared in the laboratory conditions and chosen on the basis of *in vitro* release studies and stability conditions were chosen as dosage forms for administration.

Preparation of Bilayer Tablets (4,5):

a. Preparation of immediate release

layer: Tenelegliptin, Ludiflash, mannitol were

weighed and co-sifted through sieve No. # 40 (ASTM), blended in a poly bag for 10 min, mixed well with PVP K-90 binder solution to make a damp mass. Later the damp mass was passed through sieve No. # 20 (ASTM), and dried in a hot air oven at 60°C for 1h. Finally the granules are lubricated with magnesium stearate by mixing in a poly bag, for additional 2-3 min; which is used as upper IR layer.

b. Preparation of sustained release

layer: Metformin, HPMC K100M and MCC were weighed were co-sifted through sieve No. # 40 (ASTM), blended in a poly bag for 5 min and lubricated with magnesium stearate and aerosil by mixing in the same poly bag, for additional 2-3 min; which is used as lower SR layer. Composition of Tenelegliptin (IR) layer and Metformin (SR) layer of bilayered tablets is given in Table 1.

Validation of the Bioanalytical Method (6):

Method validation was carried out according to ICH guidelines in rabbit plasma in order to evaluate the method for selectivity, linearity of response, accuracy, precision, recovery and stability of analytes during processing and storage.

Table 1: Composition of optimized tenelegliptin and metformin bilayered tablets

Ingredients	Immediate Release Layer
Tenelegliptin	20
Ludiflash	3
Starch	9
Mannitol	64
Pvp K-90	3
Mg.stearate	4
Total	100
Ingredients	Sustained release layer
Metformin	500
HPMCK100M	225
MCC	248
Aerosil	4.5
Mg.Stearate	22.5
Total	1000

a. Selectivity: Selectivity was checked by injecting blank plasma samples from six different rabbits to confirm no interfering peaks around the retention time of both Metformin & Tenelegliptin and IS.

b. Calibration, linearity and quality control samples (7): Calibration was constructed by calculating the peak area ratio of Metformin & Tenelegliptin to that of IS. For the preparation of calibration standards, working solutions of Metformin & Tenelegliptin (250 µL) and IS (500 µL) were added to blank plasma (0.25 mL) to obtain final concentrations of 65 ng/mL, 130 ng/mL, 195ng/mL, 1040 ng/mL, 1300 ng/mL, 1560 ng/mL, 2080 ng/mL and 2600 ng/mL of Metformin and 9.5 ng/mL, 19 ng/mL, 28.5 ng/mL, 152 ng/mL, 190 ng/mL, 228 ng/mL, 304 ng/mL and 380 ng/mL of Tenelegliptin and directly inject 10 µL into HPLC. The quality control (QC) samples were prepared in a similar manner as the calibration standards at three different levels: low quality control (LQC), medium quality control (MQC) and high quality control (HQC).

c. Precision and accuracy (8): The precision and accuracy of the assay were determined using QC samples of known Metformin & Tenelegliptin concentrations (i.e., LQC, MQC and HQC), which were processed freshly each validation day as described for calibration curve standards. Six replicates of each QC were analyzed on 3 days, and the intra- and inter- assay means, standard deviation (SD) and CV were calculated. The recovery of Metformin & Tenelegliptin from plasma samples was carried out at three concentration levels (LQC, MQC and HQC) by analysis of replicate (n=6) samples. The peak area of QC samples in plasma was compared with peak area of actual analyte (in mobile phase) at the same final concentrations. The recovery was expressed as percentage value, and the extent of recovery of Metformin & Tenelegliptin and of the IS should be consistent, precise and reproducible.

Metformin & Tenelegliptin Pharmacokinetic Study (9):

Healthy rabbits (New Zealand Albino) of either sex weighing 2.5-3kg were selected and housed with CPCSEA guidelines, fasted overnight and had free access to drinking water.

a. Experimental design: Animals were separated into two experimental groups, each group consisting of six animals (n=6). The test formulation of batch (F) was compared with (reference/market formulation) with the following treatment schedule under fasted condition:

Group I- Marketed formulation

Group II- Metformin & Tenelegliptin formulation (F) used as test.

b. Animal dose calculation (10):

Metformin:

$HED (mg/kg) = \text{Animal dose (mg/kg)} \times \text{Animal Km factor} / \text{Human Km factor}$.

HED: Human Equivalent Dose (500mg/60kg)

Animal Km factor=12

Human Km factor=37.

Wt. of the rabbits=3kg

So the dose of the drug taken is 8.33mg/kg.

Tenelegliptin:

$HED (mg/kg) = \text{Animal dose (mg/kg)} \times \text{Animal Km factor} / \text{Human Km factor}$.

HED: Human Equivalent Dose (20mg/60kg)

Animal Km factor =12

Human Km factor =37

Wt. of the rabbits=3kg

So the dose of the drug taken is 0.333 mg/kg.

The optimized formulation was administered via oral gavage at a dose 8.333 mg/kg for Metformin & 0.333 mg/kg for Tenelegliptin. Blood samples (each of about 1-2 mL from each animal) were withdrawn from marginal ear vein at regular time intervals after administration. The collected blood samples were immediately centrifuged at 5000rpm in ultra cooling centrifuge for 10min at 4°C. The

supernatant plasma sample was separated and stored in a clean screw capped 5ml polypropylene plasma tubes at -20°C in a deep freezer, until further analysis.

c. Estimation of drug from rabbit plasma (11): The stored plasma samples were processed at room temperature, 500 μL of plasma was added to 1 mL of acetonitrile to precipitate the proteins. The samples were vortexed on vortex mixer for 15min, followed by centrifugation at 10000rpm for 15min. The respective samples were injected into the HPLC column.

d. Data analysis (12): The total area under plasma concentration time curve ($\text{AUC}_{0-\infty}$), the maximum plasma concentration (C_{max}), and time to reach the maximum plasma concentration (Tmax) were selected as parameters for pharmacokinetic evaluation. The C_{max} and Tmax were obtained directly from the experimental data of plasma concentration versus time. $\text{AUC}_{0-\infty}$ was obtained by adding the $\text{AUC}_{0-24\text{h}}$, which was calculated by the trapezoidal rule. The

differences in average of data were compared by sample analysis of variance (one way analysis of variance) or independent sample t test. The significance of the difference was determined at 95% confident limit ($P=0.05$).

Results and Discussion

The *in vivo* experiments were conducted as per the protocol and procedure described earlier. Bioanalytical methods employed for the quantitative determination of drugs and their metabolites in biological matrix (plasma, urine, saliva, serum etc) play a significant role in evaluation and interpretation of pharmacokinetic data. For the successful conduct of pharmacokinetic study, the development of selective and sensitive bioanalytical methods plays an important role for the quantitative evaluation of drugs and their metabolites (analytes).

The HPLC method was highly sensitive and suitable for the detection of drug in plasma even in low concentrations and the respective chromatograms were shown in Figs 1, 2 & 3. Plasma concentrations of Tenueligiptin and

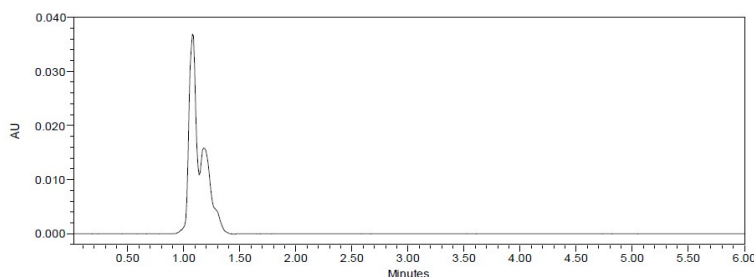


Fig 1. Chromatogram of blank plasma

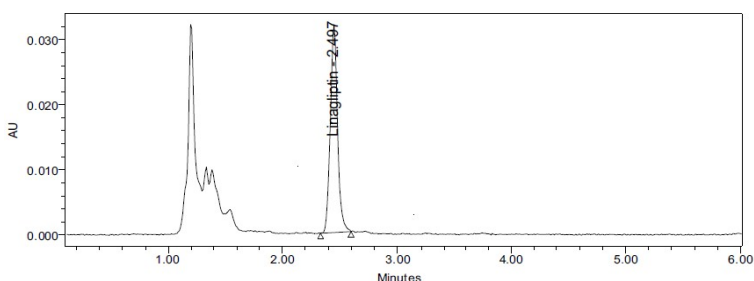


Fig 2. Chromatogram of internal standard

Antitumor Drug Delivery System

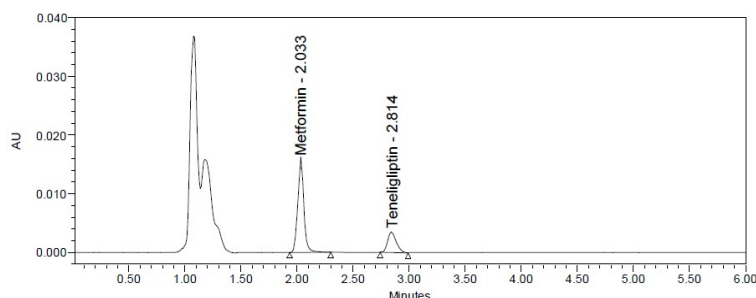


Fig 3. Chromatogram of optimized formulation with internal standard in plasma

Table 2. *In Vivo* data of metformin & teneligliptin in marketed formulation

Time (hrs)	Teneligliptin (ng/mL)	Metformin (ng/mL)
0	0	0
0.5	112.63±0.23	96.52±2.84
1	176.63±2.61	136.45±6.95
1.5	126.3±1.56	268.26±9.63
2	92.65±2.95	392.65±5.05
2.5	80.54±6.82	496.52±7.52
3	71.63±4.12	630.82±4.63
4	60.85±8.02	721.56±3.95
6	53.86±3.95	875.63±0.59
8	42.61±2.85	702.51±0.32
10	36.85±4.96	415.32±2.54
12	28.3±6.52	295.63±5.63
16	15.96±6.59	121.56±3.62
20	8.23±3.51	86.32±1.52
24	5.14±2.85	52.68±3.62

Table 3. *In Vivo* data of metformin & teneligliptin optimized formulation

Time (hrs)	Teneligliptin (ng/mL)	Metformin (ng/mL)
0	0	0
0.5	110.02±2.62	42.52±6.04
1	182.24±5.96	86.29±9.84
1.5	152.65±4.85	134.05±2.89
2	100.54±6.14	198.32±3.84
2.5	89.63±8.63	264.53±3.56
3	76.85±7.51	301.87±6.15
4	62.96±5.06	497.32±7.96
6	54.08±2.08	687.23±7.85
8	49.63±3.64	952.86±6.84
10	36.52±9.41	802.69±2.89
12	32.61±2.85	723.41±5.24
16	29.63±3.45	596.07±6.54
20	17.52±1.98	423.38±2.85
24	8.31±8.04	169.08±5.62

Metformin at different times were calculated and are shown in Table 2 & 3 and in Figs 4 & 5. Pharmacokinetic parameters such as absorption rate constant, elimination rate constant, half-life, AUC and MRT were calculated from the plot of time versus plasma concentration and subjected to statistical analysis and the results were shown in Table 4. The results from the oral

administration of Teneligliptin from marketed formulation indicated the maximum plasma concentration (C_{max}) 176.63±0.23 at 1hr (T_{max}) while optimized formulations administration exhibited the maximum plasma concentration (C_{max}) of 182.24±0.28 at 1hr (T_{max}). The oral administration of marketed formulation resulted in a low and quite variable

AUC of 925.368 ± 2.85 ng/ml/hr, whereas the optimized tablets resulted in AUC time of optimized tablets administration (4.8 ± 0.09 hrs) was found to be more than oral administration (4.3 ± 0.06 hrs). The results from

of 1100.38 ± 2.08 ng/ml/hr. The mean residence the oral administration of Metformin from marketed formulation indicated the maximum plasma concentration (C_{max}) 875.63 ± 0.63 at

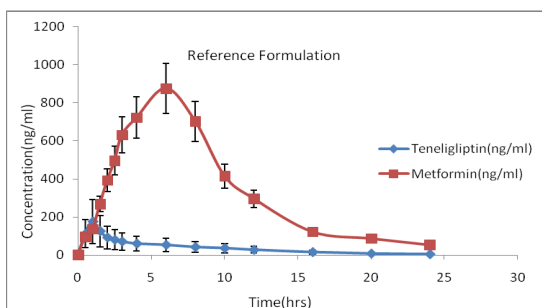


Fig 4. Plasma concentration profile of metformin & teneligliptin marketed formulation

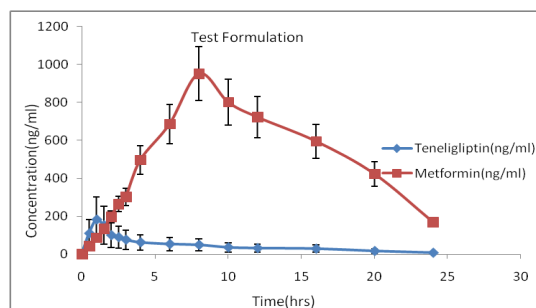


Fig 5. Plasma concentration profile of metformin & teneligliptin optimized formulation

Table 4. Statistical treatment of pharmacokinetic parameters (Mean \pm S.D.) of metformin and teneligliptin optimized formulation.

Pharmacokinetic Parameters	Optimized Formulation	Marketed Formulation	Calculated Value of 't'	Optimized Formulation	Marketed Formulation	Calculated Value of 't'
	Teneligliptin	Teneligliptin		Metformin	Metformin	
C _{max}	182.24 \pm 0.28	176.6 \pm 0.23	11.72***	952.8 \pm 0.82	875.63 \pm 0.63	16.14***
T _{max}	1.00 \pm 0.05	1.00 \pm 0.65	01.13***	8.00 \pm 0.16	6.00 \pm 0.24	5.50***
AUC(0-t)	1046.1 \pm 2.63	890.9 \pm 1.54	40.75***	12696.7 \pm 2.04	7962.756 \pm 1.85	138.67***
AUC(t- ∞)	54.2 \pm 1.58	34.4 \pm 2.63	18.87***	2312.7 \pm 2.51	516.90 \pm 1.04	47.66***
AUC(0- ∞)	1100.3 \pm 2.08	925.3 \pm 2.85	19.67***	15009.4 \pm 3.95	8479.652 \pm 2.65	219.67***
K _{el}	0.159 \pm 0.04	0.143 \pm 0.01	26.60***	0.096 \pm 0.02	0.104 \pm 0.14	12.32***
MRT (h)	4.8 \pm 0.09	4.3 \pm 0.06	6.72***	7.1 \pm 0.04	6.6 \pm 0.04	17.11***
Null hypothesis (H ₀): There is no significant difference between the pharmacokinetic parameters of marketed formulation and optimized formulations. Table value of 't' with 10 DF at the 0.001 level is 4.587.						
Result: H ₀ is not accepted as the calculated 't' value more than the table Value of 't' with 10 DF at 0.001 levels of significance. It was therefore concluded that there was significant difference between the pharmacokinetic parameters of obtained with marketed formulation and optimized formulations.						

6hr (Tmax) while optimized formulations administration exhibited the maximum plasma concentration (Cmax) of 952.86 ± 0.82 at 8hr (Tmax). The oral administration of marketed formulation resulted in a low and quite variable AUC of 8479.652 ± 2.65 ng/ml/hr, whereas the optimized tablets resulted in AUC of 15009.47 ± 3.95 ng/ml/hr. The mean residence time of optimized tablets administration (7.156 ± 0.04 hrs) was found to be more than oral administration (6.632 ± 0.04 hrs). Based on the results it was observed that greater bioavailability obtained from developed bilayer tablets showed superior bioavailability than the marketed tablets. The higher bioavailability and prolonged plasma drug concentration indicated that objective of this study was successfully achieved.

Conflict of interest

The authors declare that no conflict of interest.

References

1. Halimi S, Schweizer A, Minic B, Foley J, Dejager S. Combination treatment in the management of type 2 diabetes: focus on Vildagliptin and Metformin as a single tablet. *Vascular Health & Risk Management*. 2008; 4(3): 481-492.
2. Guarino E, Nigi L, Patti A, Fondelli C, Dotta F. Combination therapy with Metformin plus Vildagliptin in type 2 diabetes mellitus. *Expert Opinion in Pharmacotherapy*. 2012; 13(9): 1377-1384.
3. Patil M, Jani HD, Khoja SS, Pirani NA, Khoja S. A review on chemistry and pharmacological activity of Metformin hydrochloride and Teneiglipitin hydrobromide hydrate in combined dosage form. *Pharma Tutor*. 2017; 5(3): 24-30.
4. Hemalatha S, Srikanth P, Mounica Sai G. Formulation and evaluation of bilayered tablets containing immediate release layer of Glimepiride complexed with *Mangifera indica* gum and sustained release layer containing Metformin HCl by using HPMC as release retardant. *International Journal of Pharmaceutical and Clinical Research*. 2017; 9(6): 455-461.
5. Anil Kumar Ch, Sreekanth J, Raghunandhan N. Formulation and evaluation of sustained release bilayered tablets of Metformin HCl and Glimepiride. *International Journal of Pharmacy and Biological Sciences*. 2013; 3(4): 1-9.
6. Deepak P, Sufiyan A, Shastry VM, Tabrej M, Lalit T. Analytical method development and validation for the simultaneous estimation of Metformin and Teneiglipitin by RP-HPLC in bulk and tablet dosage forms. *Journal of Pharmacy Research*. 2017; 11(6): 676-681.
7. Shaikh AR, Ahmed BARK, Ibrahim M. A validated stability indicating RP-HPLC method for simultaneous estimation of Metformin and Teneiglipitin in bulk and pharmaceutical dosage form. *International Journal of Pharmaceutical Sciences and Research*. 2018; 9(4): 1705-1712.
8. Thamma NK, Kota CM, Sreenivasulu R, Raju NSV, Reddy V. Novel RP-HPLC Method for the estimation of Metformin Hydrochloride in pharmaceutical dosage forms. *International Journal of Science Innovations and Discoveries*. 2011; 1(3): 395-421.
9. Kokare V, Nagras MA, Patwardhan SK. Bioanalytical method development of Metformin co-administered with *Ocimum Sanctum* for potential bioenhancer Activity. *International Journal of Pharmaceutical Sciences and Research*. 2015; 6(5): 2056-2065.
10. Wanjari MM, There AW, Tajne MR, Umathe Rapid and Simple RP-HPLC Method for the Estimation of Metformin in Rat Plasma. *Indian Journal of Pharmaceutical Sciences*. 2008; 70(2): 198-202.
11. Gao X, Christensen M, Burghen GA, Velasquez-Mieyer P, Moore KT, Donahue SR, Reeves RA, Turner KC. Pharmacokinetics of Metformin in pediatric type 2 diabetic and healthy adult subjects. *Clinical Pharmacology & Therapeutics*. 2003; 73(2): 46-53.

12. Turner KC, Christensen M, Connor JD, Moore KT, Gao X, Donahue SR. Pharmacokinetics of a Glyburide/Metformin combination tablet in children and adolescents with type 2 diabetes. *Clinical Pharmacology & Therapeutics*. 2003; 73(2): 66-73.

Formulation and Evaluation of Cilnidipine Solid Dispersions and Oral Controlled Release Formulations

Ramakrishna Vydana* and Chandra Sekhar Kothapalli Bonnoth

¹Department of Pharmaceutical Sciences, JNTU Anantapur, Ananthapuramu, Andhra Pradesh, 515002

²Professor in Chemistry and Vice-Chancellor, Department of Chemistry, Krishna University, Machilipatnam, Andhra Pradesh, 521001

*Corresponding Author: E-Mail Id: ram.vydana@gmail.com

Abstract

The objective of the present study is to improve the solubility of Biopharmaceutical Classification System (BCS) Class-II drug, Cilnidipine by formulating them as solid dispersions and to make controlled released formulations. Solid dispersions of Cilnidipine were prepared by solvent evaporation technique using pladone K-29/32. Various physical parameters were evaluated for the prepared solid dispersions. The *in vitro* drug release studies were performed for the solid dispersions using phosphate buffer pH 6.8. The solid dispersions which showed maximum drug release were selected for the preparation of oral controlled release formulations. Tablets were prepared using Cilnidipine solid dispersions and varying concentrations of polyethylene oxide (PEO) WSR 303 by direct compression technique. Pre and post-compression parameters were evaluated along with *in vitro* drug release studies. *In vitro* dissolution studies revealed that solid dispersion CP3 containing Cilnidipine and pladone K-29/32 in 1:3 ratios showed faster drug release. Formulation CPP5 containing CP3 solid dispersion with 25% w/w of PEO WSR 303 showed prolonged drug release up to 12h. The solubility of Cilnidipine was enhanced using pladone K-29/32 and the drug release was delayed using PEO WSR 303 as polymer.

Keywords: Cilnidipine, Solid dispersions, Pladone K-29/32, Controlled release, PEO WSR 303.

Introduction

Solubility is an important factor for any drug to show its pharmacological effect in the body. Now a days, most of the drugs are facing the problem of aqueous solubility. In such cases, solubility enhancement could be helpful which could be beneficial for many patients (1). The water solubility of such drugs can be improved by various techniques. One of such most popular techniques is solid dispersions. They modify the drug properties and make them more soluble in water (2). Solid dispersions are the dosage forms with two major components; a hydrophobic drug and a hydrophilic carrier. They were made using various techniques like physical mixing, solvent evaporation and fusion (3). Solid dispersions dissolve drug in water by employing various mechanisms like making complexes, reducing the particle size, increasing wetting time (4). The drug concentration in body is maintained within the therapeutically effective range by conventional drug delivery systems only when taken multiple times in a day. This could be disadvantageous in case of geriatrics who ought to take many drugs in a day due to various disease conditions. Dosage forms which could retain in the stomach for prolonged and predictable period of time are advantageous in such cases (5). Prolonged gastric retention of drug also increases bioavailability, decreases wastage of drug and improves solubility for drugs that are less soluble in a high pH environment (6). This could be achieved by using certain polymers like polyethylene oxides (7). Poly ethylene oxides are hydrophilic in nature and are

available in various grades. They help in prolonged drug release (8).

In current study, an attempt was made to enhance the solubility of BCS (Biopharmaceutical Classification System) class-II drug, Cilnidipine which is poorly soluble in water. It shows the anti-hypertensive effect by blocking L-type calcium channels on blood vessels. It also suppresses the contraction of blood vessels (9). The bioavailability of Cilnidipine is approximately 13%. It shows high binding to plasma proteins. It has an approximate elimination half-life of 2.5h. Based on pharmacokinetic parameters, Cilnidipine is selected as drug of choice for present study.

Materials and Methods

Materials: Cilnidipine is a gift sample from M/s. NATCO Pharma Ltd. (Hyderabad, India). Plasdone K-29/32 and micro crystalline cellulose were gift samples from M/s. Pellets Pharma Ltd (Hyderabad, India). Poly ethylene oxide WSR 303 is a gift sample from M/s. Colorcon Asia Pvt Ltd., (Goa, India). Magnesium stearate and talc were procured from S.D Fine Chem. Ltd. (Mumbai, India).

Preparation of Cilnidipine Solid Dispersions by Solvent Evaporation Method: Solid dispersions of Cilnidipine were prepared using plasdone K-29/32 as polymer in different ratios by solvent evaporation

method (10). Measured quantities of Cilnidipine and Plasdone K-29/32 were placed in china dish. Few ml of methanol was added and heated at low temperature until both gets melted. The mixture was allowed to evaporate by continuous stirring. The solid mass obtained after the solvent evaporation was crushed and stored in desiccator for further study. The composition of various Cilnidipine solid dispersions. (Table 1).

Evaluation of Physical Parameters of Cilnidipine Solid Dispersions: The prepared solid dispersions were evaluated for various physical parameters such as angle of repose, Carr's index, Hausner's ratio, particle size and drug content (11). The results were indicated in (Table 2).

Table 1. Composition of Cilnidipine Solid Dispersions Prepared by Solvent Evaporation Method

Formulation	Drug:Polymer (Cilnidipine*:Plasdone K-29/32)
CP1	1:1.0
CP2	1:2.0
CP3	1:3.0
CP4	1:4.0
CP5	1:5.0
*One part is equal to 10mg	

Table 2. Physical Parameters of Cilnidipine Solid Dispersions

Solid Dispersion	Angle of Repose ($^{\circ}$)	Carr's Index (%)	Hausner's Ratio	Average Particle Size (μ m)	Drug Content* (mg) (Mean \pm S.D)
CD	33	23	1.28	42	09.64 \pm 0.98
CP1	24	19	1.22	188	10.04 \pm 0.47
CP2	22	16	1.18	172	09.99 \pm 0.63
CP3	20	12	1.15	156	10.08 \pm 0.31
CP4	22	14	1.17	164	09.95 \pm 1.03
CP5	23	15	1.18	169	10.11 \pm 0.32
*CD indicates Cilnidipine pure drug; n=3, S.D: standard deviation					

Angle of Repose: The powder flow properties were determined to know the good or bad material flow. The powder was taken into a funnel and poured through it. Below this, a graph sheet was placed to form a heap like structure for which, the radius and height of the heap was measured. Based on these, the angle of repose was calculated by using the formula;

$$\theta = \tan^{-1}(h/r)$$

Carr's Index: A simple test was used to evaluate the flow ability of a powder by comparing the poured density and the tapped density of a powder and the rate at which it is packed down.

$$\text{Carr's Index} = \frac{\text{Tapped density} - \text{Poured density}}{\text{Tapped density}} \times 100$$

Hausner's Ratio: It is an indication of flow properties of the powder. Hausner's ratio can be calculated by using the formula;

$$\text{Hausner's Ratio} = \frac{\text{Tap density}}{\text{Bulk density}}$$

Particle Size: A set of sieves were taken, properly cleaned and are stacked in descending order of mesh size (increase in the sieve number). The solid dispersion was taken in the sieve number 18. The sieves are closed with lid and sieving was done for 5min. The material retained on individual sieves were collected and weighed.

Drug Content Uniformity: Solid dispersions of Cilnidipine equivalent to 10mg was weighed and transferred into a 100ml volumetric flask. To this, small quantity of methanol was added to dissolve. It was shaken occasionally for about 15min and the volume was made up to 100ml by methanol. The solution was filtered using Whatmann filter paper. The filtrate was subsequently diluted with 6.8pH phosphate buffer and the absorbance was measured at 240nm using 6.8pH phosphate buffer as blank.

In vitro Dissolution Studies of Cilnidipine Solid Dispersions: Dissolution studies for all solid dispersions were

performed in a calibrated dissolution test apparatus (LABINDIA DS8000) equipped with paddles employing 900 ml of phosphate buffer pH 6.8 as dissolution medium. The paddles were operated at 50rpm and temperature was maintained at $37 \pm 1^\circ\text{C}$ throughout the experiment. The samples were withdrawn at 5, 10, 15, 20 and 30min and replaced with equal volume of same dissolution medium to maintain the sink conditions (12). The amount of the drug dissolved in the dispersions was estimated by double beam U.V spectrophotometer at 240nm. The dissolution profiles were indicated. (Figure 1).

Preparation of Cilnidipine Tablets:

Cilnidipine tablets were prepared by direct compression technique using the solid dispersion which showed maximum drug release. The solid dispersion concentration was maintained constant, while the concentration of PEO WSR 303 was increased the range of 5% to 30% w/w of total tablet weight. The raw materials were individually weighed and transferred to mortar. Using pestle, the components were mixed well and the prepared granules were passed through sieve no. 40. The granules were taken into a plastic bag and lubricated with talc and magnesium stearate. Then they were compressed as tablets under identical conditions (13). The compositions of various tablet formulations. (Table 3).

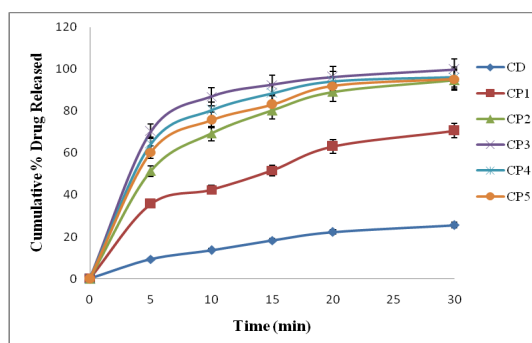


Fig 1. Drug Release Profiles of Cilnidipine Solid Dispersions

Mean \pm S.D = Mean values \pm Standard Deviation of three experiments

Evaluation of Pre-Compression

Parameters: The prepared granules were evaluated for pre compression parameters such as angle of repose, Carr's index and Hausner's ratio (14). (Table 4).

Evaluation of Post Compression

Parameters: The compressed tablets were further evaluated for post compression parameters such as weight uniformity, hardness, friability, swelling index and drug content (15)(Table 5).

Weight Uniformity: Twenty tablets were selected randomly from a batch and were individually weighed and then the average weight was calculated. The weights of individual tablets were then compared with the average weight that was already calculated. The tablets meet the specifications if not more than 2 tablets are outside the percentage limit and if no

tablet differs by more than 2 times the percentage limits.

Hardness: The crushing strength/hardness which is the force required to break the tablet in the radial direction was measured using Monsanto hardness tester (Tab-machines, Mumbai). The tablet to be tested is held in fixed and moving jaw and reading of the indicator adjusted to zero. Then force to the edge of the tablet was gradually increased by moving the screw knob forward until the tablet breaks. The reading was noted from the scale which indicates the pressure required in kg/cm² break the tablet.

Friability: Friability test was performed by using Roche friabilator (REMI Equipment, Mumbai). Ten tablets of a batch were weighted and placed in a friabilator chamber and it was allowed to rotate for 100 revolutions. During each revolution these tablets fall from a

Table 3. Composition of Cilnidipine Tablets

Ingredient (mg/tablet)	Formulations						
	CPP	CPP1	CPP2	CPP3	CPP4	CPP5	CPP6
Optimized Cilnidipine Solid Dispersion (CP3)	40	40	40	40	40	40	40
PEO WSR 303	---	12.50	25.0	37.50	50.0	62.50	75.0
MCC (PH 102)	205.0	192.50	180.0	167.50	155.0	142.50	130.0
Talc	2.5	2.5	2.5	2.5	2.5	2.5	2.5
Magnesium Stearate	2.5	2.5	2.5	2.5	2.5	2.5	2.5
Total Weight	250	250	250	250	250	250	250

Table 4. Pre-Compression Parameters of Cilnidipine Granules

Formulation	Angle of Repose (°)	Carr's Index (%)	Hausner's Ratio
CPP	30	21	1.22
CPP1	26	19	1.18
CPP2	24	17	1.17
CPP3	23	16	1.15
CPP4	22	15	1.13
CPP5	21	12	1.12
CPP6	21	12	1.12

Table 5. Post Compression Parameters of Cilnidipine Tablets

Formulation	Weight Uniformity (mg)	Hardness (kg/cm ²)	Friability (% loss)	Swelling Index (%)	Drug Content* (mg/tablet) (Mean ± S.D)
CPP	250±0.88	3.5±0.08	0.4	---	10.09±0.57
CPP1	249±0.94	3.3±0.05	0.3	90	09.96±0.82
CPP2	251±0.39	3.3±0.07	0.3	141	10.10±0.68
CPP3	250±1.01	3.2±0.10	0.3	185	10.01±1.03
CPP4	251±0.64	3.2±0.09	0.3	224	09.92±1.12
CPP5	250±0.82	3.3±0.04	0.3	262	10.05±0.93
CPP6	251±0.66	3.2±1.03	0.2	295	10.15±0.38

*n=6; S.D is standard deviation

distance of six inches to undergo shock. After completion of 100 revolutions, tablets were again weighed and the loss in weight indicated friability. The acceptance limits of weight loss should not be more than 1%. This test was performed to evaluate the ability of the tablets to withstand abrasion in packing, handling and transporting.

Swelling Index: Swelling index of the prepared tablets was measured using dissolution test apparatus (USP apparatus II method) with 900 ml of phosphate buffer pH 6.8 as dissolution medium. The paddles were operated at 50rpm and temperature was maintained at 37±1° C throughout the experiment. Weight of the tablet was taken before the study (W1). The tablet was placed in the medium for predetermined time. The swollen tablets were removed, wiped and weighed (W2). The swelling index was calculated using the formula;

$$\text{Swelling index} = \frac{W2 - W1}{W1} \times 100$$

Drug Content Uniformity: Cilnidipine tablets from a batch were taken at random and were crushed to a fine powder. The powdered material was transferred into a 100 ml volumetric flask and few ml of methanol was added to it. It was shaken occasionally for about 30 minutes and the volume was made up to 100 ml by adding

methanol. The resulting solution was set aside for few minutes and the supernatant solution was collected, filtered by using whatmann filter paper. Then the filtrate was subsequently diluted with phosphate buffer pH 6.8 and the absorbance was measured at 240 nm. This test was repeated six times (n=6) for each batch of tablets.

In vitro Dissolution Studies of Cilnidipine Tablets: Dissolution studies for Cilnidipine tablet formulations were performed in a calibrated dissolution test apparatus (USP apparatus II method) using 900 ml of phosphate buffer pH 6.8 as dissolution medium. The paddles were operated at 50rpm and temperature was maintained at 37±1° C throughout the experiment. Samples were withdrawn at 0.5, 1, 2, 4, 6, 8, 10 and 12h and replaced with equal volume of same dissolution medium to maintain the constant conditions. The amount of drug dissolved was estimated using U.V spectrophotometer at 240nm. The dissolution profiles were given in (Figure 2).

Results and Discussion

Preparation of Cilnidipine Solid Dispersions by Solvent Evaporation Method: Solid dispersions of Cilnidipine were prepared using plasdane K-29/32 as carrier in different ratios by solvent evaporation method. The composition was given the Table 1.

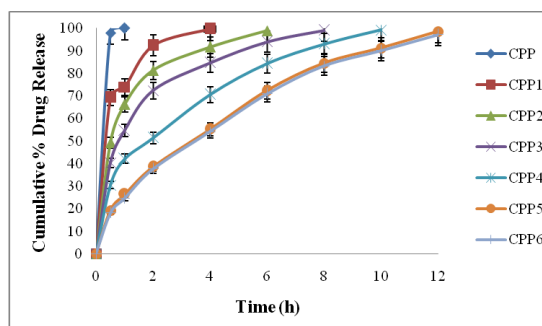


Fig 2. Dissolution Profiles of Cilnidipine Tablets

Mean \pm S.D = Mean values \pm Standard Deviation of three experiments

Evaluation of Physical Parameters of Cilnidipine Solid Dispersions: Various physical parameters for Cilnidipine solid dispersions were evaluated. All the flow properties were found to be within I.P specified limits. The obtained results were indicated in table 2.

In vitro Dissolution Studies of Cilnidipine Solid Dispersions: Formulation CP3, prepared using Cilnidipine and pladone K-29/32 in 1:3 ratios showed maximum drug release. This showed that pladone K-29/32 significantly increases drug release as suggested by past studies (16, 17). The dissolution profiles of Cilnidipine solid dispersions were given in Fig 1.

Preparation of Cilnidipine Tablets: Cilnidipine tablets were prepared using the optimized solid dispersions (CP3) along with various concentrations of PEO WSR 303 by direct compression technique. The compositions were given in table 3.

Evaluation of Pre-Compression Parameters: The pre compression parameter values obtained for various prepared granules were given in the table 4. The angle of repose, Carr's index and Hausner's ratio values for granules were within the range specified. Thus all the prepared granules were found to be stable and suitable for compression of tablets.

Evaluation of Post Compression Parameters of Cilnidipine Tablets: The direct compression method was found to be suitable for preparation of controlled release tablets. Cilnidipine tablets were prepared and evaluated for post compression parameters. The results were given in table 5. Weight uniformity, hardness and friability loss of tablet formulations were within the specified limits.

In vitro Dissolution Studies of Cilnidipine Tablets: Dissolution studies were carried on Cilnidipine tablets using U.S.P paddle method (apparatus II) with phosphate buffer pH 6.8 as dissolution medium by maintaining the bath temperature at $37 \pm 1^\circ\text{C}$ and the paddles were operated at 50rpm. The dissolution profiles of tablets were given in Table 8. The study clearly indicated that increase in the concentration of PEO WSR 303 as polymer has slowed down the drug release in the prepared tablet formulations. Formulation CPP5 containing 25% w/w of PEO WSR 303 as polymer exhibited controlled and prolonged dissolution profile. Similar drug release profile was observed with CPP6 formulation which was made using 30% w/w of PEO WSR 303. Thus the results obtained strongly suggest the usage of PEO in controlled release formulations which matches with recent findings (18, 19). The results were shown in Fig 2.

Conclusion

The present study showed that proportion of polymers used in preparation of formulations has high impact on dissolution parameters. The formulation CPP5 prepared with Cilnidipine solid dispersions using Pladone K-29/32 (1:3 ratios) and PEO WSR 303 (25%w/w) showed slower drug release.

Acknowledgements

The authors express their sincere thanks to M/s. NATCO Laboratories Ltd., (Hyderabad, India), Pellets Pharma Ltd., (Hyderabad, India) and M/s. Colorcon Asia Pvt Ltd., (Goa, India) for their generous gift samples of drug and polymers.

Conflict of Interest

Authors declare no conflict of interest.

References

1. Sundeep, M., Vidyadhara, S., Sailaja, Y., Sandeep, D., Sasidhar, R. L. and Ramu, A. (2019) Formulation and evaluation of Dolutegravir sodium solid dispersions and fast dissolving tablets using poloxamer-188 and jack fruit seed starch as excipients. *Asian Journal of Pharmaceutical and Clinical Research*, 12: 1-10.
2. Jin, X. K., Jeong, S. P., Phuong, T., Yong, C. P., Dong, H. K. and Sang, E. L. (2019) Overview of the manufacturing methods of solid dispersion technology for improving the solubility of poorly water-soluble drugs and application to anticancer drugs. *MDPI Pharmaceutics*, 11: 1-26.
3. Argade, P. S., Magar, D. D. and Sudagar, R. B. (2013) Solid dispersion: solubility enhancement technique for poorly water soluble drugs. *Journal of Advanced Pharmaceutical Education and Research*, 3: 427-439.
4. Iswarya, S., Abha, D., Bhagyashri, J., Vandana, W. and Jesal, D. (2013) Solid dispersions: an approach to enhance solubility of poorly water soluble drug. *Journal of Scientific and Innovative Research*, 2: 685-694.
5. Carla, M. L., Catarina, B., Alessandra, R., Francesca, B. and Pedro, B. (2016) Overview on gastro-retentive drug delivery systems for improving drug bioavailability. *International Journal of Pharmaceutics*, 510: 144-158.
6. Rishikesh, G., Purnima, T., Peeyush, B. and Alok, M. (2018) Recent advances in gastro-retentive drug delivery systems and its application on treatment of *H.pylori* infections. *Journal of Analytical and Pharmaceutical Research*, 7: 404-410.
7. Vidyadhara, S., Sasidhar, R. L. C. and Nagaraju, R. (2013) Design and development of polyethylene oxide based matrix tablets for Verapamil hydrochloride. *Indian Journal of Pharmaceutical Sciences*, 75: 185-190.
8. Haoyang, W., Xue, L., Yuenan, L., Haiying, W., Yanyan, W. and Tuanjie, W. (2018) *Invitro* and *Invivo* evaluation of controlled release matrix tablets of highly water soluble drug applying different mw polyethylene oxides (PEO) as retardants. *Drug Development and Industrial Pharmacy*, 44: 544-552.
9. Sarat, C. K. and Ramesh, G. (2013) The fourth generation calcium channel blocker: Cilnidipine. *Indian Heart Journal*, 65: 691-695.
10. Prashant, B. and Reeshwa, N. (2018) Formulation, development and characterization of Meclizine hydrochloride fast dissolving tablets using solid dispersion technique. *International Journal of Applied Pharmaceutics*, 10: 141-146.
11. Pinak, K., Mansi, S., Niketkumar, P., Shashank, J., Namrata, V. and Senshang, L. (2018) Preparation and characterization of Pyrimethamine solid dispersions and an evaluation of the physical nature of Pyrimethamine in solid dispersions. *Journal of Drug Delivery Science and Technology*, 45: 110-123.
12. Sharda, S., Bishambar, S., Kirtika, M., Monalisha, N., Neha, K. and Shalini, M. (2013) Solid dispersions: A tool for improving the solubility and dissolution of metronidazole. *International Journal of Drug Delivery*, 5: 94-98.
13. Mohammad, S., Sajid, B., Jabbar, A., Samiullah, K., Nargis, A. and Habibullah, J. (2018) Design, formulation and *invitro* evaluation of sustained release tablet formulations of Levosulpiride. *Turkish Journal of Pharmaceutical Sciences*, 15: 309-318.
14. Vikaas, B., Ritika, M. B., Sandeep, K., Nitesh, C. and Manjusha, C. (2016) Formulation and evaluation of fast disintegrating tablet of Telmisartan. *Journal of Chemical and Pharmaceutical Research*, 8: 61-67.

15. Remya, P. N., Saraswathi, T. S., Sangeetha, S., Damodharan, N. and Kavitha, R. (2016) Formulation and evaluation of immediate release tablets of Acyclovir. *Journal of Pharmaceutical Sciences and Research*, 8: 1258-1261.
16. Sangeetha, E., Vinay, U. R., Sudhakar, M. and Manisha, S. (2018) Enhancement of solubility and bioavailability of Hydrochlorothiazide using solid dispersion technique. *American Journal of Advances in Drug Delivery*, 3: 308-316.
17. Shirsath, N. R., Jagtap, V. and Goswami, A. K. (2019) Formulation and development of Famotidine solid dispersion tablets for their solubility enhancement. *Indian Journal of Pharmaceutical Education and Research*, 53: 548-553.
18. Nieves, I., Elsa, G., Lucia, R. A., Elena, B., Ricardo, L. and Gracia, G. M. (2020) In-depth study into polymeric materials in low-density gastroretentive formulations. *MDPI Pharmaceutics*, 12: 01-44.
19. Shah, S., Shukla, D. and Pandey, H. (2019) Formulation optimization of Polyox based modified release drug delivery system. *Journal of Drug Delivery and Therapeutics*, 9: 551-561.

***In Silico* Design and Solvent Free Synthesis of Some Novel Dihydropyrimidinthione Derivatives and Study of its Antimicrobial Activity**

G. Revathi * and Dr. K. Girija

¹Department of Pharmaceutical chemistry, Mother Theresa Post Graduate and Research Institute of Health Sciences, Indira Nagar, Gorimedu, Puducherry-6

*Corresponding Author: E-mail Id: revathi20reva@gmail.com

Abstract

According to WHO, 700,000 people were affected by antibiotic resistance per year and it becomes a serious threat to global health. Keeping in view this observation and emerging need of new drug candidates to overcome the antibiotic resistance and also to fight against the emerging diseases, the present research study focussed on to develop some novel antimicrobial agents. The study involved *In silico* design and solvent free synthesis of some novel dihydropyrimidinthione derivatives and study of its antimicrobial activity. The purity of the synthesized compounds was confirmed by TLC and melting point determination. The structures of the synthesized compounds were characterized, predicted using CHEMSKETCH, CHEM DRAW and MARVIN SKETCH software. Drug likeness properties were studied using MOLINSPIRATION software. All the synthesized compounds obey the Lipinski rule of *Five*. *In silico* ADME studies were performed using SWISS ADME online web tool, toxicity profile studied using OSIRIS property explorer software for all the designed compounds only compound F was found to be tumorigenic. The docking study was performed for all the designed compounds against the targeted enzyme Tyrosyl t-RNA Ligase Synthetase (1JIL) using AUTODOCK 4.2 software. The docking results showed Compound A, C and D produced good binding affinity and Compound B showed significant binding score (-8.30 kcal/mol) compared to standard ciprofloxacin

(-7.32 kcal/mol) Based on the docking score compounds A, B, C, and F were screened for their *in vitro* antibacterial activity against gram positive and gram-negative organisms using well diffusion method at the concentration of 100µg/ml. Compound A, B, C and D showed the good antibacterial activity compared to standard ciprofloxacin at the concentration of 100µg/ml.

Keywords: Solvent free synthesis, SWISS ADME, MOLINSPIRATION, OSIRIS, AUTODOCK 4.2.

Introduction

Antibiotic resistance is all the time more recognized as a serious and permanent public health concern and is usually considered to be a consequence of wide use and misuse of antibiotics(1). Antibiotic resistance drug discovery and development is one of the most essential and rapidly changing avenues for medicinal chemist. Despite a large number of antibiotics and for medicinal use, the treatment of infectious diseases remains an important and challenging problem(2). This is because of a combination of factors including emergence of resistance to current antimicrobial therapy and rapid increase of primary and opportunistic fungal infections in immune compromised patients like those suffering from immunodeficiency syndrome (aids) or undergoing anticancer therapy and organ transplantation. So, the drug resistivity of microbes has been increased enormously. To combat this

antimicrobial resistance, it is necessary to develop a new and effective antimicrobial drug. Dihydropyrimidinthione is one of the promising candidates attracted substantial attention of the medicinal chemists(3). Dihydropyrimidinthione were reported as therapeutic leads to develop newer and effective pharmacophores with enhanced and a versatile range of medicinal activities like such as antiviral(5), anticancer(3), antibacterial(3), antituberculosis(4), antihypertensive(6), antiarrhythmic activities(7). In keeping in view, the biological significance and medicinal utility of dihydropyrimidinthione derivative, the present study involved solvent free synthesis, molecular docking and study of some novel dihydropyrimidinthione derivatives against Tyrosyl t-RNA Ligase Synthetase as a target enzyme. Green chemistry approach under solvent free condition Simplify and improve conditions have been used traditionally to carry out the conventional Biginelli reaction involves three-component one-pot condensation of an aldehyde, β -ketoester and urea or thiourea in ethanol under strong acidic condensation HCl for the synthesis of dihydropyrimidinthione derivatives by green chemistry approach. These reactions were performed by three-component condensation of different types of an aldehyde (benzaldehyde, acetaldehyde, furfural, cinnamaldehyde, and salicaldehyde etc.), ethyl acetoacetate, and urea or thiourea at reflux temperature under solvent-free conditions with catalyst (scheme II) or without catalyst (scheme I) to afford the corresponding dihydropyrimidinthione in good yield (76–96%).

Material and Methods

All the chemicals and reagents used in experimental reactions were Analytical Grade. The melting point of the titled compounds were determined using one end sealed open capillary tube method and are uncorrected. The purity of the synthesized compounds was also checked by TLC on a pre coated silica gel using chloroform:

methanol (9:1) and spots were visualized using UV- chamber. The ^1H NMR and C^{13} NMR spectra were predicted using CHEM DRAW software. The Mass spectra were also predicted by MARVIN SKETCH software. The compounds were designed by Molecular docking study using AUTODOCK 4.2 software. All the synthesized compounds were evaluated for *in silico* ADME studies using SWISS ADME online and for its toxicity profile using OSIRIS property explorer software.

Synthesis:

General Procedure for the Synthesis of Titled Compounds: A mixture of 0.1 mole of substituted aldehydes, 0.1 mole of Ethylacetoacetate and 0.1 mole of thiourea with catalyst or without using any catalyst under solvent free condition, were taken in a round bottom flask, the reaction mixture was continuously shaken for two minutes, then heated under reflux for 2 hours, as the progress of the reaction was observed a solid compound was started to deposit. The completion of reaction was monitored by TLC using solvent system [chloroform: methanol (9: 1)]. the reaction mixture was allowed to cool and washed with cold water to remove excess of urea. It was filtered and recrystallised using ethanol to afford a pure solid product.

Scheme of Synthesis:

Scheme – I: A mixture of 0.1 mole of various substituted aldehydes, 0.1 mole of Ethylacetoacetate and 0.1 mole of thiourea without any catalyst under solvent free condition, were taken in a round bottom flask was shaken continuously for two minutes. The Reaction mixture was then heated under reflux for 2 hours, a solid product was started to deposit. The completion of reaction was monitored by TLC using solvent system [chloroform: methanol (9: 1)]. Then, the reaction mixture was allowed to cool and washed with cold water to remove excess of urea. It was filtered and recrystallised using ethanol to afford a pure solid product. The solid was taken out carefully and washed with cold water to remove excess of urea. Then, recrystallized

from rectified spirit to afford a pure solid product (Figure.1.0).

Scheme – II: To a mixture of various substituted aromatic aldehydes (0.1 mole), ethyl acetoacetate (0.1 mole), thiourea (0.1 mole) and [Btto][p-TSA] (0.15 mmol) was heated at 90°C for 30 minutes under solvent free condition with magnetic stirring. The completion of reaction was monitored by TLC. After cooling, the reaction mixture was poured on to crushed ice and stirred for 5 min. The separated solid was filtered and washed with cold water thoroughly. Then, recrystallized the synthesized products from ethanol to afford the pure product (Figure.1.1).

Physical and Spectroscopic Data of Synthesized Products

Physicochemical Properties: The Physicochemical properties of the synthesized compounds were also determined. The purity of the synthesized compounds was determined by TLC and melting point determination. All the synthesized compounds obey's the Lipinski's

rule of five. So, it has a good oral bioavailability. Determination of the Elementary analysis for all the synthesized compounds using CHEMKETCH software.

Spectroscopic Data for the Synthesized Products: The structures were characterized using predicted spectrum from CHEMSKETCH, CHEM DRAW and MARVIN SKETCH software. Drug likeness properties were studied using MOLINSPIRATION software.

A [ethyl 4- (4-chlorophenyl)-6-methyl-2-thioxo-1,2,3,4-tetrahydropyrimidine-5-carboxylate]

¹³C-NMR; δ (ppm) = 166 (-C), 61.7 (-CH₂), 174.5 (-C), 141.3 (-C), 128.3 (-CH), 15.6 (-CH₃), 54.6 (-CH₂), ¹H NMR; δ ppm: 4.19 (s,1H,-CH), 2.0 (s, 1H, NH), 4.59 (s, 3H, CH₃), 7.00 (s,1H,CH), 7.15 (s,1H,CH), 1.30 (s,2H,CH₂), Mass (m/z): 310

B [ethyl 4- (3-chlorophenyl)-6-methyl-2-thioxo-1,2,3,4-tetrahydropyrimidine-5-carboxylate]

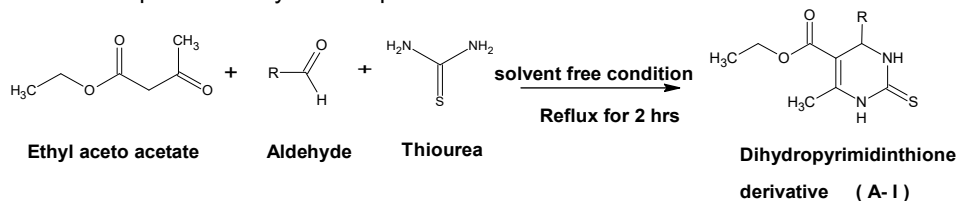


Fig 1.0. Solvent Free Synthesis of Dihydropyrimidinthione Derivative without Catalyst

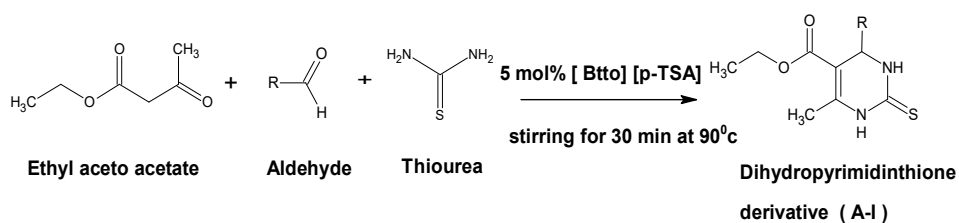


Fig 1.1 Solvent Free Synthesis of Dihydropyrimidinthione Derivative using Catalyst (p-TSA)

^{13}C -NMR; δ (ppm) = 167.2 (C=O), 61.7 (-CH₂), 104.2 (C=C), 130 (-C), 54.6 (-CH₂), 15.6 (-CH₃), 160.3 (-C=C) ^1H NMR; δ ppm: 2.0 (s, 1H, NH), 1.30 (s, 3H, CH₃), 4.19 (s, 1H, -CH), 1.71 (s, 3H, CH₃), 7.53 (tdd, 1H, -CH), 4.59 (s, 3H, CH₃), Mass (m/z): 310.

C [ethyl 4- (2-chlorophenyl)-6-methyl-2-thioxo-1,2,3,4-tetrahydropyrimidine-5-carboxylate]

^{13}C -NMR; δ (ppm) = 167.2 (C=O), 45.5 (-CH₂), 104.2 (-C), 142.8 (-C), 160.3 (-C), 180.4 (C=S), 142.8 (-C), 61.70 (-CH₂), ^1H NMR; δ ppm: 4.19 (s, 2H, -CH₂), 2.0 (s, 1H, -NH), 4.59 (tdd, 1H, -CH), 1.30 (s, 3H, -CH₃), 7.0 (s, 1H, -CH), 1.71 (s, 3H, CH₃), Mass (m/z): 310.

D [ethyl 6-methyl-4- (2-nitrophenyl)-2-thioxo-1,2,3,4-tetrahydropyrimidine-5-carboxylate]

^{13}C -NMR; δ (ppm) = 167.2 (C-O), 46.0 (-CH₂), 104.2 (C=C), 180.4 (C=S), 61.70 (-CH₂), 142.8 (-C), 137.5 (C=C), ^1H NMR; δ ppm: 4.19 (s, 2H, -CH₂), 2.0 (s, 1H, -NH), 4.59 (dd, 2H, CH-NH), 8.07 (s, 1H, -C), 1.30 (tdd, 3H, -CH₃), 7.53 (tdd, 1H, -CH), 7.32 (s, 1H, -CH), 1.71 (s, 3h, CH₃), Mass (m/z): 321.

E [ethyl 4- (4-hydroxy-3-methoxyphenyl)-6-methyl-2-thioxo-1,2,3,4-tetrahydropyrimidine-5-carboxylate]

^{13}C -NMR; δ (ppm) = 167.2 (C-O), 54.9 (-CH₂), 104.2 (C=C), 180.4 (C=S), 61.70 (-CH₂), 151.2 (-C), 160.3 (-C), ^1H NMR; δ ppm: 4.19 (s, 2H, -CH₂), 2.0 (s, 1H, -NH), 4.59 (dd, 2H, CH-NH), 6.40 (s, 1H, -C), 1.30 (tdd, 3H, -CH₃), 6.45 (tdd, 1H, -CH), 5.0 (s, 1H, -OH), 1.71 (s, 3h, CH₃), Mass (m/z): 322.

F [ethyl 4-[4- (dimethylamino)phenyl]-6-methyl-2-thioxo-1,2,3,4-tetrahydropyrimidine-5-carboxylate]

^{13}C -NMR; δ (ppm) = 167.2 (C-O), 54.6 (-CH₂), 104.2 (C=C), 180.4 (C=S), 61.70 (-CH₂), 151.2 (-C), 160.3 (-C), ^1H NMR; δ ppm: 4.19 (s, 2H, -CH₂), 2.0 (s, 1H, -NH), 4.59 (dd, 2H, CH-NH), 6.47 (s, 1H, -CH), 1.30 (tdd, 3H, -CH₃), 6.88 (s, 1H, -CH), 6.45 (tdd, 1H,

CH), 5.0 (s, 1H, -OH), 1.71 (s, 3h, CH₃), 2.85 (s, 3H, -CH₃), Mass (m/z): 319.

G [ethyl 4- (furan-2-yl)-6-methyl-2-thioxo-1,2,3,4-tetrahydropyrimidine-5-carboxylate]

^{13}C -NMR; δ (ppm) = 167.2 (C-O), 55.8 (-CH₂), 104.2 (C=C), 180.4 (C=S), 61.70 (-CH₂), 152.5 (-C), 160.3 (-C), 106.7 (-CH) ^1H NMR; δ ppm: 4.19 (s, 2H, -CH₂), 2.0 (s, 1H, -NH), 4.82 (dd, 2H, CH-NH), 6.06 (s, 1H, -CH), 1.30 (tdd, 3H, -CH₃), 6.24 (s, 1H, -CH), 7.28 (tdd, 1H, -CH), 1.71 (s, 3h, CH₃), 2.85 (s, 3H, -CH₃), Mass (m/z): 266.

H [ethyl 4- (2-hydroxyphenyl)-6-methyl-2-thioxo-1,2,3,4-tetrahydropyrimidine-5-carboxylate]

^{13}C -NMR; δ (ppm) = 167.2 (C-O), 44.4 (-CH₂), 104.2 (C=C), 180.4 (C=S), 61.70 (-CH₂), 122.9 (-C), 160.3 (-C), 128.4 (-C) ^1H NMR; δ ppm: 4.19 (s, 2H, -CH₂), 2.0 (s, 1H, -NH), 4.59 (dd, 2H, CH-NH), 6.70 (s, 1H, -CH), 1.30 (tdd, 3H, -CH₃), 6.89 (s, 1H, -CH), 6.90 (tdd, 1H, -CH), 1.71 (s, 3h, CH₃), 5.00 (s, 3H, -OH), Mass (m/z): 266.

I [ethyl 6-methyl-4-phenyl-2-thioxo-1,2,3,4-tetrahydropyrimidine-5-carboxylate]

^{13}C -NMR; δ (ppm) = 167.2 (C-O), 54.6 (-CH₂), 104.2 (C=C), 180.4 (C=S), 61.70 (-CH₂), 122.9 (-C), 160.3 (-C), 128.6 (-C) ^1H NMR; δ ppm: 4.19 (s, 2H, -CH₂), 2.0 (s, 1H, -NH), 4.59 (dd, 2H, CH-NH), 7.14 (s, 1H, -CH), 1.30 (tdd, 3H, -CH₃), 7.06 (s, 1H, -CH), 6.90 (tdd, 1H, -CH), 1.71 (s, 3h, CH₃), Mass (m/z): 276.

In Silico Studies

Evaluation of In Silico Adme Properties for the Synthesized Compounds Using Swiss Adme Software:

Swiss ADME Tool: The pharmacokinetics and drug likeness prediction of compounds were performed online on Swiss ADME tool. The online prediction was done to check the compound were inhibitors of cytochrome P450. In addition to the pharmacokinetic properties such as Gastrointestinal absorption, Blood-Brain Barrier penetration, Skin Permeation, synthetic associability and drug-likeness prediction like

Lipinski, Ghose and Veber rules and bioavailability score were also assessed.

Bioavailability Radar: The drug-likeness of a molecule can be rapidly assessed from the Bioavailability Radar. The pink colored zone is the suitable physiochemical space for oral bioavailability and the radar plot of the molecule has to fall entirely in the zone to be considered drug-like. The pink area represents the optimal range of each property LIPO (Lipophilicity): $-0.7 < XLOGP_3 < +5.0$; SIZE: $150 \text{ g/mol} < \text{MW} < 500 \text{ g/mol}$; POLAR (polarity): $20 \text{ \AA}^2 < \text{TPSA} < 130 \text{ \AA}^2$; INSOLU (Insolubility): $0 < \text{Log S (ESOL)} < 6$; INSATU (Insaturation): $0.25 < \text{Fraction of Csp}^3 < 1$; FLEX (Flexibility): $0 <$

Num. rotatable bonds < 9 . From the Swiss ADME prediction output, it is evident that all the compounds have the optimal range of all the six properties, enabling them to be considered to possess significant chemotherapeutic potentials.

Pharmacokinetics Properties: All the designed compounds (Fig.1.2 – 2.1) were observed with high intestinal absorption and hence should permeate quite easily across the intestinal lining and available for the cell membrane. drugs that act in the CNS need to pass over the blood brain barrier (BBB) to reach their molecular target. however, little or no BBB permeation might be required for drug

Compound - A

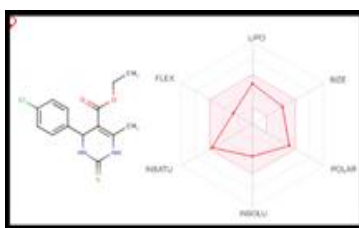


Fig 1.2

Compound - B

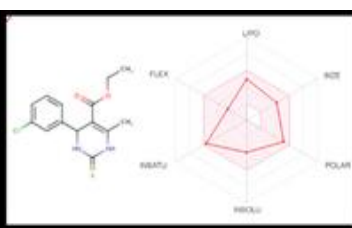


Fig 1.3

Compound - C

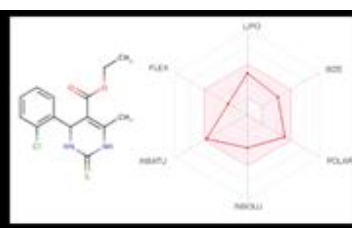


Fig 1.4

Compound - D

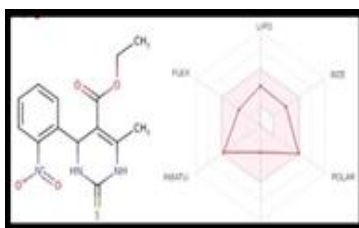


Fig 1.5

Compound - E

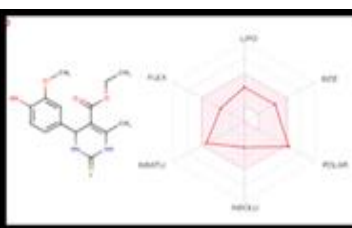


Fig 1.6

Compound - F

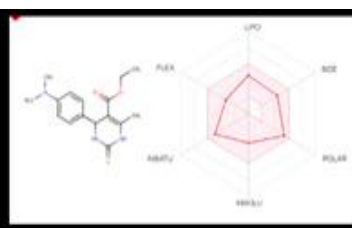


Fig 1.7

Compound - G

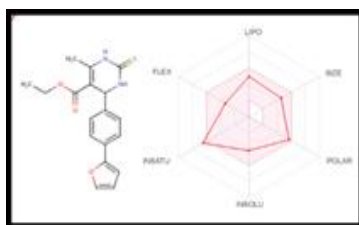


Fig 1.8

Compound - H

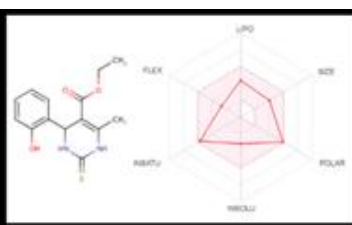


Fig 1.9

Compound - I

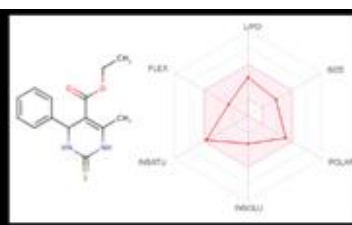


Fig 2.1

molecules with a peripheral target, so as to avoid CNS side effects.

The Blood-brain barrier (BBB) permeation expresses the relative affinity of the drug for the blood or brain tissue. It was observed that all the compounds predicted have no blood-brain barrier penetration and hence free from CNS side effects.

BOILED-Egg Model: The Brain or Intestinal permeation method (BOILED-Egg) is an intuitive graphical method to accurately predict the passive human gastrointestinal absorption (HIA) and brain permeability (BBB). This classification model relies on the descriptors: WLOGP and TPSA values, for computing lipophilicity and corresponding polarity of small molecules. The egg-shaped classification plot includes the yolk (i.e. the physicochemical space for highly probable brain permeation) and the white (i.e. the physicochemical space for highly probable passive absorption by the gastrointestinal tract). The outside grey region stands for molecules with properties implying predicted low absorption and limited brain penetration. from the boiled-egg plots, it has been observed that all the compounds were spotted in the white yolk attributed to highly probable HIA absorption Fig. 2.2.

Molecular Docking:

Ligand Preparation: Structures of molecules were drawn using ACD Labs ChemsSketch 2017 V.2.1 and saved in mol format. Open Babel V.2.4.1 mol format is used for converting formats (mol to pdb). UCSF Chimera V.1.13.1rc was used for optimization and minimizing structures by setting default options, i.e., steepest descent 100 steps, and conjugate gradient 10 steps. On adding hydrogens and assigning Gasteiger's charges, the net charge on the molecules is displayed. On saving the work, molecules were processed for docking using AutoDock Tool V.1.5.6.

Protein Preparation: Proteins were selected from PDB (w3.rcsb.org) and initially processed to remove solvent molecules, heteroatoms, and other non-standard residues. AutoDock Tool V.1.5.6 was used to prepare protein for docking by adding polar hydrogen, merging non-polar hydrogen and assigning Kollman's charges.

Grid Generation: AutoDock Tool is an interactive graphical tool for coordinate preparation, docking, and analysis. Preparation of coordinate files is the most important step of the process, as it affects docking quality. The three-dimensional (3D) grid box was created by AutoGrid algorithm to evaluate the binding energies on the macromolecule coordinates. Using AutoGrid, the grid maps expressing the intact ligand in the docking target site were



Fig 2.2

Novel Dihydropyrimidinthione Derivatives

calculated. The 3D grid box with 100 grid size (x, y, z) was created with a spacing of 0.375. The selected protein and ligand in PDBQT format were chosen, followed by the generation of GPF (grid parameter file), after which Running AutoGrid provided GLG (grid log file).

Docking: AutoDock V.4.2.6 is a computational docking program based on an empirical free energy force field and rapid Lamarckian genetic algorithm search method. In AutoDock, the overall docking energy of a given ligand molecule is expressed as the sum of intermolecular interaction energies including van der Waals attractive and repulsive energies, H-bond interaction energy, coulombic electrostatic energy, and the internal steric energy of the ligand. The selected protein and ligand on Autogrid options were subjected to docking, followed by generation of DPF (docking parameter file). Running AutoDock provides DLG (docklog file). By default, ten best conformations of protein-ligand interactions were resulted by AutoDock along with binding energy values, inhibition constant (predicted) and H-bond interactions. The docking results are presented below in Tables 1.4 and 1.5. The complexes with good binding energy values were built and subjected to LigPlot+ V.2.1 for visualizing interactions Fig.2.4. The typical interactive patterns are shown in Figs.2.6, 2.7, 2.8.

Molecular Docking for Anti-Microbial Activity:

Target Enzyme → Tyrosyl T-RNA Ligase Synthetase

Target Protein → PDB ID : 1JIL

Active Site: Active sites were selected using PDB sum by Ligplot interaction.

Standard: Ciprofloxacin

Toxicity Profile by Osiris Property Explorer:

All the synthesized compounds were studied for its toxicity profile using Osiris Property Explorer software. The results

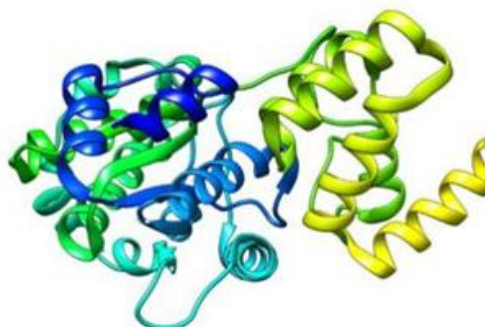


Fig 2.3

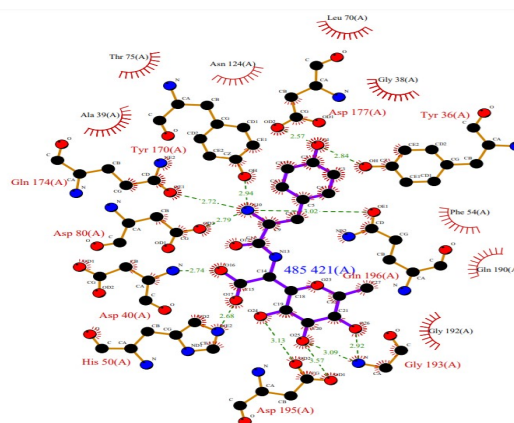


Fig 2.4

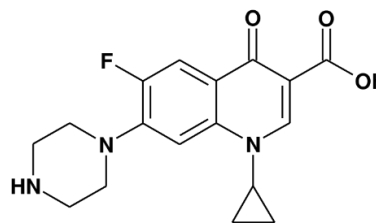


Fig 2.5

Docked Poses Of Standard, Compound B And C in the Binding Pocket with Tyrosyl T-RNA Ligase Synthetase (PDB ID: 1JIL) and Yellow Dashed Lines Represents Hydrogen Bond Interactions

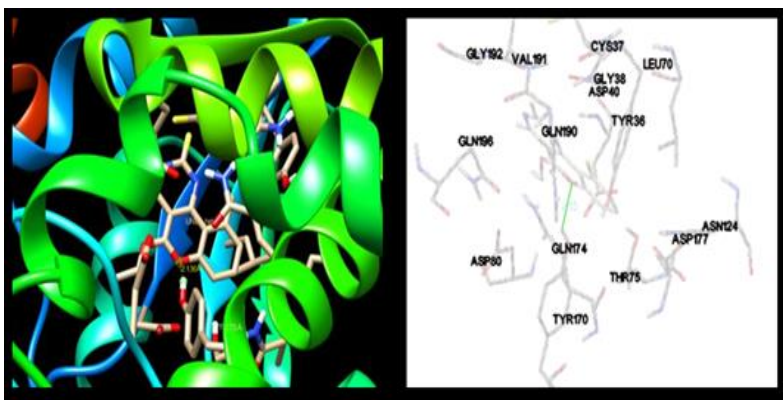


Fig 2.8 Compound C

risk except compound F which showed Tumorigenic effect.

In Vitro Antimicrobial Study

Antibacterial activity of synthesized compounds against gram negative (*E.coli* and *Pseudomonas aeruginosa*) bacteria and gram positive bacteria (*Bacillus subtilis* and MRSA) were investigated in vitro using well diffusion method.

The evaluation can be done by the following methods.

- Turbidimetric method.
- Agar streak method
- Serial dilution method.
- Agar diffusion method.

In agar diffusion methods there are about two types of techniques;

- Agar well diffusion
- Agar disc diffusion

Organism:

- *Escherichia coli* (gram negative)
- *Pseudomonas aeruginosa* (gram negative)
- *Bacillus subtilis* (gram positive bacteria)
- *Methicillin - resistant staphylococcus aureus (MRSA)* (gram positive bacteria)

Control: Distilled water

Concentration: 10 µg/ml

Method: Well diffusion method.

- All the synthesized compounds were screened for their *in vitro* antibacterial activity against gram positive (*Bacillus subtilis* and MRSA) and gram negative (*E. coli* and *Pseudomonas aeruginosa*) organisms using well diffusion method at the concentration of 100µg/ml. Compound C showed significant antibacterial activity against *E. coli* (17mm), *Pseudomonas aeruginosa* (19mm), *Bacillus subtilis* (15mm) and MRSA (14mm) respectively.
- Among the tested compounds, compound C produces a very good antibacterial activity.
- Compound A, B, C and F showed the good antibacterial activity against MRSA compared to standard ciprofloxacin.

Results

1. Chemistry and Synthesis

- A series of nine novel dihydropyrimidinthione derivatives were synthesized by condensing ethyl aceto acetate with various aromatic aldehydes under solvent free condition using catalyst (p-TSA).

- The reaction has also been carried out without using catalyst.
- The progress of reaction were checked by thin layer chromatography using the solvent system chloroform: methanol (9:1).
- The scheme details has been shown in Table.1.0

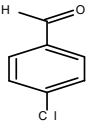
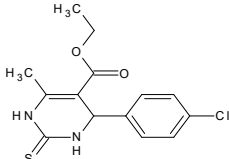
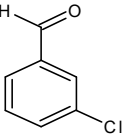
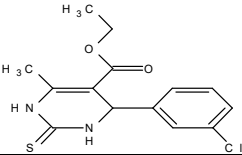
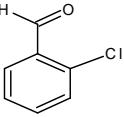
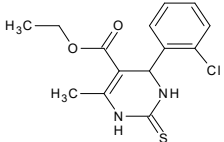
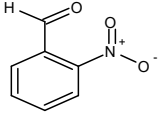
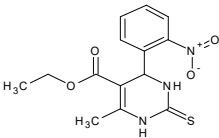
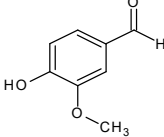
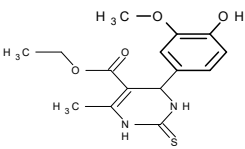
Scheme Details: The purity of the synthesized compounds were characterized by melting point determination and are uncorrected. The physiochemical properties of the synthesized compounds were studied and has been depicted in the Table 1.1 given below:

The chemical structures of synthesized compounds were characterized using PREDICTED NMR and MASS SPECTRUM by the software CHEM DRAW, CHEM SKETCH and MARVIN SKETCH softwares for elemental analysis, NMR and Mass spectra respectively.

2. In Silico Studies: The preliminary QSAR study or drug likeness of the synthesized compounds were studied using MOLINSPIRATION software was shown in the Table 1.2 and 1.3 and the parameters obeys the Lipinski rule of five. Hence, the synthesized compounds have a good oral bioavailability.

QSAR, Drug Likeness and Docking Results: Molecular docking studies of Tyrosyl

Table 1.0

Compound Code	R	Structure
A [ethyl 4- (4-chlorophenyl)- 6-methyl-2-thioxo-1,2,3,4- tetrahydropyrimidine -5-carboxylate]		
B [ethyl 4- (3-chlorophenyl)- 6-methyl-2-thioxo- 1,2,3,4-tetrahydropyrimidine -5-carboxylate]		
C [ethyl 4- (2-chlorophenyl)- 6-methyl-2- thioxo-1,2,3,4- tetrahydropyrimidine-5-carboxylate]		
D [ethyl 6-methyl- 4- (2-nitrophenyl)- 2-thioxo-1,2,3,4-tetrahydropyrimidine -5-carboxylate]		
E [ethyl 4- (4-hydroxy- 3-methoxyphenyl)-6-methyl- 2-thioxo-1,2,3,4- tetrahydropyrimidine-5-carboxylate]		

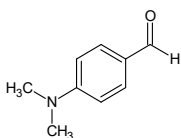
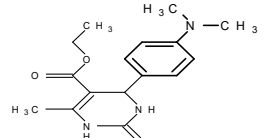
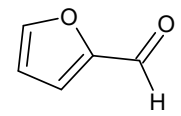
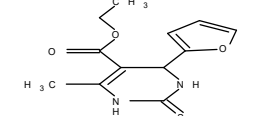
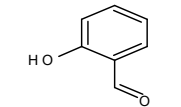
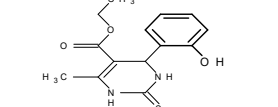
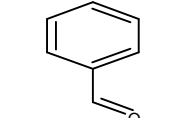
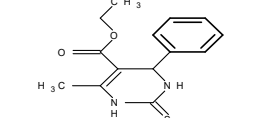
F [ethyl 4-[4- (dimethylamino) phenyl]-6-methyl-2-thioxo-1,2,3,4-tetrahydropyrimidine-5-carboxylate]		
G [ethyl 4- (furan-2-yl)-6-methyl-2-thioxo-1,2,3,4-tetrahydropyrimidine-5-carboxylate]		
H [ethyl 4- (2-hydroxyphenyl) -6-methyl-2-thioxo-1,2,3,4-tetrahydropyrimidine-5-carboxylate]		
I [ethyl 6-methyl-4-phenyl-2-thioxo-1,2,3,4-tetrahydropyrimidine-5-carboxylate]		

Table 1.1. Physicochemical Properties

Compound Code	Molecular Formula	Molecular Weight (gm/mol)	Percentage Yield (%)	Melting Point (°C)	Log P	RF Value
A	C ₁₄ H ₁₂ O ₂ N ₂ SCl	310.81	83.3	206	3.54	0.64
B	C ₁₄ H ₁₂ O ₂ N ₂ SCl	310.81	96.7	180	3.75	0.88
C	C ₁₄ H ₁₂ O ₂ N ₂ SCl	310.81	97.6	220	3.59	0.64
D	C ₁₄ H ₁₂ O ₄ N ₃ S	321.36	96.71	170	2.82	0.52
E	C ₁₅ H ₁₈ N ₂ O ₄ S	322.38	90.23	160	2.73	0.86
F	C ₁₆ H ₂₁ N ₃ O ₂ S	319.42	96.5	85	3.01	0.68
G	C ₁₂ H ₁₄ N ₂ O ₃ S	266.32	97.12	158	2.17	0.75
H	C ₁₄ H ₁₆ N ₂ O ₃ S	292.36	82.15	170	2.85	0.8
I	C ₁₄ H ₁₆ N ₂ O ₂ S	276.36	85.36	110	2.91	0.58

Table 1.2. Preliminary QSAR Study

Compound Code	Log P	Tpsa	N Atoms	Non	Nohnh	N Violations	N Rotb	Volume
A	3.59	50.36	20	4	2	0	4	261.54
B	3.57	50.36	20	4	2	0	4	261.54
C	3.54	50.36	20	4	2	0	4	261.54
D	2.82	96.18	22	7	2	0	5	271.34
E	2.25	79.82	22	6	3	0	5	281.57
F	3.01	53.60	22	5	2	0	5	293.91
G	2.17	63.50	18	5	2	0	4	227.57

Novel Dihydropyrimidinthione Derivatives

<i>H</i>	2.85	70.59	20	5	3	0	4	256.02
<i>I</i>	2.91	50.36	19	4	2	0	4	248.00

Table 1.3. Drug Likeness by Molinspiration

Compound Code	Gpcr Ligand	Ion Channel Modulator	Kinase Inhibitor	Nuclear Receptor Ligand	Protease Inhibitor	Enzyme Inhibitor
A	-0.99	-0.55	-1.57	-0.91	-1.49	-0.91
B	-0.96	-0.5	-1.46	-0.95	-1.41	-0.85
C	-0.97	-0.51	-1.44	-0.94	-1.41	-0.85
D	-0.97	-0.47	-1.52	-0.85	-1.37	-0.88
E	-0.84	-0.51	-1.23	-0.72	-1.26	-0.73
F	-0.81	-0.49	-1.19	-0.76	-1.20	-0.76
G	-1.37	-0.86	-2.08	-1.43	-1.91	-1.17
H	-9.7	-0.48	-1.44	-0.80	-1.37	-0.77
I	-1.05	-0.53	-1.54	-1.01	-1.48	-0.87

Table 1.4. Molecular Interactions of Ligand Compounds with Protein in 1jil

Compound Code	H-Bond Interaction	H-Bond Distance (Å)	Non-Bonding Interactions	Binding Energies (Kcal/Mole)
A	UNK N : VAL 224 :A	2.21	Ser 194, Leu 223, Phe 232, Asp 195, Gly 193, Leu 52, Pro 32	-6.83
B	UNK O : GLY 38: A	1.982	Tyr 170, Asp 177, Gln 174, Asp 80, Thr 75, Gln 196, Gln 190, Val 191, Gln 191, Asn 124	-8.30
C	-	-	Arg 227, Pro 336, Pro 326, Ser 382, Glu 381, Ile 338, Asp 384	-8.28
D	UNK O : ARG 65 : A	2.065	Ala 335, Pro 336, Ser 330, Leu 329, Asp 384, Phen 92, Arg 227	-6.84
E	UNK O: LYS 90 : A	2.675	Leu 329, Ser 330, Thr 332, Ile 338, Ser 330, Glu 381, Asp 384, Phen 92	-6.81
F	-	-	Pro 326, Ile 338, Ala 335, Pro 336, Asp 384, Arg 227, Arg 65	-6.20
G	-	-	Pro 326, Ile 338, Asp 384, Glu 381, Ala 335, Leu 329, Pro 336, Ser 330	-5.60
H	UNK O : SER 194: A UNK O: VAL 224 : A	2.380 1.796	Leu 329, Pro 326, Ser 382, Glu 381, Asp 384, Ile 338, Thr 332, Ala 335, Arg 227	-6.20
I	UNK O : ARG 227: B	2.152	Phen 92, Lys 90, Asp 384, Tyr 402, Val 109, Leu 108, Ala 409	-6.73
Ciprofloxacin	UNK O: LYS 231:A UNK O: HIS 47:A	1.841 1.641	Phen 92, Ser 330, Arg 227, Pro 336, Pro 326, Ile 338, Ser 382, Asp 384, Phe 383	-7.32

Table 1.5. Energy Minimization Table

S No	Compound Code	Binding Energy (Kcal/Mol)	Ligand Efficiency	Inhibitory Constant (μ M)	Vdw - Hb Desolvation Energy (K Cal/Mol)
1	A	-6.83	-0.34	9.92	-8.02
2	B	-8.30	-0.42	82.14	-8.87
3	C	-8.28	-0.32	20.83	-6.86
4	D	-6.84	-0.32	7.79	-7.54
5	E	-6.81	-0.27	38.83	-7.45
6	F	-6.20	-0.27	38.89	-7.51
7	G	-5.60	-0.29	152.96	-6.24
8	H	-6.20	-0.3	40.96	-7.09
9	I	-6.73	-0.29	106.71	-5.97
10	Ciprofloxacin	-7.32	-0.22	36.49	-8.04

RNA ligase synthetase (PDB ID: 1JIL) with designed potential inhibitors was carried out by using Auto dock 4.2. And the results has been tabulated in Table 1.4. 2D and 3D snapshots depicting the docking poses along with molecular level interactions responsible for the binding have been shown in Figs 1.13, 1.14, 1.15. for the standard control drug Ciprofloxacin and nine novel dihydropyrimidinthione derivatives respectively. Molecular docking study were performed for the synthesized compounds using AUTODOCK software version 1.5.4.

- Antimicrobial Activity - compound B showed the good binding affinity (-8.87 kcal/mol) towards the target Tyrosyl t-RNA Ligase Synthetase (1JIL) compared to standard ciprofloxacin (-8.04) respectively.
- Docking scores or binding energies for all the synthesized compounds were shown in the Table.1.4
- Energy minimization values for the obtaine compounds were also depicted in the Table 1.5

Evaluation of Pharmacokinetics, Drug Likeness and Medicinal Chemistry Friendliness of Molecules–Swiss Adme: To

be effective as a potent drug, a molecule must reach its target in the body in sufficient concentration, and stay there in a bioactive form long enough for the expected biologic events to occur. Drug development involves assessment of absorption, distribution, metabolism and excretion (ADME) increasingly earlier in the discovery process, at a stage when

considered compounds are numerous but access to the physical samples is limited. In that context, computer models constitute valid alternatives to experiments. The Swiss ADME web tool that gives easy efficient input, free access to a pool of fast yet robust predictive models for physicochemical properties, pharmacokinetics, drug-likeness and medicinal chemistry friendliness, among which in-house proficient methods such as the BOILED Egg, iLOGP and Bioavailability Radar to support drug discovery endeavors were tabulated as **Table 1.7.** Class: <10 – Insoluble, 10 – Poorly, 6- Moderetly, 4 – soluble, 2 – very, 0 highly. During the time- and resource-consuming processes of drug discovery and development, a large number of molecular structures are evaluated according to very diverse parameters in order to steer the selection of which chemicals to synthesize, test and

promote, with the final goal to identify those with the best chance to become an effective medicine for the patients. The molecules must show high biological activity together with low toxicity. Equally important is the access to and concentration at the therapeutic target in the organism. It has been demonstrated that early estimation of ADME in the discovery phase reduces drastically the fraction of pharmacokinetics-related failure in the clinical phases 1. As per the Swiss ADME predictions, results of which were tabulated in **Tables 1.6, 1.7 and 1.8**; all the synthesized dihydropyrimidinthione derivatives are as per Lipinski's rule. Hence all the synthesized compounds have potential drug likeness, lead likeness, skin permeation and synthetic accessibility. The results showed that the synthesized compounds are polar with good to moderate water solubility and are therefore

expected to have good oral absorption and bioavailability. The predicted gastro-intestinal absorption was displayed high and could assess the absence of toxicity at CNS level due to nonpermeation across the BBB. The log p values of all designed compounds were found to be optimal and hence are predicted to have good permeability and oral absorption.

Elementary Analysis: All the synthesized compounds were determined for elementary analysis using CHEMSKETCH SOFTWARE. The Elementary values are depicted in the tabular column 1.9.

Toxicity Assessment: All the synthesized compounds were studied for its toxicity profile using OSIRIS PROPERTY EXPLORER software. The results showed that the most of the studied compounds were found

Table 1.7. Drug Likeness Properties using SWISS ADME

Compound Code	Lipophilicity (Log P _{o/w})					Water Solubility (Log S)		
	iLOGP	XLOGP3	WLOGP	MLOGP	SILICOS-IT	ESOL	Ali	SILICOS-IT
A	2.96	2.61	1.61	2.03	3.83	-3.37	-3.99	-4.91
B	2.92	2.61	1.61	2.03	3.83	-3.37	-3.99	-4.91
C	2.87	2.61	1.61	2.03	3.83	-3.37	-3.99	-4.91
D	2.12	1.81	0.86	0.54	1.04	-2.84	-4.12	-3.67
E	2.74	1.60	0.67	0.66	2.77	-2.72	-3.56	-3.84
F	2.90	2.10	1.02	1.45	2.86	-3.02	-3.53	-4.40
G	2.53	1.06	0.55	0.18	2.58	-2.11	-2.68	-3.53

H	2.32	1.62	0.66	0.95	2.71	-2.63	-3.39	-3.73
I	2.70	1.98	0.96	1.51	3.19	-2.77	-3.34	-4.31

Table 1.8. *In Silico* ADME Prediction using SWISS ADME

Compound Code	GI Absorption	BBB Permeation	P-GP Substrate	CYP1A ₂ Inhibitor	CYP2C ₁₉ Inhibitor	CYP3A ₄ Inhibitor	Skin Permeation cm/s
A	High	No	No	Yes	Yes	Yes	-6.34
B	High	No	No	Yes	Yes	Yes	-6.34
C	High	No	No	Yes	Yes	Yes	-6.34
D	High	No	No	Yes	No	No	-6.98
E	High	No	Yes	No	Yes	No	-7.13
F	High	No	No	No	Yes	No	-6.76
G	High	No	No	Yes	Yes	No	-7.16
H	High	No	No	No	Yes	No	-6.93
I	High	No	No	Yes	Yes	No	-6.58

Table 1.9. Elementary Analysis

Compound Code	Molecular Formula	Molecular Weight	Composition
A	C ₁₄ H ₁₂ O ₂ N ₂ SCl	310.81	C (54.10%) H (4.86%) Cl (11.41%) N (9.01%) O (10.30%) S (10.32%)
B	C ₁₄ H ₁₂ O ₂ N ₂ SCl	310.81	C (54.10%) H (4.86%) Cl (11.41%) N (9.01%) O (10.30%) S (10.32%)
C	C ₁₄ H ₁₂ O ₂ N ₂ SCl	310.81	C (54.10%) H (4.86%) Cl (11.41%) N (9.01%) O (10.30%) S (10.32%)
D	C ₁₄ H ₁₂ O ₄ N ₃ S	321.36	C (52.33%) H (4.70%) N (13.08%) O (19.92%) S (9.98%)
E	C ₁₅ H ₁₈ N ₂ O ₄ S	322.38	C (55.88%) H (5.63%) N (8.69%) O (19.85%) S (9.95%)
F	C ₁₆ H ₂₁ N ₃ O ₂ S	319.42	C (60.16%) H (6.63%) N (13.16%) O (10.02%) S (10.04%)
G	C ₁₂ H ₁₄ N ₂ O ₃ S	266.32	C (54.12%) H (5.30%) N (10.52%) O (18.02%) S (12.04%)
H	C ₁₄ H ₁₆ N ₂ O ₃ S	292.36	C (57.52%) H (5.52%) N (9.58%) O (16.42%) S (10.97%)
I	C ₁₄ H ₁₆ N ₂ O ₂ S	276.36	C (60.85%) H (5.84%) N (10.14%) O (11.58%) S (11.60%)

Table.2.0: Osiris Property Explorer – Toxicity Profile

Compound Code	Mutagenic Effect	Tumorigenic Effect	Irritant Effect	Reproductive Effect

A				
B				
C				
D				
E				
F				
G				
H				
I				
 → indicates the non-toxic effect  → indicates the Tumorigenic effect				

Table 2.1. Evaluation of *In Vitro* Antibacterial Activity

Compound Code	Zone of inhibition			
	<i>Escherichia Coli</i> MTCC 433	<i>Pseudomonas Aeruginosa</i> MTCC 1934	<i>Bacillus Subtilis</i> MTCC 121	<i>Methicillin Resistant-Staphylococcus Aureus</i> MRSA
A	12 mm	15 mm	11 mm	11 mm
B	15 mm	17 mm	14 mm	13 mm
C	17 mm	19 mm	15 mm	14 mm
D	15 mm	18 mm	12 mm	-
E	16 mm	11 mm	11 mm	-
F	11 mm	12 mm	12 mm	13 mm
G	12 mm	13 mm	12 mm	-
H	12 mm	13 mm	11 mm	-
I	13 mm	12 mm	12 mm	-
Ciprofloxacin	22 mm	21 mm	20 mm	-

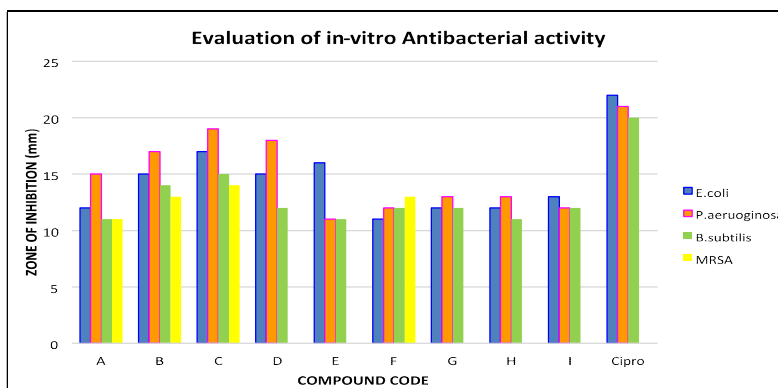


Fig.2.9

to be non-toxic except compound F which showed Tumorigenic effect. The risk of toxicity profile for the predicted compounds were depicted in the Table 2.0.

Evaluation of In Vitro Anti-Bacterial Activity: All the synthesized compounds were screened for their *in vitro* antibacterial activity against gram positive (*Bacillus subtilis* and *MRSA*) and gram negative (*E.coli* and *Pseudomonas aeruginosa*) organisms using well diffusion method at the concentration of 100µg/ml was shown in the Table 2.1. Compound C showed significant antibacterial activity against *E.coli* **MTCC 433** (17mm), *Pseudomonas aeruginosa* **MTCC 1934** (19mm), *Bacillus subtilis* **MTCC 121** (15mm) and *MRSA* (14mm) respectively.

Among the tested compounds, compound C produces a very good antibacterial activity. Compound A, B, C and F showed the good antibacterial activity against *MRSA* compared to std ciprofloxacin.

The Schematic representation for the evaluation of *In vitro* antibacterial activity were depicted in the Fig.2.9

Discussion

Antibiotic resistance is all the time more recognized as a serious and permanent public health concern and is usually considered to be a consequence of wide use

and misuse of antibiotics. So, the drug resistivity of microbes has been increased enormously². To combat this antimicrobial resistance, it is necessary to develop a new and effective antimicrobial drug³. So, we sought to design, synthesis of novel dihydropyrimidinthione is one of the promising candidates attracted substantial attention of the medicinal chemists³. Dihydropyrimidinthione²⁰ were reported as therapeutic leads to develop newer and effective pharmacophores with enhanced and a versatile range of medicinal activities like such as antiviral⁵, anticancer³, antibacterial³, antituberculosis⁴, antihypertensive⁶, antiarrhythmic activities⁷.

Most of the drugs on the market today are entirely chemically synthesized in the laboratory. Several medicinal chemists had synthesized dihydropyrimidine (DHPMs) derivatives showing a wide spectrum of therapeutic actions as antibacterials, antivirals as well as antitumor agents.

Green Chemistry approach³² shows synthesis is in good yields and in less time and also avoids problems associated with solvent and reagents use. It was found that PTSA (p-toluene sulphonic acid) works as an excellent catalyst for the one-pot three components and solvent free synthesis of dihydropyrimidinthione. This technique is superior to the existing methods. Since grinding does not require solvents leading to a

safe and environmental friendly synthesis solvent free approach opens up numerous possibilities for conducting rapid organic synthesis and functional group transformations more efficiently³³. Additionally there are distinct advantages of these solvent free reactions. It prevents pollution in organic synthesis at source³³. In solvent free organic reactions reagents react together in the absence of any solvent have been reviewed as a fast developing technology. It is required to develop safe, practical and environmental friendly process. Many exothermic reactions can be accomplished in high yield by using a technique known as "**Grindstone chemistry**" which is one of the "**Green Chemistry Technique**"³⁴.

In the conventional synthesis of dihydropyrimidinthione derivatives requires nearly 20 hours to complete the synthesis without using any catalyst and green chemistry approach. Comparison between conventional²⁷ and solvent free synthesis³⁰ was done by comparing total reaction time and percentage yield. The results suggest that solvent free synthesis¹⁵ lead to higher yields within very short reaction times. In keeping in view, the biological significance, medicinal utility and in order to minimize of solvent and also time consuming with good yield product of dihydropyrimidinthione derivative²⁵, the present study involved solvent free synthesis¹¹, molecular docking and study of some novel dihydropyrimidinthione derivatives¹³ against Tyrosyl t-RNA Ligase Synthetase as a target enzyme. solvent-free conditions with catalyst p-TPSA³¹ (scheme II) or without catalyst (scheme I) to afford the corresponding dihydropyrimidinthione in good yield (76–96%).

Conclusion

Novel dihydropyrimidinthione derivatives were designed and synthesized using Green chemistry approach, eco-friendly technique in order to increase the speed of the reaction and the percentage yield. The

purity of the synthesized compounds was determined by TLC and melting point determination. The structures were characterized using predicted spectrum from CHEMSKETCH, CHEM DRAW and MARVIN SKETCH software. Drug likeness properties were studied using MOLINSPIRATION software. All the synthesized compounds obey's the Lipinski's rule of five. All the synthesized compounds were studied for its toxicity profile using OSIRIS property explorer software. The results showed that the most of the studied compounds was non-toxic, except compound F which shows tumorigenic effect. All the synthesized compounds showed good binding energies against the target enzyme for antimicrobial activity. Compound B showed significant antibacterial activity compared to Standard ciprofloxacin at the concentration of 100µg/ml. This result showed Compound B may be suitable newer molecule for further development of potential antimicrobial agent for emerging diseases.

Acknowledgment

Dr.S. Jayanthi., DEAN, Mother Theresa post graduate and Research Institute of Health Sciences for her kind support.

DR. Joseph selvin, Department of Microbiology, Pondicherry university, Puducherry.

References

1. Centres for Disease Control and Prevention, US Department of Health and Human Services. Antibiotic resistance threats.
2. C.,Lee, Ventola, MS. 2015April. The antibiotic resistance crisis. NCBI Resources. 40 (4):277-83.
3. Rana, K., Arora, A., Bansal, S., Chawla, R. 28th January 2014. Synthesis, *in vitro* anticancer and antimicrobial evaluation of novel substituted dihydropyrimidines. Indian J PharmSci., DOI: 10.4103/0250-474X.139929.6 (4):339-47. PMID 25284932.

4. Yadlapalli, RK., Chourasia, OP., Vemuri, K., Sritharan. M., Perali, RS. March 7th 2012 Synthesis and in vitro anticancer and antitubercular activity of diarylpyrazole ligated dihydropyrimidines possessing lipophilic carbamoyl group. *Bio organic Med Chem Lett.* 22 (8):2708-11.doi: 10.1016/j.bmcl.2012.02.101, PMID 22437116.
5. Kumarasamy, D., Roy, B.G., Rocha-Pereira, J., Neyts, J., Nanjappan S., Maity S., Mookerjee M., Naesens,L.,Biswajit Gopal Roy., Joana Rocha-Pereira,C., JohanNeyts,C., Satheeshkumar, Nanjappan,D., Subhasis Maity, A., Musfiqua Mookerjee, A., and Lieve Naesens. C. 15th January 2017 Synthesis and in vitro antiviral evaluation of 4-substituted 3,4-dihydropyrimidinones.*Bioorg Med Chem Lett.*27 (2):139-42.doi: 10.1016/j.bmcl.2016.12.010, PMID 27979594.
6. Bryzgalov, AO., Dolgikh, MP., Sorokina, IV., Tolstikova,TG., Sedova, V.F., Shkurko, O.P. April 2006. Antiarrhythmic activity of 4,6-di (het)aryl-5-nitro-3,4-dihydropyrimidin- (1H)-2-ones and its effects on arterial pressure in rats. *Bioorg Med Chem Lett.*16 (5):1418-20. doi: 10.1016/j.bmcl.2005.11.043. Source: PubMed. PMID 16321526.
7. Zhang,Y., wang, B., xiaomeizhang, Jianbing L. 2015. Efficient synthesis of 3,4dihydropyrimidin-1 (1H)-ones and thiones catalyzed by a novel Bronsted acidic ionic liquid under solvent free conditions. 3811-3820.
8. Reddy, R. (December) 2008 tin (iv)catalyzed one –part synthesis of 3, 4, dihydropyrimidines- 2 (H) ones under solvent free-conditions. *Indian JChem*;47B pp1871-1875.
9. Patil, HI., Singh, MC., Gaiwkwad, P., Lade, KS., Gadhave, NA., Sawant, SD. 2011. Green chemistry why and how for sustainable chemical industry and environmentally commendable civilization. *PharmResJ.* 4; 4804:2798.
10. Wang, C. 2007 December one –pot synthesis of 3,4, dihydropyrimidine-one2 (1H)catalyzed by acidic ionic liquid.*Indian JChem.*46B 2045-2048.
11. Vingzhao. January 2015. Polyphosphoric acid catalyst for the one –pot synthesis of 3,4 dihydropyrimidine2 (H) ones by griding under solvent –free condition. *Indian J Chem vol .54B* pp139-141.
12. Pathak, V., 2008 March efficieny inexpensive route to multicomponent biginelli condensation catalyzed by cucl₂. H₂O-HCl. *Indian JChem*; 47Bpp 434-438.
13. Reddy,R., 2008 December tin (iv)catalyzed one –part synthesis of 3, 4, dihydropyrimidines- 2 (H) ones under solvent free-conditionets.*Indian JChem*;47B pp1871-1875.
14. Mohammadizadeh, MR., Firoozi., N. 2011. Trifluoroacetic acid as an effective catalyst for biginelling reaction one pot three component synthesis of 1, 4 Dihydropyrimidinone. 8;2 (1H)one and thiones. *Electronic journal of chemistry*:266-70.
15. Aslam, M., Verma, S. 2012. Biological activity of newly synthesized substituted dihydropyrimidinone and thione. *IntJ Chem Tech Res.*;4: 109-11.
16. Pansuriya, AM., Savant, MM., Bhuvu, CV., Singh, J., Naliapara, Y.T. 2009. one-pot synthesis of 5-carboxanilide-dihydropyrimidinones using etidronic acid. *ARKAT United States journal* 79-85.
17. Hatamjafari, F., Nezhad, F., G. 30th January 2014. an efficient one-pot synthesis of Dihydropyrimidinones under solvent-free conditions. *OrientJ Chem.* 355-7. doi: 10.13005/ojc/300148.
18. Nevagi, RJ., Narkhede, HI. 6th March 2014. Novel dihydropyrimidine derivatives as antibacterial agents. *Scholars Res Library.* 135-9.
19. Hojati, SF., Gholizadeh, M., Haghdoost, M., Shafiezadeh, F. 31st November 2010 1,3-dichloro5,5dimethylhydantoin as a novel and

- efficient homogeneous catalyst in Biginelli reaction. *Bull Korean Chem Soc.* 3238-40. doi: 10.5012/bkcs.2010.31.11.3238.
20. Wang, C. December 2007. one-pot synthesis of 3,4-dihydropyrimidinone-2 (1H) catalyzed by acidic ionic liquid. *Indian J Chem.* 46B 2045-2048.
21. Balalaie, S., Soleiman-Beigi, M., Rominger, F. 2005. Novel one-pot synthesis of new derivatives of dihydropyrimidinones, unusual multisubstituted imidazoline-2-ones X-ray crystallography structure. *J Iran Chem Soc.* 2 (4);319-29. doi: 10.1007/BF03245937.
22. Fu, NY., Yuan, YF., Cao, Z., Wang, W., Wang, JT., Peppe, C. 2002. Indium (III) bromide catalyzed preparation of dihydropyrimidinone: improve protocol conditions for the biginelli reaction. *Tetrahedron.* 58 (24):4801-4807. doi: 10.1016/S0040-4020 (02)00455-6.
23. Kumar, PS., Idhaya dhullal, A., Abdul Nasser, AJ., Selvin, J. 2011. Synthesis and antimicrobial activity of a new series of 1, 4-dihydropyridine derivatives. *J Serb Chem Soc.* 76:1-11.
24. Karade, HN., Sathe, M., Kaushik, MP. 2007 Synthesis of 4-aryl substituted 3,4-dihydropyrimidinones using silica-chloride under solvent free conditions. *Molecules.* 12 (7) 1341-51. doi: 10.3390/12071341, PMID 17909490.
25. Jing, X., Li, Z., Pan, X., Shi, Y., Yan, C. 2009. NaIO₄-Catalyzed one-pot synthesis of dihydropyrimidinones at room temperature under solvent-free conditions. *J Iran Chem Soc.* 6 (3):514-8. doi: 10.1007/BF03246529.
26. Patil, HI., Singh, MC., Gaiwkwad, P., Lade, KS., Gadhave, NA., Sawant, SD. 2011. Green chemistry why and how for sustainable chemical industry and environmentally commendable civilization. *PharmResJ.* 4;4804:2798.
27. Salehi, H., Kakaei, S., Ahmadi, SJ., Firooz, MA., Sadat Kiai, SM., Pakoyan, HR., Tajik Ahmadi, H. 2010. Green procedure for synthesis of 3, 4 dihydropyrimidinones using 12molybdophosphoric acid as a catalyst and solvent free condition under microwave irradiation. *J ApplChemRes.* 4:5-10.
28. Lfigueroa, valverde, December 2009. synthesis of new succinate – dihydrotestosterone – dihydropyrimidine conjugate. *Indian J Chem.* 48B.1757-60.
29. Shah, TB., January 2009. synthesis and in vitro study of biological activity of heterocyclic –N mannichbases. *Indian J Chem.* 48B pp 48-96.
30. Tawassl, T. H., Hajelsiddig, and A. E.M. Saeed, 2015. Green Chemistry Approach In Synthesis Of 3,4-Dihydropyrimidinone Derivatives Under Solvent-Free Conditions *IJPSR.* Vol. 6 (5): 2191-2196.
31. R. A., SHASTRI, P. P., JOSHI. 2018 A Green Approach for The Synthesis Of 2,4 Dihydropyrimidinones Using PTSA DOI:10.7598/cst2018.1441; *Chemical Science Transactions* ISSN:2278-3458 7 (1), 89-94.
32. Online: 2013-11-04 © (2014) SciPress Ltd., Switzerland Green synthesis of pyrimidine derivatives *International Letters of Chemistry, Physics and Astronomy* Vol. 21 (2014) pp 64-68 doi:10.18052/www.scipress.com/ILCPA.21.64
33. Online: 2014-05-11 © (2014) SciPress Ltd., Switzerland Comparative study of chemical synthesis of pyrimidine derivatives by using Grindstone chemistry Technique and Conventional method *International Letters of Chemistry, Physics and Astronomy* Vol. 33 (2014) pp 22-27 doi:10.18052/www.scipress.com/ILCPA.33.22
34. Tom Welton, (2006) *Green Chem* 8 13.

Ultrasonication Extraction Techniques for a New Approach for Development of Pharmacognostical and Phytochemical Screening of *Syzygium aromaticum*

Reena Gupta*, Ittishree and Jitendra Gupta

¹Institute of Pharmaceutical Research, GLA University, Mathura-281406, Uttar Pradesh

²G.V. M. College of Pharmacy, Sonipat-131001

*Corresponding Author: E-mail Id: rspg80@gmail.com

Abstract

Herbal therapy is becoming increasingly popular as a safe and effective treatment option for a variety of medical problems. Herbs are frequently chosen since they are natural and do not contain hazardous chemicals. Clove (*Syzygium aromaticum*) is a natural spice with antibacterial and antioxidant qualities that is used as a medicine and a preservative. Clove is being used as a larvicidal agent to treat dengue fever, which is one of the most significant health issues in tropical nations. In the present study, various standardisation procedure has been used to evaluate the extracts (Maceration and ultrasonication process) of the plant. The result showed that total ash value was found to be as 4%w/w. Furthermore, swelling index was found to be as zero indicating absence of mucilage in the sample. Phytochemical screening showed that alkaloids are present in drug in higher amount. Also, it indicated the presence of tannins and glycosides. These data can be used to make pharmaceutical preparations from the clove.

Keywords: Clove, Ultrasonication, ash value, remedies, bitterness value

Introduction

Herbal remedies are the favoured treatment choice for a variety of common diseases in virtually all areas of India due to its traditional values, fewer known adverse effects, ease of availability, cost, and other

factors (1, 2). Spices are produced, consumed, and exported in significant quantities in India. Out of the eighty-six spices grown worldwide, India produces over fifty (3). Many leaves (mint, coriander), bulbs (garlic) and buds (clove) have been used as food preservatives and traditional remedies from ancient times in addition to flavouring agents in meals (4). One of the most common spices is clove (*Syzygium aromaticum*). Cloves are the dried flower buds of the evergreen tree *Syzygium aromaticum*, belonging to family Myrtaceae (5). It is used to treat dyspepsia and stomach irritations. It is fragrant, carminative, and stimulating. Clove buds and essential oils have been recognised to have antibacterial and antioxidant effects for a long time (6). Clove oil is widely used to flavour a variety of foods, including meats, sausages, baked goods, confectionary, chocolates, table sauces, pickles, and so on. Its antibacterial, antiseptic, and antibiotic qualities make it useful in medicine (7).

Extraction is a phrase used in the pharmaceutical industry to describe the separation of medicinally active parts of plants using the right solvent. Impure liquids, semisolids, or powders are collected from the plant area, from which the pure form of active substances is removed using conventional techniques. Before moving on to biological testing, this procedure entails extracting and determining the quality and an amount of bioactive components (8-11).

Ultrasound assisted extraction is a stimulating approach for producing high-value

compounds, and it will help to raise the value of some food by-products once they are employed as a source of natural chemicals. The most significant advantages will be simpler extraction, which saves energy, and the usage of moderate temperature, which is useful for heat-sensitive chemicals. Many technique factors must be considered for effective use of ultrasound-assisted extraction, the most important of which are the supersonic power, frequency, extraction temperature, reactor parameters, and the solvent-sample interaction. The first extraction, which is the most profitable quantity, is finished within the first few minutes. A rate equation and a defined method characterization area unit were required to optimise this approach, which had previously been lacking. (12-14).

Material and Methods

Authentication

The flowe buds was procured from local market of Sonipat and authenticated by department of botany, MDU Rohtak.

Preparation of Extract

Maceration

In a weighing bottle, 20 g of coarsely powdered drug was shifted to a dry 1000 ml conical flask. The solvent (methanol) was poured to the delivery mark in a 500 mL graduated flask. The flask was corked and left for 18 hours, shaking often. After that, it was filtered and placed in a thin porcelain plate. It was then dried on a water bath. Then stored in a desiccator so that it can be use further. The percentage w/w of extractable material was determined (15).

Ultrasonication Assisted Extraction

In this investigation, ultrasonic-assisted extraction was used. The extraction procedure was carried out with methanol as the solvent. The ultrasonic effect was created with a ultra-sonicator (Model-TU60W, 20 kHz). A water bath was put underneath the

extraction set-up to regulate the temperature. The ultrasonic probe was dipped directly into the sample-holding solution. To aid in the extraction process, the ultrasonic device may generate cavitation with a bubble implosion effect (16).

Standardisation

Standardisation of *Syzygium aromaticum* was carried out for various parameters such as crude fibre content, ash values, bitterness value, loss on drying, extractive value and foaming index were evaluated according to WHO guidelines (15, 17, 18).

Ash Values

Ash is the residue left after the crude drug has been incinerated. The inorganic salt naturally existing in the drug and sticking to it is represented by the ash residue produced. It fluctuates within certain limits depending on the soils. Inorganic particles may also be intentionally introduced for the aim of adulteration. As a result, assessing the ash value provides the foundation for establishing the identity and cleanliness of any medication, as well as providing information about its adulteration/contamination with inorganic materials. As a result, ash values are valuable in identifying the quality and purity of medicinal drugs (8).

Total Ash

On completion of incineration of powdered extract(2g) at a temperature not more than 450°C, a residue is left which is known as total ash. The percentage of ash was evaluated on air dried drug basis (8) (Figure 1).

Water Soluble Ash

Water soluble ash is unambiguously recommended for drugs which are probable to be exhausted with water. The total ash was boiled with water (25 ml) for 5 min. In a crucible, insoluble material was collected and then washed with hot water. Further it was ignited at 450°C. The weight of insoluble

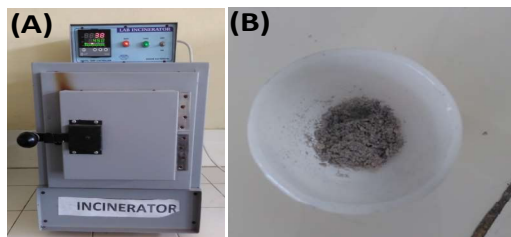


Fig 1. (A) Incinerator (B) Total ash of Powdered Drug of *Syzygium Aromaticum*

substance was deducted from weight of ash. Limit given in I.P. for water soluble ash is not less than 1.7% w/w (8).

Acid Insoluble Ash

Acid insoluble ash was calculated as per the procedure given in I.P. (8).

Sulphated Ash

Powdered extract (2g) was placed in a properly weighed crucible and gently ignited until the substance was completely burned. After cooling, with 1ml sulphuric acid, residue was wetted, heat slowly until no white vapours are released, then ignite at $800^{\circ}\text{C} \pm 25^{\circ}\text{C}$ until black particles are no longer visible. Before adding a few drops of sulphuric acid and heating, the crucible was cooled. Ignited as previously, cooled, and weighed. The technique was continued until the difference between two subsequent weighing was less than 0.5 mg (8).

Extractive Values

It is one of the imperative parameters for evaluation of a crude drug and helps in determination of polarity of chemical constituents. It can be achieved by two processes of extraction:

Cold Maceration

In a weighing bottle, 4 g of coarsely powdered drug was shifted to a dry 250 ml conical flask. The solvent was poured to the delivery mark in a 100 mL graduated flask. The flask was corked and left for 18 hours, shaking often. After that, it

was filtered and placed in a thin porcelain plate. It was then dried on a water bath before being stored in a desiccator. The percentage w/w of extractable material was determined (15).

Loss on Drying

The presence of excessive water in medicinal plant material may lead to deterioration through microbial and bacterial growth or enzyme mediated hydrolysis. There should be limit of water content for every plant material. It can be determined by weighing about 2 g of powdered drug into a weighed thin and flat porcelain dish. At 100°C , the material was dried until two consecutive weighing do not fluctuate by more than 0.5 mg. It was cooled in desiccator and weighed (15).

Foaming Index

Saponins containing drugs give persistent foam. A plant extract/ material should be evaluated for foaming index to check its capability to form foam. Foaming index was calculated according to WHO guidelines 2011.

The height of foam was measured by means of equation (i):

$$\text{Foaming Index} = \frac{100V}{a} \dots\dots\dots (i)$$

Where a is the volume in ml of filtrate in test tube showing 1cm foam height (15).

Crude Fibre Content

Crude fibre content is the deposit of resistant tissues which can be achieved after giving treatment to powdered drug with dilute acid followed by dilute alkali. It is an important tool for detection of adulteration in the drug. Crude fibre content was evaluated (17).

Swelling Index

The volume occupied by the plant material in millilitre (mL). It provides idea about the mucilage content of the drug. It can be calculated by taking the

Table 1. Serial Dilution for the Initial Test

Tube No.	Sq (ml)	Safe Drinking Water	Quinine Hydrochloride in 10 ml of Solution (°C) (mg)
1	4.2	5.8	0.042
2	4.4	5.6	0.044
3	4.6	5.4	0.046
4	4.8	5.2	0.048
5	5.0	5.0	0.050
6	5.2	4.8	0.052
7	5.4	4.6	0.054
8	5.6	4.4	0.056
9	5.8	4.2	0.058

Sq- Stock solution of quinine hydrochloride

powdered drug material in a 25 ml stoppered cylinder. Further, water was added up to 25 mL volume mark. Shaken occasionally during 23 h and then kept aside for one h. The swollen drug material's volume was calculated (17).

Bitterness Value

The bitterness value was determined through standard guidelines issued by WHO in 2011. The various compositions that were prepared by serial dilution method for initial and second test are prepared 0.042-0.058 mg/10mL and 1-10 mL respectively then bitterness value was calculated according to equation (ii):

$$\text{Bitterness value in units (per g)} = 2000 \times CA \times B \dots\dots\dots (ii)$$

Where, A = the quantity of material in mg/mL of St; B = the volume of St in mL/10mL of dilution threshold bitter concentration; C = the quantity of quinine HCL R in mg/10mL of the dilution of threshold bitter concentration (15).

Qualitative Phytochemical Screening: Detection of alkaloids, carbohydrates, proteins, flavonoids, resins,

Table 2. Serial Dilution for the Second Test

Tube No.	St (ml)	Safe Drinking Water
1	1	9
2	2	8
3	3	7
4	4	6
5	5	5
6	6	4
7	7	3
8	8	2
9	9	1
10	10	-

St = stock solution (herbal material being examined)

organic acids, volatile oils, steroids, tannins etc (17).

Result and Discussion

Morphological Evaluation of Syzygium Aromaticum

Colour- Dark Brown

Odour- Pungent

Taste- Spicy and pungent taste

Microscopy

In the microscopy, the epidermis, oil glands, collumela, clusters of calcium oxalate crystals, vascular bundles, and cortex are depicted. However, starch was absent.

Physical Evaluation

Ash Values

The *Syzygium aromaticum* had a low ash level (Total ash 4%, water-soluble ash 0.2 %, acid-insoluble ash 0.0041%, and sulphated ash 0.025 % w/w), suggesting that there were less organic compounds and foreign organic materials present as impurities.

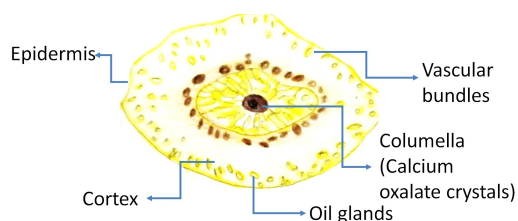


Fig 2. Microscopy of Clove

Table 3. Ash Values of Rhizomes of *Syzygium aromaticum* Linn

Ash	Values
Total ash	4% w/w
Water- soluble ash	0.2 %w/w
Acid-insoluble ash	0.0041%w/w
Sulphated ash	0.025%w/w

Table 4. Extractive Values of dried *Syzygium aromaticum*

S.No.	Extract	Extractive Values	
		Cold Maceration	Ultra- sonication
1.	Petroleum Ether (40-60 °C)	4.25%w/w	10.5 %w/w
2.	Ethanolic	6.75%w/w	10.8%w/w
3.	Hydroalcoholic	5%w/w	8.5% w/w
4.	Water	12.5%w/w	14.4%w/w

Phytochemical Screening of *Syzygium Aromaticum*

Extractive Values

In evaluation of crude drugs, the extractive value plays an important role. Further, it helps in understanding the chemical components of the drugs that was increased using ultra-sonication in comparison to cold maceration. The extraction values were found to be petroleum ether (10.5 %w/w), ethanolic (10.8%w/w), hydroalcoholic (8.5% w/w), and water (14.4%w/w).

Loss on Drying

Loss on drying gives idea about moisture content present in the drug. Loss on drying was found to as 10%w/w.

Foaming Index

Foaming index was found to as 0.0085%w/w indicating that saponins may be present in minute amount.

Swelling Index

Swelling index was found to be zero indicating that there is absence of mucilage content in the dried buds of clove.

Crude Fibre Content

Crude fibre content was found to be 10.5%w/w.

Bitterness Value

Bitterness value was found to be 7.5.

Phytochemical Investigation

Phytochemical screening of petroleum ether, alcoholic, hydroalcoholic, and aqueous extracts obtained using different extraction techniques such as maceration (MC) and ultrasonication (US). The various

phytoconstituents carbohydrates, flavonoids, and proteins were present.
 glycosides, alkaloids, tannins, amino acids

Table 5. Phytochemical Screening Results of Different Extracts of *Syzygium aromaticum*

S. No.	Test	Petroleum Ether (40-60°C)		Alcoholic		Hydroalcoholic		Aqueous	
		M C	U S	M C	U S	M C	U S	M C	U S
1.	Molisch's test	+	+	+	+	+	+	+	+
2.	Benedict's test	+	+	+	+	+	+	+	+
3.	Fehling's test	+	+	+	+	+	+	+	+
4.	Pentose sugar test	+	+	+	+	+	+	+	+
5.	Tollen's phloroglucinol test	+	+	+	+	+	+	+	+
6.	Iodine test	+	+	+	+	+	+	+	+
7.	Legal's test	+	+	+	+	+	+	+	+
8.	Keller-Killiani test	++ +	+ +	++	+ +	+ +	++	+ +	+ +
9.	Foam test	+	+	+	+	+	+	+	+
10.	Cyanogenetic glycosides	+	+	+	+	+	+	+	+
11.	Hager's test	++ +	+ + +	++ +	+ + +	+ + +	++ +	+ + +	+ + +
12.	Mayer's test	++ +	+ + +	++ +	+ + +	+ + +	++ +	+ + +	+ + +
13.	Wagner's test	++ +	+ + +	++ +	+ + +	+ + +	++ +	+ + +	+ + +
14.	Tannic acid test	++ +	+ + +	++ +	+ + +	+ + +	++ +	+ + +	+ + +
15.	Dragendroff's test	++ +	+ + +	++ +	+ + +	+ + +	++ +	+ + +	+ + +
16.	Salkowski reaction	-	-	-	-	-	-	-	-
17.	5% FeCl ₃ solution	++	+ +	++	+ +	+ +	++	+ +	+ +

18.	Lead acetate solution	++	+	++	+	+	++	+	+
19.	Acetic acid solution	++	+	++	+	+	++	+	+
20.	Dilute HNO ₃	++	+	++	+	+	++	+	+
21.	Bromine Water	++	+	++	+	+	++	+	+
22.	Biuret Test	+	+	+	+	+	+	+	+
23.	Protein containing sulphur	+	+	+	+	+	+	+	+
24.	Precipitation test								
	a. 5% HgCl ₂	+	+	+	+	+	+	+	+
	b. 5% CuSO ₄	+	+	+	+	+	+	+	+
	c. 5% lead test	+	+	+	+	+	+	+	+
25.	Ninhydrin test	+	+	+	+	+	+	+	+
26.	Cysteine	+	+	+	+	+	+	+	+
27.	Sulphuric acid test	+	+	+	+	+	+	+	+
28.	Lead acetate test	+	+	+	+	+	+	+	+

Conclusion

The different standardisation characteristics calculated in this study might aid in the botanical identification and standardisation of drugs in unrefined form. On the basis of its phytochemistry, the original plant material may also be investigated for its pharmacological and phytochemical potential. Short extraction times, minimal solvent consumption, low hazardous pollution generation, and high extraction yields were shown to be major advantages of innovative or non-conventional extraction techniques. We can use new techniques to cut down on time. Using the novel extraction of method, like ultra-sonication, the yield can be increased as the cell burst out during the process of ultrasonication. High frequency of ultrasound accommodates in the bursting of cell and penetration of solvent in the drug thus increasing the yield. Furthermore, the extraction time is lesser as compared to the conventional methods of extraction. We can

utilise the novel methods to increase the yield, lesser solvent consumption and lesser time.

Acknowledgement

Authors thank full to the management of G.V.M. College of Pharmacy, Sonipat; and Institute of Pharmaceutical Research, GLA University, Mathura-281406, U.P., India

Reference

1. Sen, S., Chakraborty. R., De B, et al. (2010). Analgesic and ant inflammatory herbs: A potential source of modern medicine. Inter J Pharm Sci Research 1: 32–44.
2. Ashok, D. B. and Devasagayam, T. P. A. (2007). Current status of herbal drugs in India: An overview. Journal of Clinical Biochemistry and Nutrition. 41(1): 1-11.
3. Ceylan, A. (1997). Medical Plants-II Volatile Oil Plants. Ege University, Faculty of

- Agriculture, Department of Field Crops, Izmir, Turkey.
4. Prabha, J. V. and Venkatachalam, P. (2016). Preliminary Phytochemical Screening of Different Solvent Extracts of Selected Indian Spices. *International Journal of Current Microbiology and Applied Sciences*. 5(2):116-122.
 5. Fu, Y., Zu, Y., Chen, L., Shi, X., Wang, Z., Sun, S. and Tomas, E. (2007.) Anti-microbial activity of clove and rosemary essential oils alone and in combination. *Phytotherapy Research*. 21(10):989-994.
 6. Shyamala, M. P., Venukumar M. R. and Latha, M. S. (2003). Antioxidant potential of this *Syzygium aromaticum* (Gaertn.) Linn. (Cloves) in rats fed with high fat diet. *Indian Journal of Pharmacology*. 35(2): 99-103.
 7. Parle, M. and Khanna, D. (2011). Clove: A champion spice. *International Journal of Research in Ayurveda and Pharmacy*. 2(1): 47-54.
 8. Saikat, S., Chakraborty, R., Biplab, D., Ganesh, T., Raghavendra, H. G. and Debnath, S. (2010). Analgesic and ant inflammatory herbs: a potential source of modern medicine. *International Journal of Pharmaceutical Sciences and Research*. 1(11):32-44.
 9. Rahman, M. M., Azmir, J. J., Zaidul, I. S. M., Sharif, K. M., Mohamed, M., Sahena, F., Jahurul, M. H. A., Ghafoor, K., Norulaini, N. A. N. and Omar, A. K. M. (2013). Techniques for extraction of bioactive compounds from plant materials. *Journal of Food Engineering*. 117:426-436.
 10. Azwanida, N. N. (2015). A review on the extraction method used in medicinal plant, principle, strength, limitation. *Medicinal and Aromatic Plants*. 4(3):1-6.
 11. Tiwari, P., Kumar, B., Kaur, M., Kaur, G. and Kaur, H. (2011). Phytochemical screening and extraction. A review, *International Pharmaceutica Scientia*. 1(1):98-106.
 12. Majek Dunni SO (2015). Review of extraction of medicinal plants for pharmaceutical research. *Merit Research Journal of Medicine and Medical Science*. 3(11):521-527.
 13. Cravotto, G. and Cintas, P. (2006). Power ultrasound in organic synthesis: Moving cavitation chemistry from academia to innovative and large-scale applications. *Chemical Society Reviews*. 35(2):180-196.
 14. Vinatoru, M. (2015). Ultrasonically assisted extraction (UAE) of natural products some guidelines for good practice and reporting. *Ultrasonic Sonochemistry*. 25:94-95.
 15. Zhang, H.-F., Yang, X.-H., Zhao, Y.-D. and Wang, Y. (2009). Ultrasonic-assisted extraction of epimedin C from fresh leaves of *Epimedium* and extraction mechanism, *Innovative Food Science and Emerging Technology*. 10(1):54-60.
 16. WHO guidelines. (2011). WHO press World Health Organization, 20 Avenue Appia, 1211 Geneva 27, Switzerland. p. 23-49.
 17. Zahari, N. A. A. R., Chong, G. H., Abdullah, L. C. and Chua, B. L. Ultrasonic-Assisted Extraction (UAE) Process on Thymol Concentration from *Plectranthus amboinicus* Leaves: Kinetic Modeling and Optimization. *Processes*. 2020; 8(3):322.
 18. Khandelwal, K. R. Practical Pharmacognosy. (20th edition), Nirali Prakashan. Pune. India., 2010; 25: 23.1-25.9.
 19. I.P. (2007), Indian Pharmacopoeia commission, sector-23, Raj Nagar, Ghaziabad, India. p. 78-79.

***Syzygium cumini* Protects Diabetic Wistar Rats Against Rosiglitazone-Induced Cardiotoxicity and Hepatotoxicity**

Prashant L. Pingale, Rupali A. Patil*, Aishwarya S. Gadkari and Sunil. V. Amrutkar

Department of Pharmacology, Gokhale Education Society's Sir Dr. M. S. Gosavi College of Pharmaceutical Education & Research, Prin. T. A. Kulkarni Vidyanagar, Nashik 422005, Maharashtra

*Corresponding Author: E-mail Id; ruupalipatil@gmail.com

Abstract

Syzygium cumini (Family: Myrtaceae), is known to show antioxidant, antidiabetic, cardioprotective and hepatoprotective activities in ayurvedic system of medicine. This study aims at determining *in vitro* and *in vivo* antioxidant activity of ethanolic extract of *S. cumini* (ESC). Effect of ESC on rosiglitazone induced cardiotoxicity and hepatotoxicity in alloxan-induced diabetic rats was studied. Results of study indicated that ESC exhibited significant protection against cardiac and hepatic damage caused by rosiglitazone in alloxan-induced diabetes in rats comparable to silymarin, used as reference standard. Cardioprotective and hepatoprotective activity may be attributed to presence of antioxidant activity.

Keywords: Alloxan, Antioxidant, Cardiotoxicity, Diabetes, Hepatotoxicity, Jambul, Rosiglitazone

Introduction

Plants based products have been in use for medicinal or other purpose right from the dawn of history. Ayurveda, the traditional Indian system of medicine, involves dispensing of plant products in various forms such as powders, extracts, decoction etc. Interest in medicinal plants has increased enormously over the last two decades. Herbal drugs constitute a major part in the traditional system of medicine of many countries. Large numbers of these herbal medicines have been incorporated into practice. Herbs have been used for easy accessibility and inexpensiveness. Several drugs of plant origin

have been used in treatment of a variety of disorders. Many medicines and formulations have significant antioxidant properties and are beneficial in treating toxicity in animals. Phytoconstituents like alkaloid, flavonoids, tannins, gallic acid and β -sitosterol are known to possess antidiabetic, hepatoprotective and cardioprotective activity.

Syzygium Cumini (Family: Myrtaceae), commonly known as *jambul*, is native of India or East India and it's found in some other countries like Thailand, Philippines, Madagascar. Seed consist of alkaloid, flavonoid and tannins. *S. cumini* seeds are used in traditional medicinal system for diarrhea, dysentery, enlargement of spleen etc (1). Seed extract of *S. cumini*, the part most often used in Ayurvedic medicine, having good level of total phenolic activity. The patient's blood sugar and glycosuria were lowered by an oral dose of dry alcoholic extract of jamun seed. The seed powder is used as an antidote for strychnine poisoning in India (2). Oxidative stress can cause hepatotoxicity and cardiotoxicity due to free radicals. Hepatotoxicity and cardiotoxicity are treated with plants possessing free radical scavenging activities. Literature review revealed that *S. cumini* seeds having significant antioxidant activity (3). Present study was aimed to explore the potential of *S. cumini* through the use of drug induced hepatotoxicity and cardiotoxicity in experimental animals.

Materials and Method

Animals: Wistar rats (150-200gm) were procured from Veterinary College, Mumbai. The

study was performed according to the CPCSEA guidelines and protocol was approved (Protocol number: MGV/PC/CPCSEA/XXXII/02/2016/06) by the IAEC.

Drugs and Chemicals: Rutin and Gallic acid used for estimation for total phenol and flavonoid content. Rosiglitazone (Yarrow Pharmaceutical, Mumbai), Silymarin, Alloxan monohydrate (Sigma-Aldrich- USA) were used. Alanine Aminotransferase (ALT or SGPT), Aspartate Aminotransferase (AST or SGOT), Alkaline Phosphatase (ALP), Bilirubin, CK-MB, and LDH were all tested using biochemical kits.

Preparation of Extract: The seed powder of *S. cumini* obtained from local market. The powdered material (190 gm) was extracted with ethanol using Soxhlet apparatus. Filtrate was obtained and evaporated to get solid ethanolic extract (Yield: 21.05%w/w).

Preliminary Phytochemical Screening: Phytochemical screening of ethanolic extract of *S. cumini* (ESC) for presence of various phytoconstituents like carbohydrate, protein, alkaloids, flavonoids, phenolic content, glycosides, tannins, steroids was done using standard procedure(2,4).

Determination of In Vitro Antioxidant Activity

Free Radical Scavenging Activity:

DPPH Method: The ability to scavenge free radicals was tested against a stable free radical of DPPH (1, 1-diphenyl-2-picryl hydrazyl). Antioxidants react with DPPH to form 1,1-diphenyl-2-picryl-hydrazine (non-radical). The amount of discoloration reflects how effective the drug is at scavenging free radicals. ESC extract of varying concentration was used. Absorbance of solutions was recorded at 517nm. [3] Percentage inhibition was calculated. % inhibition versus concentration plot was used for determination of IC50 values.

Reducing Power Assay: Due to presence of reductants (antioxidants) in the

extracts, the Fe³⁺/Ferric cyanide complex is reduced to ferrous form (Fe²⁺). Depending on the reduction power of each extract, the yellow tint of the test solution changes to various shades of green and blue. Various concentrations of the plant extracts and Ascorbic acid were used. Increased absorbance of the reaction mixture indicates increase in reducing power (5). Reducing power was measured by measuring absorbance at 700 nm by varying the concentration of the extract and the contact time.

Total Phenolic Contents: The total phenolics content of the plant extracts was determined using spectrophotometric method. A spectrophotometer set to 765 nm was used to determine the absorbance. For each analysis, the samples were produced in triplicate and the mean absorbance value was calculated. The calibration curve was generated using the same process for the standard gallic acid solution. The concentration of phenolics (mg/ml) was retrieved from the calibration curve based on the measured absorbance. In terms of gallic acid equivalent, the equivalent content of phenolics in extracts was calculated (mg of GA/g of extract) (6).]

Total Flavonoids Contents: Estimation of Total flavonoid content in ESC seeds using spectrophotometer at 415nm is dependent on the development of a flavonoid-aluminium complex. Rutin was used as a reference compound. Calibration curve was prepared for rutin using same procedure as for sample. Calibration curve was used for measuring concentration of flavonoids (mg/ml). Flavonoid content in extracts was expressed in terms of rutin equivalent (mg of rutin/g of extract)(7).

Experimental Induction of Hyperglycemia in Wistar Rats: Alloxan is the most well-known chemical substance utilized in diabetogenic research and type 1 diabetes induction. Alloxan is a urea derivative that promotes necrosis of pancreatic islet cells specifically(6). Alloxan monohydrate 120mg/kg will be administered by intraperitoneal route, blood was collected from tail

vein and glucose level was estimate by Glucometer. Rats with established hyperglycemia (blood glucose >300 mg/dl) were included for subsequent treatment.

Experimental

Animals were divided into 6 groups (n=5). Group I: Distilled water (10 ml/kg, p.o.). Group II: Alloxan Monohydrate (120 ml/kg, i.p.). Group III: Alloxan (120 ml/kg, i.p.) with Rosiglitazone (10 ml/kg, p.o.) for 21 days. Group IV & V: ESC 100 mg/kg & 300 mg/kg respectively with Rosiglitazone (10 ml/kg) for 21 days. Group VI: Silymarin (60 mg/kg) with Rosiglitazone (10 ml/kg) for 21 days.

ESC, Rosiglitazone and Silymarin were administered through oral route.

% Change in Body Weight, Relative Liver and Relative Heart Weight: Each animal's body weight was measured before treatment and sacrifice. Each animal's liver and heart samples were dissected and weighed.

Preparation of Serum and Tissue Homogenate: After the 21-day therapy, the animals were sacrificed 24 hours later. Cardiac puncture was used to get blood samples. Centrifugation at 3000 rpm for 10 minutes separated the serum. The serum samples were kept at -20 °C to be used for liver and kidney function tests. For the determination of SOD, CAT, GSH, and LPO activity, a known amount of tissue (liver and heart) was weighed and homogenised in ice cold 0.1 M Tris-HCl buffer.

Determination of In Vivo Antioxidant Activity

Estimation of Superoxide Dismutase Activity (SOD): The ability of SOD to suppress the spontaneous oxidation of adrenaline to adrenochrome was measured compared to a reagent blank as the change in optical density every minute at 480 nm. The results were represented as units of SOD activity *per mg of wet tissue* (8).

Estimation of Catalase Activity (CAT): The assay of CAT is based on ability of CAT to initiate break down of hydrogen peroxide.

The absorbance was recorded at 240 nm every 10 seconds for 1minute. The results were represented as units of CAT activity per mg of wet tissue (9).

Estimation of Reduced Glutathione Activity (GSH): It is based on the principle of development of yellow colour when 5, 5' dithiobis (2-nitro-benzoic acid) (DTNB) is added to compound containing sulfhydryl groups. Absorbance was measured at 412 nm (nM/mg of wet tissue) (10).

Estimation of Lipid Peroxidative Indices (LPO): Plants and animals both experience lipid peroxidation, which is a complex process. Formation of thiobarbituric acid reactive substances (TBARS) was measured against reference blank at 535nm (nM/mg of wet tissue) (11).

Biochemical Assays

Liver Function Tests Assessment:

Aspartate Aminotransferase (AST or SGOT): The amino group transfer between L-Aspartate and Ketoglutarate is catalysed by AST, resulting in Oxaloacetate and Glutamate. In the presence of Malate Dehydrogenase, the Oxaloacetate produced reacts with NADH to create NAD. Mean absorbance change per minute ($\Delta A/\text{min.}$) was calculated (12).

Alanine Transaminase (ALT): L-Alanine and Ketoglutarate are transaminated by ALT to generate pyruvate and L-Glutamate. Lactate Dehydrogenase (LDH) then converts Pyruvate to Lactate while simultaneously oxidising NADH to NAD⁺. At a wavelength of 340 nm, absorbance was measured after 60 seconds. Every 30 seconds, the reading was repeated. The average change in absorbance per minute ($\Delta A/\text{minute}$) was calculated (13,14,15).

Alkaline Phosphatase (ALP): Hydrolysis of colourless p-Nitro phenyl Phosphate to yellow coloured p-Nitrophenol and Phosphate occurs in presence of ALP at pH 10.3. Absorbance was recorded after every 30 seconds at 405 nm. The average change in absorbance per minute ($\Delta A/\text{minute}$) was determined (16).

Bilirubin: Total bilirubin couples with diazotised sulphanillic acid in the presence of TBA to form pink coloured azobilirubin complex of both direct and indirect bilirubin and in the absence of TBA, only direct bilirubin reacts with diazotised sulphanillic acid to form azobilirubin complex. The intensity of the colour formed is directly proportional to the bilirubin present in the sample. Absorbance was measured at 546 nm and 620 nm respectively(17).

Assessment of Cardiac Marker Enzyme

Creatine Kinase (CK)-MB: An anti-CK-M antibody in the reagent completely inhibits the CK-M portion of the CK-MM and the CK-MB in the sample. Initial absorbance was measured after 10 minutes & absorbance was repeated after every 1, 2, and 3 minute at 340nm wavelength. Mean absorbance change per minute ($\Delta A/\text{minute}$) was calculated (18).

Lactate Dehydrogenase (LDH)

Activity: LDH catalyzes the conversion of pyruvate to NAD^+ by reducing it with NADH. The rate of oxidation of NADH to NAD^+ is assessed as a decline in absorbance proportional to the sample's LDH activity. Initial absorbance was read after 10

minutes and repeated after every 1, 2, and 3 minute at 340 nm. Average change in absorbance per minute was calculated ($\Delta A/\text{minute}$) (19).

Histopathological Examination: The liver and heart tissues were immediately removed after scarification of animals and preserved in 10% formalin solution before being sent for histopathological testing. These tissues were embedded in paraffin wax, cut into tiny thin slices of 3-5 μm thickness, stained with haematoxylin-eosin, and photographed under 40X magnification to observe for histological abnormalities.

Statistical Analysis: The data was presented as a mean \pm SEM. One-way ANOVA was used in the statistical analysis, followed by Dunnett's multiple comparison tests. Statistical significance was defined as $p < 0.05$.

Results

Phytochemical analysis of Ethanolic extract of *Syzygium cumini* seed (ESC) revealed presence of alkaloids, flavonoids, tannins and phenolic compounds in Figs 1-14.

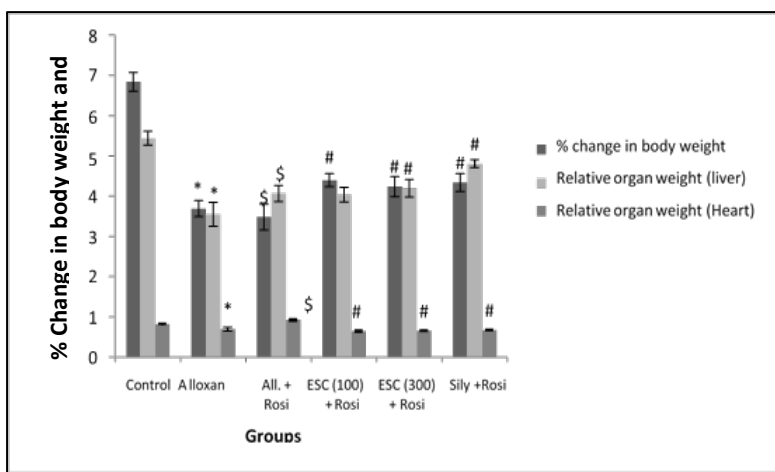


Fig 1. Effect of ethanolic extract of *S. Cumini* and RSG on percent body weight, relative organ weight (Liver and Heart) of rats. $N=5$, $^{*}\$ \# p < 0.05$ as compared to RSG treated group

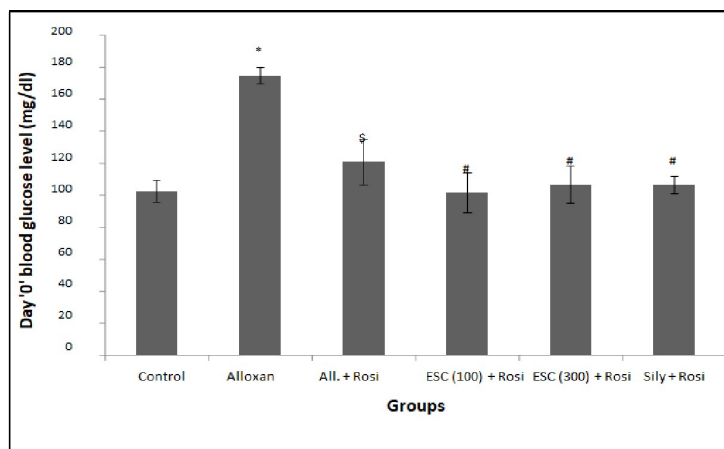


Fig 2. Effect of ethanolic extract of *S. Cumini* and RSG, alloxan on blood glucose level of rats

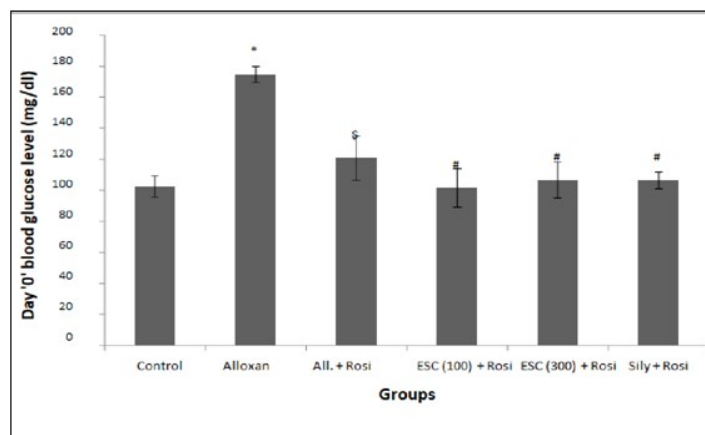


Fig 3. Effect of ethanolic extract of *S. Cumini* and RSG, alloxan on blood glucose level of rats

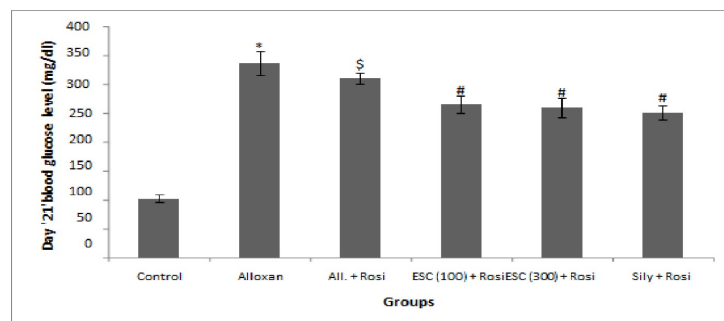


Fig 4. Effect of ethanolic extract of *S. Cumini* and RSG, alloxan on blood glucose level of rats

Cardiotoxicity and Hepatotoxicity

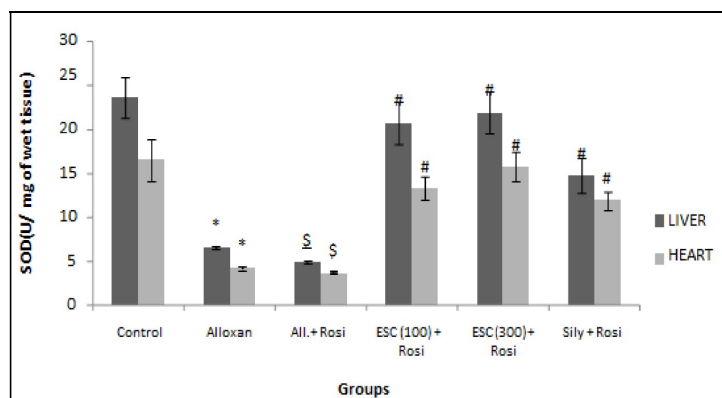


Fig 5. Effect of ethanolic extract of *S. Cumini* and RSG, alloxan on SOD level of rats

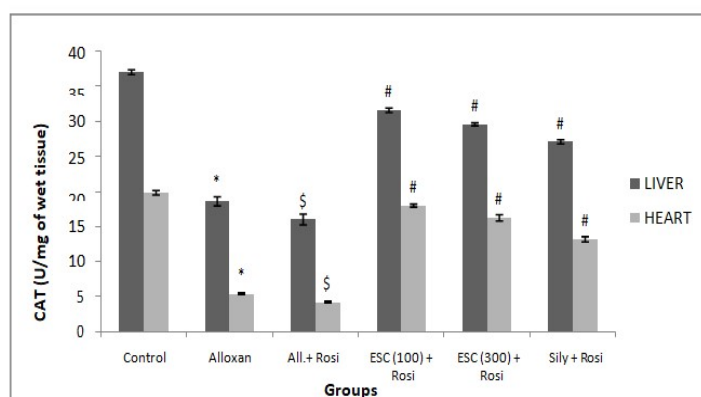


Fig 6. Effect of ethanolic extract of *S. Cumini* and RSG, alloxan on CAT level of rats

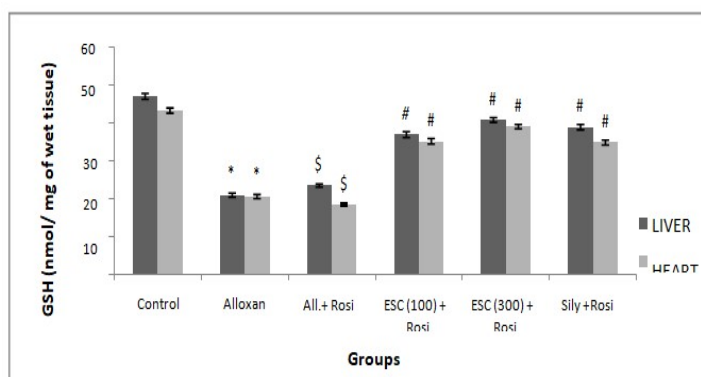


Fig 7. Effect of ethanolic extract of *S. Cumini* and RSG, alloxan on GSH level of rats

Cardiotoxicity and Hepatotoxicity

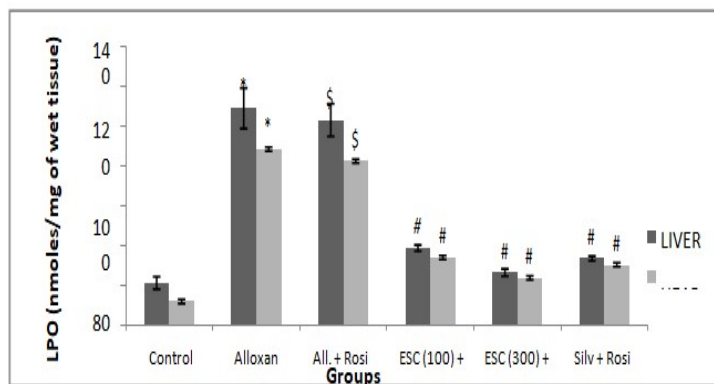


Fig 8. Effect of ethanolic extract of *Syzygium Cumini* and RSG, alloxan on LPO level of rats

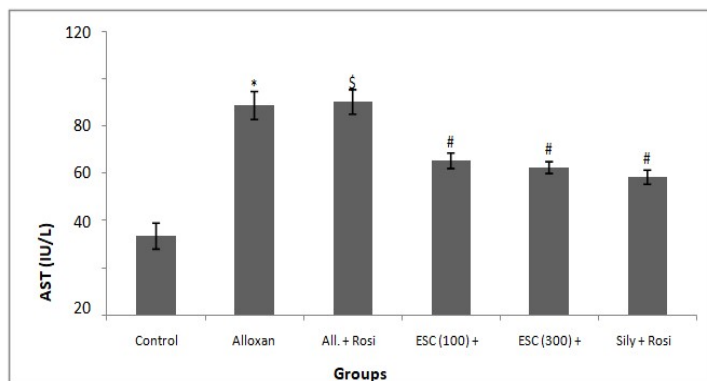


Fig 9. Effect of ethanolic extract of *Syzygium Cumini* and RSG, alloxan on AST level of rats

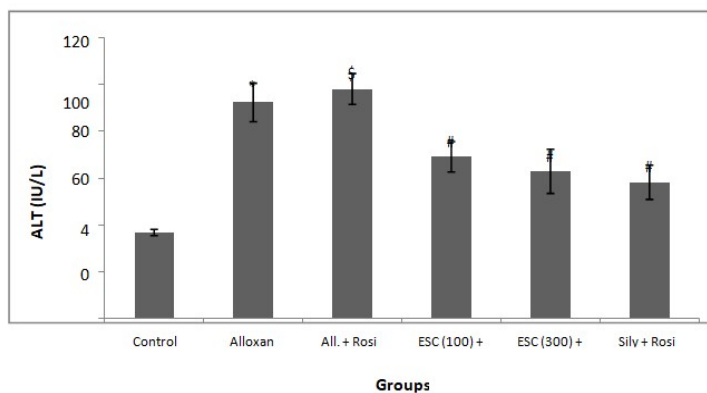


Fig 10. Effect of ethanolic extract of *Syzygium Cumini* and RSG, alloxan on ALT level of rats

Cardiotoxicity and Hepatotoxicity

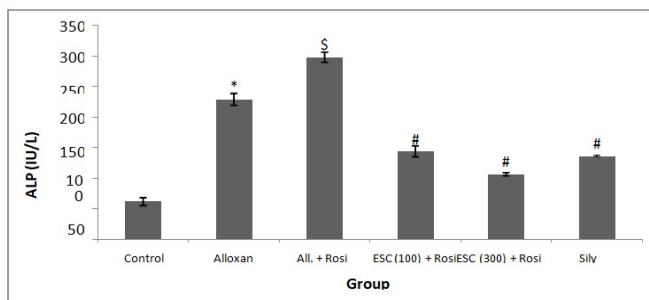


Fig 11. Effect of ethanolic extract of *Syzygium Cumini* and RSG, alloxan on ALP level of rats

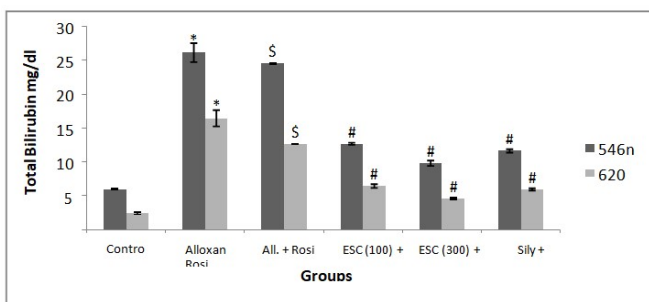


Fig 12: Effect of ethanolic extract of *Syzygium Cumini* and RSG, alloxan on bilirubin level of rats

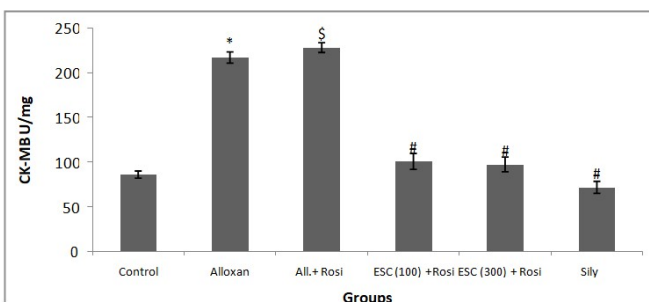


Fig 13. Effect of ethanolic extract of *Syzygium Cumini* and RSG, alloxan on CK- MB level of rats

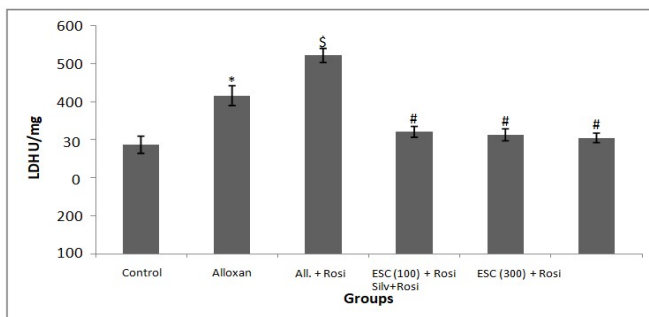


Fig 14. Effect of ethanolic extract of *S. Cumini* and RSG, alloxan on LDH level of rats

Cardiotoxicity and Hepatotoxicity

In Vitro Antioxidant Activity

Free Radical Scavenging Activity:

The % Scavenging activity increased with the increase in concentration of the ESC. *S. cumini* extract shows good inhibition of DPPH radical and IC₅₀ value was found to be 160µg/ml.

Reducing Power Assay: The % Scavenging activity increased with the increase in concentration of the ESC. Ethanolic extract of *S. cumini* shows good reducing power as compared to Vit-C and IC₅₀ value was found to be 300 µg/ml.

Total Flavonoid Content: Total flavonoid content in *S. cumini* was found to be 48µg of rutin equiv/mg extract.

Total Phenolics Content: Total phenolic content in *S. cumini* was found to be 125µg of Gallic acid equiv/mg extract.

Percent Body Weight, Relative Organ Weight (Liver and Heart)

Significant reduction in body weight was observed in Alloxan treated group as compared to normal group, while treatment group of *S. Cumini* and Silymarin shows significantly increased body weight as compared to RSG treated group. In RSG treated rats, significant increase in relative liver weight was observed as compared to Alloxan treated group, *S. Cumini* and Silymarin treated group shows significant increase in relative weight of liver as compared to RSG treated group. In RSG treated rats, significantly increase in relative heart weight was observed as compared to Alloxan treated group. *S. Cumini* and Silymarin shows significant decreased relative weight of heart as compared to RSG treated group.

Blood Glucose Level

Blood Glucose Level on Day '0': Blood glucose level on day '0' was significantly decreased in RSG treated rats as compared to Alloxan treated group. *S. Cumini* and Silymarin treatments shows significantly

decreased body weight as compared to RSG treated group.

Blood Glucose Level on Day '3':

Blood glucose level on day '3' was significant decreased in RSG treated rats as compared to Alloxan treated group. *S. Cumini* and Silymarin treatments shows significantly decreased blood glucose level as compared to RSG treated group.

Blood Glucose Level on Day '21':

Blood glucose level on day '21' was significant decreased in RSG treated rats as compared to Alloxan treated group, *S. Cumini* and Silymarin treatments shows significantly decreased blood glucose level as compared to RSG treated group.

Antioxidant Studies

Effect of ESC on Superoxide Dismutase (SOD) Level in Rosiglitazone Induced Cardiotoxicity and Hepatotoxicity in Rats:

Significant decreased SOD level in liver was observed in RSG treated rats as compared to Alloxan treated group.

Treatment of *S. Cumini* and Silymarin treated significant increase level of SOD in liver as compared to RSG treated group. Significant decreased SOD level in heart was observed in RSG treated rats as compared to Alloxan treated group. Treatment of *S. Cumini* and Silymarin significant increase level of SOD in heart as compared to RSG treated group.

Effect of ESC on Catalase (CAT) Level in Rosiglitazone Induced Cardiotoxicity and Hepatotoxicity in Rats:

Significant decreased CAT level in liver was observed in RSG treated rats as compared to Alloxan treated group. Treatment of *S. Cumini* and Silymarin treated significant increase level of CAT in liver as compared to RSG treated group. Significant decreased CAT level in heart was observed in RSG treated rats as compared to Alloxan treated group. Treatment of *S. Cumini* and Silymarin significant increase level of CAT in heart as compared to RSG treated group.

Effect of ESC on Reduced Glutathione (GSH) Level in Rosiglitazone Induced Cardiotoxicity and Hepatotoxicity in Rats:

Significant decreased GSH level in liver was observed in RSG treated rats as compared to Alloxan treated group. Treatment of *S. Cumini* and Silymarin treated significant increase level of GSH in liver as compared to RSG treated group. Significant decreased GSH level in heart was observed in RSG treated rats as compared to Alloxan treated group. Treatment of *S. Cumini* and Silymarin significant increase level of GSH in heart as compared to RSG treated group.

Effect of ESC on Lipid Peroxidation (LPO) Level in Rosiglitazone Induced Cardiotoxicity and Hepatotoxicity in Rats:

Significantly increased LPO level in liver was observed in RSG treated rats as compared to Alloxan treated group. Treatment of *S. Cumini* and Silymarin treated significant decreased level of LPO in liver as compared to RSG treated group. Significantly increased LPO level in heart was observed in RSG treated rats as compared to Alloxan treated group. Treatment of *S. Cumini* and Silymarin treated significant decreased level of LPO in heart as compared to RSG treated group.

Biochemical Assays

Effect of ESC on AST Level

Significant increase in AST level was observed in RSG treated rats as compared to Alloxan treated group. Treatment of *S. cumini* significant decrease in AST level was observed as compared to RSG treated group. Silymarin treatment shows AST level was reduced as compared to RSG treated group

Effect of ESC on ALT Level

Significant increase in ALT level was observed in RSG treated rats as compared to Alloxan treated group. Treatment of *S. cumini* significant decrease in ALT level was observed as compared to RSG treated group. Silymarin treatment shows ALT level was reduced as compared to RSG treated group.

Effect of ESC on ALP level

Significant increase in ALP level was observed in RSG treated rats as compared to Alloxan treated group. Treatment of *S. cumini* significant decrease in ALP level was observed as compared to RSG treated group. Silymarin treatment shows ALP level was reduced as compared to RSG treated group.

Effect of ESC on Bilirubin Level

Significant increase in Bilirubin activity was observed in Alloxan treated rats as compared to RSG treated group. Treatment of *S. cumini* in significant decrease in Bilirubin activity was observed as compared to RSG treated group. Silymarin treatment show reduction in Bilirubin level was reduced as compared to RSG treated group.

Estimation of Cardiac Marker Enzyme

Effect of ESC on CK-MB Level

Significant increase in CK-MB level was observed in RSG treated rats as compared to Alloxan treated group. Treatment of *S. cumini* significant decrease in CK-MB level was observed as compared to RSG treated group. Silymarin treatment shows reduction in CK-MB level compared to RSG treated group.

Effect of ESC on LDH Level

Significant increase in LDH level was observed in RSG treated rats as compared to Alloxan treated group. Treatment of *S. cumini* significant decrease in LDH level was observed as compared to RSG treated group. Silymarin treatment shows LDH level was reduced as compared to RSG treated group.

Histopathological Examination

Histopathological study of revealed disturbance in the normal liver and heart architecture due to hepatotoxin and cardiotoxin in Rosiglitazone treated animal, whereas animals treated with the ESC showed retention of the normal cellular architecture and it is comparable with the standard Silymarin group, hence confirming the significant Hepatoprotective and Cardioprotective effect of ethanolic extract of *S. cumini* seed in Figs 15 and 16.

Histopathological Examination of Liver

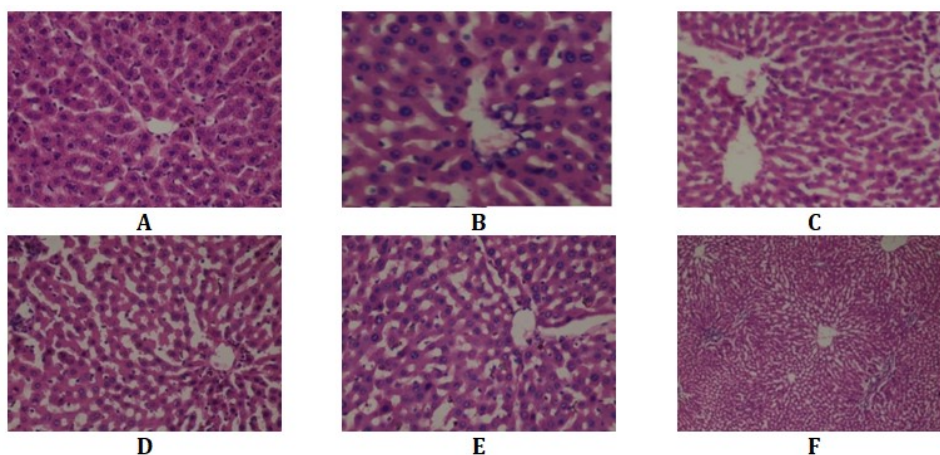


Fig 15. Histopathological studies of H & E stained section of liver showing 'A' vehicle treated animal with normal liver architecture with normal appearance of central vein, kuffer cell, and hepatocytes. RSG treated rat liver 'C' with mild fatty changes, focal necrosis and portal inflammation. ESC treated rat liver 'D' and 'E' with reversal of portal inflammation and destruction of central vein. Silymarin treated rat liver 'F' with normal liver architecture, central vein, and portal inflammation hepatocyte appearing normal

Histopathological Examination of Heart

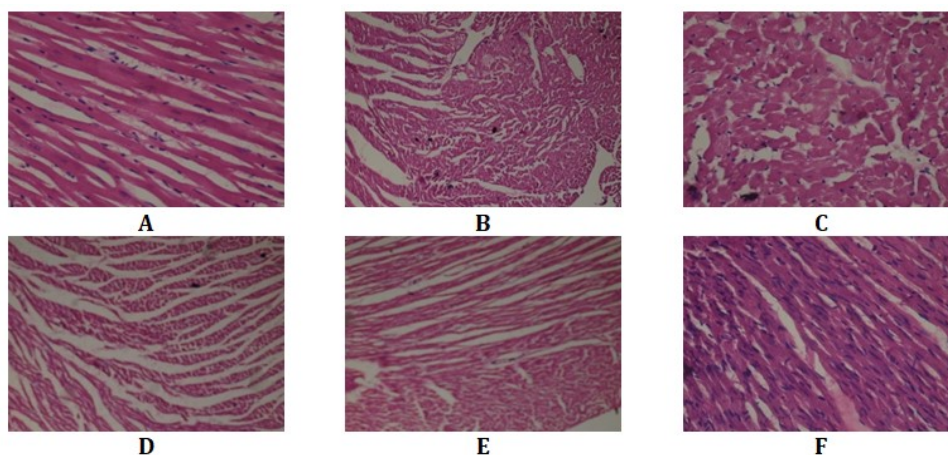


Fig 16. Histopathological studies of H & E stained section of heart showing 'A' vehicle treated animal with normal architecture of heart and to normal arrangement of the layer of myocardium, having a normal cellularity, congestion, fatty changes, atrophy and smaller nuclei. In RSG treated rat heart 'C' with myocardial inflammation, hypertrophy, and lipid accumulation and apoptosis. ESC treated rat heart 'D' and 'E' with reversal of lipid accumulation apoptosis, hypertrophy and myocardial inflammation. Silymarin treated rat heart 'F' with normal heart architecture, normal arrangement of the layer of myocardium, fatty changes and atrophy appearing normal

Discussion

The product of metabolic and physiological processes is reactive oxygen species (ROS). Environmental stress causes oxidative stress by disrupting the balance between free radical generation and antioxidant capabilities, resulting in oxidative stress due to excess ROS, antioxidant depletion, or both. When a cell's antioxidant capacity is depleted, damage to cellular macromolecules such as lipids, proteins, and DNA mutations occur, causing harm to target cells and tissues and, in some cases, cell death. This damage has been related to an elevated risk of diseases like diabetes, cardiovascular disease, cancer, and liver disease, among others [20]. Hepatotoxicity and cardiotoxicity has been reported as one of the damages caused by free radicals [21].

Rosiglitazone, an insulin sensitizer, is an antidiabetic compound. The use of RSG in diabetes, on the other hand, has been implicated in the development of cardiovascular disease [22]. In diabetic animals, RSG causes hepatotoxicity and mitochondrial dysfunction. Drugs having antioxidant activity are effective in treating RSG toxicity. RSG induced side effect such as an increased weight and fat gain upon treatment with 10mg/kg per day RSG [23]. The higher dose of ESC (300 mg/kg, p.o.) prevented the increased weight when compared to toxicity treated animals.

The ethanolic extract of *S. cumini* was subjected the presence of alkaloid, saponins, tannins, Flavonoids and antioxidant compounds. This extract contains flavonoid and phenolics which have potential to contribute in management of diabetes and its complication. ^[4] *In vitro* antioxidant activity of seed extract of *S. cumini* was performed. The result of different assay using extract exhibited antioxidant activity and reducing power. Alloxan induced diabetic rats showed a significant reduction in body weight. Insulin deficiency occurs as alloxan affects protein and lipid tissues, glucose does not enter the cells. Instead of glucose, utilization of lipid

and protein as energy sources increases and body weight losses due to severe damages in protein of tissues [24].

Toxicity group reflected a significantly increased liver and heart weight compared to other group because RSG leads lipid deposition in liver and heart [25, 26].

Furthermore, in the present study, treatment of Rosiglitazone in alloxan-induced hyperglycaemic rats shows significantly increased blood glucose level on day '0' and increased glucose level on 3rd day compared to day '0', but at the end of experiment on 21st day, the glucose level was significantly increased due to induction of alloxan monohydrate. RSG treated animals showed reduction of glucose level compared to alloxan treated animal. ESC treated animals shown significantly decreased blood glucose level compared to RSG treated animals. The continuous treatment with ESC for 21 days resulted in a considerable reduction in diabetic rats' blood glucose levels.

Alloxan causes diabetes by destroying the insulin-producing beta-islet in the pancreas. Alloxan treatment caused a multiphase glycemic response, with changes in plasma insulin concentration followed by alterations in beta cell ultrastructure, which eventually led to necrotic cell death [27].

Rosiglitazone decreases insulin resistance, an increase in glucose utilization, a decrease in hepatic glucose production, and an increase in β -cell function. The primary peripheral site of action is within adipose tissue, although other target tissues such as liver and skeletal muscle are also affected [28].

The most sensitive enzymatic indexes in liver and cardiac injury produced by ROS and oxidative stress are SOD and CAT. SOD is one of the most abundant internal antioxidant enzymes found in all aerobic cells, and it has an antitoxin impact against ROS. This dismutase superoxide anion produced during metabolism in cell. It reduces the toxicity of superoxide radicals by converting them to hydrogen peroxide [29]. CAT breaks down

hydrogen peroxide into water and oxygen. In normal homeostasis, the activity of both enzymes is sufficient to remove ROS [30]. For biological integrity to be maintained, there must be a balance between oxidation and antioxidant levels in the system. Oxidant such as superoxide anion (O_2^-) hydroxyl radical (HO^\cdot) may attack the membranes of the liver and heart cell causing oxidative stress. Results of this study shown significant decrease in anti-oxidants enzyme activity (SOD and CAT) in both liver and heart in RSG treated rats compared to alloxan treated group. Treatment of ESC and Silymarin treated group significantly increases level of SOD and CAT in both heart and liver as compared to RSG treated group. This may suggest that ESC can reduces ROS that may lessen the oxidative damage to the hepatocyte and myocardial tissue and improve the activities of the antioxidant enzyme, thus protecting liver and heart from Rosiglitazone damage.

Through the action of GSH-peroxidase, glutathione (GSH) detoxifies hydrogen peroxide and lipid peroxides. Reduced glutathione levels were found to be significantly lower in RSG-treated rats' liver and heart tissue, indicating an imbalance between oxidant and defence mechanisms, whereas ESC treatment showed a considerable rise in tissue. The detoxifying enzymes may be indicated by ESC, and these enzymes may detoxify the toxicant's ROS delivery [31].

Lipid peroxidation has been suggested as the damaging mechanism in RSG-induced liver and cardiac injury. The levels of LPO in the liver and heart of animals in the toxicity group (RSG) were found to be higher in this investigation. Increased lipid peroxidation causes tissue damage, and antioxidant defence mechanisms fail to prevent the creation of too many free radicals. Lipid peroxidation was greatly reduced after pretreatment with ESC. As a result, it's probable that ESC's hepatoprotective and cardioprotective properties are attributable to its antioxidant capability [32].

To evaluate potential toxicity related with these organs, several hepatic and cardiac marker enzymes are employed. ALT, AST, ALP and serum bilirubin are hepatic marker enzymes, while CK-MB and LDH are cardiac marker enzymes. In addition, the antioxidant status of renal and hepatic tissue was evaluated to establish whether these organs were under any toxic stress.

In acute liver damage induced by RSG, in RSG treated animal was showed increase level of liver enzyme marker as compared to ESC treated animal ESC significantly reduced the elevated serum level of AST, ALT, ALP and total bilirubin as compared to toxicity treated animals. It was observed that ethanolic extract of seed extract of *S. cumini* (100 and 300 mg/kg) showed significant Hepatoprotective effect in diabetic rat as compared to other groups. This may be due to antioxidant property of seed extract; it showed nearly normal level of liver enzymes. Antioxidant neutralize the oxidants generate in the liver. Any changes between level of oxidants and antioxidants cause development of liver damage. Plants having antioxidant effect use to treat diseases due to oxidative stress. In this study showed *S. cumini* have liver protection effect in diabetic rats [33].

Increased level of hepatic enzyme markers indicator of liver injury. The disturbance in the transport function of the hepatocyte as a result of hepatic injury causes the leakage of enzyme from cell due to altered permeability of membrane [34]. A fatty liver is characterized by elevated circulating level of ALT and AST, markers of hepatocellular damage. ALP levels were, however, significantly increased, suggesting induction of liver injury [23].

RSG causes cardiotoxicity effect, cardiac biomarkers such as CK-MB and LDH has been used as indicator for cardiac disorder. Serum LDH and CK-MB activity have previously been demonstrated to be elevated in cardiomyopathy in diabetic patients, suggesting that they could be used as a marker for cardiovascular risk and cardiac muscular injury [35]. In our study, serum LDH

and CK-MB activities were found to be increased in diabetic rats, possibly due to myocardial dysfunction. Furthermore, a significant increase in serum LDH and CK-MB level was observed with RSG treatment, which was more marked in diabetic rats than normal rats, indicating that Rosiglitazone has a cardiotoxic effect.

RSG can induce myocardial infarction, cardiomyopathy in diabetes as shown by increasing cardiac marker. These effects may be associated to alterations of cardiac ion channels and other processes rather than oxidative stress [22]. Medicinal herbs have long been considered as a source of novel cardioprotective chemicals. Methanolic extract of *S. cumini* seed has efficiently protected the myocardium against isoprotrenol-induced myocardial infarction. [36]

Histopathological study of liver and heart revealed disturbance in the normal architecture of liver and heart due to toxicity in RSG treated animals, whereas animals treated with the ESC showed retention of the normal cellular architecture and it is comparable with the standard Silymarin group, hence confirming the significant hepatoprotective and Cardioprotective effect of ethanolic extract of *S. cumini* seeds. Aqueous seed extract of *S. cumini* (500 mg/kg) showed significant hepatoprotective effect in diabetic rat's compared to other group. This may due to antioxidant property of seed extract. Antioxidant neutralize the oxidant generated in the liver. Plant having antioxidant effect use to treat disease due to oxidative stress [33]. Hepatotoxicity caused by rosiglitazone can be reversed by co-administering Silymarin, a proven hepatoprotective drug, without affecting its hypoglycemic potential [34]. Methanolic extract of *S. cumini* seeds exhibited cardioprotective effect on isoprotrenol-induced myocardial infarction of rat [36].

Silymarin administration causes the organ's morphological structure to resemble its physiological appearance. Cardiomyocytes

are cylindrical and regular, with no evidence of degeneration or necrosis observable. Silymarin has been shown to protect heart and liver tissue against doxorubicin-induced damage [37]. Study reflects good antidiabetic, cardioprotective and hepatoprotective activity of ethanolic extract of *S. cumini* seed at 100 mg/kg and 300 mg/kg orally and effect produced by the higher dose of ESC was similar to that produced by Silymarin, having hepatoprotective cardioprotective activity.

Conclusion

Our finding highlights the efficacy of ESC as protective effect against RSG induced oxidative damage to the myocardial and hepatic cell which induced toxicity. RSG induction leads to reduction in level of enzymic and non-enzymic antioxidant. However, the treatment of ESC normalised the level of all biochemical and antioxidant parameter. It can be concluded that ethanolic seed extract of *S. cumini* provide a protective and antidiabetic effect in RSG induced cardiotoxicity and hepatotoxicity in diabetic Wistar rats.

References

1. Jadhav, V. M., Kamble, S. S., & Kadam, V. J. (2009). Herbal medicine: *Syzygium cumini*: a review. *Journal of Pharmacy Research*, 2(8), 1212-1219.
2. Shrikant Baslingappa, S., Nayan Singh J, T., Meghatai M, P., & Parag M, H. (2012). *Jamun (Syzygium cumini (L.))*: a review of its food and medicinal uses. *Food and Nutrition Sciences*.
3. Nair LK, Begum M, Geetha S. (2013). In vitro-antioxidant activity of the seed and leaf extracts of *Syzygium cumini*. *J Envir Sci Toxicol Food Technol*. 7(1):54-62.
4. Kamtekar, S., Keer, V., & Patil, V. (2014). Estimation of phenolic content, flavonoid content, antioxidant and alpha amylase inhibitory activity of marketed polyherbal formulation. *Journal of Applied Pharmaceutical Science*, 4(9), 61.

5. Waghulde, H., Kamble, S., Patankar, P., Jaiswal, B., Pattanayak, S., Bhagat, C., & Mohan, M. (2011). Antioxidant activity, phenol and flavonoid contents of seeds of *Punica granatum* (Punicaceae) and *Solanum torvum* (Solanaceae). *Pharmacologyonline*, 1, 193-202.
6. Tripathi, V., & Verma, J. (2014). Different models used to induce diabetes: a comprehensive review. *International Journal of Pharmacy and Pharmaceutical Sciences*, 6(6), 29-32., 2014; 6:30-32.
7. Raza, A., Saif-ul-Malook, N. S., Qasrani, S. A., Sharif, M. N., Akram, M. N., & Ali, M. U. (2015). Extraction of bioactive components from the fruit and seed of jamun (*Syzygium cumini*) through conventional solvent extraction method. *American-Eurasian Journal of Agricultural and Environmental Sciences*, 15(6), 991-996.
8. Marklund, S., & Marklund, G. (1974). Involvement of the superoxide anion radical in the autoxidation of pyrogallol and a convenient assay for superoxide dismutase. *European journal of biochemistry*, 47(3), 469-474.
9. Beers, R. F., and Sizer, I. W. (1952) A spectrophotometric method for measuring the breakdown of hydrogen peroxide by catalase. *J. Biol. Chem.*, 195, 133-140.
10. Ellman, G. L. (1959). Determination of sulfhydryl group. *Arch. Biochem. Biophys*, 82(1), 70-77.
11. Latha S., Vijaykumar R., Shrikumar R. (2016) In vivo anti oxidative effect of Polyherbal formulation of flax seed, fenugreek and jamun seed on streptozotocin Nicotinamide Induced Diabetic Rats. *International Journal of Pharma and Bio Sciences*; 7(4):607-611.
12. Clin J., (1986) IFCC method for the measurement of catalytic concentration of enzymes. *J. Clin Chem Clin Biochem*. 24:497
13. Schumann, G., Bonora, R., Ceriotti, F., Clerc-Renaud, P., Ferrero, C.A., Féraud, G., Franck, P.F., Gella, F.J., Hoelzel, W., Jørgensen, P.J. and Kanno, T., 2002. IFCC primary reference procedures for the measurement of catalytic activity concentrations of enzymes at 37 C. Part 2. Reference procedure for the measurement of catalytic concentration of creatine kinase. 635-642.
14. Young D., (1997) In Effect of Preanalytical Variables on Clinical Laboratory Tests 2nd. AACCpress, Washington;4-489.
15. Serap T., Burcu T., Ibrhim G., Tulay G., Zeynep, Anjumana O., Teoman A (2011). Serum Alkaline Phosphatase Levels in Healthy Children and Evaluations of Alkaline Phosphatase z-scores in Different Types of Rickets, *Journal Clinical Research Pediatric Endocrinology*; 3(1): 7-11
16. Johnsan A.M., Rohifs E.M., Silverman L.M. Protein, (1999) In TIETZ Textbook of clinical chemistry, Burtis C.A., AND Ashwood E.R.,Eds. W.B.Saunders, Philadelphia, 3: 477-540
17. Billing, B., Haslam, R., & Wald, N. (1971). Bilirubin Standards and the Determination of Bilirubin by Manual and Technicon AutoAnalyzer Methods: Prepared for the Scientific and Technical Committee of the Association of Clinical Biochemists. *Annals of Clinical Biochemistry*, 8(1-6), 21-30.
18. Panteghini, M., Falsetti, F., Chiari, E., & Malchiodi, A. (1983). Determination of aspartate aminotransferase isoenzymes in hepatic diseases—preliminary findings. *Clinica Chimica Acta*, 128(1), 133-140.
19. Green, R. M., & Flamm, S. (2002). AGA technical review on the evaluation of liver chemistry tests. *Gastroenterology*, 123(4), 1367-1384.
20. Atale, N., & Rani, V. (2016). *Syzygium cumini*: an effective cardioprotective via its antiglycooxidation potential. *International Journal of Pharmaceutical Science Review and Research*, 37(1), 42-51.
21. Maheswari, R., & Manohari, S. (2015). *Syzygium cumini* (L.) seeds extract ameliorates

- cisplatin-induced hepatotoxicity in male Wistar rats. *International Journal of Pharma Sciences and Research*, 6(2), 444-50.
22. Manar AN., Dina SL., Hamdy AG., Mohammed SE. (2015) Role of oxidative stress in cardiac hypertrophy induced by Rosiglitazone in diabetic rats. *International Journal of Pharmaceutical Research and Bio-science*;4(1):238-250.
23. Hemmeryckx, B., Gaekens, M., Gallacher, D. J., Lu, H. R., & Lijnen, H. R. (2013). Effect of rosiglitazone on liver structure and function in genetically diabetic Akita mice. *Basic & clinical pharmacology & toxicology*, 113(5), 353-360.
24. Winarsi, H., Sasongko, N. D., Purwanto, A., & Nuraeni, I. (2014). Effect of cardamom leaves extract as antidiabetic, weight lost and hypocholesterolemic to alloxan-induced Sprague Dawley diabetic rats. *International Food Research Journal*, 21(6), 2253.
25. Hemmeryckx, B., Hoylaerts, M. F., Gallacher, D. J., Lu, H. R., Himmelreich, U., D'hooge, J., ... & Lijnen, H. R. (2013). Does rosiglitazone affect adiposity and cardiac function in genetic diabetic mice? *European journal of pharmacology*, 700(1-3), 23-31.
26. Wu, L., Wang, R., Champlain, J. D., & Wilson, T. W. (2004). Beneficial and deleterious effects of rosiglitazone on hypertension development in spontaneously hypertensive rats. *American journal of hypertension*, 17(9), 749-756.
27. Rohilla, A., & Ali, S. (2012). Alloxan induced diabetes: mechanisms and effects. *International journal of research in pharmaceutical and biomedical sciences*, 3(2), 819-823.
28. Papoushek, C. (2003). The "Glitazones": rosiglitazone and pioglitazone. *Journal of Obstetrics and Gynaecology Canada*, 25(10), 853-857.
29. Scandalios, J. G. (1993). Oxygen stress and superoxide dismutases. *Plant physiology*, 101(1), 7.
30. Young, I. S., & Woodside, J. V. (2001). Antioxidants in health and disease. *Journal of clinical pathology*, 54(3), 176-186.
31. Jorg BS., Jorg L., Jan S., Johannes D., (2000) Glutathione, oxidative stress and neurodegeneration. *European Journal of Biochemistry*. 267:4904- 4911.
32. Thiffault, C., Aumont, N., Quirion, R., & Poirier, J. (1995). Effect of MPTP and L-deprenyl on antioxidant enzymes and lipid peroxidation levels in mouse brain. *Journal of neurochemistry*, 65(6), 2725-2733.
33. Behera, S. R., Sekkizhar, M., & Sarath Babu, K. (2014). Hepatoprotective activity of aqueous extract of *Syzygium cumini* seed on streptozotocin induced diabetes in rats. *International journal of ayurvedic and herbal medicine*, 4(2), 1470-1477.
34. Swamy, S., Krishna, K. L., & Nidavani, R. B. (2013). Reversal of rosiglitazone hepatotoxicity by silymarin on rats. *International Journal of Pharmaceutical Sciences and Research*, 4(6), 2301.
35. Huang, E.J., Kuo, W.W., Chen, Y.J., Chen, T.H., Chang, M.H., Lu, M.C., Tzang, B.S., Hsu, H.H., Huang, C.Y. and Lee, S.D. (2006). Homocysteine and other biochemical parameters in type 2 diabetes mellitus with different diabetic duration or diabetic retinopathy. *Clinica Chimica Acta*, 366(1-2), 293-298.
36. Mastan, S. K., Chaitanya, G., Latha, T. B., Srikanth, A., Sumalatha, G., & Kumar, K. E. (2009). Cardioprotective effect of methanolic extract of *Syzygium cumini* seeds on isoproterenol-induced myocardial infarction in rats. *Der Pharmacia Lettre*, 1(1), 143-149.
37. Rašković, A., Stilinović, N., Kolarović, J., Vasović, V., Vukmirović, S., & Mikov, M. (2011). The protective effects of silymarin against doxorubicin-induced cardiotoxicity and hepatotoxicity in rats. *Molecules*, 16(10), 8601-8613.

Comparative anti-anaemic activity of methanolic extracts of *Momordica charantia* and *Luffa acutangula*

Doppalapudi Sandeep*, Suryadevara Vidyadhara and Pottella Srinivasulu

Department of Physiology and Pharmacology, Chebrolu Hanumaiah Institute of Pharmaceutical Sciences, Chandramoulipuram, Chowdavaram, Guntur, Andhra Pradesh, 522019

*Corresponding Author: E-mail Id: pharmacydeepu@gmail.com

Abstract

The present research work mainly focused on the preparation of methanolic extracts of *Momordica charantia* and *Luffa acutangula* fruits and their pharmacological evaluation for anti-anaemic property individually. The methanolic extracts were prepared by simple maceration process. Preliminary phytochemical screening of the extracts showed the presence of various phytochemicals. Anti-anaemic activity was evaluated on wistar rats using phenyl hydrazine induced anaemia model. The results of extract treated groups were compared with that of the anaemic group. Dexorange syrup was used as standard. Blood samples were collected through retro-orbital puncture from rats on day 0, 2, 7, 14, 21 and 28 of treatment and subjected to analysis of red blood cell count, haemoglobin and hematocrit using 3-part haematology analyzer. A significant increase in red blood cell count, haemoglobin and hematocrit was observed in rats treated with methanolic extract of *Momordica charantia* and *Luffa acutangula* when compared to that of the untreated anaemic group. *Momordica charantia* showed more anti-anaemic effect when compared to *Luffa acutangula*. Thus from the present study, it was concluded that the *Momordica charantia* and *Luffa acutangula* showed significant anti-anaemic activity.

Keywords: Anaemia; haemoglobin; phenyl hydrazine; rats.

Introduction

Anaemia is a condition where there is a decrease in the total amount of red blood cells (RBCs) and hemoglobin in the blood. It is affecting about a quarter of people globally. It

is more common in females, than in males(1). Haemolytic anaemia occurs due to abnormal breakdown of RBC, either in blood vessels or elsewhere in the human body. It causes several consequences, ranging from relatively harmless to life-threatening (2). Haemolytic anaemia may be due to oxidative stress or defects in RBC membrane production and haemoglobin production. It shows symptoms like fatigue, pallor, loss of weight, shortness of breath and dark colored urine. Anaemia can be induced by several chemicals. One of them is phenyl hydrazine. It causes haemolytic anaemia by increasing the absorption of iron in liver, spleen and duodenum and there by leading to altered iron metabolism in body.

Plants have been used for health and medicinal purposes for several thousands of years. They support in relieving from several types of ailments (3). *Momordica charantia* and *Luffa acutangula* belonging to the family *Cucurbitaceae* have several therapeutic benefits. *Momordica charantia*, commonly called as "Bitter gourd" and *Luffa acutangula*, commonly called as "ridged gourd" are available throughout India and are extensively used as vegetables. The fruits of *Momordica* have a distinct warty exterior and an oblong shape. The fruit is most often consumed green. It is mostly used in culinary. These are useful in treatment of diabetes mellitus, anthelmintic, anaemia and rheumatoid arthritis (4). The fruits of *Luffa* are slightly bitter in taste with slightly spongy texture. These are useful in killing of parasites and to treat gonorrhoea, eczema and anemia (5). The present study was aimed on the preparation of methanolic extracts from unripe fruits of *Momordica charantia* and *Luffa*

acutangula and to evaluate their anti-anaemic potential on Wistar rats.

Materials and Methods

Plant Material: Fruits of *Momordica charantia* and *Luffa acutangula* belonging to the family *Cucurbitaceae* were collected from the local market of Guntur, Andhra Pradesh, India. Collected material was analyzed and authenticated by Dr. K. Ammani, Professor, Department of Botany, Acharya Nagarjuna University. A voucher specimen (02/2017 and 03/2017) was preserved in the Department of Pharmacology.

Preparation of Methanolic Extract of *Momordica charantia* and *Luffa acutangula*: The fruits of *Momordica charantia* were made into small pieces, dried, powdered and subjected to maceration. In this a total amount of 100 g powder is macerated in 400ml of methanol for 72 hours with occasional stirring for every 3 hours. At the end, the extract was passed through a filter paper and filtrate was evaporated on water bath to obtain crude. After cooling 2 drops of chloroform are added for preservation. Condensed extracts were weighed and stored in air-tight containers at 4°C till further investigation. Similar procedure was followed to extract *Luffa acutangula* fruits.

Phytochemical Analysis: Preliminary phytochemical screening was performed for the methanolic extracts of *Momordica charantia* and *Luffa acutangula* to detect the presence of various constituents responsible for the pharmacological activity like carbohydrates, fixed oils, glycosides, alkaloids, flavonoids, tannins, polyphenols, steroids and saponins (6).

Drugs and Chemicals: Dexorange syrup (Franco-Indian Pharmaceuticals Pvt. Ltd., Mumbai) and phenyl hydrazine hydrochloride (Qualigens Fine Chemicals, Mumbai) were commercially procured from. All other materials used were of analytic grade and procured commercially.

Experimental Animals: Healthy adult male albino rats (Wistar strain) weighing 250–300 g, housed in polypropylene cages, maintained under standardized condition i.e., 12:12 hour light/dark cycle at 25 ± 2°C with paddy husk bedding at the animal house, Chebrolu Hanumaiah Institute of Pharmaceutical Sciences, Guntur, India. Animals were provided with standard pellet food and had free access to purified drinking water.

Pharmacological Evaluation:

Induction of Anaemia: Anaemia was induced in all groups of rats except to the control group, by intra-peritoneal administration of 40 mg/kg of phenyl hydrazine (PHZ) for two days (7).

Treatment of Animals: Rats were divided into five groups and treated daily for 4 weeks. The control group I is treated with normal saline solution. The anaemic control group II was treated with phenyl hydrazine 40 mg/kg for first two days. The standard group III was treated with dexorange syrup at a dose of 1ml/day from day 2 to day 28. Whereas the test groups IV and V were treated with methanolic extract of *Momordica charantia* and *Luffa acutangula* respectively at a dose of 200 mg/kg from day 2 to day 28. This dose was selected based on the acute toxicity tests from past studies (8-9). All administrations were done orally using oropharyngeal cannula once per day for 28 days (4 weeks).

Analysis of Haematological Parameters: Blood samples were collected from the rats through retro-orbital puncture, before induction of anaemia (day 0), after induction of anaemia with phenyl hydrazine (day 2) and on 7, 14, 21 and 28 days of treatment. The red blood cell count, haemoglobin concentration and haematocrit were determined before starting of the study and on 2, 7, 14, 21 and 28 days using a 3-part haematology analyzer (BENESPHERA) and the variations of average values of haematological parameters were calculated relative to the mean values of D0 and D2 (10).

Statistical Analysis: Graph Pad Prism 5.0 software was used for the analysis of the results obtained. The mean value is accompanied by the standard error of mean (mean \pm SD).

Results and Discussion

The present study was intended to prepare methanolic extracts of *Momordica charantia* and *Luffa acutangula* and to evaluate their anti-anaemic property.

Phytochemical Screening: The phytochemical investigation of methanolic extract of *Momordica charantia* revealed the presence of alkaloids, carbohydrates, tannins, flavonoids, glycosides and saponins which promises their huge pharmacological abilities. The methanolic extract of *Luffa* contains all the phytochemicals except glycosides (Table 1). Past studies indicate that the phytochemicals that are present in the methanolic extracts of these plants have antioxidant activity which favours tissue regeneration and enhances the resistance of blood vessels to haemolysis (11). Alkaloids also been known to possess anti-anaemic property by inhibiting phosphodiesterase enzyme thereby accumulating cyclic adenosine monophosphate (cAMP). This causes phosphorylation and

Table 1. Phytochemical Screening of Methanolic Extracts of *Momordica Charantia* and *Luffa Acutangula*

Phytochemical Constituents	Methanolic Extracts of	
	<i>Momordica charantia</i>	<i>Luffa acutangula</i>
Alkaloids	+	+
Carbohydrates	+	+
Steroids	–	+
Tannins	+	+
Flavonoids	+	+
Glycosides	+	–
Saponins	+	+

+ indicates Presence ; – indicates Absence

synthesis of proteins, which increases erythropoiesis (12). Saponins are also known to inhibit platelet aggregation and thrombosis. The methanolic extracts can detoxify the saponins which allow increase in haemoglobin and RBC(13). Flavonoids have anti-anaemic potential and also protect the blood capillaries(14).

In vivo Anti-Anaemic Activity

Effect on Body Weight: The *in vivo* anti-anaemic activity was performed by using phenyl hydrazine hydrochloride induced anaemia method. After administration of phenyl hydrazine, there is a decrease in the body weights of rats from all groups except normal group. The loss of body weight is one of the symptoms of anaemia, which would be due to lack of appetite in anaemic rats. This is mostly due to improper carbohydrate metabolism. After the study duration (28 days), the methanolic extract of *Momordica charantia* showed 14.50% increase in body weights of rats which are nearer to the standard group (17.65%). This indicates regaining of appetite in rats during treatment which lead to gain in body weight (15). The same was also observed in the rats that were treated with dexorange syrup (Table 2).

Effect on Red Blood Cell Count: The administration of phenyl hydrazine leads to decrease in red blood cell count except in normal group of rats (16). An increase in number of red blood cells was observed in following weeks in treatment groups. The animals were almost recovered by the end of the study (28 days). Significantly, the animals treated with methanolic extract of *Momordica charantia* showed 80.88% increase in red blood cell count. A bit less effect than this was found with *Luffa* extract (Table 3).

Effect on Haemoglobin Content: Haemoglobin is an important constituent of blood which maintains RBC in constant functioning and fulfils body oxygen needs. Administration of phenyl hydrazine on D2 caused a significant decrease in haemoglobin content in all groups except normal group(17).

Table 2. Effect of Methanolic Extracts of *Momordica charantia* and *Luffa acutangula* on Body Weight in Wistar Rats

Group	Treatment	Body Weight (g); Mean ± SD (%)					
		Day 0	Day 2	Day 7	Day 14	Day 21	Day 28
I	Control	300±1.12	302±1.77	300±0.81	305±1.64	300±0.14	302±0.77
II	Anemic control	298±0.93	260±1.64 (-12.75) ^a	262±0.22	275±1.55	275±1.94	270±1.86 (+03.84) ^b
III	Dexorange syrup	299±1.24	255±1.32 (-14.71) ^a	262±1.20	282±3.02	290±1.62	300±1.54 (+17.65) ^b
IV	Methanolic extract of <i>Momordica</i>	300±1.02	262±1.07 (-12.66) ^a	275±1.88	282±2.87	290±1.77	300±1.99 (+14.50) ^b
V	Methanolic extract of <i>Luffa</i>	325±1.56	275±1.99 (-15.38) ^a	282±1.05	290±1.35	300±1.64	310±1.42 (+12.72) ^b

a - Percentage variation compared to day 0; b - Percentage variation compared to day 2

Table 3. Effect of Methanolic Extracts of *Momordica charantia* and *Luffa acutangula* on Red Blood Cell Count

Group	Treatment	Red Blood Cells (10 ⁶ cells/μL); Mean ± SD (%)					
		Day 0	Day 2	Day 7	Day 14	Day 21	Day 28
I	Normal Control	8.92±1.04	9.44±1.72	9.02±1.04	9.27±2.32	9.14±1.10	9.44±0.44
II	Anemic control	8.74±1.23	4.5±0.21 (-48.51) ^a	4.63±1.54	6.63±2.41	7.05±0.66	7.39±2.01 (+64.22) ^b
III	Dexorange syrup	8.05±2.41	4.21±1.24 (-47.70) ^a	6.20±0.53	6.93±1.72	7.28±0.89	7.93±1.64 (+88.36) ^b
IV	Methanolic extract of <i>Momordica</i>	6.62±2.55	4.29±1.25 (-35.19) ^a	6.72±1.70	7.05±1.62	7.25±2.81	7.76±1.36 (+80.88) ^b
V	Methanolic extract of <i>Luffa</i>	8.17±0.36	4.59±2.08 (-43.81) ^a	5.84±1.42	7.10±0.96	7.76±1.82	8.10±0.63 (+76.47) ^b

a - Percentage variation compared to day 0; b - Percentage variation compared to day 2

After treatment, a progressive recovery was obtained. Animals treated with vitamin syrup showed higher recovery which is 80.41%. A nearer recovery value was obtained with Methanolic extract of *Momordica* which is 80%. Even the extract of *Luffa* also showed prominent effect (Table 4).

Effect on Haematocrit: Haematocrit also called as packed cell volume (PCV) is the measurement of volume percentage of red blood cells in the blood. The administration of phenyl hydrazine also decreased the haematocrit levels. After four weeks, the haematocrit value observed was very high in case of animals treated with methanolic extract

of *Momordica* which is 90.51% when compared to day 2. This was more than the standard treatment group (Table 5). The intra peritoneal administration of 40mg/kg/day of phenyl hydrazine for two days in Wistar rats caused a decrease in the concentration of body weight, haemoglobin, red blood cells and haematocrit. The results obtained were

similar to those of previous studies who observed a decrease of number of blood cells and haematocrit with a phenyl hydrazine administration(18-19). Considering the results of the groups IV, V and VI, the methanolic extract of *Momordica charantia* fruits have higher anti-anaemic potential than that of other vegetable extracts. The anti-anaemic effect of

Table 4. Effect of Methanolic Extracts of *Momordica charantia* and *Luffa acutangula* on Haemoglobin Content

Group	Treatment	Haemoglobin (in g/dL); Mean \pm SD (%)					
		Day 0	Day 2	Day 7	Day 14	Day 21	Day 28
I	Normal Control	17.21 \pm 1.30	17.31 \pm 1.68	16.71 \pm 1.60	16.91 \pm 1.20	16.30 \pm 1.60	17.10 \pm 0.53
II	Anemic control	16.12 \pm 1.52	10.73 \pm 1.58 (-33.54) ^a	11.90 \pm 1.13	12.72 \pm 2.41	13.84 \pm 1.95	13.27 \pm 1.58 (+23.36) ^b
III	Dexorange syrup	15.70 \pm 2.03	9.77 \pm 1.72 (-38.21) ^a	12.33 \pm 0.74	15.10 \pm 1.92	17.22 \pm 1.58	17.56 \pm 0.95 (+80.41) ^b
IV	Methanolic extract of <i>Momordica</i>	14.31 \pm 1.63	9.08 \pm 0.31 (-37.06) ^a	11.24 \pm 1.64	13.81 \pm 2.50	15.63 \pm 0.58	16.23 \pm 1.58 (+80.00) ^b
V	Methanolic extract of <i>Luffa</i>	14.92 \pm 0.82	9.31 \pm 1.50 (-37.58) ^a	11.95 \pm 1.34	14.32 \pm 1.67	15.54 \pm 0.39	16.16 \pm 0.86 (+73.11) ^b

a - Percentage variation compared to day 0; b - Percentage variation compared to day 2

Table 5. Effect of Methanolic Extracts of *Momordica charantia* and *Luffa acutangula* on Haematocrit

Group	Treatment	Haematocrit (%) (Mean \pm S.E.M) (%)					
		Day 0	Day 2	Day 7	Day 14	Day 21	Day 28
I	Normal Control	50.82 \pm 0.95	49.12 \pm 1.08	48.34 \pm 0.62	50.41 \pm 1.75	49.76 \pm 1.88	50.24 \pm 0.93
II	Anemic control	45.80 \pm 1.20	24.21 \pm 1.13 (-47.16)	27.66 \pm 1.43	30.20 \pm 1.31	32.81 \pm 1.71	34.93 \pm 1.51 (+44.21)
III	Dexorange syrup	45.03 \pm 0.93	27.60 \pm 1.62 (-38.66)	32.29 \pm 1.70	45.73 \pm 1.09	49.54 \pm 1.44	50.70 \pm 1.97 (+83.69)
IV	Methanolic extract of <i>Momordica</i>	42.71 \pm 1.53	27.46 \pm 1.27 (-35.83)	31.78 \pm 1.19	45.24 \pm 1.72	48.57 \pm 0.83	52.22 \pm 1.55 (+90.51)
V	Methanolic extract of <i>Luffa</i>	43.17 \pm 1.20	27.53 \pm 1.34 (-36.19)	33.02 \pm 1.88	45.70 \pm 1.03	48.26 \pm 1.28	49.14 \pm 2.55 (+78.54)

a - Percentage variation compared to day 0; b - Percentage variation compared to day 2

Anti-Anaemic Activity of Methanolic Extracts

the methanolic extracts was compared with commercially used dexorange syrup. The dexorange syrup showed a significant increase of the content in haemoglobin after the first week of treatment.

Conclusion

From the above results, it was concluded that the methanolic extracts of *Momordica charantia* and *Luffa acutangula* showed promising anti-anaemic effect and among these two, *Momordica charantia* showed more efficacy. Further work is needed to be done on the isolation of specific phytochemical component that is responsible for anti-anaemic activity.

Acknowledgement

The authors are thankful to the management of Chebrolu Hanumaiah Institute of Pharmaceutical Sciences, Chowdavaram for their sheer support during the work.

Conflict of interest

The authors declare no conflict of interest.

Ethical Statement

The guidelines of Committee for the Purpose of Control and Supervision of Experiments on Animals (CPCSEA), Government of India were followed and prior approval was sought from Institutional Animal Ethics Committee (IAEC) for conducting the study (1529/PO/Re/11/CPCSEA./CHIPS/IAEC5/PR O-11/2016-17)

References

1. Bosman, G. J.; Willekens, F. L.; Were, J. M. Erythrocyte aging: a more than superficial resemblance to apoptosis. *Cell. Physiol. Biochem.* 2005, 16, 1–8.
2. Janz, T. G.; Johnson. R. L.; Rubenstein, S. D. Anemia in the emergency

department: evaluation and treatment. *Emerg. Med. Pract.* 2013, 15, 1–15.

3. Sultan. R.; Wani, M. A.; Nawchoo, I. A. Herbal drugs - Current status and future prospects. *Int. J. Med. Plant. Alter. Med.* 2013, 1, 20-29.

4. Arunachalam, G.; Subramanian, N.; Pazhani, G. P.; Ravichandiran, V.; Karunanithi. M.; Nepolean, R. Anxiolytic, Antidepressant and Anti-Inflammatory Activities of Ethanol Extract of *Momordica charantia* Linn Leaves (Cucurbitaceae). *Iranian. J. Pharmacol. Ther.* 2003; 7, 43-47.

5. Ulaganathan, I.; Nappinnai, M.; Shanmugapandiyar, P. Anti-Inflammatory and In-Vitro Antioxidant Potential of Extracts Leaves of *Luffa Acutangula* in Rodent Model (Rats). *Int. J. Pharm. Pharm. Sci.* 2013, 5, 79-83.

6. Dibyajyoti, S.; Bindu, J.; Vibhor, K. J. Phytochemical evaluation and characterization of Hypoglycemic activity of various extracts of *Abelmoschus esculentus* Linn. *Int. J. Pharm. Pharm. Sci.* 2011, 3, 182-185.

7. Yenon, A. A.; Yapi, H. F.; Gnahoue, G.; Yapo, A. F.; Nguessan, J. D.; Djaman, A. J. Anti-anaemic activity of aqueous and ethanolic extracts of *Entandrophragma angolense* bark on phenylhydrazine- induced anaemic rats. *Asian. J. Biochem. Pharm. Res.* 2015, 5, 2231-2560.

8. Nurul, H. R.; Noriham, A.; Nooraain, H.; Azizah, A. H.; Farah, A. O. Acute oral toxicity effects of *Momordica charantia* in Sprague dawley rats. *International Journal of Bioscience, Biochemistry and Bioinformatics.* 2013, 3, 408-410.

9. Arunachalam, A.; Selvakumar, S.; Jeganath, S. Toxicological studies on ethanol extract of *Luffa acutangula* in albino Wistar rats. *Int. J. Curr. Pharm. Res.* 2012, 2, 29-33.

10. Saravanan, V. S.; Manokaran, S. Anti-anaemic activity of some plants in Cucurbitaceae on phenylhydrazine-induced anaemic rats. *Thai. J. Pharm. Sci.* 2012, 36, 150-154.

11. Shravan, K. D.; Rajeshwari, V.; Anusha, V.; Jyothi, P. J.; Ravali, T.; Mounika, M. Anti-anaemic activity of ethanol cextract of *Punica granatum* seeds on phenylhydrazine induced anaemic rats. *Asian. J. Ethnopharmacol. Med. Foods*. 2016, 2, 27-31.
12. Ndem, J. I.; Otitoju, O.; Akpanabiatiu, M. I.; Uboh, F. E.; Uwah, A. F.; Edet, O. A. Haematoprotective property of *Eremomastax speciosa* (Hochst.) on experimentally induced anaemic wistar rats. *Ann. Biol. Res.* 2013, 4, 356-360.
13. Shi, J.; Arunasalam, K.; Yeung, D.; Kakuda, Y.; Mittal, G.; Jiang, Y. Saponins from edible legumes. *J. Med. Food*. 2004, 7, 67– 78.
14. Waghmare, A. N.; Tembhurne, S. V.; Sakarkar, D. M. Anti-anaemic potential of *Murraya koenigii* fruit extracts in phenylhydrazine induced anaemic rats. *Int. J. Ayurveda. Pharma. Res.* 2015, 6, 124-127.
15. Vieira, M. R.; Galzvaio, L. C.; Fernandes, M. I. M. The haemolytic component of cancer anaemia. *Braz. J. Med. Biol. Res.* 2000, 33, 539-544.
16. Ashish, T.; Sachin, M.; Rizwan, S. K.; Gadhpayle, J.; Bhongade, S. L.; Vikas, S. Antianaemic Potential of *Swertia chirata* on Phenylhydrazine Induced Reticulocytosis in Rats. *American Journal of Phytomedicine and Clinical Therapeutics*. 2013, 1, 37-41.
17. Bhaskaran, K.; Suruthi, B. Anti-Anemic Activity of Ethanolic Leaf Extract of *Kedrostis foetidissima* in Phenylhydrazine Induced Anemic Rats. *Scholars. Acad. J. Biosci.* 2016, 4, 681-683.
18. Sylvester, C. O. Pharmacological assessment of anti-anaemic activity of aqueous leaves extracts of *Telfairia occidentalis* and *Spondias mombin* in rats. *UK. J. Pharm. Biosci.* 2016, 4, 56-59.
19. Veena, V. A.; Jyothi, Y.; Rina, P.; Rajdwip, G.; Ronak, P.; Vijay, Y. Comparative anti anemic activity of *Azadirachta indica* leaves and its combination with *Embllica officinalis* in phenyl hydrazine induced anemia using rats. *J. Chem. Pharm. Res.* 2015, 7, 1019-1022.

Synthesis, Spectral Characterization and *In vitro* Anti Cancer Activity of Pyrimidine – Imidazole coupled Heterocyclic compounds against Human Lung Cancer Cell Line

S. Shakila Banu*, G. Krishnamoorthy, R. Senthamarai and A. M. Ismail

¹Department of Pharmaceutical Chemistry, Periyar College of Pharmaceutical Sciences, Tiruchirappalli, Tamil Nadu, India

*Corresponding Author: E-mail Id: sbpharma84@gmail.com

Abstract

To Explore two heterocyclic based scaffolds; Pyrimidine and Imidazole for Anticancer activity targeting Human Lung cancer cell lines. The designed compounds were synthesized and evaluated for their *invitro* Anticancer activity against Human Lung Cancer Cell line A549. *In vitro* anticancer activity revealed that 14h showed more potent anticancer activity as compared to the standard drug Sunitinib. This compound exhibited apoptosis thus, arresting the cell cycle at G0/G1 phase itself. To conclude, the above findings clearly demonstrated that the compound 14h may serve as good anticancer agent for further development.

Keywords: Pyrimidine, Imidazole, Human Lung Cancer Cell line.

Introduction

Today, cancer is becoming a common word, with each one of us closely related with at least one nearby or a relative or a friend or a colleague, diagnosed with cancer (1). It can occur at any age, but it is more common among the people over 65 years old (2). It has been reported that cancer has become the major cause of death worldwide. As per WHO, Cancer is leading cause of death worldwide, accounting nearly 10 million deaths in 2020. The most common in 2020 (in terms of new cases of cancer) were Breast (2.26 million cases), lungs (2.21 million cases), Colon and rectum (1.93 million cases), Prostate (1.41 million cases), Skin

(1.20 million cases) and stomach (1.09 million cases). The most common causes of cancer death in 2020 were lungs, colon and rectum, liver, stomach and breast (3). This increasing burden opens the window for the research in newer anticancer molecules. Tremendous efforts are taken to combat cancer over the past few years, but there is still a demand for new and better drugs (4). Heterocycles are a good choice when designing molecules that will interact with targets and influences the biological pathways involved in cancer progression, as many of the protein targets are habited to interact with heterocyclic moieties (5). With a vision of novel drug design, the concept of molecular coupling is a significant approach which involves combination of two structurally diverse moiety in a single framework. It is well evident from the literature survey that Pyrimidine scaffold possesses significant anticancer activity.

Pyrimidine substituted with another heterocycle is widely used in the design and discovery of anticancer drugs. Pyrimidine is a versatile heterocycle and possesses many sites which enable it to combine with other potent moieties to construct a coupled framework. Such framework has multifaced mode of action or may bind to various targets to get desired activity. Imidazole ring have been lately gaining much attention due to their roles as attractive scaffolds for biologically active heterocyclic drugs. In general terms, physicochemical properties like π - π stacking interactions, co-ordination bonds with metals as ligands, hydrogen bond donor-acceptor

capability, van der Waals, polarization and hydrophobic forces have caused the increasing interest in these fragments. These properties liable for their reactivity enable derivatives to willingly bind with a series of biomolecules, including several enzymes and nucleic acids (6-9).

In the present work, we designed and synthesized Pyrimidine coupled with imidazole to explore the anticancer potential of the hybrid moieties in a single framework. The rationale behind the design of these coupled framework is to get maximum activity against Human Lung cancer.

Materials and Methods

Chemicals, Reagents and Cell Lines:

All the chemicals used were of analytical grade and procured from Sigma-Aldrich, Loba chemie Pvt Ltd, India and Sisco Research Laboratories Pvt. Ltd., India. o-Toluidine, Sulphuric acid, Nitric acid, n-Butanol, 50% aqueous solution of cyanamide, 50% Ethanol, Stannous chloride dihydrate, Methanol, Diethyl ether, N, N - Dimethylformamide dimethyl acetal, Cyclohexane, Hydrochloric acid, Ethyl acetate, Sodium sulfate, Dichloromethane, Thionyl chloride, Sodium hydroxide, Tetra Hydro Furan (THF), Tri Ethyl Amine (TEA), Propyl amine, Ammonia, and 2-Acetyl Imidazole. Cell culture was obtained from Future Bioscience, Korea. Fetal Bovine Serum, Antibiotics, Dulbecco's Modified Eagle's Medium (DMEM), Phosphate Buffered Saline, Trypsin-EDTA was purchased from HiMedia. RNase A, Propidium Iodide was purchased from HiMedia. Dichloro-Dihydro-Fluorescein Diacetate (DCFH-DA) was obtained from Sigma. Annexin V-FITC/PI apoptosis detection kit was procured from BD Biosciences (Cat.No. 556547). Human lung cancer cell line A549 was procured from National Centre for Cell Science (NCCS). A549 cells were preserved in cryopreservation medium, which contains 10% DMSO, 30% Fetal Bovine Serum and 60% DMEM.

Instrumentation:

Melting points was measured in open capillaries and were uncorrected. The purity of all the newly synthesized compounds were checked by TLC with silica gel glass plates and the spots were detected by exposure to iodine and viewed under UV light at λ 254 nm. The infrared (FT-IR) spectra were recorded using Perkin Elmer Spectrum one FT-IR instrument at a resolution of 1.0cm^{-1} and in the range of $4000\text{-}450\text{cm}^{-1}$. Proton Nuclear Magnetic Resonance (^1H NMR) spectra were recorded in CDCl_3 as solvent on a Bruker AvanceTM III 500MHz NMR Spectrometer using Tetra Methyl Silane (TMS) as an internal standard. Chemical shifts (δ) are expressed in parts per million (ppm). Mass spectra for the newly synthesized compounds were obtained from the Q-TOF Mass Spectrometer (Micromass). ELISA well plate reader (Robonik India pvt Ltd.), Flow cytometer BD FACS VERSE (BD BioSciences) was used for in vitro anticancer studies.

Synthesis:

2-Methyl-5-nitroaniline (2)

51.1mL of o-toluidine (1) was added dropwise to 122.3mL of sulphuric acid cooled to ice cold condition with vigorous stirring. Mixture of 8.9mL of 65% nitric acid and 27.2mL of sulphuric acid was cooled to ice cold condition and added 16, 17 to the above mixture for a period of 2h. Finally, it was poured into crushed ice. It was made alkaline, with aqueous sodium hydroxide. The product formed was filtered and dried in air. Recrystallization was done using 50% ethanol.

N-(2-Methyl-5-nitrophenyl)guanidinium nitrate (3)

2-methyl-5-nitroaniline (2, 25g) in n-butanol (120mL) was taken. 65% aqueous nitric acid (10.5mL) was added dropwise. 50% aqueous solution of cyanamide (22.7mL) was added to the above mixture. The mixture was refluxed for 12h and subsequently it was cooled to 0°C . The precipitate formed was collected by filtration and washed with an ice

cooled solution of 50% ethanol and diethyl ether taken in equal quantity. The product was dried in air for further use.

cold condition for 12h. White crystals. mp 30-32°C.

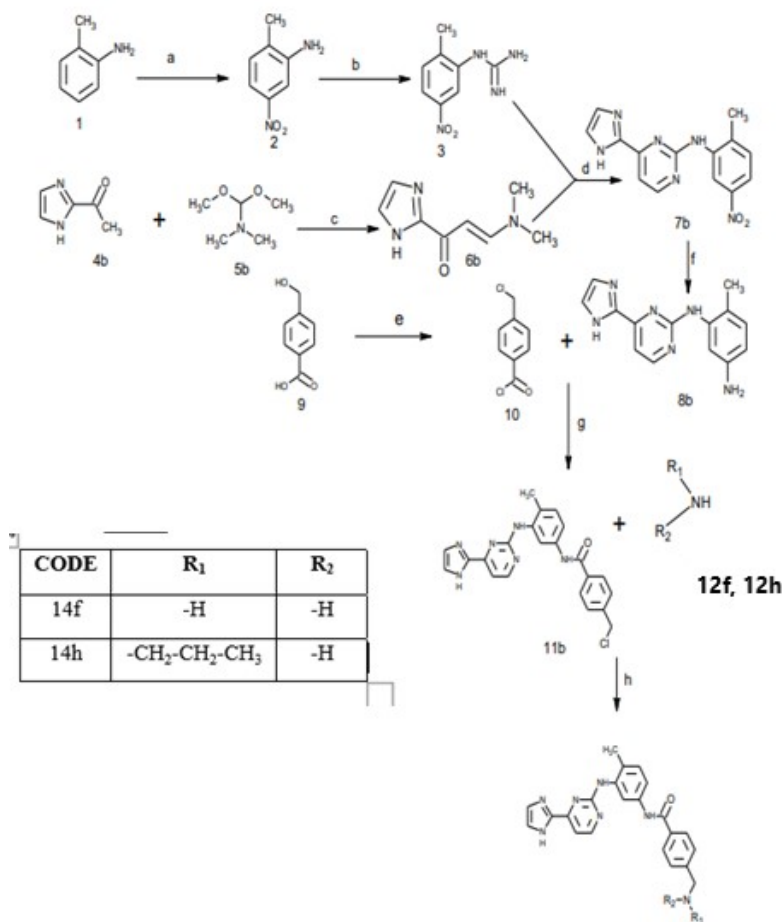
4-(Chloromethyl) benzoyl Chloride (10)

4-(hydroxyl methyl)-benzoic acid (9, 15.2g), dichloromethane (50mL), and thionyl chloride (50 mL) was added into a round bottomed flask and it was refluxed for 5h. The excess thionyl chloride and dichloromethane were removed. The residue was cooled to ice

Scheme:

3-Dimethylamino-1-(1H-imidazol-2-yl)prop-2-en-1-one (6b)

A mixture of 2-acetyl Imidazole (4b, 24.21g) and N, N-dimethylformamide dimethyl acetal (5, 34.4mL) were refluxed for 16h and then concentrated to get residue. Cyclohexane (100 mL) was added to the residue and it was cooled



Reagents and conditions: (a) H₂SO₄, HNO₃, Ice cold condition (b) 50% aqueous H₂NCN, HNO₃, n-butanol, 100 °C (c) 100 °C (d) NaOH, n-butanol, 100 °C (e) SOCl₂, CH₂Cl₂ (f) SnCl₂·2H₂O, HCl, Ice cold condition (g) THF, TEA, Ice cold condition, 3h (h) Reflux 3h

Scheme

Human Lung Cancer Cell Line

in ice. The precipitate formed was filtered and dried in air. Yellow solid. *mp* 84-86°C.

***N*-(2-methyl-5-nitrophenyl)-4-(1*H*-imidazol-2-yl)pyrimidin-2-amine (7b)**

To a mixture of 3-Dimethylamino-1-(1*H*-imidazol-2-yl)prop-2-en-1-one (6b, 26.96g) and *N*-(2-methyl-5-nitrophenyl)guanidinium nitrate (3, 51.40g) in *n*-butanol (200mL), sodium hydroxide (8.63g) was added in solid form and it was refluxed for 16h. After the completion of 16h it was cooled in ice. The precipitation formed was filtered. It was washed with methanol and diethyl ether. The product was dried in air for further use. Yellow solid. *mp* 199-201°C.

4-methyl-*N*-[4-(1*H*-imidazol-2-yl)pyrimidin-2-yl]benzene-1,3-diamine (8b)

Stannous chloride di hydrate (11.29 g in 30mL of hydrochloric acid) was cooled to 0 °C. *N*-(2-methyl-5-nitrophenyl)-4-(1*H*-imidazol-2-yl)pyrimidin-2-amine (7b, 3.69g) in portions was added to the above mixture and stirred vigorously for 6h. The mixture was poured into crushed ice and it was made alkaline using solid sodium hydroxide. Extracted three times with ethyl acetate (100mL). The combined organic phase was dried over anhydrous sodium sulfate and evaporated to dryness. Yellow solid. *mp* 145-147°C

4-(chloromethyl)-*N*-(3-[[4-(1*H*-imidazol-2-yl)pyrimidin-2-yl]amino]-4-ethylphenyl)benzamide(11b)

4-methyl-*N*-[4-(1*H*-pyrrol-2-yl)pyrimidin-2-yl]benzene-1,3-diamine (0.277g), Tetra hydro furan (5mL), and Triethylamine (0.29mL) were refluxed. The reaction mixture was cooled to 0°C and maintained for 10 min. 4-(chloromethyl)benzoyl chloride (0.217g) in Tetra Hydro Furan (2mL) was added dropwise to the above mixture within 10min. TLC of reaction mass indicated the absence of starting compound. After stirring the mixture at 0°C for 3h, 15mL of water was added dropwise. The resultant precipitate was

collected by filtration and washed with 100mL of water. The product was dried at 75-80°C. Light yellow crystals. *mp* 271-273°C

Compound 14f

4-[aminomethyl]-*N*-(3-[[4-(1*H*-imidazol-2-yl)pyrimidin-2-yl]amino]-4-methylphenyl)benzamide

4-(chloromethyl)-*N*-(3-[[4-(1*H*-imidazol-2-yl)pyrimidin-2-yl]amino]-4-methylphenyl)benzamide (0.429g) and ammonia(12f, 11.1mL) were added in a round bottomed flask and refluxed for 3h. The reaction mass was checked for the absence of compound (11b). The resultant mixture was cooled to room temperature and 10mL of water was added to it. The precipitate was collected by filtration and washed with 100mL of water. The product was dried at 75-80°C. Recrystallized using methanol. White solid. Yield 94.21%, Melting range 220-222°C; **FTIR (cm⁻¹)** 3456.09 (Ar N-H str), 3066.09 (Ar C-H str), 2948.10 (-C-H-str), 2790.01(N-H str), 1648.42 (amide -C=O str), 1578.98 (-C=C-, -C=N-ring str), 1181.66 (-C-C-str), 1081.77 (C-N str), 805.79 (N-H wag), 705.60 (C-H out of plane bending), 665.20 (N-H out of plane bend). **¹H NMR (CDCl₃)** δ 8.64 (m, 1H), 8.09 (s, 1H), 7.92 – 7.65 (m, 3H), 7.46 – 7.07 (m, 7H), 4.76 (s, 1H), 4.10 (m, 2H), 2.29 (s, 3H), 1.35 (s, 3H). **m/z [M⁺ +1]** 400.5 Peak and 382.4 Base Peak observed.

Compound 14h

4-[(propylamino)methyl]-*N*-(3-[[4-(1*H*-imidazol-2-yl)pyrimidin-2-yl]amino]-4-methylphenyl) benzamide

4-(chloromethyl)-*N*-(3-[[4-(1*H*-imidazol-2-yl)pyrimidin-2-yl]amino]-4-methylphenyl)benzamide (0.429g) and propylamine (12h, 11.1 mL) were added in a round bottomed flask and refluxed for 3h. The reaction mass was checked for the absence of compound (11b). The resultant mixture was cooled to room temperature and 10mL of water was added to it. The precipitate was collected by filtration and washed with 100mL of water. The product was dried at 75-80°C. Recrystallized using methanol [10,11]. White

powder. Yield 92.70%, Melting point 226-228°C. **FTIR (cm⁻¹)** 3430.48 (Ar N-H str), 3055.01 (Ar C-H str), 2878.57 (-C-H-str), 2797.23 (N-H str), 1648.42 (amide -C=O str), 1576.66 (-C=C-, -C=N- ring str), 747.66 (C-H out of plane bending), 1050.62 (C-N str), 809.16 (N-H wag), 611.96 (N-H out of plane bend). **¹H NMR (CDCl₃)** δ 8.64(m, 1H), 8.16 – 7.73 (m, 5H), 7.47 – 7.03 (m, 8H), 4.78 (m, 2H), 2.83 – 2.49 (m, 4H), 2.29 (s, 3H), 1.94 (m, 2H), 1.20 (s, 2H). **m/z** 442.5 (M⁺ +1) Peak, 440.2 (M⁺-1) Peak, 398.4 (Base Peak).

***In vitro* Anticancer Studies:**

Cytotoxic Activity

The cytotoxic potential of the synthesized compounds 14f and 14h was screened *in vitro* against Human Lung cancer cell line A549 according to procedures described in the literature. Sunitinib was used as standard drug. The results are summarized in **Table 1** Compound 14f and 14h showed a cytotoxic effect of 10.14% and 51.04% compared to the standard exhibiting 35.20% at the concentration of 25µM for 24h. At 48h compounds 14f and 14h showed 19.24% and 53.28% of inhibitory effect at 25 µM concentration. The IC₅₀ value was calculated using the obtained results.

Apoptosis Detection Assay

Human lung cancer cell A549 was treated with 25µM concentrations of synthesized compounds 14f, 14h and

standard, diluted in DMSO for 18h. After treatment, cells were washed with cold Phosphate Buffer Solution and then resuspended cells in 1X Binding Buffer (dilute 1 part of the 10X annexin V Binding Buffer to 9 parts of distilled water) at a concentration of 1×10⁶ cells/ml. One hundred micro liter (100µl) of the solution was transferred to a 5ml culture tube. Five micro liters (5µl) of FITC Annexin V and 5µl of Propidium Iodide were added. The cells were vortexed gently and incubated for 15min at room temperature (25°C) in the dark. After incubation, 400 µl of 1X Binding Buffer was added to each tube and analysis was carried out within 1h using flow cytometer.

Apoptosis Detection assay was used to elucidate the mode of cell death caused by the newly synthesized compounds 14f, 14h and standard drug sunitinib in Human lung cancer cell line (A549) after treatment with IC₅₀ concentration of 25µM for a period of 18h. The disruption of cell membrane phospholipid asymmetry, evidenced by Phosphatidyl Serine (PS) externalization, was examined by utilizing annexin V-FITC and propidium iodide assay and monitored via the flow cytometer protocol. The cell distributions in flow cytometric histograms are as follow: Cells in the lower left quadrant (Q3) represented live cells. Cells that are viable shows Annexin V-FITC and PI negative. The lower right quadrant (Q4) represented early apoptotic cells. Early apoptotic cells show Annexin V-FITC positive and PI negative. The upper right quadrant (Q2)

Table 1. Percentage of Scavenging Activity at 24h

Comp Code	5µM	25µM	50µM	75µM
14f	10.08	10.14	19.80	26.91
14h	42.08	51.04	54.08	59.20
Standard	26.08	35.20	44.48	59.20
Percentage of scavenging activity at 48h				
14f	28.28	19.24	26.77	30.67
14h	33.16	53.28	56.12	67.38
Standard	27.84	29.79	53.90	67.02

Human Lung Cancer Cell Line

represented late apoptotic cells. Cells that are in late apoptosis shows Annexin V-FITC and PI positive and the necrotic cells show PI positive only. The upper left quadrant (Q1) represents necrotic cells. The necrotic cells show PI positive only (Fig.1).

The addition of both early and late apoptotic cells (annexin V-FITC positives) was defined as the total percentage value of

apoptotic cells. When Human A549 lung cancer cells were treated with the newly synthesized compounds 14f, 14h and Standard drug sunitinib (25 μ M) for 18h, the total percentage of apoptotic cells increased up to 28.96%, 38.01% and 21.03% at 25 μ M respectively (Table.2). This indicates that the newly synthesized compounds 14f, 14h and Standard drug sunitinib was able to induce apoptosis of Human A549 lung cancer cells.

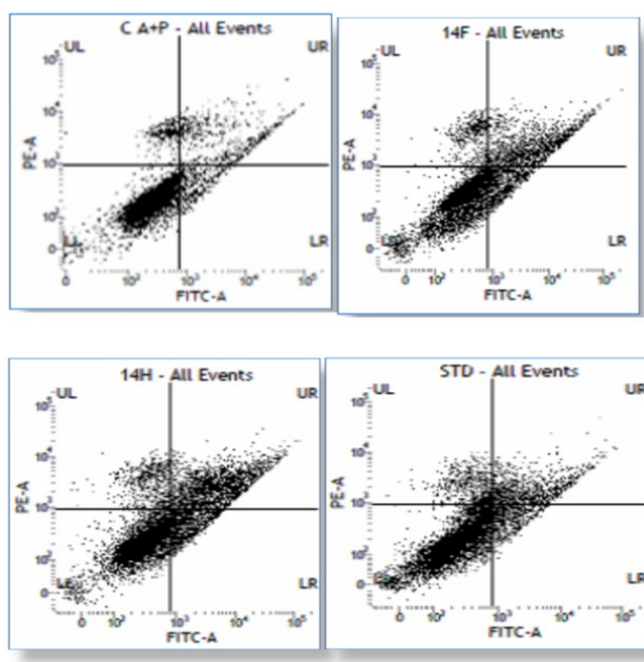


Fig 1. Apoptosis Detection Assay

Apoptosis Detection Assay - Flow cytometric analysis of the newly synthesized compounds 14f, 14h and Standard drug sunitinib in Human A549 lung cancer cells using the Annexin V-Fluorescein isothiocyanate / Propidium Iodide method. (i) Control group, (ii-iv) treatment with the newly synthesized compounds 14f, 14h and Standard drug sunitinib

Table 2. Total Percentage of Apoptotic Cells Exhibited by the Newly Synthesized Compounds at IC₅₀ Concentration

S. No.	Compound Code	Total Apoptotic Cells in % (at 25 μ M)
1	14f	28.96
2	14h	38.01
3	Standard	21.03

Human Lung Cancer Cell Line

Table 3. Percentage of Cells in each phase of Cell Cycle after Treatment with 25µM of the Newly Synthesized Compounds and Standard

Compound	P7 (G0/G1)	P8 (S)	P9 (G2)
Control	100	100	100
14f	25.14	257.13	176.57
14h	73.89	10.03	9.29
Standard	60.47	13.79	5.78

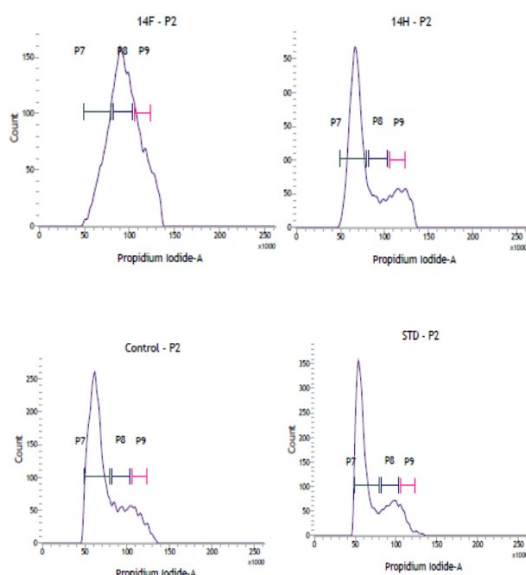


Fig 2. Graph Showing Result Generated for Cell Cycle Analysis using Flow Cytometer

Cell Cycle analysis

Changes in cell cycle due to the synthesized compounds 14f, 14h and standard were estimated using flow cytometry. Briefly, after treatment of cells with 25µM concentration of the synthesized compounds 14f, 14h and standard for 18h, cells were harvested and washed with 1X Phosphate Buffer Solution. The cells were treated with 75µg of RNase for 30 minutes at room temperature. After treatment, cells were washed with 1X Phosphate Buffer Solution.

The cells were then incubated with propidium iodide (1mg/mL) for 15 minutes. After 15 minutes, the cells were washed and resuspended in 1X Phosphate Buffer Solution. Cell cycle analysis was estimated in flow cytometry. From the flow cytometry data, the control cells in each phase of the cell cycle were considered as 100% and changes in treated cells were calculated with respect to control cells[12-18].

Further, cell cycle analysis was carried on BD FACS VERSE (BD BioSciences) flow cytometer using propidium iodide. Human A549 lung cancer cell lines was treated with 14f, 14h and standard drug sunitinib at a concentration of 25µM for a period of 15min (Fig. 2).

Treatment of newly synthesized compounds with 14h and standard drug sunitinib at 25µM showed increase in fraction of cells 73.89% and 60.47% respectively arrested in G1 phase from control (50.23%). The DNA contents of the live population (control) were 50.23%, 11.99% and 7.81% for untreated cells at 25µM, respectively for G0/G1, S and G2/M phase. Human A549 cell line treated with compound 14h showed 73.89%, 10.03% and 9.29%, standard drug sunitinib showed 60.47%, 13.79% and 5.78% respectively for G0/G1, S and G2/M phase. compound 14f showed 25.14%, 257.13% and 176.57% respectively for G0/G1, S and G2/M phase (**Table 3**). Taken together, the results of apoptosis and cell cycle analysis suggest that the compound 14h delay the cell cycle progression by arresting the cell cycle at G1phase and Compound 14f at S phase.

Human Lung Cancer Cell Line

Conclusion

The designed compounds were synthesized using chemicals of synthetic grade and obtained a good yield. The spectral data of the synthesized compounds were consistent with the assigned structure. *In vitro* anticancer activity revealed that 14h showed more potent anticancer activity as compared to the standard drug Sunitinib. This compound exhibited apoptosis thus, arresting the cell cycle at G0/G1 phase itself. To conclude, the above findings clearly demonstrated that the compound 14h may serve as good anticancer agent for further development.

Acknowledgement

The authors are grateful to the Founder Chairperson Dr. K. Veeramani of Periyar College of Pharmaceutical Sciences, Trichy-21, for extending necessary facilities to carry out this Research.

References

1. Elferink LA, Resto VA. (2011) Receptor Tyrosine Kinase - Targeted Therapies for Head and Neck Cancer. *Journal of Signal Transduction*, 2011: 01-11. 7.
2. Paul MK, Mukhopadhyay AK. (2004) Tyrosine Kinase - Role and significance in Cancer. *International Journal of Medical Sciences*, 01(02): 101-115.
3. Ferlay J, Ervik M, Lam F, Colombet M, Mery L, Piñeros M, et al. *Global Cancer Observatory: Cancer Today*. Lyon: International Agency for Research on Cancer; 2020 (<https://gco.iarc.fr/today>, accessed February 2021).
4. McMahon G. (2000). VEGF Receptor Signaling in Tumor Angiogenesis. *The Oncologist*, 5: 03-10.
5. Edon Vitaku, David T. Smith, and Jon T. Njardarson. (2014) Analysis of the Structural Diversity, Substitution Patterns, and Frequency of Nitrogen Heterocycles among U.S. FDA Approved Pharmaceuticals. *Journal of Medicinal Chemistry*, 57 (24): 10257-10274.
6. Joseph SM, Dhanaraj CJ, Joseph J, Joseyphus RS. (2017) Synthesis, Spectral Characterization and Anticancer Studies of Some Metal (II) Complexes Derived from Imidazole-2-carboxaldehyde with 2-Amino-3-carboxyethyl-4, 5- dimethylthiophene. *Oriental Journal of Chemistry*, 33(3):1477-1482.
7. Rajendran SS, Geetha G, Venkatanarayanan R and Santhi N. (2017). Synthesis, characterization and in-vitro anticancer evaluation of novel benzo[d]imidazole derivatives. *International Journal of Pharmaceutical Sciences and Research*, 8(7): 3014-3024.
8. Burungale SD and Bhitre MJ. (2013) Synthesis of 2, 4, 5- Triphenyl imidazole derivatives and biological evaluation for their Antibacterial and Anti-inflammatory activity. *International Journal of Pharmaceutical Sciences and Research*, 4(10): 4051-4057.
9. Gyanendra Kumar Sharma, Suresh Kumar and Devender Pathak et al. (2010). Synthesis, antibacterial and anticancer activities of some novel imidazoles. *Der Pharmacia Lettre*, 2(2): 223-230.
10. Yi-Feng Liu, Cui-Ling Wang, Ya-Jun Bai, Ning Han, Jun-Ping Jiao, and Xiao-Li Qi. (2008). A Facile Total Synthesis of Imatinib Base and Its Analogues. *Organic Process Research & Development*, 12: 490-495.
11. Anshu Chaudhary, Pramod Kumar Sharma, Prabhakar Verma, Rupesh Dudhe. (2011). Synthesis of Novel Pyrimidine Derivative and its Biological Evaluation, *Analele University din/ Bucuresti – Chimie (serie nouă)*, 20 (2): 123-140.
12. Li H, Zhang X, Wang W. (2017). Anticancer activity of 5,7-Dimethoxyflavone against Liver cancer cell HEPG2 involves apoptosis, ROS generation and Cell cycle arrest. *African Journal of Traditional Complementary Alternative Medicine*, 14(4): 213-220.
13. Daniel Sypniewski, Szkaradek N, Loch T, Marona H. Contribution of reactive oxygen species to the anticancer activity of aminoalkanol derivatives of xanthone. *Invest New Drugs*; 2017.

14. Kwan YP, Saito T, Ibrahim D, Al-Hassan F M S, Oon CE, Chen Y, Sasidharan S. (2016) Evaluation of the cytotoxicity, cell-cycle arrest and apoptotic induction by *Euphorbia hirta* in MCF-7 breast cancer cells. *Pharmaceutical Biology*, 54(7): 1223-1236.
15. Monika Chauhan, Gaurav Joshi, Harveen Kler, Archana Kashyap, Raj Kumar.(2016) Dual inhibitors of epidermal growth factor receptor and topoisomerase II α derived from a quinoline scaffold. *RSC Advances*, 6: 77717-77734.
16. Ji Hong Lim, Yoon Mi Lee, Sa Ra Park, Da Hye Kim and Beong ou lim. (2014). Anticancer activity of Hispidin via Reactive Oxygen Species-mediated Apoptosis in colon cancer cells. *Anticancer Research*, 34: 4087-4094.
17. Ahamad MS, Siddiqui S, Jafri A, Ahmad S, Afzal M, Arshad Md. (2014). Induction of Apoptosis and antiproliferative activity of Naringenin in Human Epidermoid Carcinoma cell through ROS generation and Cell cycle arrest. *PLOS ONE*, 9(10): 01- 08.

Preparation and characterization of oral fast dissolving film of hydralazine HCL

M. Sudhir *, V. Sruthi, T.Venkata Siva Reddy, Ch. Naveena,
B. Pamula Reddy and Sk. A. Rahaman

¹Department of Pharmaceutics, Nirmala College of Pharmacy, Atmakuru, Guntur-522503,
Andhra Pradesh, India

*Corresponding Author: E-Mail ID: sudhir.spark@gmail.com

Abstract

Hydralazine is a BCS class III antihypertensive drug. The main aim of this study is to improve the dissolution and thus the bio availability of hydralazine by preparing fast dissolving oral films of Hydralazine HCl. The objective of this study is to enhance therapeutic efficacy, compliance & convenience of geriatric and pediatric patients by preparing hydralazine fast dissolving oral films by solvent casting method. The hydralazine films were prepared by using different film forming polymers. Various grades and concentrations of hydroxypropyl methylcellulose (HPMC) E 3 and E 15, methyl cellulose (MC), sodium carboxy methyl cellulose (CMC), varying the surfactants like Sodium Lauryl Sulfate (SLS) and Poly vinyl pyrrolidone (PVP) are used. Morphological studies, Thickness uniformity, Folding endurance, Drug content uniformity test, In vitro dissolution studies, Weight variation tests were performed for evaluation of films. The film formulation F12 having HPMC E 15, PVP and Glycerol showing the greatest dissolution and bio availability and could give quick onset of action upon administration when compared to other formulations.

Keywords: Hydralazine Hcl, oral fast dissolving films, hydroxypropyl methylcellulose, sodium carboxy methyl cellulose, solvent casting method.

Introduction

Hydralazine is a BCS class III anti hypertensive drug. It is a hydralazine

derivative vasodilator used in the treatment of diseases like hypertension and heart failure. It interferes with calcium transport may be by preventing influx and efflux of calcium into cells, resulting that to relax arteriolar smooth muscle and lowers the pressure of blood. This results in decreased vascular resistance leads to increased heart rate, stroke volume, and cardiac output(1-3). Among all the drug delivery routes, the oral route is the most preferred route due to its ease of administration, non-invasiveness, adaptability, patient compliance and acceptability (4) Oral Solid dosage forms also have impervious difficulties in patients especially for geriatric and pediatric patients. Dysphasia is most common among all age group patients(5). Research and development in the oral drug delivery systems has led to transition of dosage forms from simple conventional tablets/capsules to modified release tablets or capsules to oral disintegrating tablet (ODT) to wafer to oral Dissolving Films. Many pharmaceutical firms have directed their research activity in reformulating existing drugs into new dosage forms like films. Fast dissolving oral films constitute an innovative dosage form that overcome the swallowing problem and provides speedy onset of action.

A fast-dissolving oral film drug delivery system is a film containing active pharmaceutical ingredient and hydrophilic polymers that rapidly dissolves or disintegrates in the saliva, with an in-vitro disintegration time of approximately 30 seconds without the need of water or chewing(6).

Basically the FDOFs can be considered as an ultra-thin postage stamp size strip contains active pharmaceutical ingredient and other excipients. The introduction of FDOFs in market was accompanied by educating the mass about the proper way to administer the product like giving instructions “do not swallow” or “do not chew” In this present study, the hydralazine Hcl oral films were prepared by solvent casting technique. The main advantages of this technique are greater uniformity of thickness, Greater film clarity, more flexibility, and better physical properties than other methods like hot melt and solid dispersion extrusion methods(7).

Materials and Methodology

Materials

In this present study, the hydralazine Hcl films were prepared by solvent casting technique. hydralazine hcl was purchased from aurobindo pharma and bio adhesive hydrophilic polymers like Hydroxyl propyl methyl cellulose (HPMC) E 3 and E 15 was purchased from Loba chemic pvt. Ltd, Mumbai, Yarrow chem products, methyl cellulose (MC), sodium carboxy methyl cellulose (CMC) from Merck specialitiespvt.Ltd, varying the surfactants like Sodium Lauryl Sulfate (SLS), Poly vinyl pyrrolidone(PVP) and other ingredients like SLS, PVP, Citric acid, mannitol, flavouring , colouring agents and distilled water were used in the formulation of films.

Methods

Preformulation Studies: These studies may be described as a stage of development during which the physicochemical and biotherapeutical properties of a drug substance are characterized. It is an essential step in the drug development. Pre-formulation studies are an investigation of physical and chemical properties of the drug substances alone and combined with excipients like colour, form,

melting point, and solubility studies, micrometric properties, compatibility studies, analytical studies etc. The information produced during this phase is used for making critical decisions in subsequent stages of development.(8)

The API was Tested for the Following Properties

- Organoleptic Properties
- Melting point
- Solubility
- Drug – Excipients compatibility studies

Organoleptic Properties: The drug sample was viewed under the compound microscope for the determination of drug morphology by using the black and white backgrounds. Then the results were compared with the official books and United States Pharmacopoeia.

Melting Point: Melting point of hydralazine was determined by using melting point apparatus.

Solubility: According to the Indian Pharmacopoeia the drug solubility was studied in different solvents (aqueous and organic).The drug solubility was checked in methanol, PEG, water. The drug shows maximum solubility in methanol and it is partially soluble in water.

Calibration Curve of Hydralazine HCL in Artificial Saliva Buffer

Preparation of Artificial Saliva Buffer: 0.844 gm of NaCl, 1.2 gm of KCl, 0.93 gm of CaCl₂, 0.11 gm of MgCl, 0.342 gm of KPO₄ were weighed and added one by one to 500 ml of distilled water and then the volume was made up to 1000 ml by using water then the pH was adjusted to PH 5.8 with 0.1N hydrochloric acid.(9)

Preparation of Stock Solution: 10mg of HYDRALAZINE HCL was dissolved in 10ml of pH 5.8 Artificial saliva buffer (1000µg/ml). 1ml of this solution was taken in 100 ml volumetric flask, and made up to volume with pH 5.8 Artificial saliva buffer.

Preparation of Standard Solution:

The above solution was subsequently diluted with pH 5.8 Artificial saliva buffer to obtain series of dilutions containing 10, 12, 14, 16, 18, 20 µg/ml of HYDRALAZINE HCL. The absorbance of the above dilutions was measured at 235nm by using UV- Spectrophotometer taking pH 5.8 artificial saliva buffer as blank. Then a graph was plotted by taking concentration on X-axis and absorbance on Y-axis which gives a straight line.

Manufacturing Methods

Preparation of Hydralazine Oral Fast Dissolving Films by Solvent Casting Method

- Oral dissolving films are formulated by using the solvent casting method, Drug (HydralazineHcl) was dissolved in sufficient amount of methanol.
- Then the polymers (HPMC E 3, E 15) were completely dissolved in suitable amount of hot water.
- Other ingredients like SLS, PVP, Citric acid, mannitol, flavouring and colouring agents are added one by one in a test tube containing distilled water.
- These three solutions were mixed vigorously and finally this solution was casted on a Petri dish and dried in hot air oven at 50°C for 4 hours. The films were carefully removed from Petri dish, checked for any imperfections. The samples were stored in the desiccators for further analysis(10)
- The Formulation of HYDRALAZINE HCL Oral Fast Dissolving Films was given in Table 1.

Evaluation Oral Fast Dissolving Films

- Morphological studies
- Thickness uniformity
- Folding endurance
- Drug content uniformity test
- Invitro dissolution studies

- Weight variation
- Disintegration time

Morphological Studies: A visual inspection for physical appearance of films and evaluation of texture was done by feel and touch(11)

Thickness Uniformity: All the batches were evaluated for thickness by using calibrated vernier calipers with a least count of 0.01mm. The film was placed in between anvil and pressor foot of thickness gauge and the reading on the dial was noted down. The thickness was measured at different spots of three randomly selected films of each formulation. Calculate the average thickness of film. Uniform thickness of film is essential as it is directly related to accuracy of dose distribution in the film(12). The results were given the Table 2.

Folding Endurance: Folding endurance is a procedure to estimate the mechanical properties of a film and it also gives an indication of brittleness of film. The folding endurance was measured manually for the prepared films to determine the flexibility of films. A strip of film of specific size (1*1 cm) was cut and repeatedly folded at the same place till it breaks. The film was folded at the same place until the film breaks(13). The results were given the Table 2.

Drug Content Uniformity Test: One cm² film was taken in a 100 ml volumetric flask and dissolved in 5 ml of artificial saliva buffer and then final volume was made up with artificial saliva buffer. Samples were suitably diluted with artificial saliva and the absorbance was measured at 228 nm (14). The results were given the Table 2.

Disintegration Time: Disintegration time of film is the time required by oral film to start breaking when brought in contact with water or saliva. The disintegration time depends upon the composition of the films. Generally, it ranges from 5-30 seconds. There are no official guidelines to determine the disintegration time of oral films. One of the methods is dipping the film in 25 ml water or saliva in a beaker. The beaker should be

shaken gently and the disintegration time was noted(15). The results were given the Table 2.

In Vitro Dissolution Studies

Take 500 ml of artificial saliva solution as dissolution medium to perform in vitro dissolution studies in modified type 5 dissolution apparatus. A temperature of 37°C and 25 rpm was used. Each film with a dimension of appropriate size equivalent to 30 mg of HydralazineHCl was placed on a watch glass covered with nylon wire mesh. The watch glass was then dropped into a dissolution flask. 5 ml samples were withdrawn at 1,2,3,4,5,10, 20, 30 min time intervals and every time replaced with 5 ml of fresh dissolution medium. The samples were analyzed by measuring absorbance at 228 nm (16).

Results and Discussion

Active Pharmaceutical Ingredient (API) Characterization:

Organoleptic Evaluation: These are preliminary studies of any drug substance which is useful in identification of specific material. Following physico-chemical properties of API were studied. White powder having melting point 210-220 °C and Freely soluble in water and methanol (17).

Calibration Curve of Hydralazine HCl in pH 5.8 Artificial Saliva Buffer by using UV - Visible Spectrophotometer: The calibration was used to determine the amount of HydralazineHCl in unknown solution. The series of dilutions containing 10, 12, 14, 16, 18, 20 µg/ml of Hydralazine HCl were analyzed at

Table 1. Formulation of Hydralazine HCl Oral Fast Dissolving Films

Compound	F1 (HPMC E3)	F2 (HPMC E6)	F3 (HPMC E15)	F4 (HPMC E3)	F5 (HPMC E5)	F6 (HPMC E15)	F7 (HPMC E3)	F8 (HPMC E6)	F9 (HPMC E3)	F10 (HPMC E3)	F11 (HPMC E6)	F12 (HPMC E15)
Drug (mg)	25	25	25	25	25	25	25	25	25	25	25	25
Methanol (gm)	2.5	2.5	2.5	2.5	2.5	2.5	2.5	2.5	2.5	2.5	2.5	2.5
Polymer (mg)	300	300	300	300	300	300	300	300	300	300	300	300
(SLS) (mg)	-	-	-	25	25	25	25	25	25	-	-	-
(PVP) (mg)	2	2	2	-	-	-	-	-	-	2	2	2
PEG (mg)	25	25	25	25	25	25	-	-	-	-	-	-
Glycerol (mg)	-	-	-	-	-	-	25	25	25	25	25	25
Water (gm)	1.7	1.7	1.7	1.7	1.7	1.7	1.7	1.7	1.7	1.7	1.7	1.7
Total	452	452	452	452	452	452	452	452	452	452	452	452

Hydralazine HCL

Table 2. Results of OFDFs of Hydralazine HCl Containing Evaluating Parameters as Drug Content, Weight Variation, Thickness Uniformity, Disintegrating Time, Folding Endurance

Formulation	Evaluation Parameters				
	Drug Content (1*1 cm)(mg)	Weight Variation (gm)	Thickness Uniformity (µm)	Disintegration Time (sec)	Folding Endurance
F1	15.0	0.21±0.01414	56.5±0.70711	5 sec	120
F2	9.3	0.15±0.0070	50.5±0.70711	3.1 sec	125
F3	6.4	0.19±0.01414	54±1.41421	2.2 sec	115
F4	19.2	0.13±±0.02828	52.2±0.70711	5.1 sec	95
F5	19.3	0.25±0.021213	51.5±0.70711	6.2 sec	123
F6	13.3	0.26±0.01414	56.1±2.0506	1.2 sec	122
F7	8.9	0.26±0.01414	53.5±2.969	5 sec	58
F8	15.9	0.28±0.007071	56±1.41421	2.5 sec	140
F9	6.1	0.275±0.042426	59.5±0.70711	12 sec	99
F10	15.8	0.16±0.02828	57±1.41421	1.6 sec	85
F11	18.1	0.26±0.01414	53±2.820	3.5 sec	125
F12	19.5	0.285±0.0212	51±1.41421	2.9 sec	130

absorbance of 235 nm. The absorbance values of the various concentrations of Hydralazine Hcl pure drug in pH 5.8 Artificial saliva were checked. Calibration curve of Hydralazine Hcl in pH 5.8 artificial saliva buffer was plotted between the absorbance and concentration of the HydralazineHCl. The correlation coefficient (r^2) value is about 0.994 indicates that the hydralazine follows Beer's Lambert's Law.

Analytical Methods

Spectrophotometric Method: A number of methods are reported in the literature for the Estimation of Hydralazine HCL (IP). By using pH 5.8 artificial saliva buffer as a dissolution medium to calibrate Hydralazine HCL drug.

In Vitro Dissolution Studies:

Take 500 ml of artificial saliva solution as dissolution medium to perform in vitro dissolution studies in modified type 5 dissolution apparatus. A temperature of 37°C

and 25 rpm was used. Each film with a dimension of appropriate size equivalent to 30 mg of HydralazineHCl was placed on a watch glass covered with nylon wire mesh. The watch glass was then dropped into a dissolution flask. 5 ml samples were withdrawn at 1,2,3,4,5,10, 20, 30 min time intervals and every time replaced with 5 ml of fresh dissolution medium. The samples were analyzed by measuring absorbance at 228 nm (16).

Analytical Methods

Spectrophotometric Method: A number of methods are reported in the literature for the Estimation of Hydralazine HCL (IP). By using pH 5.8 artificial saliva buffer as a dissolution medium to calibrate Hydralazine HCL drug.

Evaluation Oral Fast Dissolving Films:

Morphological Characters: Prepared Hydralazine HCl fast dissolving films were transparent and colorless, all the films were smooth in texture and glossy in appearance. The results were shown in (Table 2).

Drug Content Uniformity Test: Films of 1*1 cm were cut from different regions and the drug content in the films was evaluated and the values were found in between 6 to 20 mg. The results were shown in (Table 2).

Weight Variation: The film was cut from different regions and the weight variation was determined and the values were found in between 0.24 to 0.27 g. The results were shown in (Table 2).

Thickness Uniformity: The thickness was measured at 3 different regions of film by using vernier calipers and the values were found in between 50 to 60 µm. The results were shown in (Table 2).

Disintegration Time: The film was cut in to 1*1 mm and placed it in petri dish, now add a drop of water at the center of the film measure the time taken to disintegrate and noted. In the same manner repeat it same with the buffer. The disintegration time values were found in between 1.2 to 12 sec. The results were shown in (Table 2).

Folding Endurance: The folding endurance was measured at different regions

of film by repeated folding at 180° angle of the plane at the same place till the film breaks. The number of times the film was folded without breaking was computed as the folding endurance value. The folding endurance of films was measured at different regions and the values were found in between 96 to 147. The results were shown in (Table 2).

Dissolution Rate Studies: The in-vitro dissolution studies were conducted using pH 5.8 buffer as dissolution medium. The percent of Hydralazine HCL dissolved at the various time intervals were calculated and plotted against time. The graphical plots of percentage of Hydralazine HCL dissolved versus time were placed in (Figure. 1).

The cumulative % of hydralazine released at the end of 5min is 98.87 for F12 formulation. Complete drug release from F12 is significantly higher i.e., about 98% of drug was released when compared to other formulations.

In f12 formulation, HPMC E15, Glycerol, PVP were added to the formulation gave superior dissolution properties when compared to other formulations.

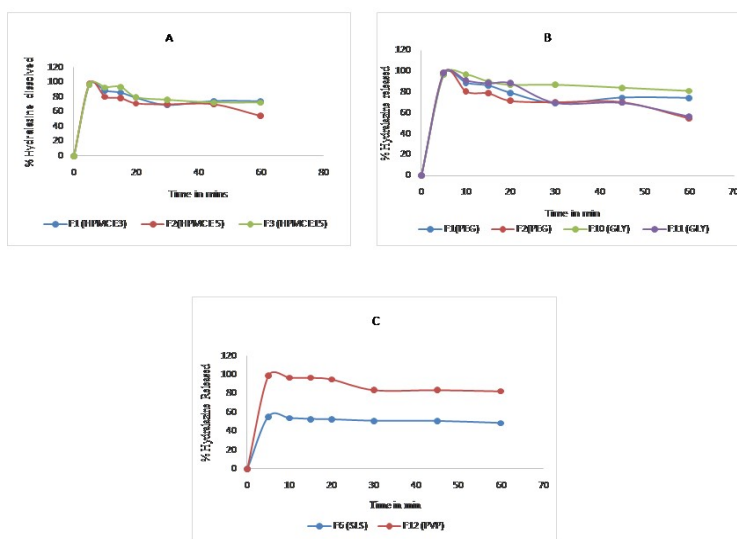


Fig 1. Comparative *In Vitro* Drug Release Profile of Hydralazine from Films A. Effect of Polymers B. HPMC E 15 with Plasticizers C. HPMC E 15 with Surfactants

Hydralazine HCL

Conclusion

The current investigation established an effective and easy method to formulate hydralazine HCl films to increase its water solubility and also its dissolution. OFDF were prepared by solvent casting method through OFDF proved to have the best results in terms of solubility and dissolution. The formulation F12 containing HPMC E 15 with glycerol and PVP gave superior dissolution properties when compared to other formulations. The rise in dissolution efficiency leads to improve bio availability. It would also facilitate quick onset of action after oral administration of films hence improving patient compliance. This can serve as a novel approach for the treatment of cardiovascular diseases.

References

1. Paul Saini, Anoopkumar. (2012) .Fast Disintegrating Oral Films: A Recent Trend of Drug Delivery, *International journal of Drug Development & Research*.
2. M.D. Nehal Siddiqui, Garima Garg and Pramod Kumar Sharma.(2011).A Short Review on "A Novel Approach in Oral Fast Dissolving Drug Delivery System and Their Patents."Biological Research.
3. Reddy LH and Ghosh BR .(2002). Fast dissolving drug delivery systems. A review of literature. *Indian J Pharm Sci*.
4. Suresh B, Halloran D and James L.(2012).Quick dissolving films: A novel approach to drug delivery. *Drug Dev Tech*.
5. Apoorva Mahajan, Neha Chhabra, Geeta Aggarwal .(2011). Formulation and Characterization of Fast Dissolving Buccal Films. A Review.Scholars Research library.
6. Indian Pharmacopoeia – 1996, volume II.
7. Raymond craowe, Paul J. sheskey. "Hand Book of Pharmaceutical Excipients".
8. Jayasravani B, Sai Kishore V, Lakshmana Rao R.(2014).Design and Development of Fast Dissolving Films of Diltiazem Hydrochloride. *Inventi Rapid: Pharm Tech*.
9. Vaishali Y. Londhe* and Kashmira B. Umalkar.(2012). "Formulation Development and Evaluation of Fast Dissolving Film of Telmisartan" *Indian J Pharm Sci*.
10. Chen M, Tirol G, Schmitt R, Chien C and DualehA.(2006). "Film forming polymers in fast dissolve oral films", *AAPS Annual meetings-posters and papers*.
11. K.Maheswari.(2014). "Development And Evaluation Of Mouth Dissolving Films Of Amlodipine Besylate For Enhanced Therapeutic Efficiency" *Journal of Pharmaceutics*.
12. Anoop Kumar. (2013). "HPMC/CMC Based Fast Dissolvable Oral Films of an Anxiolytic: In Vitro Drug Release and Texture Analysis" *International Journal of Drug Delivery*.
13. Amal S. M. Abu El-Enin."Preparation And Evaluation Of Fast Dissolving Oral Films Containing Metoclopramide Hydrochloride, *World Journal Of Pharmacy And Pharmaceutical Sciences*.
14. Buchi N. Nalluri*, B. Sravani. (2013). "Development and Evaluation of Mouth Dissolving Films of Sumatriptan Succinate for Better Therapeutic Efficacy" *Journal of Applied Pharmaceutical Science*.
15. Ravi Garala."Formulation And Evaluation Of Fast Dissolving Film Of Cyproheptadine Hydrochloride, *International Journal Of Pharmaceutical Research*.
16. Pratik Kumar, Joshi Harsha Patel.(2012). "Formulation Development And Evaluation Of Mouth Dissolving Film Of Domperidone, *J Pharm Bioallied Sci*.
17. Patel JG. (2012). "Formulation and Evaluation of Mouth Dissolving Film of Domperidone", *International Journal for Pharmaceutical Scholars (IJPRS)*, Researched Article.
18. Mashru RC, Sutariya VB, Sankalia MG and Parikh PP. (2005). "Development and

evaluation of fast dissolving film of salbutamol sulphate". *Drug Dev Ind Pharm*.

19. M Koland, VP Sandeep, NR Charyulu. (2010). Fast Dissolving Sublingual Films of Ondansetron Hydrochloride: Effect of Additives on Invitro Drug Release and mucosal Permeation" *Eur J Pharm Biopharm*.

20. Ali S and Quadir A. (2007). "High molecular weight povidone based films for fast dissolving drug delivery applications". *Drug Del Tech*.

21. Pallavi Patil, S. K. Shrivastava. (2014). "Fast Dissolving Films: An Innovative Drug Delivery System" *IJSR*.

Design and development of itraconazole loaded nanosponges for topical drug delivery

Swalin Parija* and V. Sai Kishore

¹Institute of Pharmacy & Technology, Salipur, Cuttack, Odisha-754202

²Department of Pharmaceutics, Bapatla college of Pharmacy, Bapatla-522101

*Corresponding Author: E-mail Id: Swalinpharma@gmail.com

Abstract

The aim of present research work is to develop a topical gel formulation of Itraconazole loaded nanosponges to increase the solubility, permeability, stability and to control the Itraconazole release for a prolonged period. Itraconazole loaded nanosponges was prepared by cross-linking different concentrations of β -Cyclodextrin with carbonate bonds of di phenyl carbonate in different proportions, which are porous as well as nanosized. Drug was incorporated by solvent evaporation method by dissolving the drug in various solvents like ethanol, acetone and chloroform. The prepared nanosponges were incorporated into carbopol gel. From the encapsulation efficiency of the drug loaded nanosponges formulations, it was observed that as the crosslinking ratio increased the encapsulation efficiency was found to be enhanced. It is also found that the encapsulation efficiency of drug loaded nanosponges were influenced by the solvent used for drug loading by solvent evaporation technique. Based on the drug encapsulation efficiency, drug content and extent of sustained nature, the gel prepared with β -Cyclodextrin and crosslinking agent in 1:1 ratio, chloroform as a solvent and carbopol as a gelling agent (IF12 formulation) was concluded to be the best formulation. All the formulations followed zero order release kinetics and mechanism of drug release was governed by Peppas model. The diffusion exponential coefficient(n) values were found to be in between 0.9402 to 1.1864 indicating non fickian diffusion mechanism.

Keywords: Itraconazole, β -cyclodextrin, nanosponges, diffusion rate

Introduction

Nanosponges are the progression in nano technology, which are the prominent answers for the various formulation challenges like low aqueous solubility, controlled release and targeted release. As compared to nano particles these are less prone to bursting and releases the drug in a controlled and predictable manner throughout the intended period of application or administration (1). Nanosponges are beneficial for the passive targeting of drugs to skin, there by accomplishing major benefits such as reduction of total dose, retention of dosage form on the skin for prolonged period. Nanosponge loaded topical dosage forms can act as local depot for sustained drug release as well as rate- limiting membrane barrier for inflection of systemic absorption and thus overcoming the limitations of topical formulations. They are non- irritating, non-mutagenic, non- allergenic and non- toxic. Itraconazole is an imidazole derivative and used for the treatment of local and systemic fungal infections. It is a BCS Class II drug having very low solubility and high permeability. The oral use of Itraconazole is not much recommended as it has many side effects.

Most of these infections spread only in the skin layers but upon prolonged time they may be converted to systemic infections which may be mortal. Oral administration of Itraconazole is not convenient due to its severe side effects and its short half-life (3–6 h) that requires frequent dosing(2). Itraconazole is a BCS Class II drug that has a dissolution rate limited poor bioavailability so it needs to be incorporated into a proper vehicle to have right

levels of topical absorption. The conventional topical Itraconazole formulations release the drug for a shorter period at high quantities which causes the adverse effects like stinging, zerythema, edema, vesicat, edema, vesication, desquamation, pruritus and urticaria due to the toxicity on the epithelial cells of the skin. The conventional topical dosage cannot reside at the site of application for longer times and does not release the drug in sustained manner.

Various methods are available to sustain the release of the drug. Among them the nanosponges have some unique advantages, which are three dimensional sponges like nanostructure encapsulating the drug. The nanostructure have potential for decreased skin irritation and stabilization of sensitive activities. Moreover nanosponges have good penetration into stratum corneum by overcoming the skin barrier effect and maintaining the good physical and chemical stability(3).

Materials and Methods

Itraconazole was the generous gift from Aurobindo Pharma Ltd, Hyderabad.

Carbapol 934 P was procured from SD Fine chemicals Ltd, Mumbai. β - cyclodextrin and Di phenyl carbonate were purchased from Sigma Aldrich (Milan, Italy). All other ingredients used were of analytical grade shows Table 1.

Synthesis of β - cyclodextrin nanosponges: β - cyclodextrin based nanosponges was prepared using Di phenyl carbonate as a cross-linker. Nanosponges were prepared using different ratios of β - cyclodextrin and Di phenyl carbonate [1:0.25, 1:0.5, 1:0.75 and 1:1]. Finely homogenized anhydrous β - cyclodextrin and Di phenyl carbonate were placed in a 100 ml conical flask. The system was gradually heated to 100 °C under magnetic stirring, and left to react for 5 h. During the reaction crystals of phenol appeared at the neck of the flask. The reaction mixture was left to cool and product obtained was broken up roughly. The solid was repeatedly washed with distilled water to remove unreacted β - cyclodextrin and then with acetone, to remove the unreacted Di phenyl carbonate and the phenol present as by-product of the reaction. After purification, nanosponges were stored at 25 °C until further use(4).

Table 1. Composition of Itraconazole loaded nanosponges using different solvents

S. No	Batch code	Polymer : cross linking agent (mg)	Drug (mg)	Solvent
1	ILNS1	4000:1000	4000	Ethanol
2	ILNS2	4000:2000	4000	Ethanol
3	ILNS3	4000:3000	4000	Ethanol
4	ILNS4	4000:4000	4000	Ethanol
5	ILNS5	4000:1000	4000	Acetone
6	ILNS6	4000:2000	4000	Acetone
7	ILNS7	4000:3000	4000	Acetone
8	ILNS8	4000:4000	4000	Acetone
9	ILNS9	4000:1000	4000	Chloroform
10	ILNS10	4000:2000	4000	Chloroform
11	ILNS11	4000:3000	4000	Chloroform
12	ILNS12	4000:4000	4000	Chloroform

Preparation of Itraconazole loaded nanosponges: The Itraconazole loading into β -cyclodextrin nanosponges was carried out by solvent evaporation technique. In this various solvents like chloroform, acetone and ethanol were used. In 100 ml of each solvent 4000 mg of Itraconazole was dissolved separately to form solutions. To the each solution, prepared nanosponges were added and triturated until the solvent evaporated. While triturating the clumps of nanosponges were segregated and absorbs the drug solubilised solvent. The solid dispersions were dried in an oven overnight (at 50 °C at atmospheric pressure) to remove any traces of solvents and were sieved through 60 # and used for further work(5).

Preparation of Itraconazole nanosuspension: The dried drug encapsulated nanosponges were collected and required quantities of drug equivalent nanosponges were transferred into 250ml volumetric flask containing 100ml methanol in order to remove the free unencapsulated drug by solubilising in the methanol. The drug encapsulated nanosponges were separated from the free drug by membrane filtration by using 0.22 μ membrane filter. The residual drug loaded nanosponges were collected and dispersed in distilled water by using ultra sonication to form a nanosuspension(6).

Formulation of carbopol gel containing Itraconazole loaded nanosponges: 500 mg of carbopol 934 was dispersed in 5 ml of distilled water and allowed for swelling over night. The swelled carbopol was stirred for 60 minutes at 800 rpm. The previously prepared required Itraconazole equivalent nanosuspensions, methylparaben and propylparaben were incorporated into the polymer dispersion with stirring at 500 rpm, by a magnetic stirrer for 1 h. The P^H of above mixture was adjusted to 4.5 with tri ethanolamine (0.5%). The gel was transferred in to a measuring cylinder and the volume was made up to 10ml with distilled water (7).

Evaluation studies

Fourier Transform Infrared (FTIR) spectroscopy: To confirm the formation of

nanosponges, Fourier Transform Infrared (FTIR) spectroscopy studies was used. Potassium Bromide pellet method was used in the study. The spectra was studied for the conformational changes of optimized drug when compared with the pure drug and pure excipients spectrums(8). The spectra were recorded in the wave number region of 4000-500cm⁻¹.

Encapsulation efficiency: The encapsulation efficiency of nanosponges was determined spectrophotometrically (λ_{max} = 261 nm). A sample of Itraconazole nanosponges (100 mg) was dissolved in 100 ml of methanol and kept it for overnight. 1 ml of the supernatant was taken and diluted to 10 ml with a solution containing 4.5 P^H phosphate buffer and was analysed at 260 nm using UV-visible spectrophotometer. From the absorbance the free drug content was calculated in Table 2. The methanol dispersion containing Itraconazole nanosponges was then ultra sonicated to release the encapsulated drug from the nanosponges structure(9). Then the solution was filtered by using 0.22 μ filter

Table 2. Encapsulation efficiency of Itraconazole loaded nanosponges

S. No	Batch code	%Encapsulation efficiency (n=3)
1	ILNS1	98.21 \pm 0.4
2	ILNS2	98.34 \pm 0.7
3	ILNS3	98.40 \pm 1.1
4	ILNS4	98.56 \pm 0.9
5	ILNS5	98.36 \pm 0.3
6	ILNS6	98.44 \pm 0.6
7	ILNS7	98.54 \pm 0.6
8	ILNS8	98.67 \pm 1.2
9	ILNS9	99.29 \pm 0.8
10	ILNS10	99.37 \pm 1.6
11	ILNS11	99.43 \pm 1.4
12	ILNS12	99.57 \pm 0.9

paper and the filtrate was analysed at 260 nm using UV visible spectrophotometer for the total drug content. The encapsulation efficiency (%) of the nanosponges will be calculated according to the following equation:

$$\text{Encapsulated drug content in nanosponges} \\
 \text{Encapsulation efficiency} = \frac{\text{Encapsulated drug content}}{\text{Total drug content}} \times 100$$

All measurements were performed in triplicate. The results of the best polymer and crosslinking agent ratio were analysed statistically for their significance of difference.

Determination of particle size distribution: The particle size distribution was determined by using Dynamic Light Scattering (DLS) technique. The equipment used for the particle size distribution is HORIBA particle size analyzer. In this technique the particle sizes of a batch of the nanosponges were observed and from the standard deviation and mean particle size of nanosponges, the Poly Dispersity Index (PDI) was calculated. The poly dispersity index is the indication for the nature of dispersity[10].

Determination of zeta potential: Zeta potential is a measure of surface charge of dispersed particles in relation to dispersion medium. It was determined by using HORIBA zeta sizer having the capability of determination of zeta potential. The zeta potential value is the indication of physical stability of the nanosponges(11).

Evaluation of drug loaded Nano sponges containing gels: The drug loaded Nano sponges containing gels were evaluated for P^H, Viscosity Spreadability, Extrudability and mucoadhesive time(12).

Drug content in the DLNS containing gel formulations: The sample of 1 gram of gel formulation containing 10 mg of Itraconazole was dissolved in methanol, filtered and the volume will be made to 20 ml with methanol in Table 3. The drug content

Table 3. Percentage of drug content in the Itraconazole loaded nanosponges containing gel formulations

S. No	Batch code	% Drug content
1	IF1	95.15
2	IF2	96.23
3	IF3	96.46
4	IF4	97.41
5	IF5	94.30
6	IF6	95.30
7	IF7	96.61
8	IF8	97.42
9	IF9	96.57
10	IF10	97.49
11	IF11	98.33
12	IF12	99.28

will be determined by diluting the resulting solution for 10 times with a solution containing 7.4 P^H phosphate buffer and the absorbance was measured at 260 nm using UV Visible spectrophotometer (13).

In-vitro drug diffusion study: Modified Franz diffusion cell was used for these studies. Cellophane membrane was used as the simulation for the skin. Cellophane membrane was mounted in a modified Franz diffusion cell. The known quantity (1g of gel containing 100 mg of the drug equivalent DLNS) was spread uniformly on the cellophane membrane on donor side. The solution containing 7.4 P^H phosphate buffer solution was used as the acceptor medium, from which 3ml of samples were collected for every hour and the same amount of fresh medium was replaced to maintain sink conditions for 12 hrs. While taking the samples from the acceptor medium, precautions were taken that no air bubbles were formed in the acceptor medium(14). The fresh samples were analyzed at 260 nm by UV-spectrophotometer and the

amount of drug diffused for each hour was calculated. All the samples were analysed in triplicate.

Results and Discussion

The FTIR structure of formed nano sponges were studied by comparing with unreacted β -cyclo dextrin and diphenyl carbonate FTIR spectra. In all the ratio of nanosponges, the major peaks were observed at 940 cm^{-1} which represents the α -1,4 glycoside bond which is the indication that there was no change in the cyclodextrin linkages. The absence of peaks responsible for carbonyl group of the diphenyl carbonate at 1768 cm^{-1} in the nanosponges is the indication of the removal of C=O from diphenyl carbonate. The absence of peaks responsible for $\text{C}=\text{C}$ at 1591 and 1497 cm^{-1} in the IR spectra of nanosponges is indication of absence of phenol rings which were present in the unreacted diphenyl carbonate. Similarly absence of an intense peak responsible for $\text{C}=\text{O}$ group at 1157 cm^{-1} in the IR spectra of nanosponges is the indication of removal of C=O group from the diphenyl carbonate which might be attached to the primary or secondary hydroxyl groups of β - cyclodextrin by leaving phenol as by product. All these changes infers that the formation of nanosponges by reacting of primary/secondary hydroxyl groups of betacyclo dextrin with the carbonyl groups of diphenyl carbonate. From the encapsulation efficiency of the drug loaded nanosponges formulations it was inferred that, as the crosslinking ratio increased the encapsulation efficiency was found to be enhanced. The order of encapsulation efficiency in the nanosponges is $1:1 > 1:0.75 > 1:0.5 > 1:0.25$. It is also found that the encapsulation efficiency of drug loaded nanosponges are influenced by the solvent used for drug loading by solvent evaporation technique. Chloroform $>$ Acetone $>$ Ethanol.

The change in the encapsulation efficiency with respect to solvent might be due to the solubility of Itraconazole in the

particular solvent. The extended sustained release was observed in all the 12 formulations. But the extent of sustained nature was varied from one ratio to other. The order of sustained action was as follows $1:1 > 1:0.75 > 1:0.5 > 1:0.25$.

Based on the drug encapsulation efficiency, drug content and extent of sustained nature formulation 12 was concluded to be the best formulation. The results of the present investigation overlay the path and provide substantial information for the utilization of Beta cyclodextrin in the development of drug delivery systems. The optimized formulation (IF12) were evaluated for their particle size and zeta potential. The particle size (334 nm) and zeta potential (-26.7 mV) was found to be good enough to maintain the physical stability of the nanosponges.

Carbopol gels containing nanosponges prepared with β -cyclodextrin and Di phenyl carbonate in different ratios and by using ethanol as a solvent shown drug release for a period of 7 hours, 7.5 hours, 8 hours and 9.5 hours respectively. Carbopol gels containing nanosponges prepared with β -cyclodextrin and Di phenyl carbonate in different ratios and by using acetone as a solvent shown drug release for a period of 8 hours, 8.5 hours, 9 hours and 10 hours respectively. Carbopol gels containing nanosponges prepared with β -cyclodextrin and Di phenyl carbonate in different ratios and by using chloroform as a solvent shown drug release for a period of 8.5 hours, 9 hours, 9.5 hours and 11 hours respectively. Based on the drug encapsulation efficiency, drug content and extent of sustained nature, the gel prepared with polymer and crosslinking agent in 1:1 ratio, chloroform as a solvent and carbopol as a gelling agent (IF12 formulation) was concluded to be the best formulation. The initial burst release decrease with increase in concentration of crosslinking agent. To ascertain the mechanism of drug release, the dissolution data was analyzed by zero order, first order, and Higuchi and Peppas equations. The correlation coefficient values (r) and diffusion kinetics values were shown in Table 4. Amount of drug diffused versus time

Table 4. *In vitro* drug diffusion kinetic data of Itraconazole loaded nanosponges containing gel formulations

Formulation	Correlation coefficient				Diffusion Rate Constant (mg/hr) Ko	T ₅₀ (hr)	T ₉₀ (hr)	Diffusion Exponent (n)
	Zero order	First order	Higuchi	Peppas				
IF1	0.9996	0.8771	0.9312	0.9977	13.62	3.63	6.54	0.9841
IF2	0.9996	0.8608	0.9267	0.9992	13.02	3.84	6.92	0.9919
IF3	0.9997	0.8425	0.9228	0.9995	12.25	4.08	7.34	0.9963
IF4	0.9998	0.7833	0.9221	0.9996	10.26	4.87	8.78	0.9951
IF5	0.9932	0.8964	0.9058	0.9941	12.95	3.86	6.94	0.9957
IF6	0.9973	0.8474	0.9043	0.9978	11.52	4.34	7.82	0.9968
IF7	0.9961	0.8238	0.8979	0.9983	10.50	4.76	8.57	0.9957
IF8	0.9946	0.7977	0.8909	0.9993	9.76	5.12	9.23	0.9864
IF9	0.9997	0.8721	0.9296	0.9998	12.25	4.08	7.34	0.9817
IF10	0.9987	0.8535	0.9276	0.9990	11.76	4.25	7.65	0.9923
IF11	0.9998	0.8160	0.9223	0.9990	10.50	4.76	8.57	0.9942
IF12	0.9997	0.7916	0.9214	0.9942	8.99	5.56	10.01	0.9937

curves exhibited straight line for the formulations and confirmed that the diffusion rate followed zero order release kinetics. Percentage of drug release versus square root of time curves shows linearity and proves that all the formulations followed Peppas model.

The diffusion exponential coefficient(n) values were found to be in between 0.9841 to 0.9968 indicating non

fickian diffusion mechanism. These results indicated that the diffusion rate was found to be decrease with increase in concentration of crosslinking agent. The optimized formulation has good spreadability, extrudability and mucoadhesive nature in Table 5 and Fig 1. The P^H and viscosity of the formulation were appropriate for the topical drug delivery and nanosponges technique was a better choice for sustained release.

Table 5. Physical properties of optimized gel

Formulation	Viscosity (cps)	Extrudability (N)	Spreadability (g.cm/sec.)	pH	Muco adhesive Time
IF12	3985±72	92.41± 0.05	34.61±2.11	4.46±0.02	>12 hrs

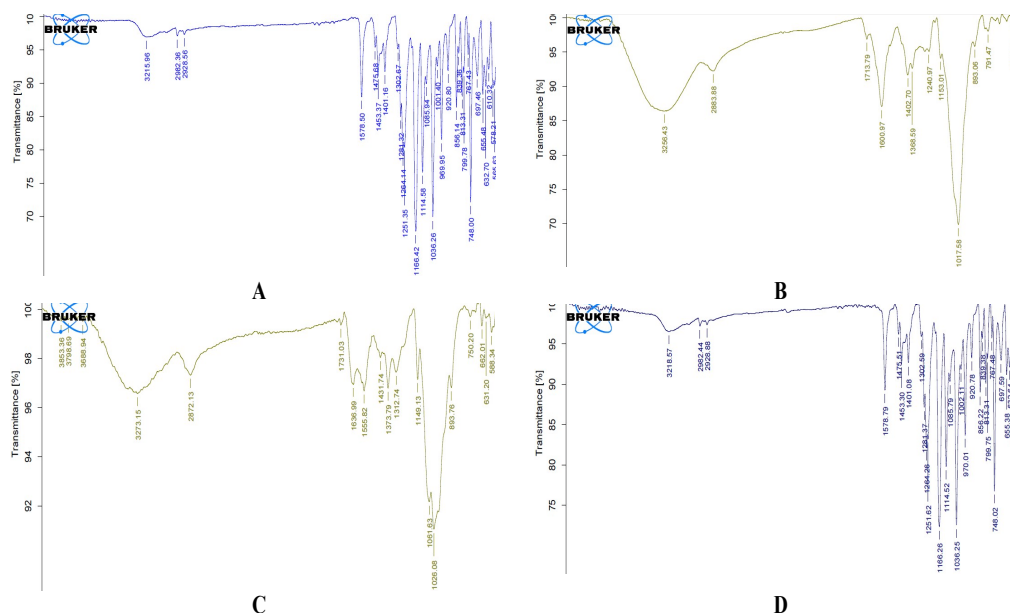


Fig 1. FT-IR spectra of Itraconazole(A) , β-Cyclodextrin (B), diphenyl carbonate (C)and optimized formulation(D)

References

- Singh A, Development and Evaluation of Cyclodextrin Based Nanosponges for Bioavailability Enhancement of Poorly Bioavailable Drug. *World Journal of Pharmaceutical Sciences*. 2017; 6(2): 805-836.
- Tripathi K D. Antifungal drugs. Tripathi K D(Ed). *Essentials of Pharmacology*, 6th edition, New Delhi: Jaypee Publication; 2008.
- Jilsha G and Viswanad V, Nanosponge Loaded Hydrogel of Cephalexin for Topical Delivery. *International Journal of Pharmaceutical Sciences and Research*, 2015; 6(7): 2781-89.
- Arvapally S, Harini M, Harshitha G, Kumar A, Formulation and *In-Vitro* Evaluation of Glipizide Nanosponges, *American Journal of PharmTech Research*, 2017; 7(3): 341-361.
- Kesar PM, Kale K, Phadtare DG, Formulation And Evaluation of Topical Antifungal Gel Containing Itraconazole, *International Journal of Current Pharmaceutical Research*, 2018; 10(4): 71-74.
- Penjuri S, Nagaraju R, Saritha D, Sailakshmi B, Srikanth R, Formulation and

Evaluation of Lansoprazole Loaded Nanosponges, Turkish Journal of Pharmaceutical Sciences, 2016; 13(3): 304-310.

7. Priyanka D, Sindhu S, Saba M. Design Development and Evaluation of Ibuprofen Loaded Nanosponges for Topical Application, International Journal of ChemTech Research, . 2018; 11(2): 218-227.

8. Manyam N, Kumar K, Budideti R, Mogili S, Formulation and *In vitro* evaluation of Nanosponge loaded Extended Release Tablets of Trimethoprim, UPI Journal of Pharmaceutical, Medical and Health Sciences, 2018; 1(1): 78-86.

9. Kamble M., Zaheer Z., Mokale S., Zainuddin R, Formulation Optimization and Biopharmaceutical Evaluation of Imatinib Mesylate Loaded β -Cyclodextrin Nanosponges, *Pharmaceutical Nanotechnology*, 2019;7:343–361.

10. Patil BS, Dr. Mohite SK, Formulation Design & Development of Artesunate Nanosponge. *European Journal of*

Pharmaceutical and Medical Research, 2016; 3(5): 206-211.

11. Swaminathan S, Vavia PR, Trotta F, Torne S, Formulation of betacyclodextrin based nanosponges of itraconazole, The Journal of *Inclusion Phenomena and Macrocyclic Chemistry*, 2017; 57:89-94.

12. Shrishail MG, Kamalapurkar Ka, Thorat Ys, Pathan Ma, Preparation and in-Vitro Evaluation of Itraconazole Loaded Nanosponges for Topical Drug Delivery. *Indo American Journal of Pharmaceutical Research*, 2019;9(04):1999-2013.

13. Caldera F., Tannous M., Cavalli R., Zanetti M., Trotta F, Evolution of Cyclodextrin Nanosponges, *International Journal of Pharmaceutics*, 017; 531:470–479.

14. Pushpalatha R., Selvamuthukumar S., Kilimozhi D. Cyclodextrin nanosponge based hydrogel for the transdermal co-delivery of curcumin and resveratrol: Development, optimization, in vitro and ex vivo evaluation, *Journal of Drug Delivery Science and Technology*, 2019;52:55–64.